Spatial modeling of invasion dynamics : applications to biological control of Aedes spp. (Diptera culicidae)

Thi Quynh Nga Nguyen

UNIVERSITÉ PARIS XIII – SORBONNE PARIS NORD

École doctorale Sciences, Technologies, Santé Galilée

Modélisation spatiale de la dynamique des invasions : Applications à la lutte biologique contre les *Aedes spp.* (Diptera: Culicidae)

Spatial modeling of invasion dynamics: Applications to biological control of Aedes spp. (Diptera: Culicidae)

THÈSE DE DOCTORAT
présentée par

Thi Quynh Nga NGUYEN

Laboratoire Analyse, Géométrie et Applications

pour l'obtention du grade de
DOCTEUR EN MATHÉMATIQUES

soutenue le 25 juin 2024 devant le jury d'examen constitué de :

PHAM NGOC Thanh Mai,	Université Sorbonne Paris Nord,	Présidente du jury
DOUMIC Marie,	École Polytechnique,	Rapportrice
GILETTI Thomas,	Université Clermont Auvergne,	Rapporteur
CORRIAS Lucilla	Université d'Evry Val d'Essonne	Examinatrice
NADIN Grégoire,	Université d'Orléans,	Examinateur
VAUCHELET Nicolas,	Université Sorbonne Paris Nord,	Directeur de thèse
BLIMAN Pierre-Alexandre,	INRIA Paris,	Co-directeur de thèse
ALMEIDA Luis	Sorbonne Université,	Co-directeur de thèse

Keywords: biological invasion, population dynamics, spatial modeling, reaction-diffusion equations, biological control

Mots clés : invasion biologique, dynamique de populations, modélisation spatiale, équations réaction-diffusion, lutte anti-vectorielle

This thesis has been prepared at

Laboratoire Analyse, Géométrie et Applications
Université Sorbonne Paris Nord
99 Av. Jean Baptiste Clément
93430 Villetaneuse
France

Web Site `https://www.math.univ-paris13.fr/laga/`

Dành cho ba mẹ và em trai yêu quý!

Life can only be understood backward; but it must be lived forward.

Soren Kierkegaard

Etre libre, ce n'est pas pouvoir faire ce que l'on veut, mais c'est vouloir ce que l'on peut.

Jean-Paul Sartre

Spatial modeling of invasion dynamics: Applications to biological control of *Aedes spp.* (Diptera: Culicidae)

Abstract

In this thesis, we focus on mathematical modeling and analysis of invasion dynamics, with application to the biological control of Aedes mosquitoes, vectors of various diseases such as dengue, zika, chikungunya, and yellow fever. We focus on the study of spatial effects on population persistence and extinction, which remains a fundamental challenge in the study of population dynamics. Biological controls based on the rear and release technique are sustainable and environmentally friendly. These techniques involve releasing large numbers of insects reared in the laboratory that are either sterile or incapable of transmitting disease, in order to reduce or replace the wild population. Reaction-diffusion models have been applied and updated in this work to describe the spatial phenomena that influence the effectiveness of these techniques. In an isolated area, we provide a critical domain size to ensure the efficacy of the control in the presence of migration of individuals on the boundary. In wide regions, we design moving release strategies to block and reverse the propagation of the population. A metapopulation model with discrete diffusion is also used to model the population in the presence of inaccessible zones. The monotonicity is the key tool to analyze the models to help design better release strategies. We also use empirical data to calibrate the models using an approach that combines the mechanistic view of differential equations and the statistical view of data to make simulations and predictions about mosquito population behavior while applying these techniques in the field.

Keywords: biological invasion, population dynamics, spatial modeling, reaction-diffusion equations, biological control

Résumé

Dans cette thèse, on étudie la modélisation mathématique et l'analyse de la dynamique des invasions, avec une application au contrôle biologique des moustiques Aedes, vecteurs de diverses maladies telles que la dengue, le zika, le chikungunya et la fièvre jaune. Nous nous concentrons sur l'étude des effets spatiaux sur la persistance et l'extinction des populations, ce qui reste un défi fondamental dans l'étude de la dynamique des populations. Les contrôles biologiques basés sur la technique de l'élevage et du lâcher sont durables et respectueux de l'environnement. Ces techniques consistent à relâcher un grand nombre d'insectes élevés en laboratoire qui sont soit stériles, soit incapables de transmettre des maladies, afin de réduire ou de remplacer la population sauvage. Des modèles de réaction-diffusion ont été appliqués et mis à jour dans ce travail pour décrire les phénomènes spatiaux qui influencent l'efficacité de ces techniques. Dans une zone isolée, on fournit une taille de domaine critique pour garantir l'efficacité du contrôle en présence d'une migration d'individus à la frontière. Dans les régions étendues, on conçoit des stratégies de lâchers mobiles pour bloquer et inverser la propagation de la population. Un modèle de métapopulation avec diffusion discrète est également utilisé pour modéliser la population en présence de zones inaccessibles. La monotonicité est l'outil clé pour analyser les modèles afin de concevoir de meilleures stratégies de relâchement. Nous utilisons également des données empiriques pour calibrer les modèles en utilisant une approche qui combine la vision mécaniste des équations différentielles et la vision statistique des données pour faire des simulations et des prédictions sur le comportement des populations de moustiques tout en appliquant ces techniques sur le terrain.

Mots clés : invasion biologique, dynamique de populations, modélisation spatiale, équations réaction-diffusion, lutte anti-vectorielle

Laboratoire Analyse, Géométrie et Applications
Université Sorbonne Paris Nord – 99 Av. Jean Baptiste Clément – 93430 Villetaneuse – France

Acknowledgement

My PhD journey started with writing letters of motivation and proposals, followed by drafting numerous paper manuscripts. And now, it may come to a conclusion with the writing of these grateful words for those without whom I would not have made it to this point.

First and foremost, I would like to thank my supervisors, Nicolas Vauchelet, Pierre-Alexandre Bliman, and Luis Almeida for their guidance and support over the years. Thank you for believing in me and for the many words of encouragement. I sincerely thank Nicolas for always listening carefully to my ideas and guiding me every step of the way. I am also grateful to Pierre-Alexandre for his detailed and constructive feedback on my work, and for the warmth of the New Year lunches (dinners) with his family, which brought much-needed joy during the long winter days away from my own family. And thanks Luis for all the helpful conversations we've had and for introducing me to various new collaborators and friends during workshops, summer schools, and conferences.

A big thank you also goes to Alexis Léculier, who has played a decisive role in my success as the coolest collaborator. His amazing ideas and passion for research have been a huge source of inspiration for me.

I want to express my immense gratitude to my collaborators at INRAE Avignon, Lionel Roques and Olivier Bonnefon. I have spent the most productive two months of my life working with them, and together we have discovered a new approach to my research.

I could not have reached this goal without the help of the Fondation Sciences et Mathématiques de Paris (FSMP) who paved the way for me to pursue my master's in France and then provided me with an opportunity to do a PhD in Paris. I want to express my deepest gratitude to Ariela Briani, Mathieu Simon, and all the individuals who have dedicated themselves to the project. Their efforts have truly provided me with a life-changing experience.

I would like to thank Marie Doumic and Thomas Giletti for accepting to be the referees of this thesis and for their careful reading and valuable comments. Also thanks to Thanh Mai Pham Ngoc, Grégoir Nadin, and Lucilla Corrias for accepting to be part of the defense jury.

My journey could not be that smooth without the help of the secretaries from all the laboratories where I work. Special thanks to Meriem Guemair from INRIA and Yolande Jimenez from LAGA for always being patient and helping me with all the complicated administrative processes.

And yes, being able to work at two different laboratories also means that my acknowledgment would be a bit longer than usual. Thank all of my friends and colleagues from both LAGA and LJLL! It is not easy to mention all of you (I have a long list), but I will try!

I am starting with my beloved office 15-16 301 at LJLL where I made my very first friends during my PhD. Thank Li Rui for being the first person to say hello to me and recognizing me from the blind conversation (in Chinese) in the French class through Zoom. Thank you for becoming my funniest ENFP friend ever. Thanks to Allen for being my very nice deskmate (always miss your keyboard sound) and a role model for me. Your desk was always empty until Liangying arrived so I have another super hard-working deskmate! Thank you, Liangying, for all the good food we shared, all the museums we visited together, and all the dump photos we took during the trips. And many thanks to Anatole for your elegant sense of humor, to Roxane, a responsible representative (and French translator), and to Lucas and Mathieu for your helpful math discussions. To all the newcomers, Aleksandra, since the day you came, our office has been full of scent and fun. Alois, Siguang, and the future office member Fédérica, thank you for organizing joyful meetings for us after working time. Thank Elisa for all of your interesting questions and *pipistrello!*

The list continues with a lot of Chinese names. I want to say thank you to Mingyue, my Pho-holic big sister, for always listening to my complaints about research and life. I promise to bring you to Vietnam some day and let you try the authentic Pho. Thank the Chinese gang for always adopting me as a lonely little sister from a communist neighbor: shout out to Liu Ruikang, Chen Zhe, Chen Gong, Bocci, Ruiyang, Ma Xiangyu, Lyu Zeyu. My PhD years could not have been completed without the lovely tulips on my desk given by Elena, the tasty pizzas, and the cozy party I enjoyed with the Italian-Spanish squad of Emma, Noémie, Giorgia, Jésus, Ramon, Agustin, Chiara. Thank you to every single one of my friends at LJLL, Chourouk, Yvonne, Charles, Kala, Jules,

Antoine, Nathalie, Cristobal, Ludovic, Lucia, Robin... Thanks Assane, Marcel and Manon for sharing with me all the cozy dinners at Pierre-Alexandre's place. Thank you, Thomas, for sharing the same anxiety of preparing the defense at almost the same time with me. And thanks to Eleanor, for always bringing the positive energy to me. We are Southeast Asian, of course we slay!

And, I want to say thank you to all of my friends at LAGA. Thank you for the kindness you gave during the time I spent at LAGA. Thank you, Elie, Neige, Mouna, Elyes, Wassim, Amine, Arthur, Maissa, Jakob, Hugo, Laila, Oisin... Thank Sawssen for helping me with all the teaching stuff.

I can not finish without showing my gratitude to my Vietnamese friends for their help during these challenging years of my PhD or even before. First of all, I want to thank Toai for being my first friend and classmate in France. Thank you for always being there whenever I need help and being the only person in the lab with whom I can discuss (gossip) in my native language. Next, I want to thank Minh Hang for being with me during this 8-year journey from bachelor to PhD. It was a long and rough time, but magically, I always have you as a reliable companion. Thank you and Khanh Hung for all the cozy meals you made for me. I am also grateful for all my lovely Vietnamese friends in Jussieu: Anh Thu (x2), Cam Linh, Xuan An, Khoa Anh, Quang, Binh, anh Trung, chi Quy, anh Long, chi Nga, anh Tuan Anh, chi Kim Anh... and my Vietnamese squad in LAGA: anh Tai, anh Dat, anh Vuong. Many thanks to all the friends who always takes beautiful pictures of me: Tan & Kien Bui, Lam le and the Erasmus Mundus friends, and especially my special guest Thai Ha. I also thank my two besties, Linh Chi and Huyen Trang, who always send love to me from a thousand miles away. Thank my two NCTzen clovers, Minh Anh and Thu Trang, for always encouraging me to follow my dream.

Last but not least, I want to express my deepest gratitude to my family, my parents, and my brother. Thank you for always supporting me and putting up with me whenever I complained about being stressed (I can't guarantee that it won't happen again). There are so many things I want to say to you, but the speech was getting too long, so I'll stop here. I hope I can come home more often to give you more hugs.

Thanks all of you, once again. I feel blessed for having been gifted with such amazing people in my life, and I could not have gotten this far without each of you.

This work has received funding from the European Union's Horizon 2020 research and innovation program under the Marie Sklodowska-Curie grant agreement No 945332.

Contents

Abstract **xi**

Acknowledgement **xiii**

Contents **xv**

1 Introduction **1**
1.1 Thesis outline . . . 1
1.2 Biological Invasion of *Aedes* Mosquitoes and Challenges . . . 1
1.2.1 Introduction of Invasive Mosquitoes . . . 2
1.2.2 Establishment . . . 3
1.2.3 Spread of *Aedes* Mosquitoes and Biological Controls . . . 5
1.2.4 Impacts of Invasion . . . 10
1.3 Spatial Modeling for Biological Control of *Aedes* Mosquitoes . . . 11
1.3.1 Reaction-diffusion models . . . 12
1.3.2 Discrete diffusion models . . . 13
1.3.3 Multi-scale models . . . 14
1.4 Contribution of the Thesis . . . 14
1.4.1 Reaction-Diffusion Model with Inhomogeneous Robin Boundary Conditions . . . 14
1.4.2 Reaction-Diffusion System with Forced Speed . . . 16
1.4.3 Global Extinction of a Two-patch Model with Control in One Patch . . . 18
1.4.4 Parameter Estimation with A Mechanistic-Statistical Approach . . . 19

I Reaction-diffusion models **21**

2 Steady-state solutions for a reaction-diffusion equation with Robin boundary conditions: Application to the control of dengue vectors. **23**
2.1 Introduction . . . 23
2.2 Results on the steady-state solutions . . . 25
2.2.1 Setting of the problem . . . 25
2.2.2 Existence of steady-state solutions . . . 26
2.2.3 Stability of steady-state solutions . . . 28
2.3 Proof of the theorems . . . 29
2.3.1 Proof of existence . . . 29
2.3.2 Stability analysis . . . 34
2.4 Application to the control of dengue vectors by the introduction of the bacterium *Wolbachia* . . . 35
2.4.1 Model . . . 35
2.4.2 Mosquito population in presence of migration . . . 36
2.4.3 Numerical illustration . . . 37
2.5 Conclusion and perspectives . . . 39

3 A control strategy for the Sterile Insect Technique using exponentially decreasing releases to avoid the hair-trigger effect **41**
3.1 Introduction . . . 41
3.1.1 The biological motivation . . . 41
3.1.2 Our model and the spreading results . . . 42
3.1.3 State of the art . . . 43
3.1.4 The traveling wave results . . . 44

3.1.5 Outline of the paper . . . 46
3.2 Numerical illustrations . . . 46
3.2.1 The numerical scheme . . . 46
3.2.2 Observations . . . 46
3.3 Study of the simplified model . . . 48
3.3.1 The simplified model . . . 48
3.3.2 Construction of a super-solution for the simplified model . . . 49
3.3.3 Construction of a sub-solution for the simplified model . . . 50
3.3.4 Conclusion: Construction of a traveling wave solution for the simplified model . . . 51
3.4 Study of the whole system . . . 51
3.4.1 Preliminary results . . . 51
3.4.2 Proof of Theorem 3.1.1 . . . 52
3.4.3 Construction of a super-solution for (3.9) . . . 54
3.4.4 Construction of a sub-solution for (3.9) . . . 57
3.4.5 Conclusion: Construction of the traveling wave for (3.9) (Proof of Theorem 3.1.2) . . . 60

4 Rolling carpet strategy to eliminate mosquitoes: 2D case 63
4.1 Introduction . . . 63
4.1.1 Formulation of the model . . . 64
4.1.2 Preliminaries . . . 65
4.1.3 Presentation of the main result . . . 66
4.1.4 Idea of the proof & Organisation of the paper . . . 68
4.2 Construction of a radially symmetric super-solution . . . 68
4.2.1 Preparation of the construction . . . 68
4.2.2 Construction of a super-solution . . . 70
4.3 Proof of the main result . . . 76
4.3.1 Proof of Theorem 4.1.1 . . . 76
4.3.2 Proof of Corollary 4.1.1 . . . 76
4.4 Numerical simulations . . . 76
4.4.1 Monostable case . . . 77
4.4.2 Bistable case . . . 77

II Metapopulation models with discrete diffusions 79

5 Efficacy of the Sterile Insect Technique in an inaccessible area: A study using two-patch models 81
5.1 Introduction . . . 81
5.2 Model . . . 82
5.2.1 Formulation of the model . . . 82
5.2.2 Preliminary results . . . 83
5.3 Mosquito dynamics without sterile males . . . 86
5.4 Elimination with releases of sterile males . . . 90
5.4.1 Principle of the method . . . 91
5.4.2 Proof of Theorem 5.4.1 . . . 93
5.5 Parameter dependence of the critical values of the release rate . . . 93
5.5.1 Diffusion rates . . . 94
5.5.2 Biological intrinsic values . . . 97
5.6 Numerical simulations . . . 97
5.6.1 Trajectories and Equilibria . . . 97
5.6.2 Critical values and bifurcation . . . 98
5.7 Discussion and conclusion . . . 103

III Model calibration: A multi-scale approach 105

6 Unveiling Mosquito Dynamics through a Mechanistic-Statistical Framework: Mark-Release-Recapture Analysis **107**
6.1 Introduction . . . 107
6.2 Material and Methods . . . 108
6.2.1 Mark-release-recapture data . . . 108
6.2.2 Models . . . 109
6.2.3 Simulated data . . . 111
6.2.4 Parameter estimation with the mechanistic-statistical approach . . . 112
6.3 Results and discussion . . . 113
6.3.1 Parameters estimation for simulated datasets . . . 113
6.3.2 Parameter estimation for real datasets . . . 115
6.4 Conclusion . . . 117

Conclusion **119**
Summary and Discussion . . . 119
Potential Future Directions . . . 120

A Monotonicity **123**
A.1 The stage-structured system . . . 123
A.2 The replacement system . . . 125

B Asymptotic limit of a Robin boundary problem **127**
B.1 Formulation of the problem . . . 127
B.2 Uniform a priori estimates . . . 128
B.3 Proof of convergence . . . 129

C Spread of Invasive Fronts **131**
C.1 Priliminary results . . . 131
C.2 Proof of Propositions 3.1.1 and 3.1.2 . . . 132

Bibliography **135**

Chapter 1

Introduction

1.1 Thesis outline

This thesis contains three parts corresponding to three modeling approaches that are used within the present work. Part I gathers studies on reaction-diffusion equations both in a bounded domain and in the whole space. The results were obtained in one- and two-dimensional spaces. Part II contains the study using discrete diffusion models and the metapopulation approach. The models in this part consist of a system of ordinary differential equations. Part III is devoted to presenting works on model calibration using empirical data.

In detail, the present chapter introduces the motivation, the methods, and the main results obtained in this thesis. The biological motivation of the thesis is described in Section 1.2 in the context of biological invasion of Aedes mosquitoes. Next, in Section 1.3, we discuss how spatial modeling can be used as a tool to address sophisticated problems in the study of biological control of *Aedes* mosquitoes. To describe the models we use in the thesis, we place them in a broader context of spatial models to highlight the circumstances under which our models provide an appropriate modeling approach. The contribution of the thesis is described in Section 1.4. From Chapter 2 to Chapter 6, we provide new results, some of which have already appeared in scientific journals (the corresponding references are given at the beginning of each chapter) as listed below.

- Chapter 2 was published in European Journal of Applied Mathematics [7]
- Chapter 3 was published in Mathematical Modeling of Natural Phenomena [126]
- Chapter 5 was submitted for peer-review. Chapter 4, and 6 are almost ready for submiting.

1.2 Biological Invasion of *Aedes* Mosquitoes and Challenges

During evolution over 100 million years, mosquitoes have developed adaptive mechanisms that allow them to survive in various environments. Among thousands of mosquito species, the two species of interest in this thesis, *Aedes albopictus* and *Aedes aegypti*, which are major vectors of many dangerous arboviruses, have a fascinating capacity to adapt to various climatic factors or environmental conditions. Nearly no aquatic habitat in the world is unsuitable for them to breed. They can lay eggs in highly polluted and clean water, and even in the smallest water containers such as buckets, vases, tires, bottle lids, or rainwater drums (see [29] and references therein). Their use of artificial containers as a larval habitat and desiccation-resistant eggs have contributed to their successful invasion worldwide.

In this section, we describe the invasion of these two species in four principal stages: *introduction, establishment, spread, and impact* (see Figure 1.1) which are commonly used to study dynamics of biological invasion (see [222, 132]). Each stage has its own issues to address in terms of the management and control of the invading species [183], and we are interested in how these issues can be addressed mathematically. Mathematical modeling and numerical simulation create a virtual laboratory to test hypotheses that are not feasible to do by using only traditional methods in ecology such as analysis and interpretation of field data. Besides, field experiments can induce adverse effects on biodiversity and the environment, and are costly while applying in large scale. The challenges that arise in each stage of the biological invasion are discussed in Section 1.2. Among these problems, we highlight the biological controls of *Aedes albopictus* and *Aedes aegypti* which is the main interest of this thesis. The starting point of mathematical modeling for these issues using a dynamical system approach is presented in this section.

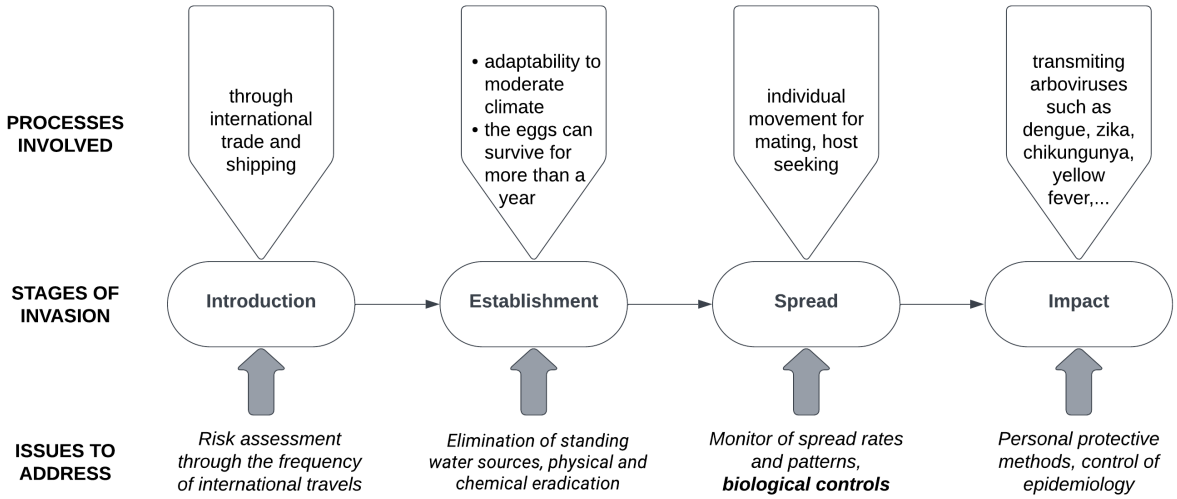

Figure 1.1 – Stages of biological invasion of *Aedes* mosquitoes

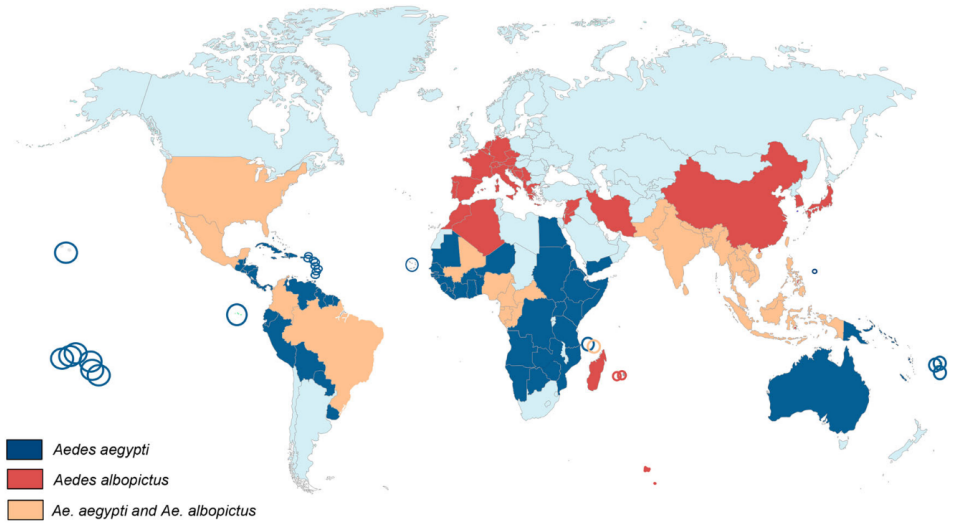

Figure 1.2 – World distribution of Aedes aegypti and *Aedes albopictus* in 2019 (Photo source: [109]).

1.2.1 Introduction of Invasive Mosquitoes

Modern human activities allow mosquitoes to be transported from one continent to another within a matter of hours to a few days by cars, aircraft, or transoceanic containers and let the mosquitoes spread globally via international trade and shipping [142, 28]. With a widespread in urbanized areas of the tropics and subtropics, their proclivity for biting humans makes *Aedes albopictus* and *Aedes aegypti* the major vectors of various dangerous arboviruses such as yellow fevers dengue, chikungunya, and Zika viruses [179]. Host-seeking females take up to 95% of their blood meals from humans in nature [149].

Aedes aegypti is a polymorphic species native of Africa that belongs to a species group known as the Aegypti Group, whose diversity is centered in the islands of the Indian Ocean. It has been brought in many areas in the tropics, especially in concurrence with the slave trade in the 16th and 17th centuries. Additionally, *Ae. aegypti* may have first invaded Portugal and Spain before reaching the Western Hemisphere on European ships [136]. In Asia, this species was first established in the late 19th century, coinciding with the first reports of dengue fever from an urban setting [190, 148]. In Australia, reports of dengue suggest the species established at a similar time as in the Asian region, possibly prior. *Ae. aegypti* is first well-known as the vector for the yellow fever virus (see e.g., [27]) and has been reported as the most efficient vector of the dengue virus (see e.g., [171]).

Aedes albopictus originates from Southeast Asia but has dramatically spread to both urban and rural areas, and to many tropical, subtropical, and temperate regions around the world in the past few decades (see e.g.,

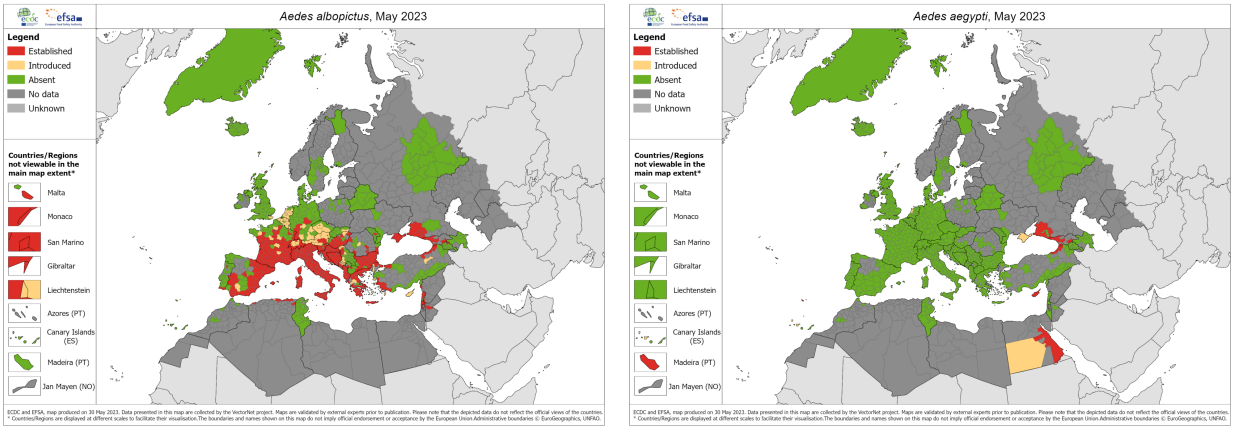

(a) *Ae. albopictus* distribution (b) *Ae. aegypti* distribution

Figure 1.3 – Distribution of *Ae. albopictus* and *Ae. aegypti* in Europe, May 2023 [111].

[31, 136]). The spread of *Ae. albopictus* is the “third wave" of mosquito invasion that was caused by human activities, following the spread of *Aedes aegypti* and *Culex pipiens* [136]. It spreads throughout the Oriental region, north through China and Japan, and west to the African island nations of Mauritius, Seychelles, and Madagascar [100, 157]. It had been detected in the transport of used tires at North American ports in 1983 [101, 136].

Nowadays, both species co-exist in many regions of the world [44, 109] (see Figure 1.2). Due to global warming, heat waves and flooding in Europe are becoming more frequent and severe. This provides more suitable conditions for invasive mosquito species like *Ae. albopictus* and *Ae. aegypti*. In 2013, the *Ae. albopictus* mosquito was established in 8 EU/EEA countries, with 114 regions being affected. In 2023, the mosquito was established in 13 countries and 337 regions (see Figure 1.3a). Also, *Ae. aegypti* has been established in Cyprus since 2022 and may continue to spread to other European countries [111] (see Figure 1.3b).

A comprehension of invasive introduction unavoidably includes the whole range of issues affecting human activities, particularly those related to human travel and transportation of agricultural products on international and intercontinental scales [64]. The introduction of *Ae. albopictus* and *Ae. aegypti* as well as other invasive species depends on the frequency of travel between the native country and the other, which could be determined by the number of tourists per year, for example. The principal challenge is to minimize the risk of new introductions of invasive species, especially the vectors of infectious diseases to avoid the epidemiology. Unfortunately, mathematical modeling of social and political processes is currently at a very early stage and is not discussed in this thesis.

1.2.2 Establishment

The invasion history proved the amazing adaptation of *Ae. albopictus* and *Ae. aegypti* to the new areas where they were brought in. The “Ten Rule” about the biological invasion of Williamson [222] stated that approximately 10% of nonindigenous alien species become established, and of the establishment, only about 10% become pests. However, the performance of biting mosquitoes is much higher than in this rule [136]. For instance, in the United States, there are 36.4 % species of mosquitoes established successfully. This proportion in Australia is about 25%. One big challenge for biologists to prevent the establishment of mosquitoes is the identification of the factors that affect the survival of the introduced species. It is efficient monitoring and eradication of the mosquitoes when they are newly introduced. Monitoring is, however, a complicated theoretical and practical problem, because the newly introduced species usually occupy only a small area. Various multi-scale approaches to modeling the establishment of invasive species have been used but often appear to be ineffective and/or very expensive [168]. For *Ae. albopictus* and *Ae. aegypti*, many works have been carried out to monitor biological factors affecting the establishment in different regions of the world (see e.g., [204, 74, 166]).

It is natural to expect that the invasive mosquito can only be established successfully if it starts growing rather than declining right after the introduction. We therefore consider a mathematical model that allows us to examine whether the invasive species will actually grow and how the answer depends on the parameter values of the model. A classical approach is to use a compartmental model which consists of a set of compartments that represent the density of, in this case, a certain life stage of the mosquito population, and which evolve according to ordinary differential equations. The mosquito life cycle can be split into two clearly distinct phases: an aquatic phase composed of three stages, egg, larvae, and pupae, and an aerial phase as adults. In the aquatic phase,

mosquitoes are developing and sexually immature. After undergoing a metamorphosis, they become adults and start to mate and reproduce. Here we do not focus on the modeling of the aquatic phase, which is a whole topic on its own. As a starting point for the kind of models that will be discussed in this thesis, we introduce a minimalistic model that was developed in the literature [19, 200]

$$\dot{E}(t) = bF\left(1 - \frac{E}{K}\right) - (\nu_E + \mu_E)E, \tag{1.1a}$$

$$\dot{F}(t) = \rho\nu_E\Gamma(M)E - \mu_F F, \tag{1.1b}$$

$$\dot{M}(t) = (1-\rho)\nu_E E - \mu_M M. \tag{1.1c}$$

Here we denote by E the aquatic phase (including eggs, larvae, pupae), M the males, F the fertilised females. This is a simplified model where the dynamics of all aquatic phases in the mosquito life cycle are simplified to the dynamics of the egg stage. Parameter b is the mean number of eggs laid by a female mosquito per day, K is the egg carrying capacity, μ_E, μ_F, μ_M are respectively the eggs, females and males daily death rates, ν_E is the emergence rate from the eggs stage to the adult stage, and ρ is the egg-hatching ratio to female. The non-linear term $bF\left(1 - \frac{E}{K}\right)$ is a behavior of *Aedes spp.* which can be interpreted as a "skip oviposition" behavior. Females will select their breeding site and may not deposit eggs or even skip their oviposition if the breeding sites already contain a lot of larvae. The term $\Gamma(M)$ represents how the density of males influenced the dynamics of females through mating. Two typical choices for function Γ are:

$$\Gamma(M) \equiv 1 \text{ (monostable case)}, \qquad \Gamma(M) = 1 - e^{-\gamma M} \text{ (bistable case)}. \tag{1.2}$$

In the first case where $\Gamma \equiv 1$, the dynamics of females do not depend on the density of males, we assume that all adult females are fertilised. While in the second case, an Allee effect is introduced through a new parameter, γ, that is related to a female mating's likelihood per male (in a given area) such that $(1 - e^{-\gamma M})$ provides the probability that an emerging female finds a male in her neighborhood to mate with. An Allee effect occurs when the population is sparse and the population growth decreases because individuals can not find a partner to mate with [61].

System (1.1) is monotone in the sense that the trajectory resulting from a larger initial value remains larger over time. Details on the monotonicity of this system is provided in Appendix A. We obtain these properties for (1.1) due to the fact that it is a cooperative system.

The population will grow and establish successfully means that the system possesses at least a positive equilibrium. By "positive" we mean that all stages in the model are positive. We introduce the basic offspring number

$$\mathcal{N} := \frac{b\rho\nu_E}{\mu_F(\nu_E + \mu_E)}.$$

The basic offspring number can be interpreted as the average number of offspring born per fertile female over its expected lifetime. In the case where $\Gamma \equiv 1$, the system (1.1) has a unique positive equilibrium (E^*, F^*, M^*) if and only if $\mathcal{N} > 1$. Due to the monotonicity of the system (see [191]), the trivial steady state corresponding to the extinction is unstable, and all trajectories resulting from non-negative initial data converge to the positive steady state. So that is why this case is called *monostable* case. Its phase portrait (of E and F) is plotted in Figure 1.4a where we can see the convergence of all trajectories to the positive equilibrium in the viable case, when $\mathcal{N} > 1$.

In the second case where $\Gamma(M) = 1 - e^{-\gamma M}$, the following constants are introduced in [200]

$$\zeta := \frac{\mu_M}{(1-\rho)\nu_E\gamma K}$$

where ζ is the ratio between the typical male population size at which the Allee effect comes into play and the male population size at wild equilibrium, as prescribed by the carrying capacity of eggs.

The result in [200] showed that when $\mathcal{N} > 4\zeta$, and

$$\max_{\theta\in[\theta_0,1]}\left[-\ln\theta - \frac{1}{2\zeta}\left(1 - \sqrt{1 + \frac{4\zeta}{\mathcal{N}}\frac{\ln\theta}{1-\theta}}\right)\right] > 0 \tag{1.3}$$

where θ_0 is the unique solution in $(0,1)$ of $1-\theta_0 = -\frac{4\zeta}{\mathcal{N}}\ln\theta_0$, then (1.1) has two positive equilibria $(e^*, f^*, m^* \ll (E^*, F^*, M^*)$. The trivial equilibrium $(0,0,0)$ and (E^*, F^*, M^*) are locally asymptotically stable, so this case is called *bistable* (see the phase portrait in Figure 1.4b). The basin of attraction of $(0,0,0)$ is narrow, and when

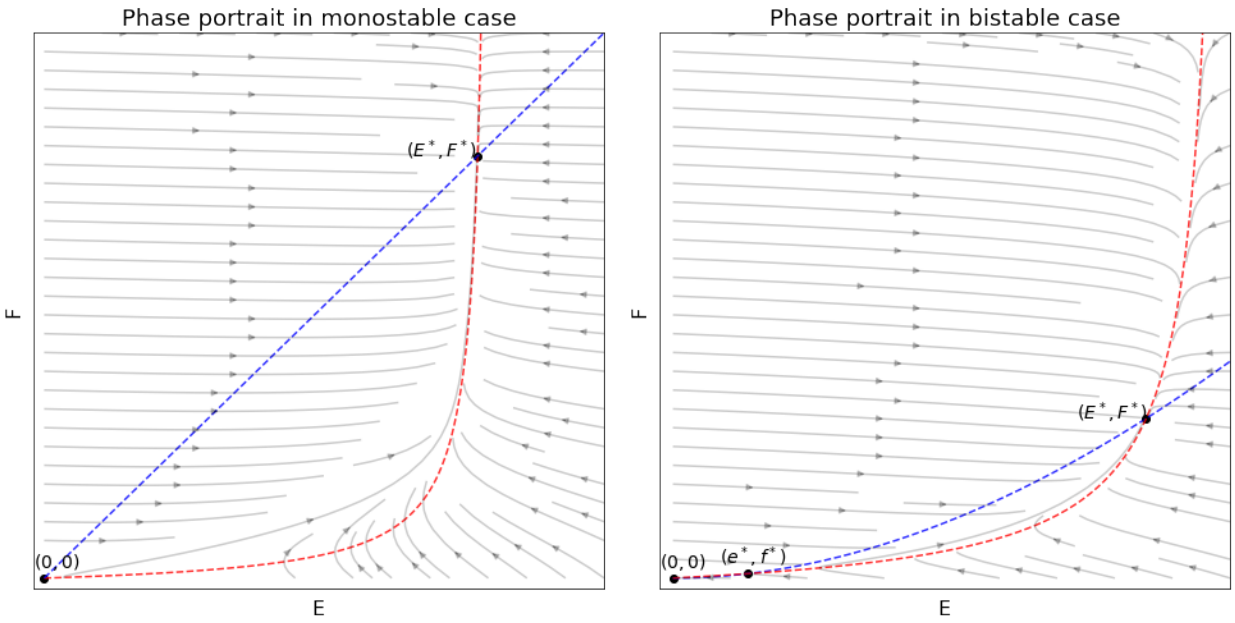

(a) Monostable case with $\mathcal{N} > 1$

(b) Bistable case with $\gamma = 0.005$, $\mathcal{N} > 4\zeta$ and (1.3) holds

Figure 1.4 – Phase portrait of E, F in model (1.1) when $\mathcal{N}$ large enough. The positive equilibria (in black) appear at the intersections of the two dashed curves on which $\dot{E}$ (in red) and $\dot{F}$ (in blue) vanish. The values of parameters are chosen following [69] for mosquitoes of species *Aedes albopictus* and presented in Table 3.1

.

the parameter γ decreases, it gets smaller.

In both cases, the model illustrates how the establishment of the mosquito population depends on the parameter values. It requires that $\mathcal{N}$ is large enough which means the population should be efficient (large birth rates and small death rates). In the bistable case where we have an Allee effect, it also requires that the probability γ of one female to mate is high. Parameter estimation from experimental data of the *Aedes* mosquito validates these conditions for establishment [200].

1.2.3 Spread of *Aedes* Mosquitoes and Biological Controls

Once the mosquitoes have been established locally, adult individuals usually start spreading and invading new areas with passive ground transportation [150] and individual movements for mating and host-seeking. For example, in France, the French Ministry of Health together with the French Regional Health Agencies have set up monitoring of the whole territory, with increased surveillance of regions where the mosquito was present or likely to become established. The data from the French Interdepartmental Agreement for Mosquito Control (EID) and the European Centre for Disease Prevention and Control (ECDC) depicted in Figure 1.5 show the spread of *Ae. albopictus* across the mainland France.

It is essential to determine the rate and pattern of spread of the invasive species to design appropriate control strategies to block the invasion. In particular, the spread is affected by interactions between the invasive mosquito and the native community as well as the biological control agents. Mathematical modeling for biological invasion has shown that these interactions can decrease the rate of spread significantly and stop the propagating invasion front completely. They can even reverse the propagation, hence stopping the invasion and eradicating the alien species (see [132] and references therein). In this section, we discuss the biological controls of *Ae. albopictus* and *Ae. aegypti* mosquitoes and some meaningful first insights into the problem by considering non-spatial models.

The spread of invasive mosquitoes has fomented the transmission of many vector-borne diseases across the regions they have been established. As the pivot for arbovirus transmission, the mosquito vector is considered the target for efficient arboviral disease control. Human efforts to control vector populations have a long and controversial history. Starting from simple environmental management like eliminating standing water sources and use of mosquito bed nets to chemical eradication using insecticide. In recent years, biological controls become an alternative strategy because of their sustainability and eco-friendliness. Biological control can be defined as the decrease of the target population by the use of predators, parasites, pathogens, competitors, or toxins from microorganisms [32]. It aims to reduce the target population to an "acceptable" level and, at the same time, to avoid unfavorable effects on the ecosystem. As far as mosquito control is concerned, biological

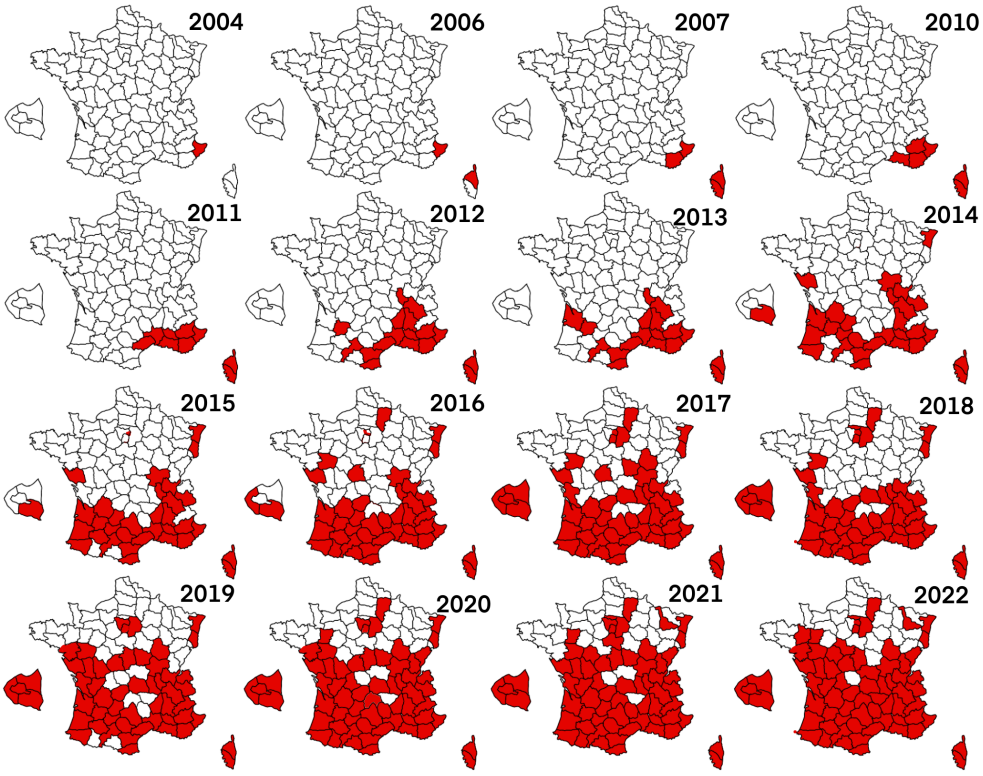

Figure 1.5 – Distribution of *Ae. albopictus* (red) in mainland France between 2004 and 2022. Paris is presented in the bottom left corner (Photo source: [67]).

control protects humans from mosquitoes by conservation of biodiversity while avoiding toxicological effects, and protecting the existing community of mosquito predators. The predators then can assist the control effort by preying upon newly hatched mosquito larvae after the control operation, thereby enhancing the efficacy of the control methods.

Among the biological control, the *rear and release* techniques can be a game changer in the fight against mosquitoes in the upcoming years [173]. These techniques consist of releasing of large numbers of insect reared in the laboratory that are either sterile or unable to transmit disease to reduce or to replace the wild population. In this thesis, we focus on two techniques that recently gained a lot of attention in the mosquito control community: the SIT and Wolbachia-based method, which represent two main approaches of the rear and release techniques: population elimination and population replacement. In this thesis, we discuss how mathematical modeling, analysis, and simulation (including the humble contributions of this thesis) help to prevent failures, improve protocols, and test assumptions while applying these strategies in the field.

The Sterile Insect Technique

Since the pioneering work of Knipling [118], who realized that the fertility of monogamous female organisms could be readily compromised as a result of mating with a sterile male, the history of genetic control of mosquitoes has begun [29]. The so-called Sterile Insect Technique (SIT) is the method aiming to suppress or even eliminate entire populations of a particular mosquito species by mass releases of sterilized male mosquitoes that mate with indigenous females yet produce no fertile offspring. This technique has been applied to fight against *Ae. albopictus* and *Ae. aegypti* and evaluated in many countries around the world, for example in Cuba [88], in Mexico [147] in China [228], and in Italy [30]. One standout advantage of SIT is that it relies on the natural ability of the male mosquitoes to locate and mate with females. This behavior will take place even in areas that cannot be reached with conventional control techniques (i.e. insecticides) (see Chapter 5).

When sterile males can be released in sufficient numbers and over a sufficiently long period, so that they outcompete the wild males in terms of mating with the females, then the population should considerably decline and reach local elimination. Different mathematical models have been studied for the SIT to assess their potential as a control tool (see [70] and references therein). The compartmental model (1.1) was modified to study the SIT [200]. A minimalistic model can be derived by assuming that the density of sterile male, denoted as M_s, is constant

$$\dot{E}(t) = bF\left(1 - \frac{E}{K}\right) - (\nu_E + \mu_E)E, \tag{1.4a}$$

$$\dot{F}(t) = \rho\nu_E\Gamma(M + \gamma_s M_s)E\frac{M}{M + \gamma_s M_s} - \mu_F F, \tag{1.4b}$$

$$\dot{M}(t) = (1-\rho)\nu_E E - \mu_M M, \tag{1.4c}$$

where we consider the proportion of fertile mating $\dfrac{M}{M + \gamma_s M_s}$, with γ_s the mating competitiveness of sterile males. The full model introduced in [200] describes different stages in the aquatic phase including eggs E, larvae L and classifies the females into two types, females F that are fertilised by mating with wild males, and sterile females F_s which mated with sterile males. The author in [200] indicated that the dynamics of the full model is not different from the simplified model (1.4). Therefore, we focus on study system (1.4) in this thesis.

A preliminary result for this system states that, if the basic offspring number $\mathcal{N}$ is large enough, there exists a critical value $M_s^{\text{crit}} > 0$ (see [19] for the monostable case and [200] for the bistable case) such that

- If $M_s \in (0, M_s^{\text{crit}})$, system (1.4) has two positive steady states $(e^*, f^*, m^*) \ll (E^*, F^*, M^*)$;
- If $M_s = M_s^{\text{crit}}$, system (1.4) has exactly one positive steady states;
- If $M_s > M_s^{\text{crit}}$, system (1.4) has no positive steady state.

This result indicates that in both cases, the SIT control can induce the Allee effect in system (1.4) and if the number of released sterile males exceeds the critical value M_s^{crit}, zero is the unique equilibrium. By use of the monotonicity of the system, one has $(0, 0, 0)$ is globally asymptotically stable, and the SIT succeeds in this case. In practice, the population of sterile males also reduces with some death rate $\mu_s > 0$, and the density of this compartment can be described by the following equation

$$\dot{M_s}(t) = \Lambda(t) - \mu_s M_s, \tag{1.5}$$

where $\Lambda(t)$ is the number of sterile males released at time t. While taking $\Lambda(t) \equiv \Lambda > 0$ constant, we plot the phase portraits of system (1.4) in Figure 1.6. Even when we consider the monostable case when $\Gamma(M) = 1$, the model (1.4) still has the bistable dynamics due to the implementation of sterile males (see Figure 1.6a). When Λ exceeds some critical value, all the positive equilibria disappear, and all trajectories converge to the trivial equilibrium (see Figure 1.6b).

Various works in the literature provided control strategies for system (1.4),(1.5) by designing different profiles for Λ. The work [200] considered different profiles of Λ where it is constant, periodic, or impulsive and provided necessary conditions to reach elimination in each case. An important assumption in [200] is that there is an Allee effect in the wild mosquito population ($\Gamma(M) = 1 - e^{-\gamma M}$), and then the application of SIT for a finite time is sufficient to drive the population into the basin of attraction of the zero steady states. In practice, this assumption may not be valid and the size of this domain may be close to zero. Other works have considered the case without that assumption and design alternatives strategy [19, 38, 39] based on the bistability induced by the SIT. The strategy in [19] consists of massive release at the beginning, then followed by a lower release rate, which can be maintained for a long time and is called the "permanent" SIT. In the thesis, this idea is extended and implemented taking into account the spatial distribution of the population (see Chapter 3 & 4). In [38, 39], robust strategies using both open and closed-loop control have been designed for the SIT. The optimization of release time and release number of sterile males is another essential question to maximize the efficiency of the technique. A clear presentation of optimal control strategies for the SIT with relevant references can also be found in the PhD thesis of Jesus Bellver Arnau [22].

Spatial distribution is an important and interesting aspect but still remains a challenge for the mathematical modeling of biological controls. A very first model combining effects of dispersal terms and growth dynamics was developed in [128] to study the SIT as a method to block and reverse the invasive waves of the wild population. Recently, many works propose spatial models for *Aedes* mosquitoes to investigate the barrier effects [185, 15], and design a control strategy based on moving releases to reverse the propagating fronts [12]. This is also the main interest in this thesis where we will use spatial modeling to investigate spatial effects on the biological control of invasive mosquitoes (see Section 1.3).

The Population Replacement Methods and *Wolbachia*-based controls

The population replacement method aims to replace the vector population with a transgenic or pathogen-refractory strain that is unable to transmit diseases [29]. Replacing the target population with a pathogen-

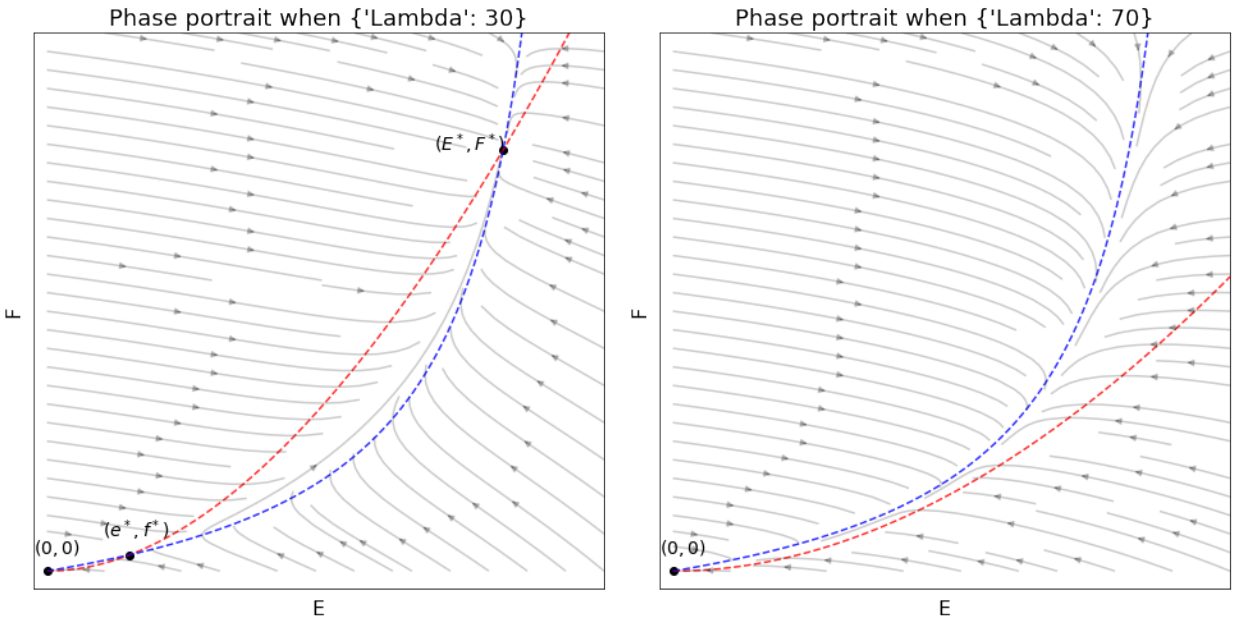

(a) $\Lambda = 30$ (b) $\Lambda = 70$

Figure 1.6 – Phase portrait of model (1.4)-(1.5) with $\Gamma(M) \equiv 1$ (monostable) while applying the SIT with different values of Λ. The equilibria (in black) appear at the intersections of the two dashed curves on which $\dot{E}$ (in red) and $\dot{F}$ (in blue) vanish.

refractory strain could specifically reduce the pathogen transmission while maintaining the population in its original ecological niche, limiting the risk of secondary pest emergence. Various mosquito antiviral factors such as siRNA, miRNA, ribozymes, immune factors, and neutralizing antibodies can be used to reduce the virus infection and transmission in genetically modified mosquitoes. They can replace the wild population in a few generations, that is to say in a few months for mosquitoes (see [226] and references therein). However, the biosafety concerns about using genetically modified insects are still controversial [158].

The biological control using *Wolbachia* is more acceptable for the public than the genetic modification-based approach as it is a naturally existing bacterium. The method has been applied successfully in the field [108] and used worldwide by the World Mosquito Program [224]. *Wolbachia* is a gram-negative bacterium, living inside the cell of the host. It was first discovered in the *Culex pipiens* mosquito in 1924 by Hertig and Wolbach [104] and now gains the spotlight due to the discovery of its ability to inhibit the replication of arboviruses, including dengue, zika, and yellow fever [43, 72] and prevent viruses transmission. The high density of *Wolbachia*, which could reach several hundred bacteria per cell [137] can cause high antiviral resistance and reduce significantly fecundity, fertility, and survival [146]. This bacterium can be found in 65% insect species [105] and is mainly transmitted vertically from mother to offspring (see Table 1.1). These characteristics allow *Wolbachia*-based technique to be viewed as a population replacement method, since once the *Wolbachia*-infected females are released, they will pass the bacteria to the next generation and replace the wild population.

Table 1.1 – Offspring outcome in a population with both *Wolbachia*-infected and uninfected mosquitoes

Male \ Female	Infected	Uninfected
Infected	Infected	CI
Uninfected	Infected	Uninfected

Another important property of *Wolbachia* is that it induces cytoplasmic incompatibility (CI) in *Aedes* mosquitoes. CI is the failure of a sperm and egg to produce viable offspring under certain conditions (see e.g., [52, 210, 209]). Various models were developed to describe CI including discrete-time population-genetics models [210, 209], following an original model for CI in [52], and continuous-time population-dynamics models taking into account the competition and coexistence of different *Wolbachia* strains [116, 79]. In the case of *Wolbachia*-carrying mosquitoes, CI is caused by the crossed infertility of a *Wolbachia*-infected male and a

wild uninfected female, see Table 1.1. Due to the CI, *Wolbachia*-infected males can be released massively to mate with wild females to reduce the reproduction of the population. This approach is similar to the SIT in the previous section and is a form of the Incompatible Insect Technique (IIT). However, unlike the SIT, the *Wolbachia*-based approach does not require a strict sex separation, since the release of both *Wolbachia*-infected males and females is meaningful. Due to this reason, we can model the biological control using *Wolbachia* by a simple Lotka-Volterra model without sex structure considering n_i and n_u the densities of *Wolbachia*-infected and uninfected mosquitoes respectively (see e.g., [54, 201, 13]). We consider in the following a simple model studied in [13]

$$\dot{n}_i(t) = b_i n_i \left(1 - \frac{n_i + n_u}{K}\right) - d_i n_i + \Lambda(t), \tag{1.6a}$$

$$\dot{n}_u(t) = b_u n_u \left(1 - \frac{n_i + n_u}{K}\right)\left(1 - s_h \frac{n_i}{n_i + n_u}\right) - d_u n_u, \tag{1.6b}$$

where we assume that the *Wolbachia*-infected (*resp.* uninfected) population has the birth rate b_i (*resp.* b_u) and death rate d_i (*resp.* d_u), and K denotes the carrying capacity of the environment. The term $\left(1 - s_h \frac{n_i}{n_i + n_u}\right)$ models the cytoplasmic incompatibility (CI) with $s_h \in [0, 1]$. When $s_h = 1$, the CI is perfect, no egg of uninfected females fertilized by infected males can hatch. The factor becomes $\frac{n_u}{n_i + n_u}$ which means the birth rate of uninfected mosquitoes depends on the proportion of uninfected parents because only an uninfected couple can lay uninfected eggs. Whereas, $s_h = 0$ means that all the eggs of uninfected females hatch. In this case, the term becomes 1, so the growth rate of the uninfected population is not altered by the pressure of the infected one. Function $\Lambda(t)$ denotes the number of *Wolbachia*-infected mosquitoes released per time unit. We emphasize that system (1.6) is competitive (see Appendix A).

The analysis of system (1.6) is studied in [13]. In the absence of control (i.e., $\Lambda \equiv 0$), if the birth rate is larger than the death rate, system (1.6) has at least three non-negative steady states

$$(0, 0), \qquad (n_i^*, 0), \qquad (0, n_u^*),$$

with $n_i^* = K\left(1 - \frac{d_i}{b_i}\right)$ and $n_u^* = K\left(1 - \frac{d_u}{b_u}\right)$. In this case, one of the two populations must prevail in the long run, eliminating the other one. In addition, the trivial equilibrium $(0, 0)$ is (locally linearly) unstable, and system (1.6) has a fourth distinct positive steady state (n_i^c, n_u^c) if and only if

$$1 - s_h < \frac{d_u b_i}{d_i b_u} < 1. \tag{1.7}$$

This coexistence equilibrium is (locally linearly) unstable (see [13] for explicit formula).

The success of the population replacement method using *Wolbachia* lies in the establishment of the *Wolbachia*-infected mosquito population which now plays the role of an invasive species. Hence, the control succeeds if the trajectories of the system converge to $(n_i^*, 0)$. The phase portrait of system (1.6) is presented in Figure 1.7 with two different values of the cytoplasmic incompatibility s_h. When s_h is small such that the condition (1.7) is not validated, almost trajectories of system (1.6) converge to equilibrium $(0, n_u^*)$ and the basin of attraction of equilibrium $(n_i^*, 0)$ is very small (see Figure 1.7a). However, in practice, the rate s_h is usually close to 1, so condition (1.7) holds and the coexistence equilibrium (n_i^c, n_u^c) exists. We can see in Figure 1.7b, this equilibrium is a saddle, and all the flows below the dashed line passing close to this equilibrium are pushed to $(n_i^*, 0)$.

The dynamics of system (1.6) can be described by the dynamics of the proportion $p = \frac{n_i}{n_i + n_u}$ (see [201]) in which two steady states 0 and 1 play an important role. Various works have provided strategies for the release function Λ in (1.6) in both temporal and spatiotemporal frameworks using this simplified model [13, 5, 6, 71]. A feedback control perspective was also provided in [37]. In addition, sex-structured models have been developed to describe more details of the mosquito population under control using *Wolbachia* to help design a sex-biased release strategy [78, 40]. The use of *Wolbachia* in the control of arboviruses transmission is also modeled using the SIR and SEI compartmental models (see [110, 14] and references therein).

Unlike the SIT control in which the target population can recover after the controls stop, the *Wolbachia*-based control performs more sustainably in both ecological and evolutionary perspectives [180]. Theoretically, once the *Wolbachia*-infected population is established in the reservoir, it persists for a long time without permanent releases. This makes it a self-sustaining, affordable, and long-term solution to control mosquito-borne diseases. However, in practice, many factors can influence the efficacy of this control technique. For example, when the area treated by the control is surrounded by one or several areas where intervention is, for some reason,

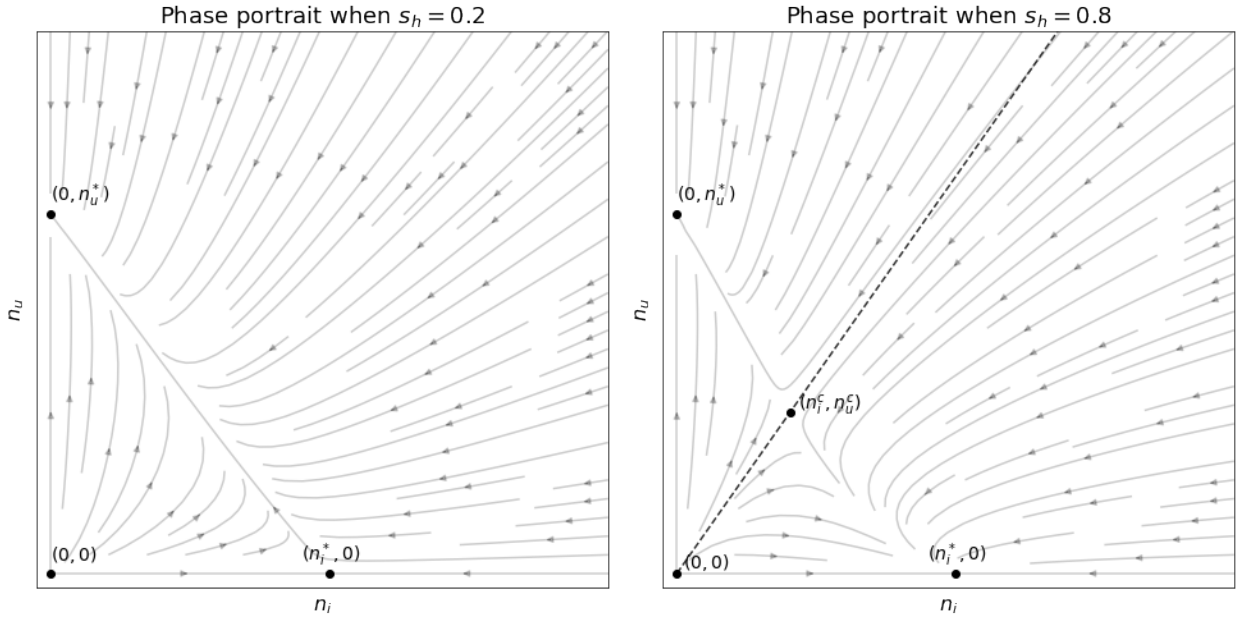

(a) $s_h = 0.2$ (b) $s_h = 0.8$

Figure 1.7 – Phase portrait of model (1.6) while applying the population replacement method using *Wolbachia*. The black dots represent the equilibria. The dashed line connects the extinction equilibrium and the coexistence equilibrium.

impossible, the migration of wild mosquitoes from the exterior towards the interior of the domain, as well as the outflow of *Wolbachia*-carrying mosquito, can affect the sustainability of the method. This is the main problem that we address in Chapter 2 by extending the model proposed in [201]. Our result suggests applying the control technique using *Wolbachia* at a large scale or in well-isolated regions to guarantee its long-term stability. Many field studies in the framework of the World Mosquito Program (see e.g., [89, 211, 212]) have confirmed the necessity of large-scale deployment of this technique on health and economic benefits.

1.2.4 Impacts of Invasion

The last stage of biological invasion is associated with the impact of alien species to the invaded areas. In the case of *Aedes aegypti* and *Aedes albopictus* mosquitoes, we focus on the spread of epidemics that they brought to the indigenous region.

In terms of morbidity and mortality caused by vector-borne diseases, mosquitoes are the most dangerous animals confronting mankind. Around 4 billion people in tropical and subtropical regions are threatened by mosquitoes, more than half of the world's population. Among 30 species known to have established in new areas throughout the world, *Ae. aegypti* and *Ae. albopictus* gain special recognition for their dispersal potential and their significance as vectors of human diseases. *Ae. albopictus* is characterized by their high vector competence for arboviruses [28] and have been able to rapidly and successfully build up and establish stable populations in new geographical regions. The invasion of mosquitoes fomented the movement of pathogens from one geographical region to another has resulted in the spread of diseases. In 1999, the introduction of *Ae. albopictus*, a vector of West Nile virus to the United States enabled this disease to spread rapidly (within 5 years from the East Coast to the West Coast) across the continent, placing another 0.5 billion people at risk. The recent introduction of this species to Southern Europe resulted in the first known indigenous European outbreak of chikungunya and Zika fever. Until the early twentieth century, in regions of North and Central America, the Caribbean, and Europe, the spread of *Ae. aegypti* caused severe yellow fever epidemics. Both *Ae. aegypti* (primary vector in urban areas) and *Ae. albopictus* (secondary vector in suburban/rural areas) are the vectors of dengue. Around 390 million dengue infections occur every year and 128 countries are at risk [66]. Currently, dengue is not endemic in Europe, but with the increasing numbers of imported cases [111] and with the spread of *Ae. aegypti* and especially *Ae. albopictus*, there is an increasing risk.

Mathematical models have been developed widely to study the dynamics of transmission of mosquito-borne diseases since the pioneering works of Sir R. Ross a century ago [181]. Mathematical approaches usually focus on estimation methods for the basic reproduction number of the pandemics and their consequences for the impact of vaccination [113]. Many deterministic models were built to describe the infection dynamics with a simplifying

assumption that the transmission probability between mosquito and host was constant [16]. However, almost all diseases transmitted by *Ae. albopictus* and *Ae aegypti* like dengue, zika, and chikungunya do not have effective vaccines or antiviral drugs, so many models have been developed to study the effects of biological controls such as the SIT or the *Wolbachia*-based technique to the transmission of diseases [110, 156, 62, 22]. Modern research in this field would benefit from an expansion around the concepts of heterogeneous mosquito biting, poorly mixed mosquito-host encounters, spatial heterogeneity, and temporal variation in the transmission process [169]. This is an intense research field but the thesis does not focus on this direction.

1.3 Spatial Modeling for Biological Control of *Aedes* Mosquitoes

The simple models we have described so far have used the dynamical system approach by assuming that all individuals experience the same homogeneous environment. In practice, populations of ecological species do not remain fixed in space. Instead, the spatial distribution of a species tends to evolve and change with time. Particularly, the redistribution of population is a fundamental feature of biological invasion, especially at the stage of geographical spread. To build a mathematical model, we need to decide how we describe the movement of individuals and how we combine it with the population dynamics to construct a growth-dispersal model.

Table 1.2 – Some different spatial models in ecology and how they treat space and keep track of population dynamics

Models	**Space**			**Population dynamics**	
	Explicit		Implicit	Individual scale	Population scale
	Continuum	Discrete			
Classical metapopulation			✓		✓
Discrete diffusion		✓			✓
Ideal free distribution		✓			✓
Cellular automata		✓			✓
Reaction-diffusion	✓				✓
Integral-kernel-based	✓				✓
Individual-based	✓			✓	

There are various ways that space and the populations inhabiting it can be represented in models (see Table 1.2). Specifically, they can treat space and time as continuous or discrete, and they can describe dispersal and population dynamics as stochastic or deterministic. Some models treat space implicitly without specifying how the population is arranged in physical space. These include the MacArthur-Wilson [141] models for island biogeography and the classical metapopulation model of Levins [127] in which they described what fraction of an environment is occupied by some species. Hanski's version of metapopulation models [99] incorporated some aspects of space explicitly by considering space as a collection of patches and describing the probability that each patch is occupied. Another version of the metapopulation model that considers a patchy space but studies the population density is known as discrete diffusion or island chain model (see e.g., [4]). The disperse between patches is assumed at some rate that can be constant or density-dependent.

Models that treat space explicitly usually incorporate a map of a spatial region and provide some sort of description of what is happening at each spatial location at any given time. In addition to the models mentioned above, there are many others that consider discrete space like ideal free distribution [84] or cellular automata models [58]. Besides, a majority of spatial models treat space as a continuum such as reaction-diffusion models [50, 176]. The key idea to derive the dispersal in these models is to envision individuals dispersing via random walks, then at large spatial scales, a collection of dispersing individuals will behave analogously to a collection of particles diffusing as a Brownian motion [159, 208]. Diffusion can also be derived from Fick's law which describes the flux of a diffusing substance in terms of its gradient [159, 154], or from stochastic differential equations [86]. These models were first introduced into ecology by Skellam [189] and Kierstead and Slobodkin [117] and will be discussed in the context of the mosquito population in this thesis. It is important to note the reaction-diffusion equation ignores the long-distance dispersal since Fick's law relates the population flux to the local value of the population density gradient. When long-distance dispersal cannot be neglected, transport becomes nonlocal and Fick's law is no longer valid [165] and reaction-diffusion equations can then be replaced by integrodifferential

equations (integral-kernel based models).

The models we described so far are not explicit in the sense of keeping track of the locations of individuals as they move around in space. The models that capture the behavior of each individual are called individual-based models (see [65]). They can provide enough details of behavior and life history to make predictions of specific natural systems by computer simulations, but they seem to be too complicated to solve mathematically by existing analytical methods. Population-based models, in contrast, can be analyzed with various tools of mathematical analysis but usually only provide broad insights about general systems. Both specific prediction and general understanding are worthy goals, but it is not always feasible to achieve both with the same model.

With such a wide range of spatial models that have been developed to study ecological phenomena, how can we decide which to use in a given situation? The way we choose the type of models in this thesis is based on the biology of the mosquito population and the challenges that arise in the implementation of biological controls (see 1.2.3). *Ae. albopictus* and *Ae. aegypti* species usually breed and rest close to the habitat of their hosts and therefore do not fly long distances [29], so non-local dispersal is negligible. Moreover, the biological control agents (e.g. sterile males, *Wolbachia*-infected mosquitoes) are usually released in a single patch habitat, possibly with some internal heterogeneity, and can often be viewed as a continuum, so that it is appropriate to use **reaction-diffusion models** to describe the density of mosquito population inhabiting it. This kind of model is the heart of mathematical modeling in ecology as well as this thesis. In the present work, we also study some other spatial models with a strong connection with reaction-diffusion models. More details of the models are presented in the following.

1.3.1 Reaction-diffusion models

Models of local growth are considered in Section 1.2 and now can be coupled with the diffusion and form a reaction-diffusion model as follows

$$\begin{cases} \partial_t \mathbf{u}(t,\mathbf{x}) & = D\Delta_{\mathbf{x}}\mathbf{u} + \mathbf{f}(\mathbf{u}), \\ \mathbf{u}(t=0,\mathbf{x}) & = \mathbf{u}_0(\mathbf{x}), \end{cases} \tag{1.8}$$

where $\mathbf{x} \in \mathbb{R}^d$ is the space variable, $\mathbf{u} = (u_1, u_2, \dots u_n)$ a vector function in $\mathbb{R}^n$ that describes the density of n stages of the mosquito population ($\mathbf{u} = (E, F, M, M_s)$ in the SIT case and $\mathbf{u} = (n_i, n_u)$ in the *Wolbachia* case), and $D \in \mathcal{M}^{n\times n}$ is a non-negative diagonal matrix. The continuous function $\mathbf{f} : \mathbb{R}^n \to \mathbb{R}^n$ describes the growth of population, D is the diffusion coefficient.

In a bounded domain: To study the effect of migration of mosquitoes on a treated habitat, we consider model (1.8) in a bounded domain Ω and develop specific boundary conditions to describe the flux on the boundary. Solutions of nonlinear parabolic equations can exhibit various and sometimes complicated behavior. However, in a bounded domain and with small nonlinearities $\mathbf{f}$, the solutions of this model relax to the constant or simple steady states and we cannot expect spectacular behavior [167]. For example, with the homogeneous Dirichlet condition, $\mathbf{u} = 0$ on $\partial\Omega$, the Laplace operator has a positive dominant eigenvalue, then the solution of (1.8) converges towards a stable steady state. With the Neumann condition $\frac{\partial \mathbf{u}}{\partial \nu} = 0$, the first eigenvalue of the Laplace operator is 0 and possible long-term behavior of (1.8) is the relaxation towards a homogeneous (i.e., independent of x) solution, which is not constant in time.

In our work, we use an inhomogeneous Robin boundary condition to describe the inflow and outflow on the boundary $\partial\Omega$ (see Chapter 2)

$$\frac{\partial u_i}{\partial \nu} = -D_b(u_i - u_i^{\text{ext}}), \tag{1.9}$$

with $i = 1, 2, \dots,$ and $u_i^{\text{ext}} > 0$ is the density of stage i outside Ω, $D_b > 0$ is the migration rate on the boundary. The boundary condition (1.9) models the tendency of the population to cross the boundary, with rates proportional to the difference between the surrounding density and the density inside Ω. The model (1.8) with boundary condition (1.9) has some non-homogeneous steady state that provides insights into the study of the efficacy of the biological controls.

In the whole space: To investigate the spread of invasive waves in a wide area, we consider the reaction-diffusion model in an unbounded domain and study its traveling wave analysis. When the model has a steady state 0 which corresponds to the case the population is absent and a positive steady state $\mathbf{u}^*$, the spread of the population is described in [219, 131] and we will present the definition in the following for the sake of completeness. The population spreads at roughly the speed c^* if for any non-zero initial data $\mathbf{u}_0$ lies between 0 and $\mathbf{u}^*$ and $\mathbf{u}_0$ has a compact support, and for any positive ε, solution $\mathbf{u}$ of (1.8) satisfies that

$$\lim_{t\to+\infty} \sup_{|x|\geqslant(c^*+\varepsilon)t} |\mathbf{u}(x)| = 0, \tag{1.10}$$

and

$$\lim_{t\to+\infty}\sup_{|x|\leqslant(c^*-\varepsilon)t}|\mathbf{u}(x)-\mathbf{u}^*|=0. \tag{1.11}$$

Equation (1.10) states that if an observer were to move at a fixed speed greater than c^*, the local population density would eventually look like 0. Equation (1.11) states that if an observer were to move at a fixed speed less than c^*, the local population density would eventually look like $\mathbf{u}^*$.

Traveling waves is an interesting behavior that one can observe while working with the reaction-diffusion systems in the whole space. Recall that a traveling wave solution of (1.8) with speed $c_+ > 0$ refers to a pair (U, c_+), where $\mathbf{u}(t,x) = \mathbf{U}(x + c_+t)$ is a nontrivial and bounded solution of (1.8). We call $\mathbf{U} = (U_1, \ldots, U_n)$ the wave profile and c_+ the wave speed. We say $(\mathbf{U}, c_+)$ is a wavefront if $\mathbf{U}(\pm\infty)$ exist and $\mathbf{U}(-\infty) \neq \mathbf{U}(+\infty)$.

System (1.8) is called non-degenerate if all diagonal entries of matrix D are positive. When $\mathbf{f}$ is a monostable nonlinearity, for any wave speed c_+ larger than some minimal speed $c_{\min}$, system (1.8) admits a traveling front. The existence of the minimal wave speed and the stability of wavefronts for the non-degenerate case were presented in [214]. The author in [219] proved the existence and estimate of the spreading speed c^* for general cooperative reaction-diffusion systems. The results in [133] showed that the spreading speed c^* coincides with the minimal wave speed $c_{\min}$. In the bistable case, a complete result about the existence and stability of the unique (up to translation) wavefront when (1.8) is non-degenerate was given in [214].

While applying the reaction-diffusion model (1.8) to describe the mosquito population with $\mathbf{u} = (E, F, M)$ as in (1.1), we take into account the fact that the aquatic stage E of the population does not move. Thus, the model we obtain is partially degenerate with $D_{11} = 0, D_{ii} > 0$ with $i > 1$. The existence of wavefronts of partially degenerate systems in both monostable and bistable cases was proved in [77].

In this thesis, we design a space-dependent release function (see Chapter 3 and 4) and move it with a constant speed $c < 0$ in the opposite direction of the natural front. Thus, the nonlinearity $\mathbf{f}$ in (1.8) can be written as the form $\mathbf{f}(\mathbf{x} - ct, \mathbf{u})$. We are interested in the question of whether such a 'forced' moving nonlinearity can give rise to traveling waves with the same speed. This can be interpreted that the release strategy succeeds in reversing the propagation of the wild population.

1.3.2 Discrete diffusion models

Another issue we want to address is the inaccessibility of the target region. Due to the natural ability to move and mate with females of male mosquitoes, the SIT can reach the inaccessible area which other control methods (like insecticides) can not do. To study this phenomenon, we consider space as a combination of two patches: the directly treated zone and the unreachable zone, then use the **discrete diffusion model** to describe the population dynamics (see Chapter 5). Discrete approaches offer a better and simpler way of modeling heterogeneity (see e.g., [20, 21, 112]), especially when resources such as hosts and breeding sites are variable across regions. This kind of model was also used to study the dispersal of mosquito population in [140, 143] and references therein.

The discrete model can be obtained using a finite difference scheme of (1.8) (see [4]). For example in one-dimensional space, we can discretize a spatial domain $(0, L)$ into N intervals. Let $\sum_{j=1}^{N} l_j = L$ and denote $x_0 = 0, x_1 = l_1, x_2 = l_1 + l_2, \ldots x_N = L$. For $j = 1, 2, \ldots, N$, consider $\mathbf{v}^j(t) = \mathbf{u}(t, x_j)$ and $\mathbf{u}(x_j) = \mathbf{v}_0^j$, then the discrete approximation $\mathbf{v}^j$ satisfies

$$\begin{cases} \dot{\mathbf{v}}^j & = \mathbf{f}(\mathbf{v}^j) + D_{j,j+1}(v_{j+1} - v_j) + D_{j-1,j}(v_{j-1} - v_j), \\ \mathbf{v}^j(t=0) & = \mathbf{v}_0^j. \end{cases}$$

In more general scenarios, the discrete diffusion models are written in the form

$$\dot{\mathbf{v}}^j = \mathbf{f}(\mathbf{v}^j) + \sum_{k\neq j}(D_{k,j}\mathbf{v}_k - D_{j,k}\mathbf{v}_j), \tag{1.12}$$

with $D_{k,j} > 0$ for any $k \neq j$. The study of the discrete diffusion model for single-species populations has a long history (see [4, 202, 138]). The critical patch number such that the population persists was provided in [4, 138]. This number depends on the nonlinearity $\mathbf{f}$ and the diffusion rates $D_{j,k}$. In [202], the authors showed that if the population in each patch can survive when the patches are isolated, then the whole model remains persistent for any diffusion rates. However, there is still no general theoretical result for the multi-group system like in our case.

In our model in Chapter 5, we consider a multi-group system on each patch. While considering the release function only on one patch, we investigate the conditions in which both patches go extinct depending on the

dynamics of the population, the number of sterile males released as well as the diffusion rates.

1.3.3 Multi-scale models

The movement of each individual in the population can be described by a stochastic process, where X_t denotes its position at time t and satisfies the following stochastic differential equation

$$dX_t = \mu(X_t, t)dt + \sigma(X_t, t)dW_t, \tag{1.13}$$

where dX_t and dt can be viewed as ordinary differentials, W_t is the standard Wiener process, μ is a drift. Then the probability density $p(t, x)$ of the random variable X_t can be described by a parabolic equation called the Fokker-Planck equation [172]. In the one-dimensional case, the formulation of the equation is as below

$$\partial_t p(t, x) = -\mu(x, t)\partial_x p(t, x) + \partial_{xx}\left[\frac{\sigma^2(t, x)}{2}p(t, x)\right]. \tag{1.14}$$

We have the diffusion coefficient $D(t, x) = \dfrac{\sigma^2(x, t)}{2}$. This equation is also known as the Kolmogorov forward equation. The stochastic differential equation in (1.13) describes the movement in the individual scale, and the Fokker-Planck equation (1.14) translates it into the population scale.

Equation (1.13) is convenient to do simulation, keep tracks, and make predictions of the individual movements. While the diffusion equation (1.14) can be studied analytically to provide broad insights into general systems. Therefore, a multi-scale approach combining these two models can provide both specific predictions and a general understanding of our problem (see Chapter 6).

1.4 Contribution of the Thesis

1.4.1 Reaction-Diffusion Model with Inhomogeneous Robin Boundary Conditions

The principal motivation of this work is to study the establishment of the *Wolbachia*-carrying mosquitoes released to the control area with the presence of migration on the boundary. The biological control agents now play the role of an invasive species.

In a bounded domain Ω, we consider a reaction-diffusion model with the population dynamics as in (1.6), and develop a mixed-type boundary condition to take into account the inflow and outflow of mosquitoes on the boundary. We assume that the individuals tend to cross the boundary with a rate proportional to the difference between the surrounding density and the density just inside Ω. Denote n_i^{ext}, n_u^{ext} respectively the density surrounding the boundary $\partial\Omega$ of *Wolbachia*-infected and uninfected mosquitoes, then for some $T > 0$, and for any $t \in (0, T)$,

$$\partial_t n_i(x, t) = D\Delta_x n_i + b_i n_i\left(1 - \frac{n_i + n_u}{K}\right) - d_i n_i \qquad \text{for } x \in \Omega, \tag{1.15a}$$

$$\partial_t n_u(x, t) = D\Delta_x n_u + b_u n_u\left(1 - \frac{n_i + n_u}{K}\right)\left(1 - s_h\frac{n_i}{n_i + n_u}\right) - d_u n_u \qquad \text{for } x \in \Omega, \tag{1.15b}$$

$$n_i(0, x) = n_i^0(x), \quad n_u(0, x) = n_u^0(x) \qquad \text{for } x \in \Omega, \tag{1.15c}$$

$$\frac{\partial n_i}{\partial \nu} = -D_b(n_i - n_i^{\text{ext}}) \qquad \text{for } x \in \partial\Omega, \tag{1.15d}$$

$$\frac{\partial n_u}{\partial \nu} = -D_b(n_u - n_u^{\text{ext}}) \qquad \text{for } x \in \partial\Omega, \tag{1.15e}$$

with $D > 0$ the diffusion coefficient, $D_b > 0$ the migration rate on the boundary, and ν is the normal outward vector through x on $\partial\Omega$. By extending the result in [201], we have shown in [7] (see Appendix B) that for $\Lambda \equiv 0$, by replacing b_i by $\dfrac{b_i}{\varepsilon}$, b_u by $\dfrac{b_u}{\varepsilon}$ with some positive parameter ε, then the proportion of *Wolbachia*-infected population $p = \dfrac{n_i}{n_i + n_u}$ converges as $\varepsilon \to 0$ to the solution of

$$\partial_t p = D\Delta_x p + d_i s_h \frac{p(1 - p)(p - \theta)}{s_h p^2 - (s_f + s_h)p + 1} \qquad \text{for } x \in \Omega, \tag{1.16a}$$

$$p(0, x) = \frac{n_i^0}{n_i^0 + n_u^0} \qquad \text{for } x \in \Omega, \tag{1.16b}$$

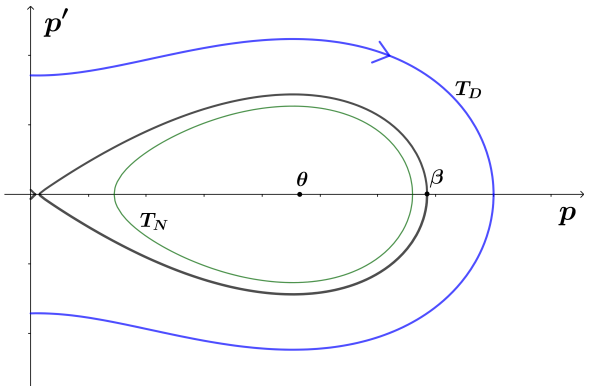

(a) Phase portrait of Dirichlet case

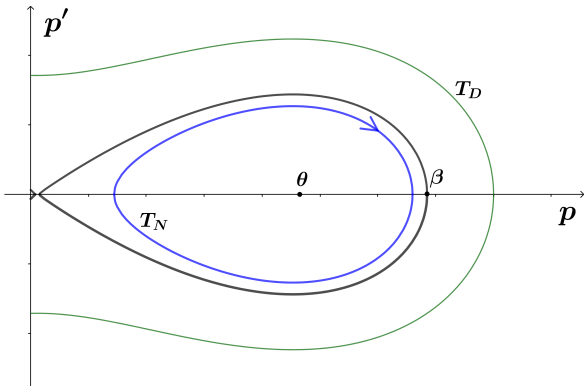

(b) Phase portrait of Neumann case

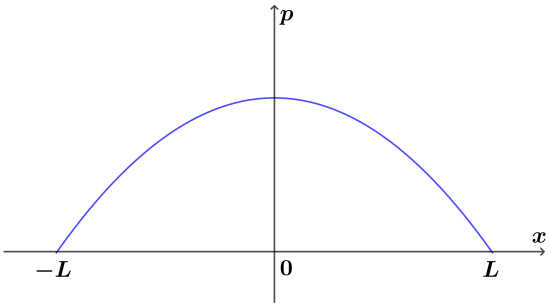

(c) Equilibrium shape in Dirichlet case

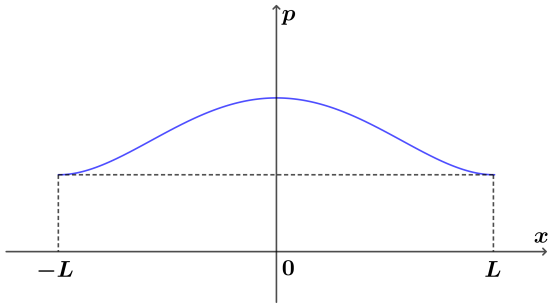

(d) Equilibrium shape of Neumann case

Figure 1.8 – Phase diagram of (1.17a) presenting the orbits and the corresponding shape of equilibria (in blue) in Dirichlet and Neumann cases

$$\frac{\partial p}{\partial \nu} = -D_b(p - p^{\text{ext}}) \qquad \text{for } x \in \partial\Omega, \tag{1.16c}$$

where

$$s_f = 1 - \frac{b_i}{b_u}, \quad \delta = \frac{d_i}{d_u}, \quad \theta = \frac{s_f + \delta - 1}{\delta s_h},$$

and $p^{\text{ext}} = \dfrac{n_i^{\text{ext}}}{n_i^{\text{ext}} + n_u^{\text{ext}}}$. The proof is based on a relative compactness argument but here, the use of the trace theorem is necessary to prove the limit on the boundary (see Appendix B). The parameter ε here charaterises the large fecundity rate of the population.

Our work in [7] (Chapter 2) discovers a slightly more general reaction term of (1.16a) where f is assumed to be cubic-like and has three roots 0, 1, and $\theta \in (0, 1)$ to consider the strong Allee effect. We consider here an idealized case of a system with one spatial dimension to gain insight into the principal features of the problem. We study the model in an interval $(-L, L)$ and normalize the diffusion coefficient $D = 1$. For the biological control to succeed, the population n_i needs to not only establish but also replace the population n_u, so we expect the solution p of (1.16) to converge to a steady state close to 1. The following stationary problem has been studied

$$-p''(x) = f(p(x)), \qquad x \in (-L, L), \tag{1.17a}$$
$$p'(L) = -D_b(p(L) - p^{\text{ext}}), \tag{1.17b}$$
$$-p'(-L) = -D_b(p(-L) - p^{\text{ext}}). \tag{1.17c}$$

By using the phase diagram of this system as well as the time mapping method, we provide the critical domain sizes such that different kinds of non-constant steady-state solutions exist. More precisely, by denoting $F(p) = \displaystyle\int_0^p f(s)ds$, the "energy" functional

$$\mathcal{E}(p, p') = \frac{(p')^2}{2} + F(p)$$

is constant along the orbit of (1.17). Moreover, it is simple to show that the solution of (1.17) can not be monotone in $(-L, L)$, so there exists at least one point $x_0 \in (-L, L)$ such that $p'(x_0) = 0$. Hence, for any $x \in (-L, L)$, one has $\mathcal{E}(p(x_0), 0) = \mathcal{E}(p(x), p'(x))$, which deduces that

$$p' = \pm\sqrt{2F(p(x_0)) - 2F(p)}.$$

Using this relation, we can draw a phase diagram for p and p'. It is classical for the case with homogeneous Dirichlet and Neumann boundary conditions that there exist some non-constant equilibria for equations when the size L is large enough (see [194]). The examples of equilibrium shapes and the corresponding orbits in these cases can be depicted in Figure 1.8. The orbits in the Dirichlet case "begin" and "end" on the axis $p = 0$ (see curve T_D in Figure 1.8a), while in the Neumann case, they end on the axis $p' = 0$ (see curve T_N Figure 1.8b).

The introduction of an inhomogeneous Robin boundary condition as in (1.17) changes the analysis of the equilibria. Their orbits do not end on the axes but on the lines, $p' = \pm D_b(p - p^{\text{ext}})$ (see Figure 2.3) and the critical domain sizes in this case depend on the migration rate D_b and the density in the boundary p^{ext}. Theorem 2.2.1 provides the critical values of L for different p^{ext} above and below the Allee effect threshold θ such that the symmetric non-contant steady-state solutions exist. These equilibria are important since their values is close to 0 or 1 which are the states that we are interested in. Theorem 2.2.2 studies the existence of other types of non-uniform equilibria. The principal eigenvalue of the Laplacian with homogeneous Robin boundary condition is used to provide some sufficient conditions for the stability of equilibria (see Theorem 2.2.3).

The main results say that there always exists a symmetric steady-state solution that is monotone on each half of the domain. For p^{ext} large, there always exists a steady-state solution that is close to 1; otherwise, it is close to 0. Besides, the larger value of L, the more steady-state solutions this problem admits. In realistic situations, the proportion p^{ext} of mosquitoes carrying Wolbachia outside the domain is usually low. Using the theoretical results proved in [7] (Chapter 2), one obtains that, to have major chances of success, one should try to treat large regions (L large), well-isolated (D_b small) and possibly applying a population replacement method in a zone outside Ω (to increase p^{ext} by reducing its denominator).

1.4.2 Reaction-Diffusion System with Forced Speed

The motivation of this part is to study the spread of the wild mosquito population in a wide area and design moving releases of sterile males for the SIT to block and reverse the natural propagation waves. We consider a released function Λ moving with a constant speed c in the opposite direction of the natural fronts. In order to gain insight into the principal features of the problem, we first study an idealized case of a system with one spatial dimension in Chapter 3. Results in a more realistic two-dimensional system will be considered in Chapter 4. We emphasize that the one-dimensional space is idealized but not completely unrealistic since it can be used to represent a long strip region in practice. In one dimension, we study the problem in the real line $\mathbb{R}$. We assume that the initial density of the wild population is compactly supported in $\mathbb{R}^-$. The natural front moves to the right with a positive speed c_+ so we move our release to the left with speed $c < 0$ (see Figure 1.9a). In the two-dimensional case, we consider a radially symmetric space, and the release is carried out in the torus $\{R_1 \leqslant |\mathbf{x}| \leqslant R_2\}$ and we keep releasing a small amount of sterile mosquitoes in the ball $\{|\mathbf{x}| < R_1\}$ (see Figure 1.9b).

To study the population dynamics under control, we consider a partially degenerate reaction-diffusion system in which the aquatic stage is assumed to be immobile. Both monostable and bistable cases are considered with Γ defined in (1.2)

$$\partial_t E = bF\left(1 - \frac{E}{K}\right) - (\nu_E + \mu_E)E, \tag{1.18a}$$

$$\partial_t F - D\Delta F = \rho\nu_E E\frac{M}{M + \gamma_s M_s}\Gamma(M + \gamma_s M_s) - \mu_F F, \tag{1.18b}$$

$$\partial_t M - D\Delta M = (1 - \rho)\nu_E E - \mu_M M, \tag{1.18c}$$

$$\partial_t M_s - D\Delta M_s = \Lambda(t, x) - \mu_s M_s, \tag{1.18d}$$

$$(E, F, M, M_s)(t = 0, \cdot) = (E^0, F^0, M^0, M_s^0). \tag{1.18e}$$

The moving releases are described in model (1.18) by taking $\Lambda(t, x) = \phi(x - ct)$ with c the speed of the release. We study in Chapter 3 and 4 the existence of solution of (1.18) spreading with the same forced speed c. Existing results on reaction-diffusion models with forced speed are mostly based on the study of the generalized principal eigenvalue of an associated operator (see e.g., [35, 36, 33, 34, 42]) of the scalar model. The generalization of this approach to a partially degenerate system like (1.18) remains challenging. In this thesis, our proof relies on the comparison principle for system (1.18) and the sophisticated construction of a super-solution that converges to

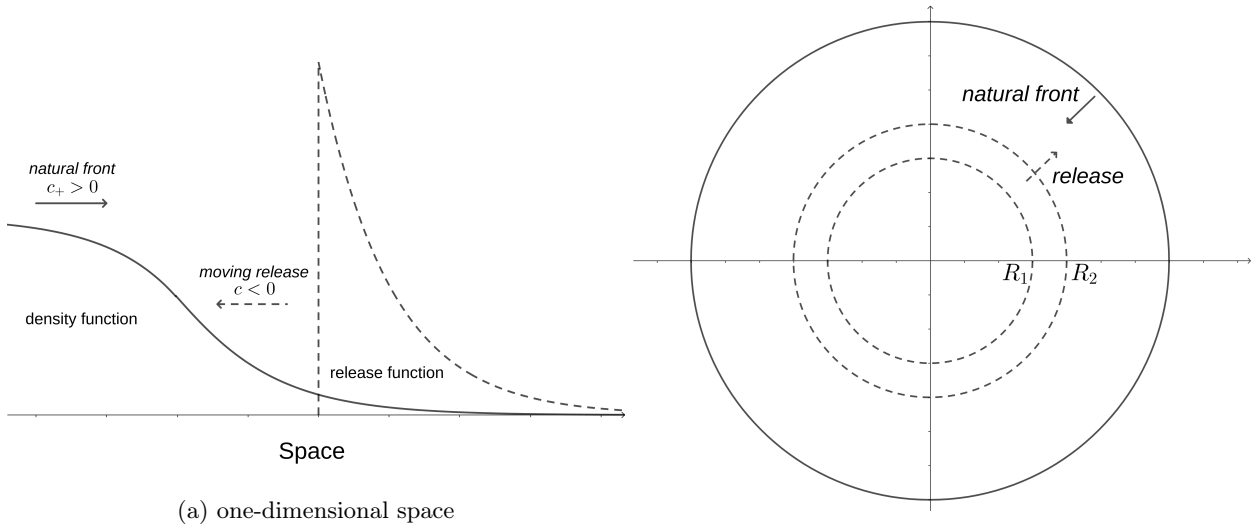

(a) one-dimensional space

(b) two-dimensional space

Figure 1.9 – Sketch of release strategies in one- and two-dimensional space. The release function is moved with a constant speed in the opposite direction of the natural front.

zero in the set $\{|x| \leqslant (c-\varepsilon)t\}$ and a sub-solution that goes to (E^*, F^*, M^*) in the set $\{|x| \geqslant (c+\varepsilon)t\}$.

One-dimensional space

As mentioned in the previous section, many works in the literature consider the case in which there is a strong Allee effect on the wild population so it is sufficient to apply the SIT in a bounded interval to block the propagation [15] and reverse it by moving the release [12]. In practice, the assumption of strong Allee effect may not be validated. The dynamics without control of the wild population can be described by the following system

$$\partial_t E = bF\left(1 - \frac{E}{K}\right) - (\nu_E + \mu_E)E, \tag{1.19a}$$

$$\partial_t F - D\partial_{xx} F = \rho\nu_E E - \mu_F F, \tag{1.19b}$$

$$\partial_t M - D\partial_{xx} M = (1-\rho)\nu_E E - \mu_M M, \tag{1.19c}$$

In this work, we consider the monostable case in which ($\Gamma(M) \equiv 1$). The bistable case was well-studied in the literature (see e.g., [15, 12]). By applying the linear determinacy in [219], we show in Appendix C that with only a few females at the initial time, invasion still occurs. More precisely, there exists a minimal speed $c^* > 0$ such that system (1.19) has a non-increasing wavefront $\mathbf{U}(x - c_+ t)$ connecting the positive equilibrium (E^*, F^*, M^*) and the zero equilibrium $(0, 0, 0)$ if and only if $c_+ \geqslant c^*$. And c^* is also the spreading speed of the solution of (1.19).

Also due to the monostable properties, the arrival of only a few individuals in the controlled zone can lead to reinvasion. In this thesis, we introduce a release strategy to deal with this difficulty and present it in model (1.18) as follows

$$\Lambda(t,x) = \begin{cases} 0 & \text{for } x - ct \leqslant 0, \\ Ae^{-\eta(x-ct)} & \text{for } x - ct > 0, \end{cases} \tag{1.20}$$

with constants $A > 0$, $\eta > 0$ and speed $c < 0$.

The release function shown in (1.20) means that we need to release a large amount of sterile males near the natural front and keep releasing a small amount behind it to avoid the reinvasion in the treated zone (see Figure 1.9a). Our results in Chapter 3 show that if the initial data is compactly supported in $\mathbb{R}_-$ and below (E^*, F^*, M^*), with constant $A > 0$ large enough and $\eta > 0$ small enough, the invasion does not occur: the equilibrium $(0, 0, 0)$ invades the positive equilibrium (E^*, F^*, M^*) (see Theorem 3.1.1). We can also construct a traveling front connecting these two equilibria of the wild population and moving with the same speed of the release Λ (see Theorem 3.1.2). We emphasize that (E^*, F^*, M^*) is the positive steady state of the wild population in system (1.19) without releasing sterile males. It is natural to expect that in the area where sterile males are not released ($\Lambda = 0$), the density of the wild population still converges to this state. However, our main model (1.18) also takes into account the diffusion of sterile male population M_s in (1.18d), which means that

the number of sterile males in the non-release area can be positive due to this diffusion. This raises a technical difficulty in constructing a sub-solution that connects $(0,0,0)$ and (E^*,F^*,M^*). A method of perturbation is developed to tackle this issue.

Two-dimensional space

In a more realistic scenario, we consider model (1.18) in $\mathbb{R}^2$ and assume the space to be radially symmetric (see Figure 1.9b). It becomes challenging to extend the results to two-dimensional space since the analysis of the system changes due to the emergence of the drift term in the equation of variable $r=|\mathbf{x}|$. Existing results in the two-dimensional case (see e.g. [68, 175]) indicate that the solution of the system without control still converges to the traveling front of 1D equation $\partial_t \mathbf{u} = \partial_{rr}\mathbf{u} + \mathbf{f}(\mathbf{u})$ with a logarithmic delay in time coming from the drift.

In Chapter 4, for any speed $c>0$, we consider the release function as follows

- In the bistable case, for some $\overline{\Lambda}>0$

$$\Lambda(t,\mathbf{x}) = \begin{cases} \overline{\Lambda} & \text{for } R_1+ct \leqslant |\mathbf{x}| \leqslant R_2+ct \\ 0 & \text{otherwises .} \end{cases} \tag{1.21}$$

- In the monostable case, for some $\eta>0$

$$\Lambda(t,\mathbf{x}) = \begin{cases} \overline{\Lambda} e^{\eta(|x|-(R_1+ct))} & \text{for } |x| \leqslant R_1+ct, \\ \overline{\Lambda} & \text{for } R_1+ct \leqslant |\mathbf{x}| \leqslant R_2+ct, \\ 0 & \text{otherwises .} \end{cases} \tag{1.22}$$

In order to reverse the natural propagation, we need the initial to be well-prepared, that is, we have already eradicated mosquitoes in a set with positive measures, e.g. a ball. This assumption is natural since we need to ensure the elimination in a smaller area before extending to the larger region. With such assumptions, again we can show in Chapter 4 that for $\overline{\Lambda}>0$ large enough and $\eta>0$ small enough, we succeed in reversing the invasion (see Theorem 4.1.1). We generalize the construction of super- and sub-solutions in the one-dimensional case to two dimensions. The key idea is to divide properly the space into different zones and design the super-solution by parts to guarantee the convergence to zero in the set $\{|x| \leqslant (c-\varepsilon)t\}$.

1.4.3 Global Extinction of a Two-patch Model with Control in One Patch

The motivation of this work is to study the efficacy of the SIT in the presence of inaccessible areas, such as crab burrows in which mosquito oviposition takes place. We consider a two-patch model with the growth of population in each patch described by a dynamical system like (1.4) in the monostable case and two patches are connected by the discrete diffusion.

$$\dot{E}_1 = bF_1\left(1-\frac{E_1}{K_1}\right) - (\nu_E+\mu_E)E_1, \tag{1.23a}$$

$$\dot{F}_1 = \rho\nu_E E_1 \frac{M_1}{M_1+\gamma_s M_1^s} - \mu_F F_1 - d_{12}F_1 + d_{21}F_2, \tag{1.23b}$$

$$\dot{M}_1 = (1-\rho)\nu_E E_1 - \mu_M M_1 - \beta d_{12}M_1 + \beta d_{21}M_2, \tag{1.23c}$$

$$\dot{M}_1^s = \Lambda - \mu_s M_1^s - \alpha d_{12}M_1^s + \alpha d_{21}M_2^s, \tag{1.23d}$$

$$\dot{E}_2 = bF_2\left(1-\frac{E_2}{K_2}\right) - (\nu_E+\mu_E)E_2, \tag{1.23e}$$

$$\dot{F}_2 = \rho\nu_E E_2 \frac{M_2}{M_2+\gamma_s M_2^s} - \mu_F F_2 - d_{21}F_2 + d_{12}F_1, \tag{1.23f}$$

$$\dot{M}_2 = (1-\rho)\nu_E E_2 - \mu_M M_2 - \beta d_{21}M_2 + \beta d_{12}M_1, \tag{1.23g}$$

$$\dot{M}_2^s = -\mu_s M_2^s - \alpha d_{21}M_2^s + \alpha d_{12}M_1^s. \tag{1.23h}$$

In this model, system (1.23a) - (1.23d) describes the dynamics of the controlled zone, and system (1.23e) - (1.23h) describes the dynamics of the inaccessible area. The release function Λ is only included in (1.23d) for the first patch, and the sterile males move naturally to the second patch. We consider d_{ij} the diffusion rate of the females from patch i to move to patch j $(i,j=1,2,\ i\neq j)$. While the fertile males and sterile males move slower but with proportional rates respectively βd_{ij} and αd_{ij}, where typically $0<\alpha<\beta<1$ in practice.

The question we want to solve is whether the release in one patch can succeed in driving the whole system to elimination, and how the diffusion rates and other parameters influence the result. As mentioned in Section 1.2.3, without the diffusion between patches, with the release of a sufficiently large number of sterile males, the extinction equilibrium is unique and globally asymptotically stable (GAS) (see Figure 1.6b). In Chapter 5, we investigate the same behavior for the model (1.23). The main idea is to set the proportion $\frac{M_i}{M_i + \gamma_s M_i^s}$ with $i = 1, 2$ lower than a certain level so that the new basic offspring number of system (1.23) is smaller than 1. Then, we shape the release function such that the previous setting is valid. Two release strategies have been studied in Chapter 5

- Constant release $\Lambda(t) \equiv \Lambda > 0$ per time unit.
- Impulsive periodic release with period $\tau > 0$ by taking $\Lambda(t) = \sum_{k=0}^{+\infty} \tau \Lambda^{\text{per}} \delta_{k\tau}$.

In Theorem 5.4.1, we prove the existence of a critical value $\overline{\Lambda}$ such that if $\Lambda > \overline{\Lambda}$, the zero equilibrium is GAS. We also provide an upper bound for $\overline{\Lambda}$ which depends on the diffusion rates and the biological parameters. The value of $\overline{\Lambda}$ is shown in Theorem 5.5.2 to be monotone with respect to these biological parameters. The results indicate that if the diffusion rate is large, the system requires a lower number of sterile males to reach elimination. The proofs are based on the comparison principle for system (1.23).

1.4.4 Parameter Estimation with A Mechanistic-Statistical Approach

In this part, we work with the data from the mark-release-recapture (MRR) experiments of *Aedes aegypti* mosquitoes carried out in La Havana city in Cuba. The MRR experiments consist of the release of marked (usually with colored powder) adults (or even pupae) from the lab into the field, with a trapping network around the release locations. The data obtained is the number of individuals being trapped at different positions and times. MRR experiments are carried out while applying the rear and release techniques in order to keep track of the released individuals and test their fitness under field conditions. We are interested in estimating of parameters that can provide useful insight to improve the release protocols. The set of parameters we want to infer, denote Θ, consists of several constants or functions such as the diffusion coefficient, the survival rates, and the recapture rates in the MRR experiments.

The spread of individuals in the experiments can be governed by the reaction-diffusion equations as in (1.8). The parameters listed above can be incorporated into the model to describe the population dynamics. However, in practice, one can rarely observe the density $\mathbf{u}$. The observation process is usually stochastic and implies a loss of information such as spatial or temporal censorship, and measurement uncertainty. The combination between the mechanistic vision of the PDE-based model and the statistical vision of the data can be made with the mechanistic-statistical approach (see e.g., [196, 197, 177, 178]).

Our general strategy of the mechanistic-statistical approach is as follows. Let $\mathbf{u}(t, \mathbf{x})$ be the population density described by a reaction-diffusion model. We know that the experiments were carried out in N days and there are P traps set up around the release point, with N_0 mosquitoes released at once. Denote the observed variable Y_{ij} the number of individuals captured in the trap i, on day j, with $i = 1, 2, \dots P,\ j = 1, 2, \dots, N$. This variable is a function of the density $\mathbf{u}$, say $Y_{ij}(\mathbf{u})$. Each time the variable Y_{ij} is observed, a number $\widetilde{Y}_{ij}$ is reported. This number is assumed to follow independent Poisson distributions with mean values Y_{ij}, since it can be viewed as the sum of N_0 independent Bernoulli trials with N_0 very large. Then, we have

$$\widetilde{Y}_{ij} | \Theta \sim \text{Poisson}[Y_{ij}(\mathbf{u})].$$

From this model of observation process, one can compute a likelihood function according to the parameter set Θ. Note that, for a given value of the parameter set, the reaction-diffusion model with a given initial condition admits a unique solution $\mathbf{u}$. This solution may not be computed explicitly but we can approximate it numerically. The parameter estimation then can be carried out using the maximum likelihood estimator (MLE) or the posterior distribution using the Bayesian statistics (see Chapter 6).

Another contribution of our work in Chapter 6 is to provide insights at the individual scale from data at the population scale. In order to do that, we describe the dynamics of individuals by a stochastic process as in (1.13) together with some random variables. We derive a reaction-diffusion equation for the probability density function corresponding to the stochastic process as in 1.3.3. Due to this strong connection between the two models, we can use the individual-based model to generate simulated data to validate our method of parameter estimation, and on the one hand, we can use the parameters obtained from the population-based model to unveil the dynamics of individuals.

Finally, we can apply the parameters estimated in our models to provide a numerical simulation of mosquito dynamics that can not be observed by the data. This is one of the most important advantages that mathematical modeling offers to the study of ecological problems.

Part I

Reaction-diffusion models

Chapter 2

Steady-state solutions for a reaction-diffusion equation with Robin boundary conditions: Application to the control of dengue vectors.

This chapter is a joint work with Luis Almeida, Pierre-Alexandre Bliman, and Nicolas Vauchelet. It was published as an article in European Journal of Applied Mathematics [7].

Abstract. In this work, we investigate an initial-boundary-value problem of a reaction-diffusion equation in a bounded domain with a Robin boundary condition and introduce some particular parameters to consider the non-zero flux on the boundary. This problem arises in the study of mosquito populations under the intervention of the population replacement method, where the boundary condition takes into account the inflow and outflow of individuals through the boundary. Using phase-plane analysis, the present paper studies the existence and properties of non-constant steady-state solutions depending on several parameters. Then, we prove some sufficient conditions for their stability. We show that the long-time efficiency of this control method depends strongly on the size of the treated zone and the migration rate. To illustrate these theoretical results, we provide some numerical simulations in the framework of mosquito population control.

2.1 Introduction

The study of scalar reaction-diffusion equations $\partial_t p - \Delta p = f(p)$ with a given nonlinearity f has a long history. For suitable choices of f, this equation can be used to model some phenomena in biology such as population dynamics (see e.g. [82], [155], [192]). To investigate the structure of the steady-state solutions, the semilinear elliptic equation $\Delta p + f(p) = 0$ has been studied extensively.

Many results about the multiplicity of positive solutions for the parametrized version $\Delta p + \lambda f(p) = 0$ in a bounded domain are known. Here, λ is a positive parameter. Various works investigated the number of solutions and the global bifurcation diagrams of this equation according to different classes of the nonlinearity f and boundary conditions. For Dirichlet problems, in [135], Lions used many "bifurcation diagrams" to describe the solution set of this equation with several kinds of nonlinearities f, and gave nearly optimal multiplicity results in each case. The exact number of solutions and the precise bifurcation diagrams with cubic-like nonlinearities f were given in the works of Korman *et. al.* [123], [122], Ouyang and Shi [163] and references therein. In these works, the authors developed a global bifurcation approach to obtain the exact multiplicity of positive solutions. In the case of one-dimensional space with a two-point boundary, Korman gave a survey of this approach in [120]. Another approach was given by Smoller and Wasserman in [193] using phase-plane analysis and the time mapping method. This method was completed and applied in the works of Wang [215], [216]. While the bifurcation approach is convenient to solve the problem with more general cubic nonlinearities f, the phase-plane method is more intuitive and easier to compute.

Although many results were obtained concerning the number of solutions for Dirichlet problems, relatively little seems to be known concerning the results for other kinds of boundary conditions. For the Neumann problem, the works of Smoller and Wasserman [193], Schaaf [184], and Korman [121] dealt with cubic-like nonlinearities f in one dimension. Recently, more works have been done for Robin boundary conditions (see e.g. [63], [186], [227]), Neumann-Robin boundary conditions (see e.g. [207]), or even nonlinear boundary conditions (see e.g. [94], [95]

and references therein). However, those works only focused on other types of nonlinearities such as positive or monotone f. An analogous problem with advection term was studied in [218], [217] for cubic-like nonlinearities, but in these works, they used a homogeneous non-symmetric Robin boundary condition to characterize the open or closed environment boundary. To the best of our knowledge, the study of inhomogeneous symmetric Robin problems with cubic-like nonlinearities remains quite open.

In this paper, we study the steady-state solutions with values in $[0, 1]$ of a reaction-diffusion equation in one dimension with inhomogeneous Robin boundary conditions

$$\partial_t p^0 - \partial_{xx} p^0 = f(p^0), \qquad (t, x) \in (0, T) \times \Omega, \tag{2.1a}$$

$$\frac{\partial p^0}{\partial \nu} = -D_b(p^0 - p^{\text{ext}}), \qquad (t, x) \in (0, T) \times \partial\Omega, \tag{2.1b}$$

$$p^0(0, x) = p^{\text{init}}(x), \qquad x \in \Omega, \tag{2.1c}$$

where $\Omega = (-L, L)$ is a bounded domain in $\mathbb{R}$, time $T > 0$. The steady-state solutions satisfy the following elliptic boundary-value problem,

$$-p''(x) = f(p(x)), \qquad x \in (-L, L), \tag{2.2a}$$

$$p'(L) = -D_b(p(L) - p^{\text{ext}}), \tag{2.2b}$$

$$-p'(-L) = -D_b(p(-L) - p^{\text{ext}}), \tag{2.2c}$$

where $L > 0$, $D_b > 0$, $p^{\text{ext}} \in (0, 1)$ are constants. The reaction term $f : [0, 1] \to \mathbb{R}$ is of class $\mathcal{C}^1$, with three roots $\{0, \theta, 1\}$ where $0 < \theta < 1$ (see Figure 2.1a). The dynamics of (2.1) can be determined by the structure of steady-state solutions which satisfy (2.2). Note that, by changing variable from x to $y = x/L$, then (2.2) becomes $p''(y) + L^2 f(p(y)) = 0$ on $(-1, 1)$ with parameter L^2. Thus, we study problem (2.2) with three parameters $L > 0, D_b > 0$, and $p^{\text{ext}} \in (0, 1)$.

The Robin boundary condition considered in (2.1) and (2.2) means that the flow across the boundary points is proportional to the difference between the surrounding density and the density just inside the interval. Here we assume that p^{ext} does not depend on space variable x nor time variable t.

The existence of classical solutions for such problems was studied widely in the theory of elliptic and parabolic differential equations (see, for example, [164]). In our problem, due to difficulties caused by the inhomogeneous Robin boundary condition and the variety of parameters, we cannot obtain the exact multiplicity of solutions. However, our main results in Theorems 2.2.1 and 2.2.2 show how the existence of solutions and their "shapes" depend on parameters D_b, p^{ext} and L. The idea of phase plane analysis and time-map method as in [193] are extended to prove these results.

Since the solutions of (2.2) are equilibria of (2.1), their stability and instability are the next problems that we want to investigate. The stability analysis of the non-constant steady-state solutions is a delicate problem especially when the system under consideration has multiple steady-state solutions. In Theorem 2.2.3, we use the principle of linearized stability to give some sufficient conditions for stability. Finally, as a consequence of these theorems, we obtain Corollary 2.2.1 which provides a comprehensive result about existence and stability of the steady-state solutions when the size L is small.

The main biological application of our results is the control of dengue vectors. *Aedes* mosquitoes are vectors of many vector-borne diseases, including dengue. Recently, a biological control method using an endosymbiotic bacterium called *Wolbachia* has gathered a lot of attention. *Wolbachia* helps reduce the vectorial capacity of mosquitoes and can be passed to the next generation. Massive release of mosquitoes carrying this bacterium in the field is thus considered as a possible method to replace wild mosquitoes and prevent dengue epidemics. Reaction-diffusion equations have been used in previous works to model this replacement strategy (see [26, 53, 201]). In this work, we introduce the Robin boundary condition to describe the migration of mosquitoes through the boundary. Since inflows of wild mosquitoes and outflows of mosquitoes carrying *Wolbachia* may affect the efficiency of the method, the study of existence and stability of steady-state solutions depending on parameters D, p^{ext} and L as in (2.2), (2.1) will provide necessary information to maintain the success of the control method using *Wolbachia* under the effects of migration.

Problem (2.1) arises often in the study of population dynamics. p^0 is usually considered as the relative proportion of one population when there are two populations in competition. This is why, we only focus on solutions with values that belong to the interval $[0, 1]$. Problem (2.1) is derived from the idea in paper [201], where the authors reduce a reaction-diffusion system modeling the competition between two populations n_1 and n_2 to a scalar equation on the proportion $p = \frac{n_1}{n_1+n_2}$. More precisely, they consider two populations with a very high fecundity rate scaled by a parameter $\epsilon > 0$ and propose the following system depending on ϵ for

$t > 0, x \in \mathbb{R}^d$,

$$\partial_t n_1^\epsilon - \Delta n_1^\epsilon = n_1^\epsilon f_1(n_1^\epsilon, n_2^\epsilon), \tag{2.3a}$$
$$\partial_t n_2^\epsilon - \Delta n_2^\epsilon = n_2^\epsilon f_2(n_1^\epsilon, n_2^\epsilon). \tag{2.3b}$$

The authors obtained that under some appropriate conditions, the proportion $p^\epsilon = \frac{n_1^\epsilon}{n_1^\epsilon + n_2^\epsilon}$ converges strongly in $L^2(0,T;L^2(\mathbb{R}^d))$, and weakly in $L^2(0,T;H^1(\mathbb{R}^d))$ to the solution p^0 of the scalar reaction-diffusion equation $\partial_t p^0 - \Delta p^0 = f(p^0)$ when $\epsilon \to 0$, where f can be given explicitly from f_1, f_2. Now, in order to describe and study the migration phenomenon, we aim here to consider system (2.3) in a bounded domain Ω and introduce the boundary conditions to characterize the inflow and outflow of individuals as follows

$$\frac{\partial n_1^\epsilon}{\partial \nu} = -D_b(n_1^\epsilon - n_1^{\text{ext},\epsilon}), \qquad (t,x) \in (0,T) \times \partial\Omega, \tag{2.4a}$$
$$\frac{\partial n_2^\epsilon}{\partial \nu} = -D_b(n_2^\epsilon - n_2^{\text{ext},\epsilon}), \qquad (t,x) \in (0,T) \times \partial\Omega, \tag{2.4b}$$

where $n_1^{\text{ext},\epsilon}, n_2^{\text{ext},\epsilon}$ depend on ϵ but do not depend on time t and position x. (2.4) models the tendency of the population to cross the boundary, with rates proportional to the difference between the surrounding density and the density just inside Ω. Reusing the idea in [201], we prove in Appendix B that the proportion $p^\epsilon = \frac{n_1^\epsilon}{n_1^\epsilon + n_2^\epsilon}$ converges on any bounded time-domain to the solution of (2.1) when ϵ goes to zero. Hence, we can reduce the system (2.3), (2.4) to a simpler setting as in (2.1). The proof is based on a relative compactness argument that was also used in previous works about singular limits (e.g. [201, 106, 107]), but here, the use of the trace theorem is necessary to prove the limit on the boundary.

The outline of this work is the following. In the next section, we present the setting of the problem and the main results. In Section 2.3, we provide detailed proof of these results. Section 2.4 is devoted to an application to the biological control of mosquitoes. We also present numerical simulations to illustrate the theoretical results we obtained. Appendix B is devoted to proving the asymptotic limit of a 2-by-2 reaction-diffusion system when the reaction rate goes to infinity. Finally, we end this article with a conclusion and perspectives section.

2.2 Results on the steady-state solutions

2.2.1 Setting of the problem

In one-dimensional space, consider the system (2.1) in a bounded domain $\Omega = (-L, L) \subset \mathbb{R}$. Let $D_b > 0$, $p^{\text{ext}} \in (0,1)$ be some constant an $p^{\text{init}}(x) \in [0,1]$ for all $x \in (-L,L)$. The reaction term f satisfies the following assumptions

Assumption 2.2.1 (bistability)**.** *Function $f : [0,1] \to \mathbb{R}$ is of class $\mathcal{C}^1([0,1])$ and $f(0) = f(\theta) = f(1) = 0$ with $\theta \in (0,1)$, $f(q) < 0$ for all $q \in (0,\theta)$, and $f(q) > 0$ for all $q \in (\theta,1)$. Moreover, $\int_0^1 f(s)ds > 0$.*

Assumption 2.2.2 (convexity)**.** *There exist $\alpha_1 \in (0,\theta)$ and $\alpha_2 \in (\theta,1)$ such that $f'(\alpha_1) = f'(\alpha_2) = 0$, $f'(q) < 0$ for any $q \in [0,\alpha_1) \cup (\alpha_2, 1]$, and $f'(q) > 0$ for $q \in (\alpha_1, \alpha_2)$. Moreover, f is convex on $(0,\alpha_1)$ and concave on $(\alpha_2, 1)$.*

A function f satisfying Assumptions 2.2.1 and 2.2.2 is illustrated in Figure 2.1a.

Remark 2.2.1.

1. *Due to Assumption 2.2.1 and the fact that $p^{\text{ext}} \in (0,1), p^{\text{init}}(x) \in [0,1]$ for any x, one has that 0 and 1 are respectively sub- and super-solution of problem (2.1). Since f is Lipschitz continuous on $(0,1)$ then by Theorem 4.1, Section 2.4 in [164], we obtain that problem (2.1) has a unique solution p^0 that is in $\mathcal{C}^{1,2}((0,T] \times \Omega)$ with $0 \leqslant p^0(t,x) \leqslant 1$ for all $x \in (-L,L), t > 0$.*

2. *Again by Assumption 2.2.1, 0 and 1 are respectively sub- and super-solutions of (2.2). For fixed values of D_b, p^{ext} and L, we use the same method as in [164] to obtain that there exists a $\mathcal{C}^2$ solution of (2.2) with values in $[0,1]$. However, Assumption 2.2.1 and 2.2.2 on f are not enough to conclude the uniqueness of the solution. In the following section, we prove that the stationary problem (2.2) may have multiple solutions and their existence depends on the values of the parameters.*

The following proposition shows that solutions of system (2.2) always have at least one extreme value in $(-L, L)$.

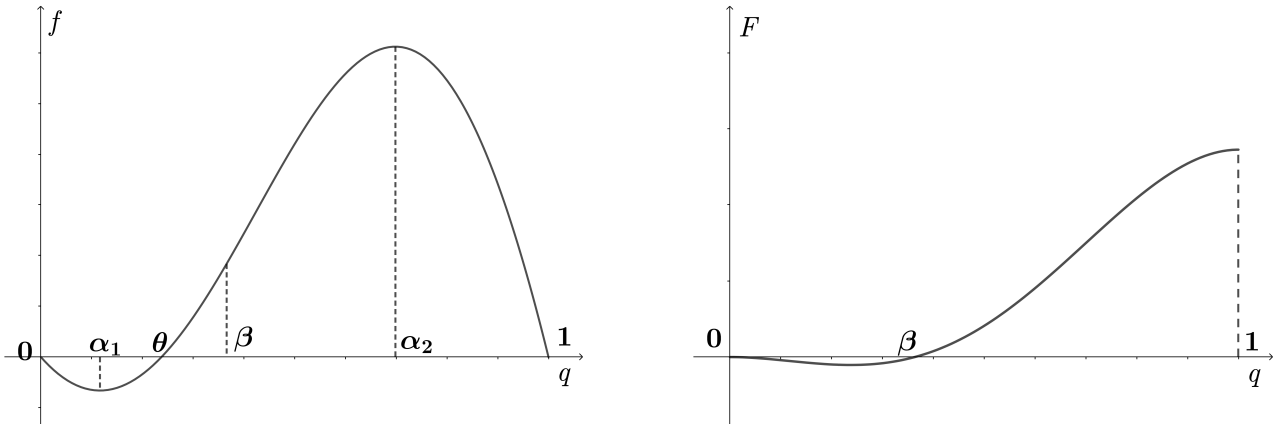

(a) $f(q)$ (b) $F(q)$

Figure 2.1 – Sketch of the functions f and F

Proposition 2.2.1. *For any $p^{\text{ext}} \in (0,1)$ and $p^{\text{ext}} \neq \theta$, system (2.2) does not have any non-constant monotone solution on the whole interval $(-L, L)$.*

Proof. Assume that (2.2) admits an increasing solution p on $(-L, L)$ (the case when p is decreasing on $(-L, L)$ is analogous). Thus, we have $p'(x) \geqslant 0$ for all $x \in [-L, L]$ and $p(L) > p(-L)$. So thanks to the boundary condition of (2.2), one has

$$D_b p^{\text{ext}} = p'(L) + D_b p(L) \geqslant D_b p(L) > D_b p(-L) \geqslant -p'(-L) + D_b p(-L) = D_b p^{\text{ext}},$$

which is impossible. Therefore, we can deduce that the solutions of system (2.2) always admit at least one local extremum on the open interval $(-L, L)$. □

To study system (2.2), we define function F (see Figure 2.1b) as below

$$F(q) = \int_0^q f(s)ds, \tag{2.5}$$

then $F'(q) = f(q)$ and $F(0) = 0$. From Assumption 2.2.1, F reaches the minimal value at $q = \theta$ and the (locally) maximal values at $q = 0$ and $q = 1$. Since $\displaystyle\int_0^1 f(s)ds > 0$, then $F(1) > F(0)$, it implies that $F(1) = \max_{[0,1]} F$; $F(\theta) = \min_{[0,1]} F$. Moreover, since $F(\theta) < F(0)$ and function F is monotone in $(\theta, 1)$ ($F'(q) = f(q) > 0$ for any $q \in (\theta, 1)$). Thus, there exists a unique value $\beta \in (\theta, 1)$ such that

$$F(\beta) = F(0) = 0. \tag{2.6}$$

The main results of the present work concern the existence and stability of steady-state solutions of (2.1), i.e. solutions of (2.2).

2.2.2 Existence of steady-state solutions

In our result, we first focus on two types of steady-state solutions defined as follows

Definition 2.2.1. *Consider a steady-state solution $p(x)$,*

p is called a symmetric-decreasing (SD) solution when p is symmetric on $(-L, L)$ with values in $[0, 1]$, decreasing on $(0, L)$ and $p'(0) = 0$ (see Figure 2.2a).

Similarly, p is called a symmetric-increasing (SI) solution when p is symmetric on $(-L, L)$ with values in $[0, 1]$, increasing on $(0, L)$ and $p'(0) = 0$ (see Figure 2.2b).

Any solution which is either (SD) or (SI) is called a symmetric-monotone (SM) solution.

The following theorems present the main result of the existence of (SM) solutions depending upon the parameters. For each value of $p^{\text{ext}} \in (0, 1)$ and $D > 0$, we find the critical values of L such that (2.2) admits solutions.

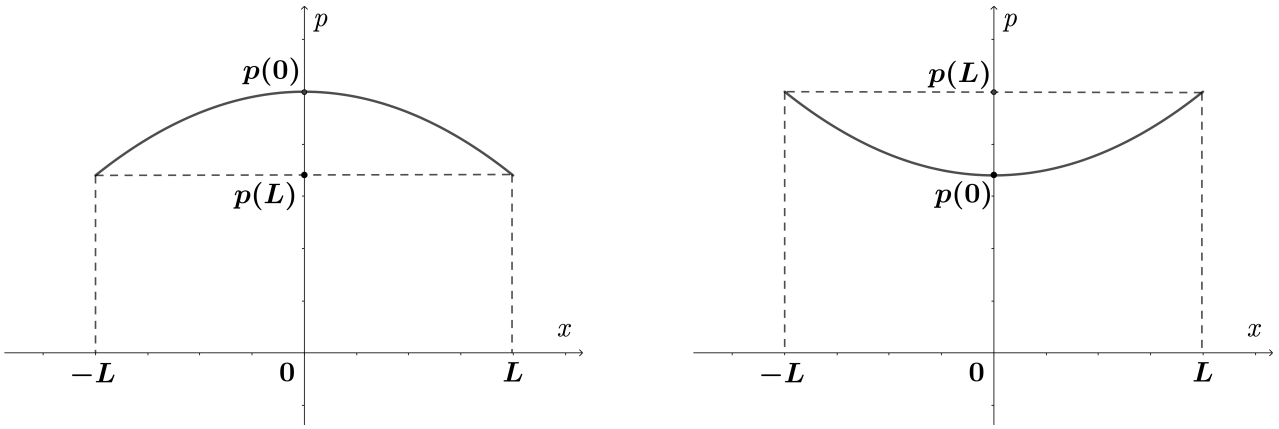

(a) (SD): p is decreasing on $(0, L)$ (b) (SI): p is increasing on $(0, L)$

Figure 2.2 – Sketch of the symmetric steady-state solutions p

Theorem 2.2.1. *In a bounded domain $\Omega = (-L, L) \subset \mathbb{R}$, consider the stationary problem (2.2). Assume that the reaction term f satisfies Assumptions 2.2.1 and 2.2.2. Then, there exist two functions*

$$\begin{array}{rccl} M_d, M_i: & (0,1)\times(0,+\infty) & \longrightarrow & [0,+\infty], \\ & (p^{\text{ext}}, D_b) & \longmapsto & M_d(p^{\text{ext}}, D_b), M_i(p^{\text{ext}}, D_b), \end{array} \tag{2.7}$$

such that for any $p^{\text{ext}} \in (0,1), D_b > 0$, problem (2.2) admits at least one (SD) solution (resp., (SI) solution) if and only if $L > M_d(p^{\text{ext}}, D_b)$ (resp., $L > M_i(p^{\text{ext}}, D_b)$) and the values of these solutions are in $[p^{\text{ext}}, 1]$ (resp., $[0, p^{\text{ext}}]$). More precisely,

1. *If $0 < p^{\text{ext}} < \theta$, then for any $D_b > 0$, $M_i(p^{\text{ext}}, D_b) = 0$ and $M_d(p^{\text{ext}}, D_b) \in (0, +\infty)$.*
   Moreover, if $p^{\text{ext}} \leqslant \alpha_1$, the (SI) solution is unique.
2. *If $\theta < p^{\text{ext}} < 1$, then for any $D_b > 0$, $M_d(p^{\text{ext}}, D_b) = 0$. If $\alpha_2 \leqslant p^{\text{ext}}$, the (SD) solution is unique. Moreover, consider β as in (2.6),*
   - *if $p^{\text{ext}} \leqslant \beta$, then $M_i(p^{\text{ext}}, D_b) \in (0, +\infty)$ for any $D_b > 0$;*
   - *if $p^{\text{ext}} > \beta$, then there exists a constant $D_* > 0$ such that $M_i(p^{\text{ext}}, D_b) \in (0, +\infty)$ for any $D_b < D_*$, and $M_i(p^{\text{ext}}, D_b) = +\infty$ for $D_b \geqslant D_*$.*
3. *If $p^{\text{ext}} = \theta$, then $M_d(\theta, D_b) = M_i(\theta, D_b) = 0$. Moreover, there exists a constant solution $p \equiv \theta$.*

In the statement of the above result, $M_i = 0$ means that for any $L > 0$, (2.2) always admits (SI) solutions. $M_i = +\infty$ means that there is no (SI) solution even when L is large. The same interpretation applies for M_d.

Besides, problem (2.2) can also admit solutions that are neither (SD) nor (SI). The following theorem provides an existence result for those solutions.

Theorem 2.2.2. *In a bounded domain $\Omega = (-L, L) \subset \mathbb{R}$, consider the stationary problem (2.2). Assume that the reaction term f satisfies Assumption 2.2.1 and 2.2.2. Then, there exists a function*

$$\begin{array}{rccl} M_*: & (0,1)\times(0,+\infty) & \longrightarrow & [0,+\infty], \\ & (p^{\text{ext}}, D_b) & \longmapsto & M_*(p^{\text{ext}}, D_b), \end{array} \tag{2.8}$$

such that for any $p^{\text{ext}} \in (0,1), D_b > 0$, problem (2.2) admits at least one solution which is not (SM) if and only if $L \geqslant M_*(p^{\text{ext}}, D_b)$. Moreover,
• If $p^{\text{ext}} \leqslant \beta$, then for any $D_b > 0$, one has

$$0 < M_i(p^{\text{ext}}, D_b) + M_d(p^{\text{ext}}, D_b) < M_*(p^{\text{ext}}, D_b) < +\infty. \tag{2.9}$$

• If $p^{\text{ext}} > \beta$, then for any $D_b < D_*$, one has $0 < M_i(p^{\text{ext}}, D_b) < M_*(p^{\text{ext}}, D_b) < +\infty$. Otherwise, for $D_b \geqslant D_*$, $M_*(p^{\text{ext}}, D_b) = +\infty$. Here, D_* was defined in Theorem 2.2.1.

The construction of M_i, M_d, M_* will be done in the proof in Section 2.3. The idea of the proof is based on a careful study of the phase portrait of (2.2). To make the results more reader-friendly, we present the types of steady-state solutions corresponding to different parameters in Table 2.1.

In the next section, we present a result about the stability and instability of steady-state solutions of (2.2).

Table 2.1 – The existence of steady-state solutions corresponding to values of parameters.

Parameters	$0 < p^{\text{ext}} < \theta,\ D_b > 0$		
	$0 = M_i < L < M_d$	$M_d \leqslant L < M_*$	$M_* \leqslant L < +\infty$
Types of solutions	(SI)	(SI), (SD)	(SI), (SD), non-(SM)
Parameters	$p^{\text{ext}} = \theta,\ D_b > 0$		
	$0 = M_d = M_i = M_* < L$		
Types of solutions	(SD), (SI), non-(SM)		
Parameters	$\theta < p^{\text{ext}} \leqslant \beta,\ D_b > 0$ or $p^{\text{ext}} > \beta,\ 0 < D_b < D_*$		
	$0 = M_d < L < M_i$	$M_i \leqslant L < M_*$	$M_* \leqslant L < +\infty$
Types of solutions	(SD)	(SI), (SD)	(SI), (SD), non-(SM)
Parameters	$\beta < p^{\text{ext}} < 1,\ D_b > D_*$		
	$0 = M_d < L < M_i = M_* = +\infty$		
Types of solutions	(SD)		

2.2.3 Stability of steady-state solutions

The definition of stability and instability used in the present work comes from Lyapunov stability

Definition 2.2.2. *A steady-state solution $p(x)$ of (2.1) is called stable if for any constant $\epsilon > 0$, there exists a constant $\delta > 0$ such that when $||p^{\text{init}} - p||_\infty < \delta$, one has*

$$||p^0(t,\cdot) - p||_\infty < \epsilon, \quad \text{for all } t > 0 \tag{2.10}$$

where $p^0(t,x)$ is the unique solution of (2.1). If, in addition,

$$\lim_{t\to\infty} ||p^0(t,\cdot) - p||_\infty = 0, \tag{2.11}$$

then p is called asymptotically stable. The steady-state solution p is called unstable if it is not stable.

The following theorem provides sufficient conditions for the stability of steady-state solutions given in Section 2.2.2.

Theorem 2.2.3. *In the bounded domain $\Omega = (-L, L) \subset \mathbb{R}$, consider the problem (2.1) with the reaction term satisfying Assumptions 2.2.1 and 2.2.2. There exists a constant $\lambda_1 \in \left(0, \frac{\pi^2}{4L^2}\right)$ such that for any steady-state solution p of (2.1),*

- *If $f'(p(x)) > \lambda_1$ for all $x \in (-L, L)$, then p is unstable.*
- *If $f'(p(x)) < \lambda_1$ for all $x \in (-L, L)$, then p is asymptotically stable.*

More precisely, λ_1 is the principal eigenvalue of the linear problem (2.12)

$$-\phi''(x) = \lambda\phi(x), \qquad x \in (-L, L), \tag{2.12a}$$
$$\phi'(L) = -D_b\phi(L), \tag{2.12b}$$
$$\phi'(-L) = D_b\phi(-L), \tag{2.12c}$$

where λ is an eigenvalue with associated eigenfunction ϕ. It may be proved that its value is the smallest positive solution of equation $\sqrt{\lambda}\tan\left(L\sqrt{\lambda}\right) = D_b$ (see more details in Section 2.3).

Note that we cannot apply the first statement if $\sup_{q\in(0,1)} f'(q) \leqslant \lambda_1$. However, due to the fact that $\lambda_1 \in \left(0, \frac{\pi^2}{4L^2}\right)$, when L gets larger, the value of λ_1 gets closer to zero and the inequality in the first statement becomes valid.

Remark 2.2.2. *By Assumption 2.2.2, $f'(q) \leqslant 0 < \lambda_1$ for all $q \in [0, \alpha_1] \cup [\alpha_2, 1]$, we can deduce that the steady-state solutions with values smaller than α_1 or larger than α_2 are asymptotically stable.*

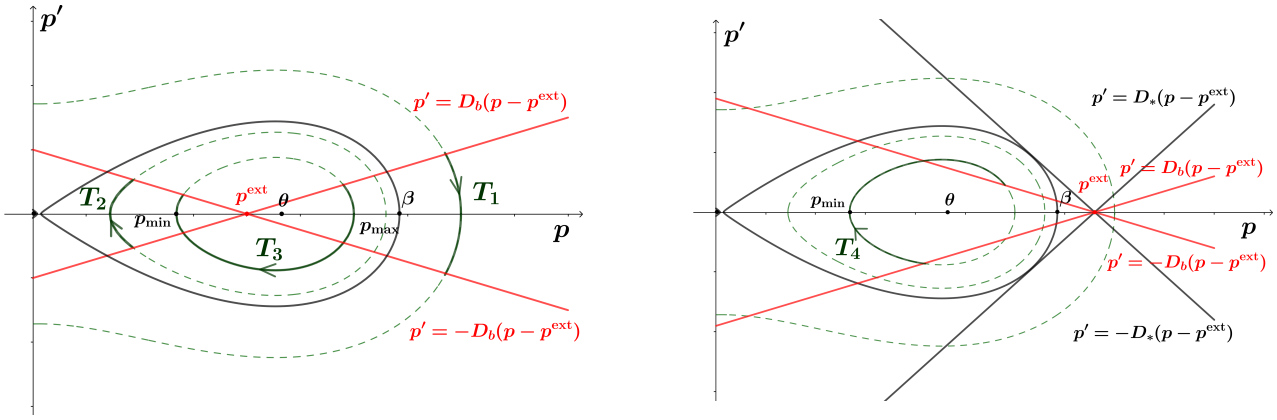

(a) $p^{\text{ext}} < \theta < \beta, D_b > 0$

(b) $p^{\text{ext}} > \beta, D_b \leqslant D_*$

Figure 2.3 – Phase portraits of (2.2): straight lines illustrate the boundary conditions, solid curves show relations between p' and p. Figure (a): curves T_1, T_2, and T_3 correspond to orbits of (SD), (SI), and non-(SM) solutions, respectively. Figure (b): curve T_4 corresponds to an orbit of a non-(SM) solution.

As a consequence of Theorems 2.2.1, 2.2.2, and 2.2.3, the following important result provides complete information about the existence and stability of steady-state solutions in some special cases.

Corollary 2.2.1. *In the bounded domain $\Omega = (-L, L) \subset \mathbb{R}$, consider the problem (2.1) with the reaction term satisfying Assumption 2.2.1 and 2.2.2. Then for any $D_b > 0$, we have*

- *If $p^{\text{ext}} \leqslant \alpha_1$, for any $L > 0$, there exists exactly one (SI) steady-state solution p and it is asymptotically stable. Moreover, if $L < M_d(p^{\text{ext}}, D_b)$, then p is the unique steady-state solution of (2.1).*
- *If $p^{\text{ext}} \geqslant \alpha_2$, for any $L > 0$, there exists exactly one (SD) steady-state solution p and it is asymptotically stable. Moreover, if $L < M_i(p^{\text{ext}}, D_b)$, then p is the unique steady-state solution of (2.1).*

Remark 2.2.3. *This corollary gives us a comprehensive view of the long-time behavior of solutions of (2.1) when the size L of the domain is small. In this case, the unique steady-state solution p is symmetric, monotone on each half of Ω, and asymptotically stable. Its values will be close to 0 if p^{ext} is small and close to 1 if p^{ext} is large. We discuss an essential application of this result in Section 2.4.*

2.3 Proof of the theorems

2.3.1 Proof of existence

In this section, we use phase-plane analysis to prove the existence of both (SM) and non-(SM) steady-state solutions depending on the parameters. The studies of (SD) and (SI) solutions will be presented respectively in Sections 2.3.1 and 2.3.1. Then, using these results, we prove Theorem 2.2.1. The proof of Theorem 2.2.2 will be presented after that using the same technique.

First, we introduce the following function

$$\mathcal{E}(p, p') = \frac{(p')^2}{2} + F(p). \tag{2.13}$$

Since $\frac{d}{dx} E(p, p') = p'(p'' + f(p)) = 0$, then $E(p, p')$ is constant along the orbit of (2.2). From Proposition 2.2.1, we can deduce that there exists an $x_0 \in (-L, L)$ such that $p'(x_0) = 0$, thus one has

$$\mathcal{E}(p(x_0), 0) = \mathcal{E}(p(x), p'(x)), \tag{2.14}$$

for all $x \in (-L, L)$. Therefore, the relation between p' and p is as below

$$p' = \pm\sqrt{2F(p(x_0)) - 2F(p)}. \tag{2.15}$$

According to this relation, one has a phase plane as in Figure 2.3a, in which the curves illustrate the relation between $p'(x)$ and $p(x)$ in (2.15) with respect to different values of $p(x_0)$. We can see that some curves do not end on the axis $p = 0$ but wrap around the point $(\theta, 0)$. This is dues to the fact that for any $p_1 \in [\theta, \beta]$, there exists a value $p_2 \in [0, \theta]$ such that $F(p_1) = F(p_2)$. Thus, if the curve passes through the point $(p_1, 0)$, it will also

pass through the point $(p_2, 0)$ on the axis $p' = 0$. Moreover, those curves only exist if their intersection with the axis $p' = 0$ has p-coordinate less than or equal to β. Besides, the two straight lines show the relation between p' and p at the boundary points. Solutions of (2.2) correspond to those orbits that connect the intersection of the curves with the line $p' = D_b(p - p^{\text{ext}})$ to the intersection of the curves with the line $p' = -D_b(p - p^{\text{ext}})$.

In the phase plane in Figure 2.3a, orbit T_1 describes an (SD) solution, while orbit T_2 corresponds to a (SI) solution. On the other hand, the solid curve T_3 shows the orbit of a steady-state solution that is not symmetric-monotone.

Remark 2.3.1. *(Graphical interpretation of D_*) The (SI) solutions (see Figure 2.2b) have orbit as T_2 in Figure 2.3a. This type of orbits only exists when the lines $p = \pm D_b(p - p^{\text{ext}})$ intersect the curves wrapping around the point $(\theta, 0)$. In the case when $p^{\text{ext}} > \beta$, the constant $D_* > 0$ in Theorem 2.2.1 is the slope of the tangent line to the curve passing through $(\beta, 0)$ as in Figure 2.3b. Hence, if $D_b > D_*$, there exists no (SI) solution. We construct explicitly the value of D_* in Proposition 2.3.2 below.*

Next, we establish some relations between the solution p and the parameters based on the phase portrait above. For any $x > x_0$, if p is monotone on (x_0, x), we can invert $x \mapsto p(x)$ into function $p \mapsto X(p)$. We obtain $X'(p) = \frac{\pm 1}{\sqrt{2F(p(x_0)) - 2F(p)}}$. By integrating this equation, we obtain that

$$x - x_0 = \int_{p(x_0)}^{p(x)} \frac{(-1)^k ds}{\sqrt{2F(p(x_0)) - 2F(s)}}, \tag{2.16}$$

where $k = 1$ if p is decreasing and $k = 2$ if p is increasing on (x_0, x). We can obtain the analogous formula for $x < x_0$.

First, we focus on symmetric-monotone (SM) solutions for which $p'(0) = 0$, then we analyze the integral in (2.16) with $x = L, x_0 = 0$. For any $p^{\text{ext}} \in (0, 1)$, using (2.15), we have

$$F(p(0)) = F(p(L)) + \frac{1}{2} D_b^2 \left(p(L) - p^{\text{ext}}\right)^2 = G(p(L)), \tag{2.17}$$

for F defined in (2.5) and

$$G(q) := F(q) + \frac{1}{2} D_b^2 (q - p^{\text{ext}})^2, \tag{2.18}$$

and from (2.16) with $x = L, x_0 = 0$, we have

$$L = \int_{p(0)}^{p(L)} \frac{(-1)^k ds}{\sqrt{2F(p(0)) - 2F(s)}}, \tag{2.19}$$

where $k = 1$ if p is decreasing on $(0, L)$, $k = 2$ if p is increasing on $(0, L)$.

Thus, the (SM) solution of (2.2) exists if there exist values $p(L)$ and $p(0)$ that satisfy (2.17) and (2.19). When such values exist, we can assess the value of $p(x)$ for any x in $(-L, L)$ using (2.16).

Before proving the existence of such values of $p(0)$ and $p(L)$, we establish some useful properties of the function G defined in (2.18). It is continuous in $[0, 1]$ and $G(q) \geqslant F(q)$ for all $q \in [0, 1]$. Moreover, the following lemma shows that G has a unique minimum point.

Lemma 2.3.1. *For any $p^{\text{ext}} \in (0, 1)$, there exists a unique value $\overline{q} \in (0, 1)$ such that $G'(\overline{q}) = 0$, $G'(q) < 0$ for all $q \in [0, \overline{q})$ and $G'(q) > 0$ for all $q \in (\overline{q}, 1]$. Particularly, $G(\overline{q}) = \min_{[0,1]} G$.*

Proof. We have $G'(q) = f(q) + D_b^2(q - p^{\text{ext}})$. We consider the following cases.

Case 1: When $p^{\text{ext}} = \theta$, we have $G'(p^{\text{ext}}) = G'(\theta) = f(\theta) = 0, G'(q) < 0$ for all $q \in (0, \theta)$ and $G'(q) > 0$ for all $q \in (\theta, 1)$. Thus $\overline{q} = \theta = p^{\text{ext}}$.

Case 2: When $p^{\text{ext}} < \theta$, we have $G'(q) < 0$ for all $q \in [0, p^{\text{ext}}]$ and $G'(q) > 0$ for all $q \in [\theta, 1]$. So there exists at least one value $\overline{q} \in (p^{\text{ext}}, \theta)$ such that $G'(\overline{q}) = 0$.

For any $\overline{q} \in (p^{\text{ext}}, \theta)$ such that $G'(\overline{q}) = 0$, we have $f(\overline{q}) + D_b^2(\overline{q} - p^{\text{ext}}) = 0$ so that $D_b^2 = -\frac{f(\overline{q})}{\overline{q} - p^{\text{ext}}}$. We can prove that $G''(\overline{q})$ is strictly positive. Indeed, from Assumption 2.2.2 we have that α_1 is the unique value in $(0, \theta)$ such that $f'(\alpha_1) = 0$, thus $f(\alpha_1) = \min_{[0,\theta]} f < 0$.

If $\alpha_1 \leqslant \overline{q} < \theta$ then $f'(\overline{q}) \geqslant 0$. One has $G''(\overline{q}) = f'(\overline{q}) + D_b^2 > 0$.

If $p^{\text{ext}} < \overline{q} < \alpha_1$, due to the fact that f is convex in $(0, \alpha_1)$ one has $f'(\overline{q}) \geqslant \frac{f(\overline{q}) - f(p^{\text{ext}})}{\overline{q} - p^{\text{ext}}}$. Since $f(p^{\text{ext}}) < 0$, one has $G''(\overline{q}) = f'(\overline{q}) + D_b^2 = f'(\overline{q}) - \frac{f(\overline{q})}{\overline{q} - p^{\text{ext}}} > f'(\overline{q}) + \frac{f(p^{\text{ext}}) - f(\overline{q})}{\overline{q} - p^{\text{ext}}} \geqslant 0$. One can deduce that $\overline{q}$ is the unique value in $(0, 1)$ such that $G'(\overline{q}) = 0$ and $G(\overline{q}) = \min_{[0,1]} G$, so it satisfies Lemma 2.3.1.

Case 3: When $p^{\text{ext}} > \theta$, the proof is analogous to case 2 but using the concavity of f in $(\alpha_2, 1)$. We obtain that there exists a unique value $\overline{q}$ in (θ, p^{ext}) that satisfies Lemma 2.3.1. □

When $p^{\text{ext}} = \theta$, it is easy to check that $p \equiv \theta$ is a solution of (2.2). We now analyze two types of (SM) solutions (see Figure 2.2) in the following parts.

Existence of (SD) solutions

In this part, the solution p we study is symmetric on $(-L, L)$ and decreasing on $(0, L)$ (see Figure 2.2a). So $p(L) < p(x) < p(0)$ for any $x \in (0, L)$. But from (2.15), we have that $F(p(x)) \leqslant F(p(0))$, so $F'(p(0)) \geqslant 0$. It implies that $p(0) \in [\theta, 1]$. Next, we use two steps to study the existence of (SD) solutions:

Step 1: Rewriting as a non-linear equation on $p(L)$

For any $q \in (\theta, 1)$, we have $F'(q) = f(q) > 0$ so $F|_{(\theta,1)} : (\theta, 1) \longrightarrow (F(\theta), F(1))$ is invertible. Define $F_1^{-1} := (F|_{(\theta,1)})^{-1} : (F(\theta), F(1)) \longrightarrow (\theta, 1)$, and $F_1^{-1}(F(\theta)) = \theta, F_1^{-1}(F(1)) = 1$. Then, F_1^{-1} is continuous in $[F(\theta), F(1)]$. For any $y \in (F(\theta), F(1))$, one has $\left(F_1^{-1}\right)'(y) = \frac{1}{F'\left(F_1^{-1}(y)\right)} = \frac{1}{f\left(F_1^{-1}(y)\right)} > 0$, so F_1^{-1} is an increasing function in $(F(\theta), F(1))$. From (2.17) and (2.19), since p is decreasing in $(0, L)$, we have $L = \displaystyle\int_{p(L)}^{p(0)} \frac{ds}{\sqrt{2G(p(L)) - 2F(s)}}$. Denote

$$\mathcal{F}_1(q) := \int_q^{F_1^{-1}(G(q))} \frac{ds}{\sqrt{2G(q) - 2F(s)}}. \tag{2.20}$$

Hence, a (SD) solution p of system (2.2) has $p(0) = F_1^{-1}(G(p(L)))$, and $p(L)$ satisfies

$$L = \mathcal{F}_1(p(L)). \tag{2.21}$$

Moreover, one has $p'(x) \leqslant 0$ for all $x \in (0, L)$ thus $-D_b(p(L) - p^{\text{ext}}) = p'(L) \leqslant 0$. One can deduce that

$$p(L) \geqslant p^{\text{ext}}. \tag{2.22}$$

Step 2: Solving (2.21) in $[p^{\text{ext}}, 1]$

The following proposition states the existence of a solution of (2.21).

Proposition 2.3.1. *For any $D > 0, p^{\text{ext}} \in (0, 1)$, we have*

1. *If $0 < p^{\text{ext}} < \theta$, then there exists a constant $M_1 > 0$ such that equation (2.21) has at least one solution $p(L) \geqslant p^{\text{ext}}$ if and only if $L \geqslant M_1$.*

2. *If $\theta \leqslant p^{\text{ext}} < 1$, then equation (2.21) admits at least one solution $p(L) \geqslant p^{\text{ext}}$ for all $L > 0$. If $p^{\text{ext}} \geqslant \alpha_2$, then this solution is unique.*

Proof. Since F_1^{-1} is only defined in $[F(\theta), F(1)]$, we need to find $p(L) \in [p^{\text{ext}}, 1]$ such that $G(p(L)) \in [F(\theta), F(1)]$.

For all $q \in (0, 1)$, we have $G(q) \geqslant F(q) \geqslant F(\theta)$ and from Lemma 2.3.1, there exists a value $\overline{q} \in (0, 1)$ such that $\min\limits_{[0,1]} G = G(\overline{q}) \leqslant G(p^{\text{ext}}) = F(p^{\text{ext}}) < \max\limits_{[0,1]} F = F(1)$. Moreover, one has $G(1) > F(1)$, thus there exists a value $p^* \in (p^{\text{ext}}, 1)$ such that $G(p^*) = F(1)$. Then, for all $q \in [p^{\text{ext}}, p^*], G(q) \in [F(\theta), F(1)]$ and we will find $p(L)$ in $[p^{\text{ext}}, p^*]$. Since F_1^{-1} increases in $(F(\theta), F(1))$, then $p(0) = F_1^{-1}(G(p(L))) \geqslant F_1^{-1}(F(p(L))) \geqslant p(L)$.

Function $\mathcal{F}_1$ in (2.20) is well-defined and continuous in $[p^{\text{ext}}, p^*)$, $\mathcal{F} \geqslant 0$ in $[p^{\text{ext}}, p^*)$. Moreover, since $F'(1) = 0$, one has $\lim\limits_{p \to p^*} \mathcal{F}_1(p) = \displaystyle\int_{p^*}^1 \frac{ds}{\sqrt{2F(1) - 2F(s)}} = +\infty$.

Case 1: If $0 < p^{\text{ext}} < \theta$, we will prove that $\mathcal{F}_1$ is strictly positive in $[p^{\text{ext}}, p^*)$. Indeed, for any $y \in [0, 1]$, if $y < \theta$, by the definition of F_1^{-1}, we have $F_1^{-1}(G(y)) \in [\theta, 1]$ so $F_1^{-1}(G(y)) > y$. If $y \geqslant \theta > p^{\text{ext}}$ then $G(y) = F(y) + \frac{1}{2} D_b^2 (y - p^{\text{ext}})^2 > F(y)$ so again $F_1^{-1}(G(y)) > y$. Hence $\mathcal{F}_1(y) > 0$ for all $y \in [p^{\text{ext}}, p^*)$. We have $\mathcal{F}_1(p) \to +\infty$ when $p \to p^*$, so there exists $p \in [p^{\text{ext}}, p^*)$ such that $M_1 := \mathcal{F}_1(p) = \min\limits_{[p^{\text{ext}}, p^*]} \mathcal{F}_1 > 0$, and system (2.21) admits at least one solution if and only if $L \geqslant M_1$.

Case 2: If $\theta \leqslant p^{\text{ext}} < 1$, one has $G(p^{\text{ext}}) = F(p^{\text{ext}})$, then $F_1^{-1}(G(p^{\text{ext}})) = p^{\text{ext}}$ so $\mathcal{F}_1(p^{\text{ext}}) = 0$. On the other hand, $\mathcal{F}_1(p) \to +\infty$ when $p \to p^*$. Thus, for any $L > 0$, there always exists at least one value $p(L) \in (p^{\text{ext}}, p^*)$ such that $\mathcal{F}_1(p(L)) = L$.

Proof of uniqueness: When $p^{\text{ext}} \geqslant \alpha_2$, we can prove that $\mathcal{F}_1' > 0$ on (p^{ext}, p^*). Indeed, denoting $\gamma(q) = F_1^{-1}(G(q))$, and changing the variable from s to t such that $s = t\gamma(q) + (1-t)q$, one has

$$\mathcal{F}_1(q) = \int_0^1 \frac{[\gamma(q) - q]dt}{\sqrt{2F(\gamma(q)) - 2F(t\gamma(q) + (1-t)q)}}.$$

To simplify, denote $s(q) = t\gamma(q) + (1-t)q$. For any $t \in (0,1)$, one has $q < s(q) < \gamma(q)$. Let us define $\Delta F = F(\gamma(q)) - F(s(q))$, then one has

$$\begin{aligned}\sqrt{2}\mathcal{F}_1'(q) &= \int_0^1 (\gamma'(q)-1)(\Delta F)^{-1/2}dt - \frac{1}{2}\int_0^1 (\Delta F)^{-3/2}(\gamma(q)-q)\frac{d\Delta F}{dq}dt \\ &= \int_0^1 (\Delta F)^{-3/2}\left[(\gamma'(q)-1)\Delta F - \frac{1}{2}(\gamma(q)-q)(f(\gamma(q))\gamma'(q) - f(s(q))s'(q))\right].\end{aligned}$$

Let P be the formula in the brackets, then

$$\begin{aligned}P &= (\gamma'-1)\Delta F - \tfrac{1}{2}(\gamma-q)\left[f(\gamma)\gamma' - f(s)(t\gamma'+1-t)\right] \\ &= (\gamma'-1)\left[\Delta F - \tfrac{1}{2}(\gamma-q)f(\gamma) + \tfrac{1}{2}(s-q)f(s)\right] - \tfrac{1}{2}(\gamma-q)(f(\gamma)-f(s)),\end{aligned}$$

Define $\psi(y) := F(y) - \frac{1}{2}f(y)(y-q)$ for any $y \in [q, \gamma(q)]$, then one has $\psi'(y) = \frac{1}{2}[f(y) - f'(y)(y-q)] \geqslant \frac{f(q)}{2} > 0$ since $y \geqslant q > p^{\text{ext}} \geqslant \alpha_2$ and f is concave in $(\alpha_2, 1)$, $f(q) > 0$. Moreover, f is decreasing on $(\alpha_2, 1)$ so $0 < f(\gamma(q)) < f(s(q)) < f(q)$, and $\gamma'(q) = \frac{G'(q)}{f(F_1^{-1}(G(q)))} = \frac{f(q) + D_b^2(q - p^{\text{ext}})}{f(\gamma(q))} > 1$. Hence, we can deduce that $P = (\gamma'-1)(\psi(\gamma) - \psi(s)) - \frac{1}{2}(\gamma - q)(f(\gamma) - f(s)) > 0$ for any $t \in (0,1)$. This proves that function $\mathcal{F}_1$ is increasing on (p^{ext}, p^*), so the solution of equation (2.21) is unique. □

Existence of (SI) solutions

In this case, the technique we use to prove the existence of (SI) solutions is analogous to (SD) solutions except in the case when $p^{\text{ext}} > \beta$ (case 3 below). Since the proof is not straightforward, it is worth to re-establish this technique for (SI) solutions in two following steps:

Step 1: Rewriting as a non-linear equation on $p(L)$

Since now p is symmetric on $(-L, L)$ and increasing in $(0, L)$ (see Figure 2.2b), then $p(0) < p(x) < p(L)$ for any $x \in (0, L)$. But from (2.15), we have that $F(p(x)) \leqslant F(p(0))$, so $F'(p(0)) \leqslant 0$. This implies that $p(0) \in [0, \theta]$.

For any $q \in (0, \theta)$, we have $F'(q) = f(q) < 0$ so $F|_{(0,\theta)} : (0,\theta) \longrightarrow (F(\theta), F(0))$ is invertible. Define $F_2^{-1} := (F|_{(0,\theta)})^{-1} : (F(\theta), F(0)) \longrightarrow (0, \theta)$, $F_2^{-1}(F(\theta)) = \theta, F_2^{-1}(F(0)) = 0$, and F_2^{-1} is continuous in $[F(\theta), F(0)]$. For any $y \in (F(\theta), F(0))$, $\left(F_2^{-1}\right)'(y) = \frac{1}{F'\left(F_2^{-1}(y)\right)} = \frac{1}{f\left(F_2^{-1}(y)\right)} < 0$, so F_2^{-1} is a decreasing function in $(F(\theta), F(0))$.

From (2.17) and (2.19), we have $L = \displaystyle\int_{p(0)}^{p(L)} \frac{ds}{\sqrt{2G(p(L)) - 2F(s)}}$. Denote

$$\mathcal{F}_2(q) := \int_{F_2^{-1}(G(q))}^{q} \frac{ds}{\sqrt{2G(q) - 2F(s)}}. \tag{2.23}$$

Hence, a (SI) solution of system (2.2) has $p(0) = F_2^{-1}(G(p(L)))$, and $p(L)$ satisfies

$$L = \mathcal{F}_2(p(L)), \tag{2.24}$$

and in this case, one needs to find $p(L)$ in $[0, p^{\text{ext}}]$.

Step 2: Solving of (2.24) in $[0, p^{\text{ext}}]$

The following proposition states the existence of a solution of (2.24).

Proposition 2.3.2. *For any $p^{\text{ext}} \in (0,1)$, considering the value β as in (2.6), we have:*

1. *If $0 < p^{\text{ext}} \leqslant \theta$, then equation (2.24) admits at least one solution p with $p(L) \leqslant p^{\text{ext}}$ for all $L > 0, D_b > 0$. If $p^{\text{ext}} \leqslant \alpha_1$, this solution is unique.*
2. *If $\theta < p^{\text{ext}} \leqslant \beta$, then for all $D_b > 0$, there exists a constant $M_2 > 0$ such that equation (2.24) has at least one solution p with $p(L) \leqslant p^{\text{ext}}$ if and only if $L \geqslant M_2$.*
3. *If $\beta < p^{\text{ext}} < 1$, then there exists a constant $D_* > 0$ such that when $D_b \geqslant D_*$, equation (2.24) has no solution. Otherwise, there exists a constant $M_3 > 0$ such that equation (2.24) has at least one solution p with $p(L) \leqslant p^{\text{ext}}$ if and only if $L \geqslant M_3$.*

Proof. As we assume that $F(0) < F(1)$ and $F(\theta) < F(0)$ then, due to the continuity of F, one can deduce that there exists a value $\beta \in (\theta, 1)$ such that $F(\beta) = F(0) = 0$.

Since F_2^{-1} is only defined in $[F(\theta), F(0)]$, we need to find $p(L) \in [0, p^{\text{ext}}]$ such that $G(p(L)) \in [F(\theta), F(0)]$. For all $q \in (0,1)$, we have $G(q) \geqslant F(q) \geqslant F(\theta)$, thus equation (2.24) has solutions if and only if $\min_{[0,1]} G < F(0)$. Even when $\min_{[0,1]} G = G(\overline{q}) = F(0)$, $\mathcal{F}_2$ is still not defined in $[0,1]$ since $\mathcal{F}_2(\overline{q}) = +\infty$.

One has the following cases:

Case 1: $0 < p^{\text{ext}} \leqslant \theta$:

We have $\min_{[0,1]} G = G(\overline{q}) \leqslant G(p^{\text{ext}}) = F(p^{\text{ext}}) < \max_{[0,\theta]} F = F(0)$, and $G(0) > F(0)$ so there is a value $p_* \in (0, p^{\text{ext}})$ such that $G(p_*) = F(0)$. Moreover $F'(0) = 0$, then $\lim_{p \to p^*} \mathcal{F}_2(p) = +\infty$. Thus, function $\mathcal{F}_2$ is only well-defined and continuous in $(p_*, p^{\text{ext}}]$.

When $0 < p^{\text{ext}} \leqslant \theta$, $F_2^{-1}(G(p^{\text{ext}})) = F_2^{-1}(F(p^{\text{ext}})) = p^{\text{ext}}$ so $\mathcal{F}_2(p^{\text{ext}}) = 0$. We can deduce that for any $L > 0$, there always exists at least one value $p(L) \in (p_*, p^{\text{ext}})$ such that $\mathcal{F}_2(p(L)) = L$. When $p^{\text{ext}} \leqslant \alpha_1$, arguing analogously to the second case of Proposition 2.3.1, one has $\mathcal{F}_2' < 0$ on (p_*, p^{ext}), thus the solution is unique.

Case 2: $\theta < p^{\text{ext}} \leqslant \beta$:

Since F increases on $(\theta, 1)$, then $\min_{[0,1]} G = G(\overline{q}) < G(p^{\text{ext}}) = F(p^{\text{ext}}) \leqslant F(\beta) = F(0)$. Analogously to the previous case, $\mathcal{F}_2$ is well-defined and continuous in $(p_*, p^{\text{ext}}]$, $\lim_{p \to p^*} \mathcal{F}_2(p) = +\infty$, and $\mathcal{F}_2$ is strictly positive in $(p_*, p^{\text{ext}}]$. Therefore, there exists $p \in (p_*, p^{\text{ext}}]$ such that

$$M_2 := \mathcal{F}_2(p) = \min_{[p_*, p^{\text{ext}}]} \mathcal{F}_2 > 0, \tag{2.25}$$

and system (2.24) admits as least one solution if and only if $L \geqslant M_2$.

Case 3: $\beta < p^{\text{ext}} < 1$:

Consider the function $H(q) = F(q) + \frac{1}{2} f(q)(p^{\text{ext}} - q)$ defined in an interval $[\theta, p^{\text{ext}}]$. For any $\theta < q < p^{\text{ext}}$, one can prove that $H'(q) \geqslant 0$.

Indeed, if $q \leqslant \alpha_2$, then $f'(q) \geqslant 0$, and $f(q) > 0$. One has $H'(q) = \frac{1}{2} f(q) + \frac{1}{2} f'(q)(p^{\text{ext}} - q) > 0$. If $q > \alpha_2$, from Assumption 2.2.2, the function f is concave in $(\alpha_2, 1)$, and hence $f'(q)(p^{\text{ext}} - q) \geqslant f(p^{\text{ext}}) - f(q)$. Thus,

$$H'(q) = \tfrac{1}{2}(p^{\text{ext}} - q)\left(f'(q) + \tfrac{f(q)}{p^{\text{ext}} - q}\right) > \tfrac{1}{2}(p^{\text{ext}} - q)\left(f'(q) + \tfrac{f(q) - f(p^{\text{ext}})}{p^{\text{ext}} - q}\right) \geqslant 0.$$

Therefore, function H increases in (θ, p^{ext}). Moreover $H(\theta) = F(\theta) < F(0)$ and $H(p^{\text{ext}}) = F(p^{\text{ext}}) > F(\beta) = F(0)$, and so there exists a unique value $\overline{p}_* \in (\theta, p^{\text{ext}})$ such that $H(\overline{p}_*) = F(0)$. Take $D_* > 0$ such that $D_*^2 = \frac{f(\overline{p}_*)}{p^{\text{ext}} - \overline{p}_*}$. Then, for any $D_b > 0$, from Lemma 2.3.1, there is a unique value $\overline{q} \in (\theta, p^{\text{ext}})$ such that $G'(\overline{q}) = 0$, $G(\overline{q}) = \min_{[0,1]} G$, and $D_b^2 = \frac{f(\overline{q})}{p^{\text{ext}} - \overline{q}}$. If $D_b < D_*$, then $\frac{f(\overline{q})}{p^{\text{ext}} - \overline{q}} < \frac{f(\overline{p}_*)}{p^{\text{ext}} - \overline{p}_*}$.

Let $h(q) = \frac{f(q)}{p^{\text{ext}} - q}$, then $h'(q) = \frac{1}{p^{\text{ext}} - q}\left(f'(q) + \frac{f(q)}{p^{\text{ext}} - q}\right) > 0$ for $q \in (\theta, p^{\text{ext}})$. So function h is increasing in (θ, p^{ext}), and we can deduce that $\overline{q} < \overline{p}_*$. Hence, $\min_{[0,1]} G = G(\overline{q}) = F(\overline{q}) + \frac{1}{2} D_b^2 (p^{\text{ext}} - \overline{q})^2 = F(\overline{q}) + \frac{1}{2} f(\overline{q})(p^{\text{ext}} - \overline{q}) = H(\overline{q}) < H(\overline{p}_*) = F(0)$.

Moreover, $G(p^{\text{ext}}) = F(p^{\text{ext}}) > F(\beta) = F(0)$, $G(0) > F(0)$. Thus, there exists a maximal interval $(q_*, q^*) \subset [0, p^{\text{ext}}]$ such that $G(q) \in (F(\theta), F(0))$ for all $q \in (q_*, q^*)$. We have $0 < q_* < \overline{q} < q^* < p^{\text{ext}}$ and $G(q_*) = G(q^*) = F(0)$. Therefore, $\mathcal{F}_2$ is well-defined and continuous in (q_*, q^*), and $\lim_{p \to q^*} \mathcal{F}_2(p) = \lim_{p \to q_*} \mathcal{F}_2(p) = +\infty$. Reasoning like in the previous case, (2.24) admits solution if and only if $L \geqslant M_3$, where

$$M_3 := \min_{[q_*, q^*]} \mathcal{F}_2 > 0, \tag{2.26}$$

On the other hand, if $D_b \geqslant D_*$, $\min_{[0,1]} G \geqslant F(0)$, and equation (2.24) has no solution. □

Proof of Theorem 2.2.1. As we showed in Section 2.3.1, the (SD) steady-state solution p of (2.2) has $p(L)$ satisfying equation (2.21). From Proposition 2.3.1, we can deduce that for fixed $p^{\text{ext}} \in (0,1), D_b > 0$, $M_d(p^{\text{ext}}, D_b) = \min_q \mathcal{F}_1(q)$. Thus, we obtain the results for (SD) steady-state solutions of (2.2) in Theorem 2.2.1.

Similarly, Proposition 2.3.2 provides that for fixed $p^{\text{ext}} \in (0,1), D_b > 0$, we have $M_i(p^{\text{ext}}, D_b) = \min_q \mathcal{F}_2(q)$ when $p^{\text{ext}} \leqslant \beta$ or $D_b < D_*$. Otherwise, $M_i(p^{\text{ext}}, D_b) = +\infty$. □

Existence of non-(SM) solutions

As we can see in the phase portrait in Figure 2.3, there exist some solutions of (2.2) which are neither (SD) nor (SI). These solutions can be non-symmetric or can have more than one (local) extremum. By studying these cases, we prove Theorem 2.2.2 as follows

Proof of Theorem 2.2.2. We can see from Figure 2.3a that for fixed $p^{\text{ext}} \leqslant \beta, D_b > 0$, the non-(SM) solutions p of (2.2) have more than one (local) extreme value because their orbits have at least two intersections with the axis $p' = 0$ (see e.g. T_3). Those solutions have the same local minimum values, denoted $p_{\min}$, and the same maximum values, denoted $p_{\max}$. Moreover, we have $p_{\min} < \theta < p_{\max}$, and $F(p_{\min}) = F(p_{\max})$.

Since the orbits make a round trip of distance $2L$, then the more extreme values a solution has, the larger L is. Hence, to find the minimal value M_*, we study the case when p has one local minimum and one local maximum with orbit as T_3 in Figure 2.3a. Then we have

$$G(p(-L)) = G(p(L)) = F(p_{\min}) = F(p_{\max}), \tag{2.27}$$

and by using (2.16), we obtain

$$\begin{aligned} 2L &= \mathcal{F}_1((p(-L)) + \int_{p_{\min}}^{p_{\max}} \frac{ds}{\sqrt{2F(p_{\min}) - 2F(s)}} + \mathcal{F}_2(p(L)) \\ &= 2\left[\mathcal{F}_1(p(-L)) + \mathcal{F}_2(p(L))\right] + \int_{p(L)}^{p(-L)} \frac{ds}{\sqrt{2G(p(L)) - 2F(s)}}. \end{aligned}$$

Using the same idea as above, we can show that L depends continuously on $p(L)$. Moreover, we know that $M_d = \min \mathcal{F}_1$, $M_i = \min \mathcal{F}_2$, therefore there exists a constant M_* such that (2.2) admits at least one non-(SM) solution p if and only if $L \geqslant M_* > M_d + M_i$.

On the other hand, for fixed $p^{\text{ext}} > \beta, D_b < D_*$, it is possible that (2.2) admits a non-symmetric solution with only one minimum. The orbit of this solution is as T_4 in Figure 2.3b. In this case, we have $G(p(L)) = G(p(-L)) = F(p_{\min})$ with $p(-L) < p(L)$ and

$$2L = \mathcal{F}_2(p(-L)) + \mathcal{F}_2(p(L)) > 2M_i.$$

Hence, we only need $M_* > M_i$. □

2.3.2 Stability analysis

We first study the principal eigenvalue and eigenfunction for the linear problem. Then by using these eigenelements, we construct the super- and sub-solution of (2.1) and prove the stability and instability corresponding to each case in Theorem 2.2.3.

Proof of Theorem 2.2.3. Consider the corresponding linear eigenvalue problem (2.12). We can see that $\phi = \cos\left(\sqrt{\lambda}x\right)$ is an eigenfunction iff $\sqrt{\lambda}\tan\left(L\sqrt{\lambda}\right) = D_b$. Denote λ_1 the smallest positive value of λ which satisfies this equality, thus $L\sqrt{\lambda_1} \in \left(0, \frac{\pi}{2}\right)$. Hence, $\lambda_1 \in \left(0, \frac{\pi^2}{4L^2}\right)$. Moreover, for any $x \in (-L, L)$, the corresponding eigenfunction $\phi_1(x) = \cos\left(\sqrt{\lambda_1}x\right)$ takes values in $(0, 1)$.

Proof of stability: Now let p be a steady-state solution of (2.1) governed by (2.2). First, we prove that if $f'(p(x)) < \lambda_1$ for any $x \in (-L, L)$ then p is asymptotically stable. Indeed, since $f'(p(x)) < \lambda_1$, there exist positive constants δ, γ with $\gamma < \lambda_1$ such that for any $\eta \in [0, \delta]$,

$$f(p + \eta) - f(p) \leqslant (\lambda_1 - \gamma)\eta, \qquad f(p) - f(p - \eta) \leqslant (\lambda_1 - \gamma)\eta, \tag{2.28}$$

on $(-L, L)$. Now consider

$$\overline{p}(t, x) = p(x) + \delta e^{-\gamma t}\phi_1(x), \qquad \underline{p}(t, x) = p(x) - \delta e^{-\gamma t}\phi_1(x).$$

Assume that $p^{\text{init}}(x) \leqslant p(x) + \delta\phi_1(x)$. Then by (2.28), we have that $\overline{p}$ is a super-solution of (2.1) because

$$\partial_t\overline{p} - \partial_{xx}\overline{p} = (\lambda_1 - \gamma)\delta e^{-\gamma t}\phi_1(x) + f(p) \geqslant f(p + \delta e^{-\gamma t}\phi_1(x)) = f(\overline{p}),$$

due to the fact that $0 < \delta e^{-\gamma t}\phi_1(x) < \delta$ for any $t > 0$, $x \in (-L, L)$. Moreover, at the boundary points one has $\frac{\partial\overline{p}}{\partial\nu} + D_b(\overline{p} - p^{\text{ext}}) = \frac{\partial p}{\partial\nu} + D_b(p - p^{\text{ext}}) = 0$.

Similarly, if we have $p^{\text{init}}(x) \geqslant p(x) - \delta\phi_1(x)$, and so $\underline{p}$ is a sub-solution of (2.1). Then, by the method of super- and sub-solution (see e.g. [164]), the solution p^0 of (2.1) satisfies $\underline{p} \leqslant p^0 \leqslant \overline{p}$. Hence, $|p^0(t,x) - p(x)| \leqslant \delta e^{-\gamma t}\phi_1(x)$. Therefore, we can conclude that, whenever $|p^{\text{init}}(x) - p(x)| \leqslant \delta\phi_1(x)$ for any $x \in (-L, L)$, the solution p^0 of (2.1) converges to the steady-state p when $t \to +\infty$. This shows the stability of p.

Proof of instability: In the case when $f'(p(x)) > \lambda_1$, there exist positive constants δ, γ, with $\gamma < \lambda_1$, such that for any $\eta \in [0, \delta]$,

$$f(p+\eta) - f(p) \geqslant (\lambda_1 + \gamma)\eta, \tag{2.29}$$

on $(-L, L)$.

For any $p^{\text{init}} > p$, there exists a positive constant $\sigma < 1$ such that $p^{\text{init}} \geqslant p + \delta(1-\sigma)$. Then $\widetilde{p}(t,x) = p(x) + \delta(1 - \sigma e^{-\gamma' t})\phi_1(x)$, with $\gamma' < \gamma$ small enough, is a sub-solution of (2.1). Indeed, by applying (2.29) with $\eta = \delta(1 - \sigma e^{-\gamma' t})\phi_1(x) \in [0, \delta]$ for any $x \in (-L, L)$, we have

$$\partial_t \widetilde{p} - \partial_{xx}\widetilde{p} = \gamma'\delta\sigma e^{-\gamma' t}\phi_1(x) + \lambda_1\delta(1 - \sigma e^{-\gamma' t})\phi_1(x) + f(p) \leqslant f(p + \delta(1 - \sigma e^{-\gamma' t})\phi_1(x))$$

if $\gamma \geqslant \frac{\gamma'\sigma e^{-\gamma' t}}{1 - \sigma e^{-\gamma' t}} = \frac{\gamma'\sigma}{e^{\gamma' t} - \sigma}$ for any $t \geqslant 0$. This inequality holds when we choose $\gamma' \leqslant \frac{\gamma(1-\sigma)}{\sigma}$. Now, we have that $\widetilde{p}$ is a sub-solution of (2.1), thus for any $t \geqslant 0, x \in (-L, L)$, the corresponding solution p^0 satisfies

$$p^0(t,x) - p(x) \geqslant \tilde{p}(t,x) - p(x) \geqslant \delta(1 - \sigma e^{-\gamma' t})\phi_1(x).$$

Hence, for a given positive $\epsilon < \delta \min_x \phi_1(x)$, when $t \to +\infty$, solution p^0 cannot remain in the ϵ-neighborhood of p even if $p^{\text{init}} - p$ is small. This implies the instability of p. □

Proof of Corollary 2.2.1. For $p^{\text{ext}} \leqslant \alpha_1 < \theta, D_b > 0$, from Theorem 2.2.1, the (SI) steady-state solution p exists for any $L > 0$ and is unique, $p(x) \leqslant p^{\text{ext}} \leqslant \alpha_1$ for all $x \in (-L, L)$. Moreover, from Assumption 2.2.2, the reaction term f has $f'(q) < 0$, for any $q \in (0, \alpha_1)$. Then, for any $x \in (-L, L)$, $f'(p(x)) \leqslant 0 < \lambda_1$. Hence, p is asymptotically stable.

Besides, from Theorems 2.2.1 and 2.2.2, for any $L > 0$ such that $L < M_d(p^{\text{ext}}, D_b) < M_*(p^{\text{ext}}, D_b)$, (2.1) has neither (SD) nor non-(SM) steady-state solutions. So the (SI) steady-state solution is the unique steady-state solution.

Using a similar argument for the case $p^{\text{ext}} \geqslant \alpha_2$, we obtain Corollary 2.2.1. □

2.4 Application to the control of dengue vectors by the introduction of the bacterium *Wolbachia*

2.4.1 Model

In this section, we show an application of our model to the control of mosquitoes using *Wolbachia*. Mosquitoes of genus *Aedes* are the vector of many dangerous arboviruses, such as dengue, zika, chikungunya and others. There exists neither effective treatment nor vaccine for these vector-borne diseases, and in such conditions, the main method to control them is to control the vector population. A biological control method using a bacterium called *Wolbachia* (see [108]) was discovered and developed with this purpose. Besides reducing the ability of mosquitoes to transmit viruses, *Wolbachia* also causes an important phenomenon called *cytoplasmic incompatibility* (CI) on mosquitoes. More precisely, if a wild female mosquito is fertilized by a male carrying *Wolbachia*, its eggs almost cannot hatch. For more details about CI, we refer to [220]. In the case of *Aedes* mosquitoes, *Wolbachia* reduces lifespan, changes fecundity, and blocks the development of the virus. However, it does not influence the way mosquitoes move.

In [201], model (2.3), (2.4) was considered with $n_1 = n_i$ the density of the mosquitoes which are infected by *Wolbachia* and $n_2 = n_u$ the density of wild uninfected mosquitoes. Consider the following positive parameters:

- $d_u, \delta d_u$: death rate of, respectively uninfected mosquitoes and infected mosquitoes, $\delta > 1$ since *Wolbachia* reduces the lifespan of the mosquitoes;
- $b_u, (1 - s_f)b_u$: birth rate of, respectively uninfected mosquitoes and infected ones. Here $s_f \in [0, 1)$ characterizes the fecundity decrease;
- $s_h \in (0, 1]$: the fraction of uninfected females' eggs fertilized by infected males that do not hatch, due to the cytoplasmic incompatibility (CI);
- K: carrying capacity, A: diffusion coefficient.

Parameters δ, s_f, s_h have been estimated in several cases and can be found in the literature (see [26] and references therein). We always assume that $s_f < s_h$ (in practice, s_f is close to 0 while s_h is close to 1).

Several models have been proposed using these parameters. In the present study, a system of Lotka-Volterra type is proposed, where the parameter $\epsilon > 0$ is used to characterize the high fertility as follows

$$\partial_t n_i^\epsilon - A\partial_{xx} n_i^\epsilon = (1 - s_f)\frac{b_u}{\epsilon} n_i^\epsilon \left(1 - \frac{n_i^\epsilon + n_u^\epsilon}{K}\right) - \delta d_u n_i^\epsilon, \tag{2.30a}$$

$$\partial_t n_u^\epsilon - A\partial_{xx} n_u^\epsilon = \frac{b_u}{\epsilon} n_u^\epsilon \left(1 - s_h \frac{n_i}{n_i^\epsilon + n_u^\epsilon}\right)\left(1 - \frac{n_i^\epsilon + n_u^\epsilon}{K}\right) - d_u n_u^\epsilon, \tag{2.30b}$$

where the reaction term describes birth and death. The factor $\left(1 - s_h \frac{n_i^\epsilon}{n_i^\epsilon + n_u^\epsilon}\right)$ characterizes the cytoplasmic incompatibility. Indeed, when $s_h = 1$, no egg of uninfected females fertilized by infected males can hatch, that is, there is complete cytoplasmic incompatibility. The factor becomes $\frac{n_u^\epsilon}{n_i^\epsilon + n_u^\epsilon}$ which means the birth rate of uninfected mosquitoes depends on the proportion of uninfected parents because only an uninfected couple can lay uninfected eggs. Whereas, $s_h = 0$ means that all the eggs of uninfected females hatch. In this case, the factor $\left(1 - s_h \frac{n_i^\epsilon}{n_i^\epsilon + n_u^\epsilon}\right)$ becomes 1, so the growth rate of uninfected population is not altered by the pressure of the infected one.

In paper [201], the same model was studied in the entire space $\mathbb{R}$. In that case, the system (2.30) has exactly two stable equilibria, namely the *Wolbachia* invasion steady state and the *Wolbachia* extinction steady state. In this paper, the authors show that when $\epsilon \to 0$ and the reaction terms satisfy some appropriate conditions, the proportion $p^\epsilon = \frac{n_i^\epsilon}{n_i^\epsilon + n_u^\epsilon}$ converges to the solution p^0 of the scalar equation $\partial_t p^0 - A\partial_{xx} p^0 = f(p^0)$, with the reaction term

$$f(p) = \delta d_u s_h \frac{p(1-p)(p-\theta)}{s_h p^2 - (s_f + s_h)p + 1}, \tag{2.31}$$

with $\theta = \frac{s_f + \delta - 1}{\delta s_h}$. We will always assume that $s_f + \delta(1 - s_h) < 1$, so $\theta \in (0, 1)$, and f is a bistable function on $(0, 1)$. The two stable steady states 1 and 0 of (2.1) correspond to the success or failure of the biological control using *Wolbachia*.

2.4.2 Mosquito population in presence of migration

In this study, the migration of mosquitoes is taken into account. Typically, the inflow of wild uninfected mosquitoes and the outflow of the infected ones may influence the efficiency of the method using *Wolbachia*. Here, to model this effect, system (2.30) is considered in a bounded domain with appropriate boundary conditions to characterize the migration of mosquitoes. In one-dimensional space, we consider $\Omega = (-L, L)$ and Robin boundary conditions as in (2.4) at points $x = -L$, and $x = L$

$$\frac{\partial n_i^\epsilon}{\partial \nu} = -D_b(n_i^\epsilon - n_i^{\text{ext},\epsilon}), \tag{2.32a}$$

$$\frac{\partial n_u^\epsilon}{\partial \nu} = -D_b(n_u^\epsilon - n_u^{\text{ext},\epsilon}), \tag{2.32b}$$

where $n_i^{\text{ext},\epsilon}, n_u^{\text{ext},\epsilon}$ do not depend on t and x but depend on parameter $\epsilon > 0$. Denote $p^\epsilon = \frac{n_i^\epsilon}{n_i^\epsilon + n_u^\epsilon}, n^\epsilon = \frac{1}{\epsilon}\left(1 - \frac{n_i^\epsilon + n_u^\epsilon}{K}\right)$. In Appendix B, we prove that when $\epsilon \to 0$, up to extraction of sub-sequences, n^ϵ converges weakly to $n^0 = h(p^0)$ for some explicit function h, and p^ϵ converges strongly towards solution p^0 of (2.1) where p^{ext} is the limit of $\frac{n_i^{\text{ext},\epsilon}}{n_i^{\text{ext},\epsilon} + n_u^{\text{ext},\epsilon}}$ when $\epsilon \to 0$, and the reaction term f as in (2.31). Function f satisfies Assumptions 2.2.1 and 2.2.2, so the results in Theorem 2.2.1 and 2.2.3 can be applied to this problem. By changing the spatial scale, we can normalize the diffusion coefficient into $A = 1$.

In this application, the parameters L, D_b, p^{ext} correspond to the size of Ω, the migration rate of mosquitoes, and the proportion of infected mosquitoes surrounding the boundary. The main results in the present paper give information about the existence and stability of equilibria depending upon different conditions for these parameters. Especially, from Corollary 2.2.1, we obtain that when the size L of the domain is small, there exists a unique equilibrium for this problem and its values depend on the proportion of mosquitoes carrying *Wolbachia* outside the domain (p^{ext}). More precisely, when p^{ext} is small (i.e., $p^{\text{ext}} \leqslant \alpha_1$), the solution of (2.1) converges to the steady-state solution close to 0, which corresponds to the extinction of mosquitoes carrying *Wolbachia*. Therefore, in this situation, the replacement strategy fails because of the migration through the boundary. Otherwise, when the proportion outside the domain is high (i.e., $p^{\text{ext}} \geqslant \alpha_2$), then the long-time behavior of solutions of (2.1) has values close to 1, which means that the mosquitoes carrying *Wolbachia* can invade the whole population.

Table 2.2 – Parameters for the numerical illustration

Parameters	b_u	d_u	δ	σ	s_f	s_h
Values	1.12	0.27	$\frac{10}{9}$	1	0.1	0.8

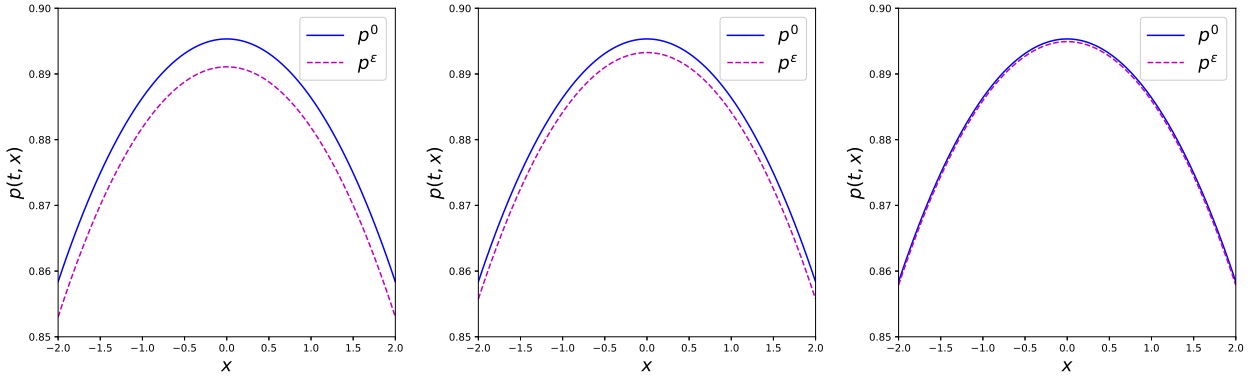

(a) $\epsilon = 0.1$ (b) $\epsilon = 0.05$ (c) $\epsilon = 0.01$

Figure 2.4 – Convergence of p^ϵ to p^0 as ϵ goes to zero. The solid lines represent the solution $p^0(t,x)$ of (2.1) at $t = 50$ days. The dashed lines represent the proportion $p^\epsilon = \frac{n_i^\epsilon}{n_i^\epsilon + n_u^\epsilon}$ of solution n_i^ϵ, n_u^ϵ of system (2.30), (2.32) at $t = 50$.

2.4.3 Numerical illustration

In this section, we present the numerical illustration for the above results. Parameters are fixed according to biologically relevant data (adapted from [83]). Time unit is the day, and parameters per day are in Table 2.2. Then, the reaction term f in (2.31) has $\theta = 0.2375$, $\beta \approx 0.3633, \alpha_1 \approx 0.12, \alpha_2 \approx 0.7$. As proposed in section 3 of the modeling article [162], we may pick the value $830m^2$ per day for the diffusivity of *Aedes* mosquitoes. Choose $A = 1$, so the x-axis unit in the simulation corresponds to $\sqrt{830/1} \approx 29$ m.

In the following parts, we check the convergence of p^ϵ when $\epsilon \to 0$ in 2.4.3. In 2.4.3, corresponding to different parameters, we compute numerically the solutions of (2.1) and (2.2) to check their existence and stability.

Convergence to the scalar equation

Consider a mosquito population with a large fecundity rate, that is, $\epsilon \ll 1$. Model (2.30) with boundary condition in (2.32) takes into account the migration of mosquitoes.

Fix $D_b = 0.05, p^{\text{ext}} = 0.1$ and $L = 2$, the system (2.30), (2.32) is solved numerically thanks to a semi-implicit finite difference scheme with 3 different values of the parameters ϵ. The initial data are chosen such that $n_i^\epsilon(t = 0) = n_u^\epsilon(t = 0)$, that is, $p^{\text{init}} = 0.5$. In Figure 2.4, at time $t = 50$ days, the numerical solutions of (2.1) are plotted with blue solid lines, the proportions $p^\epsilon = \frac{n_i^\epsilon}{n_i^\epsilon + n_u^\epsilon}$ are plotted with dashed lines. We observe that when ϵ goes to 0, the proportion p^ϵ converges to the solution p^0 of system (2.1).

Steady-state solutions

For the different values of p^{ext}, the values of the integrals $\mathcal{F}_1$ and $\mathcal{F}_2$ as functions of $p(L)$ in (2.20) and (2.23) are plotted in Figure 2.5. For fixed values of D and p^{ext}, Figure 2.5 can play the role of bifurcation diagrams that show the relation between the value $p(L)$ of symmetric solutions p and parameter L. Then, we can obtain the critical values of parameter L. Next, we compute numerically the (SM) steady-state solutions of (2.1) with different values of $L > 0, D_b > 0, p^{\text{ext}} \in (0, 1)$.

Numerical method: To approximate the (SM) steady-state solution, we use the Newton method to solve nonlinear equations and follow these steps:

- Step 1: Solve $L = \mathcal{F}_i(p(L))$ for $i = 1$ or 2, and obtain the values of $p(L)$.
- Step 2: Find $p(0)$ by solving (2.17).

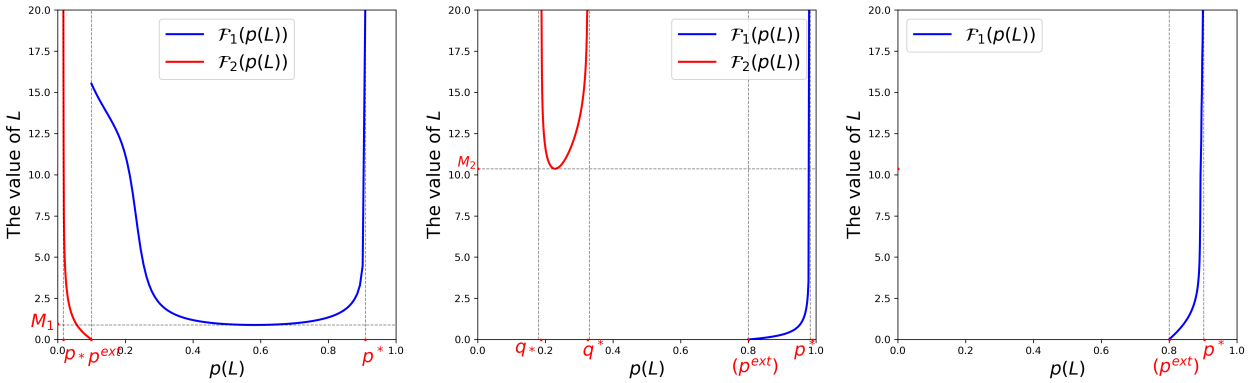

(a) $p^{\text{ext}} = 0.1, D_b = 0.05$ (b) $p^{\text{ext}} = 0.8, D_b = 0.05$ (c) $p^{\text{ext}} = 0.8, D_b = 0.5$

Figure 2.5 – The blue and red solid lines represent respectively functions $\mathcal{F}_1$ and $\mathcal{F}_2$ of $p(L)$

.

◦ Step 3: For each x in $(0, L)$, interpolate $p(x)$ by solving $x = \displaystyle\int_{p(0)}^{p(x)} \frac{(-1)^k ds}{\sqrt{2F(p(0)) - 2F(s)}}$ due to (2.16) with $k = 1$ if p is decreasing and $k = 2$ if p is increasing on $(0, x)$.

The construction of a non-(SM) steady-state solution is more sophisticated since it is hard to find $p(L)$ for a fixed L like in step 1. We presented a numerical non-(SM) equilibrium in Figure 2.6c where we first fixed a value $p(L)$. Then similarly to step 2, we solved (2.27) to find all the extreme values of p. Finally, we applied step 3 with $p(0)$ replaced by $p_{\min}$ or $p_{\max}$.

We also plot the time dynamics of the solution $p^0(t, x)$ of (2.1) at $t = 10, 20, 40, 60, 100$ to verify the asymptotic stability of steady-state solutions. Next, we consider different values of p^{ext} and present our observation in each case.

- **Case 1:** $p^{\text{ext}} = 0.1 < \alpha_1$.

For $D_b = 0.05$ fixed, we observe in Figure 2.5a that for any $L > 0$, equation $\mathcal{F}_2(p(L)) = L$ always admits exactly one solution. Thus, there always exists one (SI) steady-state solution with small values. We approximate that

$$M_d(0.1, 0.05) = M_1 \approx 0.8819, \quad M_*(0.1, 0.05) \approx 8.625.$$

Also from Figure 2.5a, we observe that when $L = M_1$, a bifurcation occurs and (2.1) admits an (SD) steady-state solution, and when $L > M_1$ one can obtain two (SD) solutions. Moreover, when $L \geqslant M_*$, there exist non-symmetric steady-state solutions. We do numerical simulations for two values of L as follows.

For $L = 0.5 < M_1$, the unique equilibrium $\overline{p}_{21}$ is (SI) and has values close to 0 (see Figure 2.6a). Solution p^0 of (2.1) with any initial data converges to $\overline{p}_{21}$. This simulation is coherent with the asymptotic stability that we proved in Corollary 2.2.1.

For $L = 8.96 > M_* > M_1$, together with $\overline{p}_{21}$, there exist two more (SD) steady-state solutions, namely $\overline{p}_{11}$, $\overline{p}_{12}$, (see Figure 2.6b). This plot shows that these steady-state solutions are ordered, and the time-dependent solutions converge to either the largest one $\overline{p}_{11}$ or the smallest one $\overline{p}_{21}$, while $\overline{p}_{12}$ with intermediate values is not an attractor. In Figure 2.6c, we find numerically a non-symmetric solution $\overline{p}$ of (2.2) corresponding to orbit T_3 as in Figure 2.3a. Let the initial value $p^{\text{init}} \equiv \overline{p}$, then we observe from Figure 2.6c that p^0 still converges to the symmetric equilibrium $\overline{p}_{21}$.

Moreover, the value λ_1 of Theorem 2.2.3 in this case is approximately equal to 0.0063. We also obtain that for any $x \in (-L, L)$,

$$f'(\overline{p}_{11}(x)) < 0, \quad f'(\overline{p}_{21}(x)) < 0, \quad f'(\overline{p}_{12}(x)) > 0.0462, \quad f'(\overline{p}(x)) > 0.022.$$

Therefore, by applying Theorem 2.2.3, we deduce that the steady-state solutions $\overline{p}_{11}, \overline{p}_{21}$ are asymptotically stable, $\overline{p}_{12}$ and the non-symmetric equilibrium $\overline{p}$ are unstable. Thus, the numerical simulations in Figure 2.6 are coherent to the theoretical results that we proved.

- **Case 2:** $p^{\text{ext}} = 0.8 > \alpha_2 > \beta$.

In this case, we obtain $D_* \approx 0.16$. We present numerical illustrations for two cases: $D_b = 0.05 < D_*$ and $D_b = 0.5 > D_*$.

◦ For $D_b = 0.05 < D_*$, we have $M_i(0.8, 0.05) = M_2 \approx 10.3646$ (see Figure 2.5b).

For $L = 2 < M_2$, the unique equilibrium $\overline{p}_{11}$ is (SD) and has values close to 1 (see Figure 2.7a). The time-dependent solution p^0 of (2.1) with any initial data converges to $\overline{p}_{11}$. This simulation is coherent to the

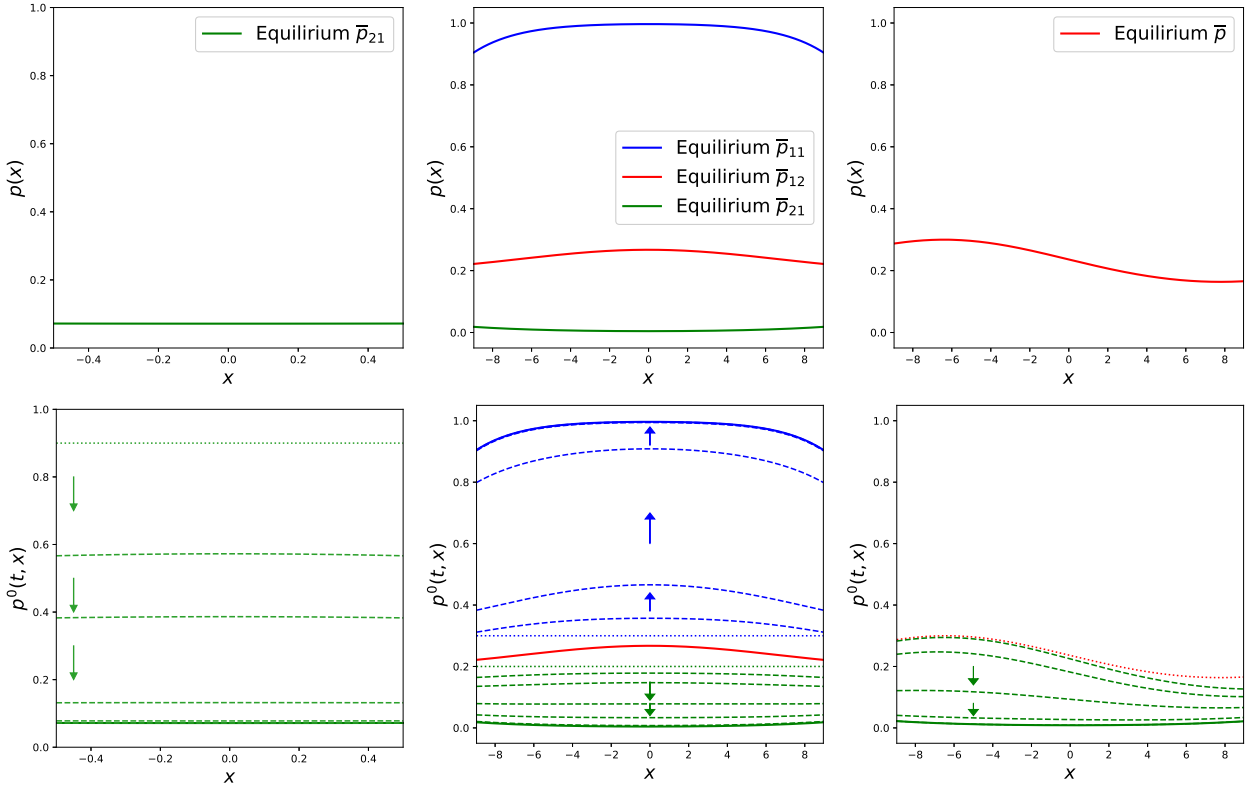

(a) $L = 0.5 < M_1$ (b) $L = 8.96 > M_* > M_1$ (c) $L = 8.96 > M_* > M_1$

Figure 2.6 – Case $p^{\text{ext}} = 0.1, D_b = 0.05$: The solid lines illustrate the steady-state solutions. The dotted lines show the initial data of problem (2.1). The dashed lines represent the solution $p^0(t,x)$ with $t \in \{10, 20, 40, 60, 100\}$. The color of the dashed lines corresponds to the color of the equilibrium that they converge to.

asymptotic stability we obtained in Corollary 2.2.1.

For $L = 12 > M_2$, together with $\overline{p}_{11}$, there exist two more (SI) steady-state solutions, namely $\overline{p}_{21}$, $\overline{p}_{22}$, and they are ordered (see Figure 2.7b). In this case, we obtain approximately that $\lambda_1 \approx 0.0063$ and for any $x \in (-L, L)$, one has

$$f'(\overline{p}_{11}(x)) < 0, \quad f'(\overline{p}_{21}(x)) \in (-0.0398, 0.0368), \quad f'(\overline{p}_{22}(x)) \in (-0.0195, 0.0673).$$

By sufficient conditions in Theorem 2.2.3, we obtain that $\overline{p}_{11}$ is asymptotically stable but we can not conclude the stability for $\overline{p}_{21}$ and $\overline{p}_{22}$. The time dynamics of p^0 in Figure 2.7b suggests that the smallest steady-state solution $\overline{p}_{21}$ is asymptotically stable and $\overline{p}_{22}$ seems to be unstable.

◦ For $D_b = 0.5 > D_*$, function $\mathcal{F}_2$ is not defined (see Figure 2.5c), so problem (2.2) admits only one (SD) steady-solution, and we obtain that it is unique and asymptotically stable (see Figure 2.7c).

2.5 Conclusion and perspectives

We have studied the existence and stability of steady-state solutions with values in $[0, 1]$ of a reaction-diffusion equation

$$\partial_t p - \partial_{xx} p = f(p)$$

on an interval $(-L, L)$ with cubic nonlinearity f and inhomogeneous Robin boundary conditions

$$\frac{\partial p}{\partial \nu} = D_b(p - p^{\text{ext}}),$$

where constant $p^{\text{ext}} \in (0, 1)$ is an analogue of p, and constant $D_b > 0$. We have shown how the analysis of this problem depends on the parameters p^{ext}, D_b, and L. More precisely, the main results say that there always exists a symmetric steady-state solution that is monotone on each half of the domain. For p^{ext} large, the value of this steady-state solution is close to 1, otherwise, it is close to 0. Besides, the larger value of L, the more steady-state solutions this problem admits. We have found the critical values of L so that when the parameters surpass these critical values, the number of steady-state solutions increases. We also provided some sufficient

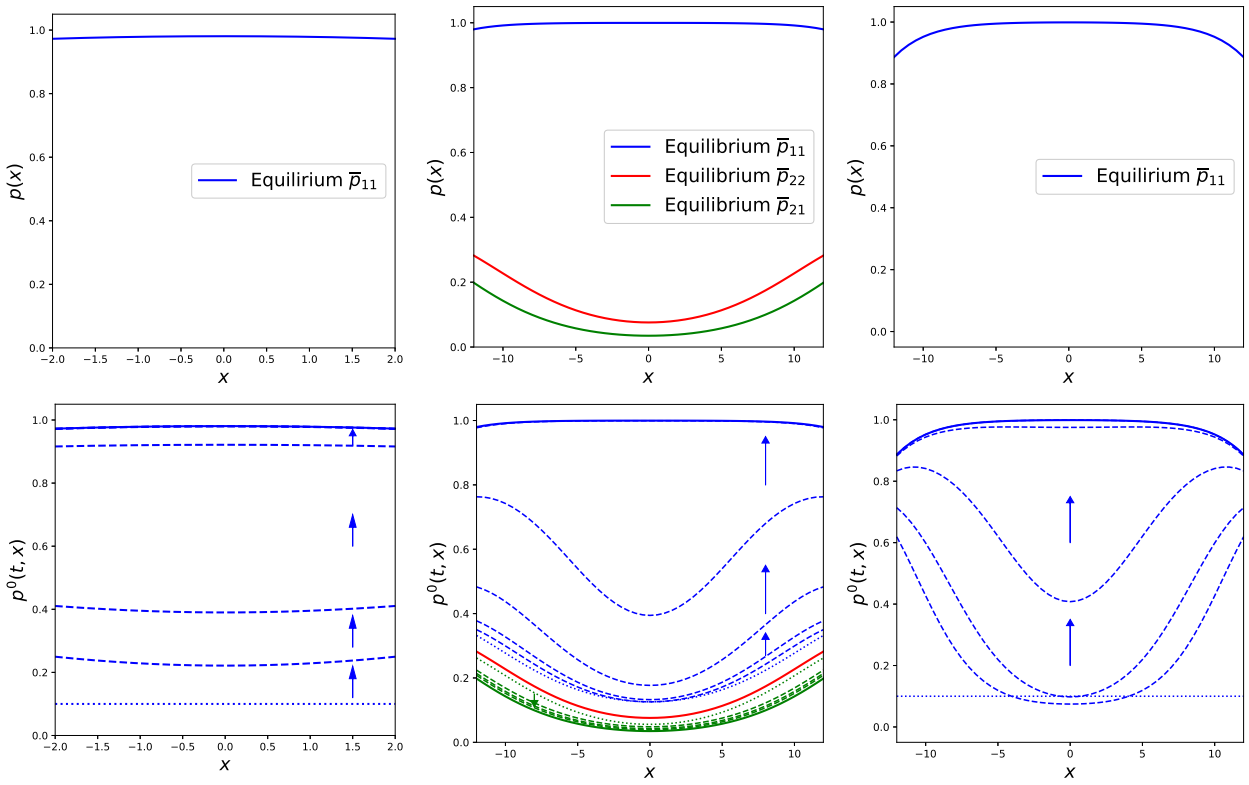

(a) $L = 2, D_b = 0.05 < D_*$ (b) $L = 12, D_b = 0.05 < D_*$ (c) $L = 12, D_b = 0.5 > D_*$

Figure 2.7 – Case $p^{\text{ext}} = 0.8$: The solid lines illustrate the steady-state solutions. The dotted lines show the initial data of problem (2.1). The dashed lines represent the solution $p^0(t,x)$ with $t \in \{10, 20, 40, 60, 100\}$. The color of the dashed lines corresponds to the color of the equilibrium that they converge to.

conditions for the stability and instability of the steady-state solutions.

We presented an application of our results on the control of dengue vector using *Wolbachia* bacterium that can be transmitted maternally. Since *Wolbachia* can help reduce vectorial capacity of the mosquitoes, the main goal of this method is to replace wild mosquitoes by mosquitoes carrying *Wolbachia*. In this application, we considered p as the proportion of mosquitoes carrying *Wolbachia* and used the equation above to model the dynamic of the mosquito population. The boundary condition describes the migration through the border of the domain. This replacement method only works when p can reach an equilibrium close to 1. Therefore, the study of the existence and stability of the steady-state solution close to 1 is meaningful and depends strongly on the parameters p^{ext}, D_b, and L. In realistic situations, the proportion p^{ext} of mosquitoes carrying *Wolbachia* outside the domain is usually low. Using the theoretical results proved in this article, one sees that, to have major chances of success, one should try to treat large regions (L large), well isolated (D_b small) and possibly applying a population replacement method in a zone outside Ω (to increase p^{ext} by reducing its denominator).

As a natural continuation of the present work, higher dimension problems and more general boundary conditions can be studied. In more realistic cases, p^{ext} can be considered to depend on space and the periodic solutions can be the next problem for our study. Besides, when an equilibrium close to 1 exists and is stable, one may consider multiple strategies using multiple releases of mosquitoes carrying *Wolbachia*. To optimize the number of mosquitoes released to guarantee the success of this method under the difficulties enlightened by this paper is an interesting problem for future works.

Chapter 3

A control strategy for the Sterile Insect Technique using exponentially decreasing releases to avoid the hair-trigger effect

This chapter is a joint work with Alexis Léculier. It was published as an article in Mathematical Modelling of Natural Phenomena [126].

Abstract. In this paper, we introduce a control strategy for applying the Sterile Insect Technique (SIT) to eliminate the population of *Aedes* mosquitoes which are vectors of various deadly diseases like dengue, zika, chikungunya... in a wide area. We use a system of reaction-diffusion equations to model the mosquito population and study the effect of releasing sterile males. Without any human intervention, and due to the so-called *hair-trigger effect*, the introduction of only a few individuals (eggs or fertilized females) can lead to the invasion of mosquitoes in the whole region after some time. To avoid this phenomenon, our strategy is to keep releasing a small number of sterile males in the treated zone and move this release forward with a negative forcing speed c to push back the invasive front of wild mosquitoes. By using traveling wave analysis, we show in the present paper that the strategy succeeds in repulsing the population while consuming a finite amount of mosquitoes in any finite time interval even though we treat a moving half-space $\{x > ct\}$. Moreover, we succeed in constructing a 'forced' traveling wave for our system moving at the same speed as the releases. We also provide some numerical illustrations for our results.

3.1 Introduction

3.1.1 The biological motivation

Pest and disease vector controls have become a global issue because of the spread of these species all around the world causing crop losses and disease epidemics. For example, the oriental fruit fly is a serious pest of a wide variety of fruit crops in Asia and has also invaded a number of other countries and is a very damaging pest wherever it occurs. It was first detected in French Polynesia in 1996 and invaded Africa in 2004. Few individuals have been detected in Italy in 2018 and hence southern Europe is at high risk. Similarly, according to the World Health Organization, the global incidence of dengue has grown dramatically with about half of the world's population now at risk. It was first identified in the 1950s during dengue epidemics in Philippines and Thailand due to the travel and invasion of its vectors, female mosquitoes of the species *Aedes aegypti* and *Ae. albopictus*. They are also vectors of chikungunya, yellow fever, Zika viruses..., and, until now, there is neither effective treatment nor vaccine for these diseases. So pest/vector controls play an important role in getting rid of these problems. The classical control method based on insecticides induces resistance, which reduces its own efficiency and is detrimental to the environment. Among others, the Sterile Insect Technique (SIT) aiming at reducing the size of the insect population recently gathered much attention. The SIT is a biological method where people release sterile individuals (modified in laboratories) of pest species to introduce sterility into the wild population, and thus control it (see [73] for an overall presentation of SIT). It is a promising control method against many agricultural pests and disease vectors, most notably screw worms and fruit flies (see [73]), and recently mosquitoes of genus *Aedes*. This technique has been applied successfully for *Aedes* mosquitoes in the field in many different countries, for instance, in Italy [51], Cuba [88], and China [228]. In our work, we focus on applying SIT in a vast region using the idea of the "rolling carpet": a large number of sterile insects are released near the front of the invasion, and as soon as this area is free from wild insects, we move the front of release and

continue to release a few sterile individuals in the already treated area (see [73]). The purpose of these small releases at the back is to prevent reinvasion by the so-called *hair-trigger effect* (where the existence of just a few individuals leads to the total invasion of the territory). The notion of 'hair-trigger' was first introduced in [23] to refer to the persistence in the long-time of the solution with respect to any non-trivial initial data. In our case, it has been observed in [73] that the mosquitoes reinvade the treated territory without this small amount of releases of sterile males. By implementing such a process, we succeed in eradicating wild insects, preventing reinvasion, and keeping the number of released sterile insects below a threshold in a finite time interval $[0, T]$. It is in our interest to consume as few sterile males as possible since it is one of the main costs of the strategy. We propose in the present work to study a mathematical model of such release strategy used in the field for *Aedes* mosquitoes.

3.1.2 Our model and the spreading results

Following ideas in e.g. [12], [200], we model the mosquito population by a partially degenerate reaction-diffusion system for time $t > 0$, position $x \in \mathbb{R}$:

$$\partial_t E = bF\Big(1 - \frac{E}{K}\Big) - (\nu_E + \mu_E)E, \tag{3.1a}$$

$$\partial_t F - D\partial_{xx} F = \rho\nu_E E \frac{M}{M + \gamma_s M_s} - \mu_F F, \tag{3.1b}$$

$$\partial_t M - D\partial_{xx} M = (1-\rho)\nu_E E - \mu_M M, \tag{3.1c}$$

$$\partial_t M_s - D\partial_{xx} M_s = \Lambda(t,x) - \mu_s M_s, \tag{3.1d}$$

$$(E, F, M, M_s)(t = 0, x) = (E^0, F^0, M^0, M_s^0)(x). \tag{3.1e}$$

In this system, we have:

- E, M, M_s and F denote respectively the number of mosquitoes in the aquatic phase, adult males, sterile adult males and fertilized adult females depending on time t and position x;
- $\Lambda(t,x)$ is the number of sterile mosquitoes that are released at position x and time t;
- the fraction $\frac{M}{M+\gamma_s M_s}$ corresponds to the probability that a female mates with a fertile male, and parameter γ_s models the competitivity of sterile males;
- $b > 0$ is a birth rate; $\mu_E > 0$, $\mu_M > 0$, and $\mu_F > 0$ denote the death rates for the mosquitoes in the aquatic phase, for adult males and for adult females, respectively;
- K is an environmental capacity for the aquatic phase, accounting also for the intraspecific competition;
- $\nu_E > 0$ is the rate of emergence;
- $D > 0$ is the diffusion rate;
- $\rho \in (0,1)$ is the probability that a female emerges, then $(1-\rho)$ is the probability that a male emerges;
- the initial data $(E^0, F^0, M^0, M_s^0) \geqslant (0,0,0,0)$ (component by component).

We introduce the basic offspring number as follows

$$\mathcal{R}_0 = \frac{b\rho\nu_E}{\mu_F(\nu_E + \mu_E)}. \tag{3.2}$$

When there is no regulation of sterile males, our model becomes

$$\partial_t E = bF\Big(1 - \frac{E}{K}\Big) - (\nu_E + \mu_E)E, \tag{3.3a}$$

$$\partial_t F - D\partial_{xx} F = \rho\nu_E E - \mu_F F, \tag{3.3b}$$

$$\partial_t M - D\partial_{xx} M = (1-\rho)\nu_E E - \mu_M M, \tag{3.3c}$$

It is obvious that $(0,0,0)$ is an equilibrium of (3.3). When the basic offspring number $\mathcal{R}_0 > 1$, this system has a second equilibrium (E^*, F^*, M^*) where

$$E^* = K\frac{b\rho\nu_E - \mu_F(\nu_E + \mu_E)}{b\rho\nu_E} > 0, \tag{3.4a}$$

$$F^* = K\frac{b\rho\nu_E - \mu_F(\nu_E+\mu_E)}{b\mu_F} > 0, \tag{3.4b}$$

$$M^* = K\frac{1-r}{r}\frac{b\rho\nu_E - \mu_F(\nu_E+\mu_E)}{b\mu_M} > 0. \tag{3.4c}$$

Note that, the positive equilibrium (E^*, F^*, M^*) is stable and $(0,0,0)$ is unstable. Thus, in the case without sterile males, the following result shows the spread of the population toward the positive equilibrium and provides the existence of the spreading speed for the solution of the system (3.3).

Proposition 3.1.1. *If the basic offspring number $\mathcal{R}_0 > 1$, then there exists a spreading speed $c^* > 0$ such that for any positive ε, the solution (E,F,M) of system (3.3) satisfies*

- *if the initial data (E^0,F^0,M^0) is compactly supported and $0 \leqslant (E^0,F^0,M^0) < (E^*,F^*,M^*)$, then*

$$\lim_{t\to+\infty}\left[\max_{|x|\geqslant t(c^*+\varepsilon)}\max(E,F,M)(t,x)\right] = 0, \tag{3.5}$$

- *if the initial data $(E^0,F^0,M^0) < (E^*,F^*,M^*)$ and if there exists a set with a positive measure $\Omega \subset \mathbb{R}$, such that $\max(\min_{x\in\Omega}E^0, \min_{x\in\Omega}F^0) > 0$ then*

$$\lim_{t\to+\infty}\left[\max_{|x|\leqslant t(c^*-\varepsilon)}\max(E^*-E, F^*-F, M^*-M)(t,x)\right] = 0. \tag{3.6}$$

We present in Appendix C a proof for this result based on the result in the work of Lui [139] with an extension for reaction-diffusion system in Weinberger et al. [219] for a monostable system. We also underline that, with only females at the initial time (i.e. $E^0 \equiv 0$, $M^0 \equiv 0$, and $F^0 > 0$ in some ball), invasion still occurs. This is due to the fact that in our model we consider F to be the fertilized females. Therefore, if $F^0 > 0$ on a set with a positive measure, then the same holds for the aquatic phase at any $t > 0$ in the whole domain $\mathbb{R}$, and the dynamics of invasion start to occur.

The main result in the present work shows that when a release function of sterile males Λ moving with a certain speed $c < 0$ is imposed in the system, we can succeed in suppressing the mosquitoes and avoiding reinvasion. In the present work, we consider the release function

$$\Lambda(t,x) = \begin{cases} 0 & \text{for } x - ct \leqslant 0, \\ Ae^{-\eta(x-ct)} & \text{for } x - ct > 0, \end{cases} \tag{3.7}$$

with constants $A > 0$, $\eta > 0$.

Theorem 3.1.1. *If the basic offspring number $\mathcal{R}_0 > 1$, $(E^0,F^0,M^0) \leqslant (E^*,F^*,M^*)$, $(E^0,F^0,M^0)_{|\mathbb{R}_+} = (0,0,0)$ and $M_s^0 \in L^1(\mathbb{R})$ such that $M_s^0 \geqslant \phi_s$, where ϕ_s is the solution of*

$$-c\phi_s' - \phi_s'' = Ae^{-\eta x}\mathbb{1}_{\{x>0\}} - \mu_s\phi_s \qquad \text{and} \qquad \phi_s(\pm\infty) = 0$$

then for any speed $c < 0$, there exist $\widetilde{A}_c > 0$, $\widetilde{\eta}_c > 0$ such that for any $A \geqslant \widetilde{A}_c$, $0 < \eta \leqslant \widetilde{\eta}_c$, we have the solution (E,F,M,M_s) of system (3.1) and (3.7) satisfies

$$\lim_{t\to+\infty}\sup_{x>ct}\max(E,F,M)(t,x) = 0.$$

From this result, we can see that if the initial data is compactly supported in $\mathbb{R}_-$ and below (E^*,F^*,M^*), the invasion does not occur: the equilibrium $(0,0,0)$ invades the positive equilibrium (E^*,F^*,M^*). We also remark that the number of sterile males released in the field in a finite time interval $[0,T]$ is $T \times \frac{A}{\eta}$ finite even though the space is infinite. However, if $T \to +\infty$, the total amount of released mosquitoes also tends to $+\infty$. Finally, we point out that in the above results, the number of sterile males released $(A,\ \eta)$ depends on the speed c of the rolling carpet. This can be observed more precisely in the proof in section 3.4 and discussed in section 3.2 with some numerical illustrations. However, finding $A,\ \eta$ that minimizes the number of released mosquitoes each time remains a challenge.

3.1.3 State of the art

Based on biological knowledge, mathematical modeling and numerical simulations can be additional and useful tools to prevent failures, improve protocols, and test assumptions before applying the SIT strategy in the field.

Many works have been done using mean-field temporal models to assess the SIT efficiency for a long-term period (see e.g. [38], [200] and references therein).
Only a few works exist modeling explicitly the spatial component due to the lack of knowledge about vectors in the field. Moreover, from the mathematical point of view, the studies of spatial-temporal models are more sophisticated. A reaction-diffusion equation was first used in [144] to model the spreading of a pest in the SIT model. Then, the model was completed by considering the release of sterile females in [128]. In this article, the author assumed that the same amount of sterile insect is released in the whole field (i.e. $\Lambda \equiv constant$). It follows that if the number of released sterile insects is large enough, the reaction term becomes strictly negative, and the extinction of the wild population follows. However, this hypothesis is unrealistic in a large area since the number of sterile insects to release tends to infinity as the size of the domain increases. The main contribution of our work is to tackle this problem by following what has been done in the field experiment: we assume that the releases are not homogeneous. By considering only releases supported in $\mathbb{R}_+$ with exponential decay, the amount of sterile males released in a finite time interval is constant.
In [185], the authors studied SIT control with barrier effect using a system of two reaction-diffusion equations for the wild and the sterile populations. Recently, a sex-structured system including the aquatic phase of mosquitoes has been studied in [17]. Using the theory of traveling waves, the authors proved, for a similar system to (3.1), the existence of natural invading traveling wave when $\{M_s = 0\}$ and the system is either monostable or bistable. They also provide some numerical implementation of the SIT but only for the bistable case.

In the bistable case, one can release the mosquitoes in a compact set since the equilibrium 0 is stable. The main result in [12] shows that if the initial wild mosquitoes distribution behaves as $1_{\mathbb{R}_-}$ and we release enough sterile males in some compact set $(ct, L + ct)$ with a speed $c < 0$, then the wild population remains close to 0 in the set $\{x > L + ct\}$ thanks to the assumed natural dynamics of the mosquitoes. We also quote [9, 15], which was done before [12] where the authors studied the analogous system of reaction-diffusion equations to (3.1) in a bistable context taking into account the strong Allee effects. They proved that for large enough constant releases in a bounded interval, there exists a barrier that blocks the invasion of mosquitoes. However, for the monostable case, they obtain numerically that there is no blocking. The so-called "hair-trigger effect" makes the monostable case become more complicated since one can not rely on the natural dynamics of the mosquitoes. So the main purpose of the present work is to study an efficient strategy for the SIT to deal with the difficulty in this case.

The control of sterile insect techniques in a bistable context in a bounded domain is studied in [206, 205]. We also quote [45, 11] that focus on the optimal form to stop or repulse an invading traveling wave by spreading a killing agent (such as insecticide). In [45] the authors study the optimal shape of spreading in order to repulse an invasion. In [11], the authors study the optimal shape of spreading in order to block an invasion but consider more constraints on the spreading area than in [45]. The key argument in these works is to consider that the reaction term is bistable. In the present work, we propose a way to deal with the difficulty of the monostable case with a finite amount of control agents (such as sterile insects or insecticides, or other kinds of control) in any finite time interval.

3.1.4 The traveling wave results

Another natural question that arises in the study of our model of reaction-diffusion equations is the existence of a traveling wave solution. First, we study the traveling wave problem for the system (3.3) in which there are no sterile male. Then, by imposing a control function Λ that moves with a speed $c < 0$, we will construct a traveling wave for the main system (3.1) moving with the same speed.

Recall that a traveling wave solution of (3.3) with any speed c is the pair (U, c) where $U = (E, F, M)^T$ and $U(x - ct)$ is a nontrivial and bounded solution of (3.3). We say (U, c) is a wavefront if $U(\pm\infty)$ exist and $U(-\infty) \neq U(+\infty)$. The existence of such wavefronts for reaction-diffusion systems has been studied widely in the literature. In our case, the nonlinearity is monostable and it is well-known that there exists a minimal speed such that the monostable system admits traveling wave solutions with any speed larger than this minimum value. For example, in the book [214], the authors studied the existence of minimal speed and the stability of wavefronts for the non-degenerate system. However, our systems are partially degenerate because the first stage E is quiescent (does not diffuse). The paper [77] studied monotone wavefronts for partially degenerate systems and they proved that the spreading speed of the solution is the minimal wave speed of monotone wavefronts in the monostable cooperative case. The authors of [17] proved the same result for a similar system to (3.3) and for the sake of completeness, we present it in the following

Proposition 3.1.2. *Let c^* be defined in Proposition 3.1.1, then for each $c_+ \geqslant c^*$, system (3.3) has a non-increasing wavefront $U(x - c_+t)$ connecting (E^*, F^*, M^*) and $(0, 0, 0)$. While for any $c_+ \in (0, c^*)$, there is no wavefront connecting (E^*, F^*, M^*) and $(0, 0, 0)$.*

The general system (3.1) (with $M_s > 0$) is not cooperative at first glance. Some works in the recent literature have tackled the lack of comparison principle for non-cooperative Fisher-KPP systems (see e.g. [92, 91, 90]). However, due to the fact that the system (3.1) in the present paper is partially degenerate, that is, it does not satisfy that $\min \mathbf{D}_{ii} > 0$ where $\mathbf{D}$ is the diffusive matrix, we can not apply these results in our work. Fortunately, the system (3.1) can be put in the setting of cooperative systems by the change of variable ($\widetilde{M_s} = C - M_s$ with C a large constant). With this change of variable, we define a new order for the solutions (E, F, M, M_s) of (3.1) such that $(E^1, F^1, M^1, M_s^1) \geqslant (E^2, F^2, M^2, M_s^2)$ if $E^1 \geqslant E^2,\ F^1 \geqslant F^2,\ M^1 \geqslant M^2,\ M_s^1 \leqslant M_s^2$. In section 3.4.1, we present more precisely the comparison principle used in our problem.

One of the main interests of this article is the establishment of a 'forced' traveling wave solution for (3.1) with a control function Λ as in (3.7). Dealing with the whole system of ODE-PDE like (3.1) is by no means an easy task, so our first idea is to try to simplify the system to a single reaction-diffusion equation by adding some assumptions and then find a general strategy to study the full model. When we assume that the equilibrium of the aquatic phase is attained instantaneously (i.e. $\partial_t E = 0$) then from the first equation of (3.1), one has $E = \dfrac{bF}{b\frac{F}{K} + \nu_E + \mu_E}$. Thus, if the number of females F is equal to the number of males M, and the sterile males are assumed to be equal to Λ in the treating time interval $[0, T]$, using the second equation of (3.1), we end up with only a single equation :

$$\partial_t F - D\partial_{xx} F = \frac{F}{F + \Lambda} \frac{bF}{\frac{bF}{K} + \nu_E + \mu_E} - \mu_F F. \tag{3.8}$$

The model of a scalar reaction-diffusion equation was used widely in the literature studying SIT (see e.g. [128], [229]) or in other contexts, for e.g. in climate change [33], [34]. In our case, the source term $\Lambda(t, x)$ moving with a certain speed $c < 0$, we can construct the 'forced' traveling wave solution of (3.8) moving with the same speed. Equation (3.8) having the form $\partial_t u - \partial_{xx} u = f(x - ct, u)$ with $f(s, u) : \mathbb{R} \times \mathbb{R}_+ \to \mathbb{R}$ is asymptotic of F-KPP type as $s \to \pm\infty$ and was studied in the literature (see e.g. [34] and references therein). In the present work, even if it has been already studied, we provide in Section 3.3 an explicit construction of the 'forced' wave for (3.8) which can help to grasp the general idea of the proof for the whole system.

Indeed, back to the main model of the present paper, we infer from the scalar model that the main difficulty lies in the construction of the super-solution of (3.1). The forced wave has the form $(E, F, M, M_s)(t, x) = (\phi_E, \phi_F, \phi_M, \phi_s)(x - ct)$, where $c < 0$ is the forced speed and $(\phi_E, \phi_F, \phi_M, \phi_s)$ is the profile satisfying

$$-c\phi_E' = b\phi_F\Big(1 - \frac{\phi_E}{K}\Big) - (\nu_E + \mu_E)\phi_E, \tag{3.9a}$$

$$-c\phi_F' - D\phi_F'' = \rho\nu_E\phi_E \frac{\phi_M}{\phi_M + \gamma_s\phi_s} - \mu_F\phi_F, \tag{3.9b}$$

$$-c\phi_M' - D\phi_M'' = (1 - \rho)\nu_E\phi_E - \mu_M\phi_M, \tag{3.9c}$$

$$-c\phi_s' - D\phi_s'' = \phi - \mu_s\phi_s, \tag{3.9d}$$

$$\tag{3.9e}$$

where $\phi(x - ct) = \Lambda(t, x)$ in (3.7). To overcome the difficulty of the construction of the super-solution, we use the fact that the dynamic is governed, in some sense, by F. Thanks to what was observed for the scalar equation, we have a natural candidate to be the super-solution for F. More in detail, by denoting $\overline{\phi_E}, \overline{\phi_F}, \overline{\phi_M}$ respectively the super-solution of ϕ_E, ϕ_F, ϕ_M, we proceed as follows:

- **Step 1.** Fix $\phi_s = \overline{\phi_s} = C_s e^{-\eta x} 1_{\{x>0\}}$. We insert $\overline{\phi_F} = F^*\big(1_{\{x\leqslant 0\}} + 1_{\{x>0\}} e^{-\lambda x}\big)$ in the first equation of (3.9),
- **Step 2.** We prove that with such a $\overline{\phi_F}$ the associated ϕ_E satisfies $\phi_E \leqslant Ce^{-\lambda x}$ for x large enough,
- **Step 3.** We insert $\overline{\phi_E} = E^*\big(1_{\{x\leqslant 0\}} + 1_{\{x>0\}} e^{-\lambda x}\big)$ in the third equation of (3.9),
- **Step 4.** We prove that with such a $\overline{\phi_E}$ the associated ϕ_M satisfies $\phi_M \leqslant Ce^{-\lambda x}$ for x large enough
- **Step 5.** We define $\overline{\phi_M} = M^*\big(1_{\{x\leqslant 0\}} + 1_{\{x>0\}} e^{-\lambda x}\big)$,
- **Step 6.** We prove that $(\overline{\phi_E}, \overline{\phi_F}, \overline{\phi_M}, \phi_s)$ is a super-solution of (3.9), where ϕ_s is the solution of the last equation with $\phi_s(\pm\infty) = 0$.

We present precisely this construction of a super-solution in section 3.4.3 and we also construct a sub-solution in section 3.4.4. Therefore, we obtain the main result:

Table 3.1 – Parameters for the numerical illustration

Parameters	b	K	ν_E	μ_E	μ_F	μ_M	μ_s	γ_s	r	D
Values	10	200	0.08	0.05	0.1	0.14	0.14	1	0.5	0.5

Theorem 3.1.2. *If the basic offspring number $\mathcal{R}_0 > 1$, then for any speed $c < 0$, there exist $\widetilde{A}_c > 0$, $\widetilde{\eta}_c > 0$ such that for any $A \geqslant \widetilde{A}_c$, $0 < \eta \leqslant \widetilde{\eta}_c$, system (3.9) with $\phi(x - ct) = \Lambda(t, x)$ defined in (3.7) admits a solution $(\phi_E, \phi_F, \phi_M, \phi_s)$ such that (ϕ_E, ϕ_F, ϕ_M) converges to (E^*, F^*, M^*) at $-\infty$ and to $(0, 0, 0)$ at $+\infty$.*

We underline that to obtain the exact limits at $-\infty$ is technical since the sterile males diffuse, $\phi_s > 0$ everywhere and the system is not heterogeneous in $\mathbb{R}^-$ (contrary to the super-solutions). Using a perturbation of the equilibrium (E^*, F^*, M^*), we succeed in obtaining a sub-solution $(\underline{\phi_E}, \underline{\phi_F}, \underline{\phi_M}, \underline{\phi_s})$. However, this sub-solution satisfies $\lim\limits_{x\to-\infty}(\underline{\phi_E}, \underline{\phi_F}, \underline{\phi_M}, \underline{\phi_s}) = (E^* - \varepsilon_E, F^* - \varepsilon_F, M^* - \varepsilon_M, \varepsilon_0)$ (where $\varepsilon_{E,F,M,0}$ are small positive constants) so we can not deduce directly the limit of $(\phi_E, \phi_F, \phi_M, \phi_s)$ at $-\infty$. We prove that the solution of (3.9) satisfies the desired limit at $-\infty$ by contradiction (see Section 3.4.5).

3.1.5 Outline of the paper

The outline of the rest of this paper is the following: section 3.2 is devoted to showing some numerical illustrations to support our theoretical results. Next, in section 3.3 we provide the technical details for the results stated for the simplified model. Finally, section 3.4 is devoted to the technical details that allow proving Theorems 3.1.1 and 3.1.2. As mentioned in the introduction, the results for the case without any sterile males (Propositions 3.1.1 and 3.1.2) are applications of former works. For the sake of completeness, we present the proofs in Appendix C.

3.2 Numerical illustrations

3.2.1 The numerical scheme

In this section, we present some numerical illustrations for our theoretical results using a simple finite difference scheme. Since we study the model in one-dimensional space, we use a semi-implicit second-order scheme for space discretization, and a first-order explicit scheme for time discretization, with the time step following a CFL condition. We use Neumann boundary conditions on the boundary of a very large spatial interval. It is well-known that such a spatial domain approximates correctly $\mathbb{R}$, or at least regarding spreading properties of reaction–diffusion systems.

3.2.2 Observations

The values of parameters are chosen following [69] for mosquitoes of species *Aedes albopictus* and presented in Table 3.1. With these parameters, we first verify that the basic offspring number $\mathcal{R}_0 \approx 30.77 > 1$, thus the condition in our theorems is satisfied. The positive equilibrium is $(E^*, F^*, M^*) \approx (193.5, 77.4, 55.3)$.

In our plots, the time unit is a day, space unit is 1 km. We consider the domain $[-50, 50]$ of width 100 km discretized by 500 points, with a 60-day time interval. We show in Figure 3.1 the dynamics of the female population over time and space. In this simulation, the initial data are taken as compactly supported functions. When there is no SIT control, the wave of mosquitoes invades the space (see Figure 3.1a) and approaches the steady state $F^* = 77.4$. This illustrates the invasion phenomenon in Proposition 3.1.1.

To stop this invasion, we keep releasing sterile mosquitoes over time with a release function that decays exponentially on half of the space $\Lambda(t, x) = Ae^{-\eta(x-ct)}\mathbb{1}_{\{x>ct\}}$.

In practice, the number of sterile males to release is usually fixed and one can adjust the speed of the releases to obtain the best result. To illustrate our result, first, we fix $A = 600$, $\eta = 0.2$ and vary the speeds $c \leqslant 0$ to observe the dynamics of mosquitoes while applying SIT. When we do not move the release ($c = 0$), we observe in Figure 3.1b that the wave is blocked near $x = 0$ and cannot pass through the release zone. Then, by moving this release domain to the left with velocity $c = -0.3$, we succeed to push back the wave to the left (see Figure 3.1c), and there is no mosquito behind the releases which illustrates the main result in Theorems 3.1.2 and 3.1.1. However, we observe in Figure 3.1d that if we move the releases faster to the left with velocity $c = -0.7$, there is a reinvasion on the right of the zone. It seems that the faster we move the release domain, the faster we push back the mosquito waves, but we need to release more sterile males in the treated zone to prevent reinvasion.

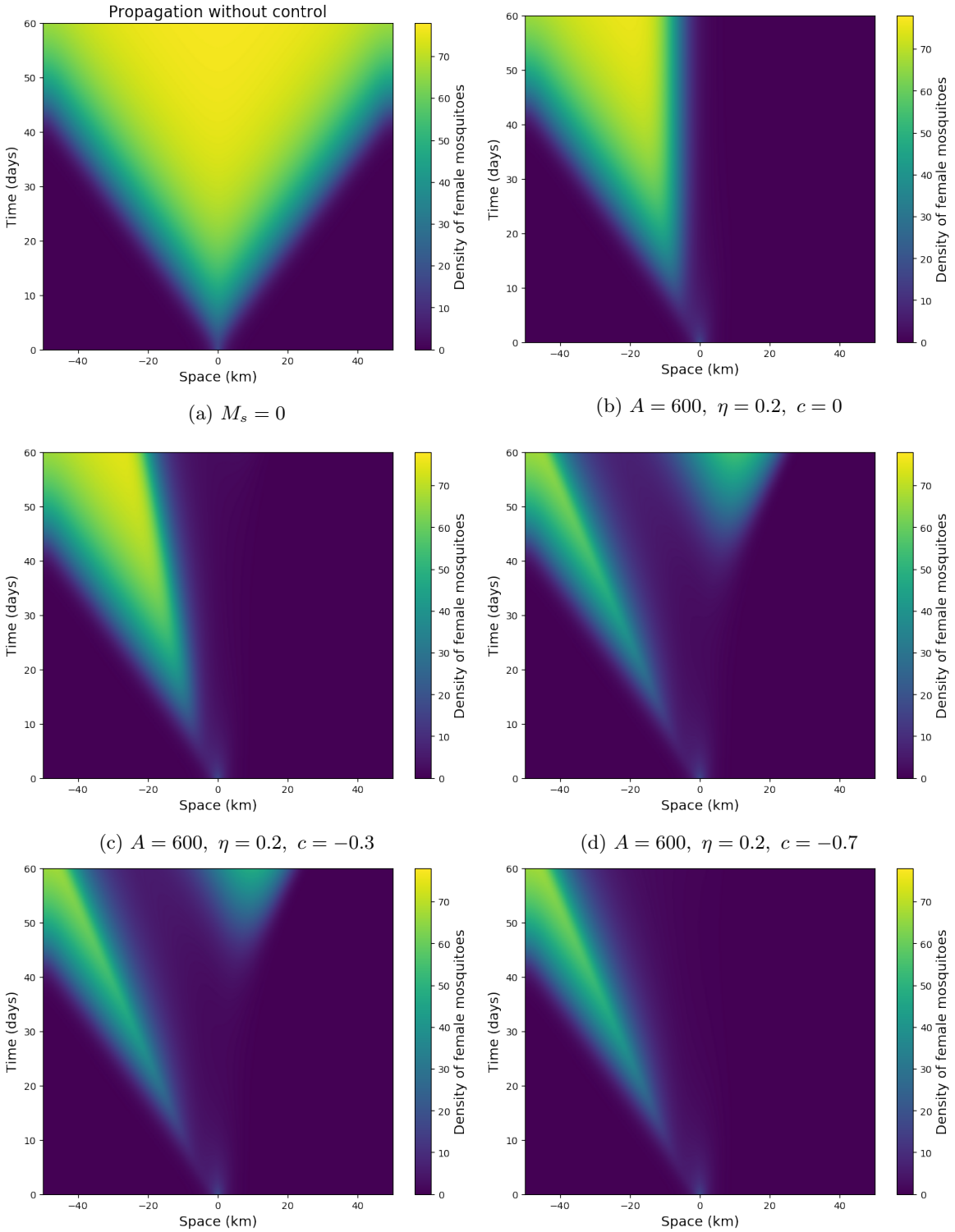

(a) $M_s = 0$

(b) $A = 600,\ \eta = 0.2,\ c = 0$

(c) $A = 600,\ \eta = 0.2,\ c = -0.3$

(d) $A = 600,\ \eta = 0.2,\ c = -0.7$

(e) $A = 800,\ \eta = 0.2,\ c = -0.7$

(f) $A = 800,\ \eta = 0.1,\ c = -0.7$

Figure 3.1 – Dynamics of the female density in system (3.1).

Indeed, when the speed $c = -0.7$ is fixed and the number of sterile males is increased by taking $A = 800$ (see 3.1e), and $\eta = 0.1$ (see 3.1f), one can see that the reinvasion in the treated zone gets slower and disappears.

3.3 Study of the simplified model

3.3.1 The simplified model

From (3.8) we study in this section the following scalar equations:

$$\partial_t u - \partial_{xx} u = \frac{u}{u + \Lambda} \frac{bu}{\frac{bu}{K} + \delta} - \mu u, \qquad \text{for } x \in \mathbb{R}, t > 0, \tag{3.10a}$$

$$u(t = 0, x) = u_0(x). \tag{3.10b}$$

where b, δ, μ, K are parameters, u is the density of mosquitoes, and the function $\Lambda(t, x)$ is the control (i.e. the number of sterile males released). In order to ensure the existence of a non-trivial steady state, we need the following assumption:

Assumption 3.3.1. *The parameters b, δ, μ, K are positive and $b - \mu\delta > 0$.*

We first treat briefly the case without any control (i.e. $\Lambda = 0$) and then we explain how to obtain a similar result to Theorem 3.1.1.

The case $\Lambda \equiv 0$

In this case, when Assumption 3.3.1 holds, the equation has two equilibria $u_0 = 0$ and $u_* = \dfrac{K(b - \mu\delta)}{b\mu} > 0$. The reaction term $f(u) := \dfrac{bu}{\frac{bu}{K} + \delta} - \mu u > 0$ for any $u \in (0, u_*)$, $f'(0) = \dfrac{b}{\delta} - \mu > 0$, and $f(u) < \dfrac{bu}{\delta} - \mu u = f'(0)u$. Then, from the result in [119], there exists a number $c_* > 0$ such that (3.10) possesses "natural" traveling wave solutions $u(t, x) = v_N(x - c_+ t)$ for all speed $c_+ \geqslant c_*$ with v_N solutions of

$$-c_+ v_N' - v_N'' = \frac{bv_N}{\frac{bv_N}{K} + \delta} - \mu v_N, \tag{3.11a}$$

$$v_N(-\infty) = u_*, \quad v_N(+\infty) = 0. \tag{3.11b}$$

Hence, when $t \to +\infty$, the positive state $u = u_*$ invades the extinction state $u = 0$ (see [24, Theorem 4.1] for more details). We recall the following classical result

Proposition 3.3.1. *[24, Theorem 4.1] For any positive initial data u_0, the solution of (3.10) with $\Lambda \equiv 0$ satisfies*

$$\forall c_+ \geqslant c_*, \quad \lim_{t \to +\infty} \sup_{|x| < c_+ t} |u(t, x) - u_*| = 0, .$$

Remark 3.3.1. *Depending on the initial data, the front can go faster and even accelerate (see [97]). But, in any case, the steady-state u_* invades the steady state 0 at least with a speed c_*.*

The controlled case

In this case, function Λ is considered as in (3.7), and we prove the existence of a forced traveling wave moving with the same speed as Λ satisfying

$$-cv' - v'' = \frac{v}{v + \phi} \frac{bv}{\frac{bv}{K} + \delta} - \mu v, \tag{3.12a}$$

$$v(-\infty) = u_*, \quad v(+\infty) = 0, \tag{3.12b}$$

with $\phi(x - ct) = \Lambda(t, x)$ and speed c negative. The result is the following:

Theorem 3.3.1. *For any $c < 0$, there exists constants $\widetilde{A}$, $\widetilde{\eta} > 0$ such that for any $A \geqslant \widetilde{A}$, $0 < \eta \leqslant \widetilde{\eta}$, and the release function $\phi(x - ct) = \Lambda(t, x)$ defined in (3.7), problem (3.12) admits a solution v.*

Then, we have the following result for the space-time model (3.10) (which is an analog to Theorem 3.1.1):

Theorem 3.3.2. *For any initial data $u_0 \geqslant 0$ with $u_0 \leqslant u_*$ and $u_{0|\mathbb{R}_+} = 0$ and $c \leqslant 0$, there exist constants $\widetilde{A}$, $\widetilde{\eta} > 0$ such that for any $A \geqslant \widetilde{A}$, $0 < \eta \leqslant \widetilde{\eta}$, and the release function $\phi(x - ct) = \Lambda(t, x)$, one has that the solution u of (3.10) satisfies, with any $\epsilon > 0$, that*

$$\lim_{t \to +\infty} \sup_{x > (c+\epsilon)t} u(t, x) = 0.$$

By imposing a control with exponential decay, we succeed in suppressing the insects in the region behind the release. It is contrary to what happens naturally (when the stable steady state u_* invades the unstable steady state 0). Notice that the hypothesis on the initial data u_0 takes into account any positive and compactly supported initial data bounded by u_* (up to a translation of the support in $\mathbb{R}_-$).

In the following section, we construct a super-solution for (3.12) in Proposition 3.3.2, then we can apply this result to prove Theorem 3.3.2. The existence of a sub-solution of (3.12) is presented in Proposition 3.3.3 in section 3.3.3. Finally, by using comparison principle for a scalar reaction-diffusion equation, we prove Theorem 3.3.1.

3.3.2 Construction of a super-solution for the simplified model

The existence of super-solution for (3.12) is shown in the following proposition

Proposition 3.3.2. *For any fixed speed c and any fixed parameter $\alpha \in \left(0, \dfrac{\delta\mu}{b}\right)$, there exists a constant $r(\alpha) < 0$ depending on α, c such that the function*

$$\overline{w}(x) = \begin{cases} u_* & \text{when } x < 0, \\ u_* e^{r(\alpha)x} & \text{when } x \geqslant 0, \end{cases} \tag{3.13}$$

is a super-solution of (3.12) with $\phi(x - ct) = \Lambda(t, x)$ for any $\eta \in [0, -r(\alpha)]$ and $A \geqslant \dfrac{u_*}{\alpha} - u_* > 0$.

Proof of Proposition 3.3.2. For a constant $c < 0$, we study the following problem

$$-c\overline{w}' - \overline{w}'' = \left(\frac{\alpha b}{\delta} - \mu\right)\overline{w}, \qquad \text{on } [0, +\infty), \tag{3.14a}$$

$$\overline{w} > 0 \text{ on } [0, +\infty), \quad \overline{w}(+\infty) = 0. \tag{3.14b}$$

Consider the characteristic polynomial $r^2 + cr + \dfrac{\alpha b}{\delta} - \mu = 0$, since $\dfrac{\alpha b}{\delta} - \mu < 0$ then for any $c < 0$, the polynomial admits two distinct roots $r_\pm = \dfrac{-c \pm \sqrt{c^2 - 4\left(\frac{\alpha b}{\delta} - \mu\right)}}{2}$ where $r_+ > 0$ and $r_- < 0$.

Since we look for a solution w of (3.14) with $w(+\infty) = 0$, then the solution of (3.14) is

$$\overline{w}(x) = u_* e^{r(\alpha)x} \qquad \text{for } x > 0, \tag{3.15}$$

with $r(\alpha) = r_- = \dfrac{-c - \sqrt{c^2 - 4\left(\frac{\alpha b}{\delta} - \mu\right)}}{2} < 0$.

Now, remarking that Assumption 3.3.1 provides $\frac{\delta\mu}{b} \leqslant 1$, it follows for any $\alpha \in (0, \frac{\delta\mu}{b})$ and any constant $\eta \in [0, -r(\alpha)]$ and $A \geqslant \dfrac{u_*}{\alpha} - u_* > 0$, one defines $\phi(x - ct) = \Lambda(t, x)$ as in (3.7), then for all $x \in [0, \infty)$, one has $\dfrac{\overline{w}(x)}{\overline{w}(x) + \phi(x)} = \dfrac{u_* e^{r(\alpha)x}}{u_* e^{r(\alpha)x} + Ae^{-\eta x}} = \dfrac{u_*}{u_* + Ae^{-(\eta + r(\alpha))x}} \leqslant \alpha$. We deduce that

$$-c\overline{w}' - \overline{w}'' - \frac{\overline{w}}{\overline{w} + \phi}\frac{b\overline{w}}{\frac{b\overline{w}}{K} + \delta} + \mu\overline{w} \geqslant -c\overline{w}' - \overline{w}'' - \left(\frac{\alpha b}{\delta} - \mu\right)\overline{w} = 0.$$

For any $x < 0$, one has $\overline{w}(x) = u_*$ and

$$-c\overline{w}' - \overline{w}'' - \frac{\overline{w}}{\overline{w} + \phi}\frac{b\overline{w}}{\frac{b\overline{w}}{K} + \delta} + \mu\overline{w} = -\frac{bu_*}{\frac{bu_*}{K} + \delta} + \mu u_* = 0.$$

Moreover, we have $\lim\limits_{x \to 0^-} \overline{w}'(x) = 0 > r(\alpha)u_* = \lim\limits_{x \to 0^+} \overline{w}'(x)$. Hence, function $\overline{w}$ as in (3.13) is a super-solution of (3.12) with any $\phi(x - ct) = \Lambda(t, x)$ of the form in (3.7). □

From the existence of this super-solution we have the following proof of Theorem 3.3.2:

Proof of Theorem 3.3.2. Let $\overline{u}(t,x) = \overline{w}(x-ct)$, $\Lambda(t,x) = \phi(x-ct)$, and $\overline{w}, \phi$ provided by Proposition 3.3.2 with a certain speed $c < 0$. It is clear that with such a choice of $\Lambda(t,x)$, we have that $\overline{u}$ is a super-solution of (3.10). Thanks to the definition of $\overline{w}$, we have $u_0(x) \leqslant \overline{u}(t=0,x)$, therefore, the comparison principle implies that for any $t > 0,\ x \in \mathbb{R}$, $u(t,x) \leqslant \overline{u}(t,x)$. For any $\epsilon > 0$, $x > (c+\epsilon)t$, one has $\overline{u}(t,x) \leqslant u_* e^{r(\alpha)\epsilon t} \to 0$ when $t \to +\infty$, then the result follows. □

3.3.3 Construction of a sub-solution for the simplified model

We are going to construct this sub-solution by part. In the part where $\phi \equiv 0$, we recall $f(s) = \dfrac{bs}{\frac{bs}{K}+\delta} - \mu s$ which corresponds to the reaction term of (3.12) with $\phi \equiv 0$. Consider the following system

$$-w'' = f(w) \quad \text{in } \mathbb{R}_-, \tag{3.16a}$$

$$w(0) = 0; \quad \lim_{x\to 0^-} w'(x) = -\sqrt{2\int_0^{u_*} f(s)ds}. \tag{3.16b}$$

We have the following Lemma

Lemma 3.3.1. *System (3.16) admits a solution $w \geqslant 0$ such that for any $x < 0$ $w'(x) < 0$ and $\lim_{x\to-\infty} w(x) = u_*$.*

Proof. By Cauchy-Lipschitz theorem, problem (3.16) admits a solution $w \geqslant 0$ in $[-L_0, 0)$ for some $L_0 \in (0, +\infty]$. Multiplying the first equation of (3.16) by w' and integrating in $(-L, 0)$ for some $L \in (0, L_0]$, we have

$$-\int_{-L}^0 \left[\frac{(w')^2}{2}\right]' dx = \int_{-L}^0 f(w)w'dx,$$

then

$$\frac{w'(-L)^2}{2} - \frac{w'(0)^2}{2} = -\int_0^{w(-L)} f(s)ds.$$

From (3.16), we have $w'(0)^2 = 2\displaystyle\int_0^{u_*} f(s)ds$ then

$$\frac{w'(-L)^2}{2} = \int_{w(-L)}^{u_*} f(s)ds. \tag{3.17}$$

Since f is monostable, then $w'(-L) = 0$ if and only if $w(-L) = u_*$.

Define

$$L := \inf\{x > 0 : w'(-x) = 0\} = \inf\{x > 0 : w(-x) = u_*\} \leqslant +\infty. \tag{3.18}$$

If $L < +\infty$, from the definition of L one has $w'(-L) = 0$ and $w(-L) = u_*$. However, u_* is a stable equilibrium of equation $-w'' = f(w)$, so $w(-L) = u_*$ implies that $w \equiv u_*$. This is contradictory to the fact that $w(0) = 0$.

Hence, $L = +\infty$. So we have $w'(x) < 0$ and $w(x) < u_*$ for any $x < 0$. We can deduce from this bound that w converges when $x \to -\infty$. Since $\lim_{x\to-\infty} w(x) < w(0) = 0$, then w converges to u_*. □

Now, we can use the solution w of (3.16) to construct a sub-solution of (3.12).

Proposition 3.3.3. *For any $c < 0$, problem (3.12) has a sub-solution $\underline{w}$ which is defined as follows*

$$\underline{w}(x) = \begin{cases} w(x) & \text{when } x < 0, \\ 0 & \text{when } x \geqslant 0, \end{cases} \tag{3.19}$$

with $\phi(x-ct) = \Lambda(t,x)$.

Proof. For any $c < 0$, for any $x < 0$, one has $\phi(x) = 0, \underline{w}(x) = w(x), \underline{w}'(x) < 0$, then

$$-c\underline{w}' - \underline{w}'' - \frac{\underline{w}}{\underline{w}+\phi}\frac{b\underline{w}}{\frac{b\underline{w}}{K}+\delta} + \mu\underline{w} = -c\underline{w}' - \underline{w}'' - f(\underline{w}) = -c\underline{w}' < 0.$$

Moreover, $\lim_{x\to 0^-} \underline{w}(x) = -\sqrt{2\displaystyle\int_0^{u_*} f(s)ds} < 0 = \lim_{x\to 0^+} \underline{w}(x)$. Hence, $\underline{w}$ is a sub-solution of (3.12). □

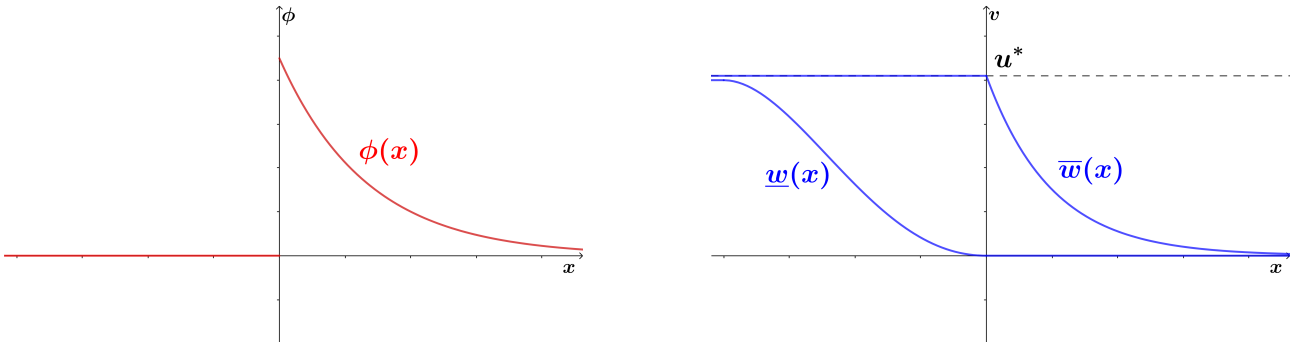

Figure 3.2 – Control function ϕ and super-, sub-solutions.

3.3.4 Conclusion: Construction of a traveling wave solution for the simplified model

We construct a solution from the above sub- and super-solutions.

Proof of Theorem 3.3.1. According to Propositions 3.3.2 and 3.3.3, for the control function $\phi(x-ct) = \Lambda(t,x)$, problem (3.12) has the super-solution $\overline{w}$ as in (3.13) and the sub-solution $\underline{w}$ as in (3.16). Moreover, the sub- and super-solutions are well-ordered : $\underline{w} \leqslant \overline{w}$ (see Figures 3.2). By applying the classical technique of sub- and super-solution (see e.g. [194]), there exists a classical solution of (3.12). Moreover, we have $\int_{\mathbb{R}} \phi(x)dx = C_s \int_0^{+\infty} e^{-\lambda x}dx = \dfrac{C_s}{\lambda} < +\infty$. □

3.4 Study of the whole system

In subsection 3.4.1, we provide some preliminary results such as a comparison principle adapted to system (3.1). In subsection 3.4.2, we prove the main Theorem 3.1.1 by introducing a super-solution. The proof of the result which states that it is indeed a super-solution is postponed to subsection 3.4.3. Subsection 3.4.4 is devoted to the establishment of a sub-solution of (3.9). Finally, in subsection 3.4.5, we provide the proof of Theorem 3.1.2.

3.4.1 Preliminary results

In this part, we focus on studying the existence of traveling wave solutions for system (3.1) and then apply it to prove Theorem 3.1.1. In the rest of the paper, we study this system in the subset $\{E \leqslant K\}$ of the positive cone since we have the following property.

Lemma 3.4.1. *On the positive cone $\{E \geqslant 0, F \geqslant 0, M \geqslant 0, M_s \geqslant 0\}$, the subset $\{E \leqslant K\}$ is time invariant, that is, if $0 \leqslant E^0 \leqslant K$, then $E(t,\cdot) \leqslant K$ for all $t > 0$.*

Proof. Assume that there exists a time $t_0 > 0$ such that $E(t_0, x) > K$ for some x. Since $0 \leqslant E^0 \leqslant K$, and E is continuous over time, we can deduce that there exists a time $t_1 \in (0, t_0)$ such that $E(t_1, x) > 0$ and $\partial_t E(t_1, x) > 0$. However, we also have $\partial_t E(t_1, x) = bF(t_1, x)\left(1 - \dfrac{E(t_1, x)}{K}\right) - (\nu_E + \mu_E)E(t_1, x) < 0$. This contradiction proves the result. □

We recall that in the subset $\{E \leqslant K\}$, system (3.1) is not cooperative due to the introduction of sterile males $M_s > 0$. Indeed, from the second equation of (3.1), we have the reaction term

$$g(E, F, M, M_s) := \rho\nu_E E \frac{M}{M + \gamma_s M_s} - \mu_F F,$$

and $\dfrac{\partial g}{\partial M_s} = -\dfrac{\gamma_s \rho \nu_E E M}{(M + \gamma_s M_s)^2} < 0$ on the positive cone. Hence, we introduce a new comparison principle that

can be applied to system (3.1) in the following part. We first define the nonlinear vector-valued function

$$\mathbf{f}(E,F,M;\psi)=\begin{bmatrix} f_1(E,F,M)\\ f_2(E,F,M)\\ f_3(E,F,M)\end{bmatrix}=\begin{bmatrix} bF\left(1-\frac{E}{K}\right)-(\nu_E+\mu_E)E\\ \rho\nu_E E\frac{M}{M+\gamma_s\psi}-\mu_F F\\ (1-\rho)\nu_E E-\mu_M M\end{bmatrix}, \tag{3.20}$$

where $\psi(t,x)$ is a fixed function. Denote $U(t,x)=(E,F,M)(t,x)\in\mathbb{R}^3_+$ then we obtain the following system

$$\partial_t U-D\partial_{xx}U=\mathbf{f}(U;\psi). \tag{3.21}$$

Next, we introduce the following theorem

Theorem 3.4.1 (Comparison principle for (3.1)). *Consider two functions $M_s^1, M_s^2\in L^1_{\text{loc}}((0,+\infty)\times\mathbb{R})$ such that $0\leqslant M_s^2(t,x)\leqslant M_s^1(t,x)$ for all $t\geqslant 0, x\in\mathbb{R}$. Suppose that*

- *(E^1,F^1,M^1) is a sub-solution of system (3.21) with $\psi\equiv M_s^1$,*
- *(E^2,F^2,M^2) is a super-solution of system (3.21) with $\psi\equiv M_s^2$,*
- *$(E^1,F^1,M^1)(t=0)\leqslant(E^2,F^2,M^2)(t=0)$, for any $x\in\mathbb{R}$,*

then

$$(E^1,F^1,M^1)(t,x)\leqslant(E^2,F^2,M^2)(t,x),$$

for all $t>0, x\in\mathbb{R}$.

Proof. Recall that system (3.21) with $\psi(t,x)$ fixed is a cooperative system. Indeed,

$$\frac{\partial f_1}{\partial F}=b\left(1-\frac{E}{K}\right)>0,\quad \frac{\partial f_1}{\partial M}=0,$$

$$\frac{\partial f_2}{\partial E}=\rho\nu_E\frac{M}{M+\gamma_s\psi}>0,\quad \frac{\partial f_2}{\partial M}=\frac{\gamma_s\psi\rho\nu_E E}{(M+\gamma_s\psi)^2}>0,$$

and

$$\frac{\partial f_3}{\partial E}=(1-\rho)\nu_E>0,\quad \frac{\partial f_3}{\partial F}=0.$$

On the other hand, from the assumption of Theorem 3.4.1, one has $0\leqslant M_s^2(t,x)\leqslant M_s^1(t,x)$ for any $t>0, x\in\mathbb{R}$, we deduce that $\mathbf{f}(U;M_s^1)\leqslant\mathbf{f}(U;M_s^2)$ for any $U\in\mathbb{R}^3_+$. Hence, recalling that $U^1=(E^1,F^1,M^1)$ is a sub-solution of system (3.21) with $\psi\equiv M_s^1$, it follows

$$\partial_t U^1-D\partial_{xx}U^1-\mathbf{f}(U^1;M_s^2)\leqslant\mathbf{f}(U^1;M_s^1)-\mathbf{f}(U^1;M_s^2)\leqslant 0.$$

This inequality deduces that U^1 is also a sub-solution of system (3.21) with $\psi\equiv M_s^2$. From assumptions in Theorem 3.4.1, we also have $U^2=(E^2,F^2,M^2)$ is a super-solution of this system. Moreover, $U^1(t=0)\leqslant U^2(t=0)$. Therefore, by applying the comparison principle for this cooperative system (see e.g. [214], Chapter 5, §5), we obtain that $(E^1,F^1,M^1)(t,x)\leqslant(E^2,F^2,M^2)(t,x)$ for any $t>0, x\in\mathbb{R}$. □

Next, we will use Theorem 3.4.1 for studying system (3.1) and prove the main result in Theorem 3.1.1.

3.4.2 Proof of Theorem 3.1.1

Before treating the main system, we first fix the distribution of sterile males by assuming that the sterile males neither die nor diffuse, and we assign $M_s(t,x)=\overline{\phi_s}(x-ct)$ where

$$\overline{\phi_s}(x)=\begin{cases}0 & \text{for } x<0,\\ C_s e^{-\eta x} & \text{for } x\geqslant 0,\end{cases} \tag{3.22}$$

with constants $C_s>0,\ \eta>0$. We consider the traveling wave solution $(E,F,M)(t,x)=(\phi_E,\phi_F,\phi_M)(x-ct)$ where (ϕ_E,ϕ_F,ϕ_M) satisfies the following system

$$-c\phi_E'=b\phi_F\Big(1-\frac{\phi_E}{K}\Big)-(\nu_E+\mu_E)\phi_E, \tag{3.23a}$$

$$-c\phi_F'-D\phi_F''=\rho\nu_E E\frac{\phi_M}{\phi_M+\gamma_s\overline{\phi_s}}-\mu_F\phi_F, \tag{3.23b}$$

$$-c\phi_M' - D\phi_M'' = (1-\rho)\nu_E\phi_E - \mu_M\phi_M, \tag{3.23c}$$
$$(\phi_E,\phi_F,\phi_M)(-\infty) = (E^*,F^*,M^*), \qquad (\phi_E,\phi_F,\phi_M)(+\infty) = (0,0,0). \tag{3.23d}$$

with speed $c<0$. Note that, system (3.23) is cooperative on the positive cone $\{E\geqslant 0, F\geqslant 0, M\geqslant 0\}$, thus we can apply directly the comparison principle for a cooperative system (see e.g. [214], Chapter 5, §5). Our idea is to construct a super-solution for the system (3.23) where the sterile males' distribution is fixed and then deduce a super-solution for the main system (3.9). First, we need to show that the solution ϕ_s of (3.9) is larger than $\overline{\phi_s}$ in the whole $\mathbb{R}$. It will follow that the solution $M_s(t,x)$ of the Cauchy problem with appropriate initial data is also larger than $\overline{\phi_s}$.

Lemma 3.4.2. *For a certain speed $c<0$ and function $\phi(x-ct)=\Lambda(t,x)$ defined in (3.7), there exists a solution ϕ_s of equation*

$$-c\phi_s' - D\phi_s'' = \phi - \mu_s\phi_s, \quad \phi_s(\pm\infty)=0,$$

such that for $A>C_s$ large enough and $\eta>0$ small enough, one has $\overline{\phi_s}\leqslant\phi_s$ in $\mathbb{R}$.

Moreover, for the initial data $M_s^0\in L^1(\mathbb{R})$ such that $M_s^0\geqslant\phi_s$, the solution M_s of

$$\partial_t M_s - D\partial_{xx}M_s = \Lambda - \mu_s M_s, \tag{3.24a}$$
$$M_s(t=0) = M_s^0 \tag{3.24b}$$

satisfies $M_s(t,x)\to\phi_s(x-ct)$ uniformly with respect to time and $M_s(t,x)\geqslant\overline{\phi_s}(x-ct)$.

Proof. Denote $\sigma_\pm = \dfrac{-c\pm\sqrt{c^2+4D\mu_s}}{2D}$ two roots of the characteristic polynomial of equation $-c\phi_s' - D\phi_s'' + \mu_s\phi_s = 0$, then we have $\sigma_- < 0 < \sigma_+$. Assume that $0<\eta<-\sigma_-$, and define $A_s := \dfrac{A}{-D\eta^2+c\eta+\mu_s}$, then we have solution

$$\phi_s(x) = \begin{cases} B_+e^{\sigma_+x} + B_-e^{\sigma_-x} & \text{for } x\leqslant 0,\\ A_+e^{\sigma_+x} + A_-e^{\sigma_-x} + A_se^{-\eta x} & \text{for } x>0,\end{cases}$$

for some $A_\pm$, $B_\pm$. Since we have $\phi_s(\pm\infty)=0$, then $B_- = A_+ = 0$. To ensure that ϕ_s is $\mathcal{C}^1$, we need $B_+ = A_- + A_s$, $\sigma_+B_+ = \sigma_-A_- + \eta A_s$. Hence, we obtain that

$$A_- = \frac{\eta+\sigma_+}{\sigma_--\sigma_+}A_s < 0, \qquad B_+ = \frac{\eta+\sigma_-}{\sigma_--\sigma_+}A_s > 0,$$

since $0<\eta<-\sigma_-$. Now for any $x\leqslant 0$, one has $\phi_s(x) = \dfrac{\eta+\sigma_-}{\sigma_--\sigma_+}\dfrac{A}{-D\eta^2+c\eta+\mu_s}e^{\sigma_+x} > 0 = \overline{\phi_s}(x)$. Otherwise, if $x>0$, one has $\phi_s(x) = \dfrac{\eta+\sigma_+}{\sigma_--\sigma_+}A_se^{\sigma_-x} + A_se^{-\eta x} > \dfrac{\eta+\sigma_-}{\sigma_--\sigma_+}\dfrac{A}{-D\eta^2+c\eta+\mu_s}e^{-\eta x} > C_se^{-\eta x}$ if $A>C_s$ large enough.

For the second claim, we split the solution M_s into two parts: $M_s = M_s^1 + M_s^2$ solutions of

$$\begin{cases}\partial_t M_s^1 - D\partial_{xx}M_s^1 = -\mu_s M_s^1,\\ M_s^1(t=0) = M_s^0 - \phi_s\end{cases} \quad\text{and}\quad \begin{cases}\partial_t M_s^2 - D\partial_{xx}M_s^2 = \Lambda - \mu_s M_s^2,\\ M_s^2(t=0) = \phi_s\end{cases}$$

By linearity, it is clear that $M_s^1 + M_s^2$ is a solution of (3.24). Moreover, we have $M_s^1 = \left[H*(M_s^0-\phi_s)\right]e^{-\mu_s t}$ (where H stands for the heat kernel in $\mathbb{R}\times[0,+\infty[$ and $*$ stands for the convolution) and $M_s^2(x-ct) = \phi_s(x-ct)$. Since $(M_s^0-\phi_s)\in C_b^0(\mathbb{R})\cap L^1(\mathbb{R})$ we deduce that M_s^1 converges uniformly to 0 as $t\to+\infty$. Finally, remarking that $(M_s^0-\phi_s)\geqslant 0$ we deduce that $M_s^1\geqslant 0$ and $M_s\geqslant\phi_s>\overline{\phi_s}$. □

The next Proposition shows that we can construct a super-solution of (3.9) by studying system (3.23)

Proposition 3.4.1. *Assume that the basic offspring number $\mathcal{R}_0>1$, then for any speed $c<0$ and the control function $\overline{\phi_s}$ defined in (3.22) with $C_s>0$ large enough and $\eta>0$ small enough, there exists a non-negative super-solution $(\overline{\phi_E},\overline{\phi_F},\overline{\phi_M})$ of system (3.23) such that $\overline{\phi_E}\leqslant E^*$, $\overline{\phi_F}\leqslant F^*$, $\overline{\phi_M}\leqslant M^*$, and when $x\to+\infty$, $(\overline{\phi_E},\overline{\phi_F},\overline{\phi_M})$ converges to $(0,0,0)$.*

Hence, we deduce that $(\overline{\phi_E},\overline{\phi_F},\overline{\phi_M},\phi_s)$ is a super-solution of (3.9) where ϕ_s is defined in Lemma 3.4.2.

The proof of Proposition 3.4.1 is long and technical therefore, we postpone it to section 3.4.3. We finally provide the details of the proof of Theorem 3.1.1.

Proof of Theorem 3.1.1. We define $(\overline{E},\overline{F},\overline{M})(t,x) = (\overline{\phi_E},\overline{\phi_F},\overline{\phi_M})(x-c't)$ where $c'<c<0$, $(\overline{\phi_E},\overline{\phi_F},\overline{\phi_M})$ is defined in Proposition 3.4.1 with a speed c'. It is clear that $(\overline{E},\overline{F},\overline{M})$ is a super-solution of system (3.21) with $\psi(t,x)=\overline{\phi_s}(x-ct)$ and $\overline{\phi_s}$ defined in (3.22). Denote (E,F,M,M_s) solution of system (3.1) with Λ defined in (3.7). Then (E,F,M) is a sub-solution of system (3.21) with $\psi\equiv M_s$. From Lemma 3.4.2, we can choose $A>C_s$ such that $M_s(t,x)\geqslant\overline{\phi_s}(x-ct)$ for any $t>0$ and $x\in\mathbb{R}$. Moreover, by the construction of $(\overline{\phi_E},\overline{\phi_F},\overline{\phi_M})$ in Proposition 3.4.1 (see Section 3.4.3), we have $(E^0,F^0,M^0)(x)\leqslant(\overline{E},\overline{F},\overline{M})(t=0,x)$. Now, we apply the comparison principle in Theorem 3.4.1 and we obtain that $(E,F,M)(t,x)\leqslant(\overline{E},\overline{F},\overline{M})(t,x)$ for any time $t>0$ and $x\in\mathbb{R}$. Since $(\overline{\phi_E},\overline{\phi_F},\overline{\phi_M})(x)\to(0,0,0)$ when $x\to+\infty$, we conclude that

$$\begin{aligned}\limsup_{t\to+\infty}\sup_{x<ct}(E,F,M)(x,t)&\leqslant\limsup_{t\to+\infty}\sup_{x<ct}(\overline{E},\overline{F},\overline{M})(x,t)\\&=\limsup_{t\to+\infty}\sup_{x<ct}(\overline{\phi_E},\overline{\phi_F},\overline{\phi_M})(x-c't)\\&\leqslant\lim_{t\to+\infty}Ce^{(c-c')t}(1,1,1)=(0,0,0).\end{aligned}$$

□

In the following parts, we construct super- and sub-solutions for (3.9), then conclude by proving Theorem 3.1.2.

3.4.3 Construction of a super-solution for (3.9)

We first remark that if $(\overline{\phi_E},\overline{\phi_M},\overline{\phi_F})$ is a super-solution of (3.23) then $(\overline{\phi_E},\overline{\phi_M},\overline{\phi_F},\phi_s)$ is a super-solution of (3.9). Indeed, by applying Lemma 3.4.2, we have $\phi_s\geqslant\overline{\phi_s}$ in $\mathbb{R}$, thus, we have

$$-c\overline{\phi_F}'-D\overline{\phi_F}''-\rho\nu_E\overline{\phi_E}\frac{\overline{\phi_M}}{\overline{\phi_M}+\gamma_s\phi_s}+\mu_F\overline{\phi_F}\geqslant-c\overline{\phi_F}'-D\overline{\phi_F}''-\rho\nu_E\overline{\phi_E}\frac{\overline{\phi_M}}{\overline{\phi_M}+\gamma_s\overline{\phi_s}}+\mu_F\overline{\phi_F}\geqslant0.$$

Following the idea we used with the simplified model, we construct super-solutions for (3.23) established by two parts, a constant part on $(-\infty,x_*]$ and a tail on $(x_*,+\infty)$ that decays to 0 at $+\infty$, with some $x_*\geqslant0$. We start by considering $\overline{\phi_F}$ as follows

$$\overline{\phi_F}(x)=\begin{cases}F^* & \text{when } x\leqslant0,\\ F^*e^{-\lambda x} & \text{when } x>0,\end{cases}\tag{3.25}$$

with some $\lambda>0$. Next, we construct the tails for $\overline{\phi_E}$ and $\overline{\phi_M}$, and clarify the value of x_*. After that, we provide proof of Proposition 3.4.1.

• **Construction of function $\overline{\phi_E}$:** First, on $\mathbb{R}_+$, we consider function $\widetilde{\phi_E}(x)$ such that

$$-c\widetilde{\phi_E}'=bF^*e^{-\lambda x}\Big(1-\frac{\widetilde{\phi_E}}{K}\Big)-(\nu_E+\mu_E)\widetilde{\phi_E},\tag{3.26a}$$

$$\widetilde{\phi_E}>0,\quad\lim_{x\to+\infty}\widetilde{\phi_E}=0,\quad\widetilde{\phi_E}(0)=E^*.\tag{3.26b}$$

Hence, for any $x\geqslant0$, we obtain $\widetilde{\phi_E}$ of the form

$$\widetilde{\phi_E}(x)=e^{\delta(x)}\left(-\frac{bF^*}{c}\int_0^x e^{-\lambda s-\delta(s)}ds+E^*\right)>0,\tag{3.27}$$

where $\delta(x)=-\dfrac{bF^*}{\lambda cK}e^{-\lambda x}+\dfrac{\nu_E+\mu_E}{c}x+\dfrac{bF^*}{\lambda cK}$. One has $\delta(0)=0$ and $\lim\limits_{x\to+\infty}\delta(x)=-\infty$. We have the following lemma

Lemma 3.4.3. *Assume that $\lambda+\dfrac{\nu_E+\mu_E}{c}<0$, then there exists a constant $C_E>E^*$ such that $\widetilde{\phi_E}(x)\leqslant C_Ee^{-\lambda x}$ for any $x\geqslant0$.*

Proof. Since $\lambda+\dfrac{\nu_E+\mu_E}{c}<0$ and $c<0$, for any $x\geqslant0$, we obtain that $\delta(x)\leqslant\dfrac{\nu_E+\mu_E}{c}x\leqslant-\lambda x$. Therefore, $e^{\delta(x)}\leqslant e^{\frac{\nu_E+\mu_E}{c}x}\leqslant e^{-\lambda x}$. On the other hand, one has

$$e^{\delta(x)}\int_0^x e^{-\lambda s-\delta(s)}ds\leqslant e^{\frac{\nu_E+\mu_E}{c}x}\int_0^x e^{-\lambda s-\frac{\nu_E+\mu_E}{c}s}e^{-\frac{bF^*}{c\lambda K}(1-e^{-\lambda s})}ds\leqslant\frac{-e^{-\frac{bF^*}{c\lambda K}}}{\lambda+\frac{\nu_E+\mu_E}{c}}e^{-\lambda x}.$$

Then one has $C_E := E^* + \dfrac{bF^*}{c}\dfrac{e^{-\frac{bF^*}{c\lambda K}}}{\lambda + \frac{\nu_E+\mu_E}{c}} > E^*$. This induces the result of the lemma. □

From Lemma 3.4.3, we can deduce that $\lim_{x\to+\infty} \widetilde{\phi_E}(x) = 0$. Moreover, we define

$$x_E := \sup\{x \geqslant 0 : \widetilde{\phi_E}(x) = E^*\} < +\infty, \tag{3.28}$$

and $\widetilde{\phi_E}(x) < E^*$ for any $x > x_E$. We define function $\overline{\phi_E}$ as follows

$$\overline{\phi_E}(x) = \begin{cases} E^* & \text{when } x \leqslant x_E \\ \widetilde{\phi_E}(x) & \text{when } x > x_E. \end{cases} \tag{3.29}$$

Then for any x, we have $\overline{\phi_E}(x) \leqslant \min\{E^*, C_E e^{-\lambda x}\}$, $\lim_{x\to+\infty} \overline{\phi_E}(x) = 0$, and $\lim_{x\to x_E^-} \overline{\phi_E}'(x) = 0 \geqslant \widetilde{\phi_E}'(x_E) = \lim_{x\to x_E^+} \overline{\phi_E}'(x)$.

• **Construction of function $\overline{\phi_M}$:** Next, on $\mathbb{R}_+$, we consider function $\widetilde{\phi_M}$ which satisfies

$$-c\widetilde{\phi_M}' - D\widetilde{\phi_M}'' = (1-\rho)\nu_E C_E e^{-\lambda x} - \mu_M \widetilde{\phi_M}, \tag{3.30a}$$

$$\widetilde{\phi_M}(x) > 0, \quad \lim_{x\to+\infty} \widetilde{\phi_M}(x) = 0, \quad \widetilde{\phi_M}(0) = M^*. \tag{3.30b}$$

Consider the characteristic polynomial $-D\delta^2 - c\delta + \mu_M = 0$ with two roots $\delta_\pm = \dfrac{-c \pm \sqrt{c^2 + 4D\mu_M}}{2D}$, where $\delta_+ > 0, \delta_- < 0$. Then any solution of (3.30) has the form $\widetilde{\phi_M}(x) = C_M e^{-\lambda x} + C_1 e^{\delta_- x} + C_2 e^{\delta_+ x}$, where

$$C_M = \frac{(1-\rho)\nu_E C_E}{-D\lambda^2 + c\lambda + \mu_M}. \tag{3.31}$$

Since we look for $\lim_{x\to+\infty} \widetilde{\phi_M}(x) = 0$, then $C_2 = 0$. Moreover, $M^* = \widetilde{\phi_M}(0) = C_M + C_1$, thus $C_1 = M^* - C_M$.

Assume that $\lambda + \delta_- < 0$, so we have $\mu_M > -D\lambda^2 + c\lambda + \mu_M > 0$ and

$$C_M > \frac{(1-\rho)\nu_E C_E}{\mu_M} = M^* \frac{C_E}{E^*} \geqslant M^*.$$

Moreover, since $\delta_- < -\lambda$, then for any $x > 0$, we have

$$C_M e^{-\lambda x} > \widetilde{\phi_M}(x) = C_M e^{-\lambda x} + (M^* - C_M) e^{\delta_- x} > M^* e^{\delta_- x} > 0.$$

and we have $\lim_{x\to+\infty} \widetilde{\phi_M}(x) = 0$, so $\widetilde{\phi_M}$ is a solution of problem (3.30). We define

$$x_M = \sup\{x \geqslant 0 : \widetilde{\phi_M}(x) = M^*\} < +\infty, \tag{3.32}$$

and

$$\overline{\phi_M}(x) = \begin{cases} M^* & \text{when } x \leqslant x_M \\ \widetilde{\phi_M}(x) & \text{when } x > x_M. \end{cases} \tag{3.33}$$

Again we have $\overline{\phi_M}(x) \leqslant \min\{M^*, C_M e^{-\lambda x}\}$ for any x, $\lim_{x\to+\infty} \overline{\phi_M}(x) = 0$, and $\lim_{x\to x_M^-} \overline{\phi_M}'(x) = 0 \geqslant \widetilde{\phi_M}'(x_M) = \lim_{x\to x_M^+} \overline{\phi_M}'(x)$.

Now we prove that for C_s large enough, $(\overline{\phi_E}, \overline{\phi_F}, \overline{\phi_M})$ defined as above is a super-solution of (3.23).

Proof of Proposition 3.4.1. Fix a positive parameter α such that $\alpha < \dfrac{\mu_F F^*}{\rho\nu_E C_E} = \dfrac{E^*}{C_E} < 1$. Then, we choose a

positive constant λ such that

$$\lambda \leqslant \min\left\{-\frac{\nu_E+\mu_E}{c}, \frac{c+\sqrt{c^2+4D\mu_M}}{2D}, \frac{c+\sqrt{c^2+4D\mu_F\left(1-\alpha\frac{C_E}{E^*}\right)}}{2D}\right\}. \tag{3.34}$$

Recalling C_M defined respectively in (3.31), we take $\eta<\lambda$ and C_s large enough such that $\frac{C_s}{C_M}\geqslant\frac{1}{\gamma_s}\left(\frac{1}{\alpha}-1\right)$. Then for any $x>0$, $\frac{\overline{\phi_s}}{\phi_M}\geqslant\frac{C_s e^{-\eta x}}{C_M e^{-\lambda x}+(M^*-C_M)e^{\delta_- x}}\geqslant\frac{C_s e^{-\eta x}}{C_M e^{-\lambda x}}\geqslant\frac{C_s}{C_M}$, thus we obtain that $\frac{\phi_M}{\phi_M+\gamma_s\overline{\phi_s}}=\frac{1}{1+\gamma_s\frac{\overline{\phi_s}}{\phi_M}}\leqslant\alpha$.

We now check that $(\overline{\phi_E},\overline{\phi_F},\overline{\phi_M})$ is a super-solution of (3.23).

∘ **Checking for $\overline{\phi_E}$:** For any $x\leqslant x_E$, since $\overline{\phi_E}(x)=E^*,\overline{\phi_F}(x)\leqslant F^*$, then

$$-c\overline{\phi_E}'-b\overline{\phi_F}\left(1-\frac{\overline{\phi_E}}{K}\right)+(\nu_E+\mu_E)\overline{\phi_E}\geqslant -bF^*\left(1-\frac{E^*}{K}\right)+(\nu_E+\mu_E)E^*=0,$$

and for $x>x_E>0$, one has

$$-c\overline{\phi_E}'-b\overline{\phi_F}\left(1-\frac{\overline{\phi_E}}{K}\right)+(\nu_E+\mu_E)\overline{\phi_E}=-c\widetilde{\phi_E}'-bF^*e^{-\lambda x}\left(1-\frac{\widetilde{\phi_E}}{K}\right)+(\nu_E+\mu_E)\widetilde{\phi_E}=0.$$

∘ **Checking for $\overline{\phi_F}$:** For any $x\leqslant 0$, we have $\overline{\phi_F}=F^*,\overline{\phi_E}\leqslant E^*$, then

$$-c\overline{\phi_F}'-D\overline{\phi_F}''-\rho\nu_E\overline{\phi_E}\frac{\overline{\phi_M}}{\overline{\phi_M}+\gamma_s\overline{\phi_s}}+\mu_F\overline{\phi_F}\geqslant-\rho\nu_E E^*+\mu_F F^*=0.$$

For any $x>0$, we have $\overline{\phi_E}(x)\leqslant C_E e^{-\lambda x},\overline{\phi_F}(x)=F^*e^{-\lambda x},\frac{\overline{\phi_M}}{\overline{\phi_M}+\gamma_s\phi}\leqslant\alpha$.

From (3.4), we note that $\frac{\mu_F F^*}{E^*}=\rho\nu_E$, thus

$$-c\overline{\phi_F}'-D\overline{\phi_F}''-\rho\nu_E\overline{\phi_E}\frac{\overline{\phi_M}}{\overline{\phi_M}+\gamma_s\overline{\phi_s}}+\mu_F\overline{\phi_F}\geqslant F^*e^{-\lambda x}\left(-D\lambda^2+c\lambda-\mu_F\alpha\frac{C_E}{E^*}+\mu_F\right)\geqslant 0$$

since $0<\lambda\leqslant\frac{c+\sqrt{c^2+4D\mu_F\left(1-\alpha\frac{C_E}{E^*}\right)}}{2D}$.

∘ **Checking for $\overline{\phi_M}$:** For any $x\leqslant x_M$, one has $\overline{\phi_M}(x)=M^*,\overline{\phi_E}(x)\leqslant E^*$, thus

$$-c\overline{\phi_M}'-D\overline{\phi_M}''-(1-\rho)\nu_E\overline{\phi_E}+\mu_M\overline{\phi_M}\geqslant-(1-\rho)\nu_E E^*+\mu_M M^*=0.$$

On the other hand, when $x>x_M$, one has $\overline{\phi_E}(x)\leqslant C_E e^{-\lambda x}$, $\overline{\phi_M}(x)=\widetilde{\phi_M}(x)$ with $\widetilde{\phi_M}$ defined in (3.30) thus

$$-c\overline{\phi_M}'-D\overline{\phi_M}''-(1-\rho)\nu_E\overline{\phi_E}+\mu_M\overline{\phi_M}\geqslant-c\widetilde{\phi_M}'-D\widetilde{\phi_M}''-(1-\rho)\nu_E C_E e^{-\lambda x}+\mu_M\widetilde{\phi_M}=0.$$

In conclusion, for $\lambda>0$ small such that (3.34) holds, $(\overline{\phi_E},\overline{\phi_F},\overline{\phi_M})$ defined as above is a super-solution of (3.23) where C_s is large enough and $0<\eta<\lambda$. Then, we deduce that $(\overline{\phi_E},\overline{\phi_F},\overline{\phi_M},\phi_s)$ is a super-solution of (3.9). □

3.4.4 Construction of a sub-solution for (3.9)

First, we remark that the sub-solution is established only to prove Theorem 3.1.2. Therefore, according to Theorem 3.4.1, we need to establish $(\underline{\phi_E}, \underline{\phi_F}, \underline{\phi_M}, \underline{\phi_s})$ such that

$$\underline{\phi_s} \geqslant \phi_s \qquad \text{and} \qquad \begin{cases} -c\underline{\phi_E}' \leqslant b\underline{\phi_F}\Big(1 - \dfrac{\underline{\phi_E}}{K}\Big) - (\nu_E + \mu_E)\underline{\phi_E}, \\ -c\underline{\phi_F}' - D\underline{\phi_F}'' \leqslant \rho\nu_E \dfrac{\underline{\phi_M}}{\underline{\phi_M} + \gamma_s\underline{\phi_s}}\underline{\phi_E} - \mu_F\underline{\phi_F}, \\ -c\underline{\phi_M}' - D\underline{\phi_M}'' \leqslant (1-\rho)\nu_E\underline{\phi_E} - \mu_M\underline{\phi_M}. \end{cases}$$

The first difficulty is that the sterile males diffuse so $\phi_s > 0$ on $\mathbb{R}$. It is clear that $\phi_s(x) \underset{|x|\to+\infty}{\longrightarrow} 0$ uniformly. Therefore, we deduce that

$$\forall \varepsilon > 0,\ \exists x_\varepsilon = \inf\{x \in \mathbb{R}\ :\ \phi_s(x) < \varepsilon\} \qquad \text{and} \qquad x_\varepsilon < +\infty.$$

Moreover, taking ε small enough, we can consider $x_\varepsilon \leqslant 0$. Then, we take

$$\underline{\phi_s}(x) = \begin{cases} \varepsilon & \text{for } x < x_\varepsilon, \\ \phi_s & \text{for } x > x_\varepsilon. \end{cases} \tag{3.35}$$

The second difficulty is that (E^*, F^*, M^*) is no more an equilibrium if we impose $\underline{\phi_s}(-\infty) = \varepsilon$. Nevertheless, thanks to the implicit function theorem, we obtain

Proposition 3.4.2. *There exists $\varepsilon_0 > 0$ such that for any $\varepsilon \in [0, \varepsilon_0)$, there exists a strictly positive solution $(E^*_\varepsilon, F^*_\varepsilon, M^*_\varepsilon)$ of*

$$bF^*_\varepsilon\Big(1 - \frac{E^*_\varepsilon}{K}\Big) - (\nu_E + \mu_E)E^*_\varepsilon = 0, \tag{3.36a}$$

$$\rho\nu_E E^*_\varepsilon \frac{1}{1+\varepsilon} - \mu_F F^*_\varepsilon = 0, \tag{3.36b}$$

$$(1-\rho)\nu_E E^*_\varepsilon - \mu_M M^*_\varepsilon = 0. \tag{3.36c}$$

Moreover, one has $(E^*_\varepsilon, F^*_\varepsilon, M^*_\varepsilon)$ is decreasing continuously with respect to ε, and $(E^*_0, F^*_0, M^*_0) = (E^*, F^*, M^*)$.

Proof. We define

$$\mathbf{f_2}(E, F, M, \varepsilon) = \begin{pmatrix} bF\Big(1 - \frac{E}{K}\Big) - (\nu_E + \mu_E)E \\ \rho\nu_E E \frac{1}{1+\varepsilon} - \mu_F F \\ (1-\rho)\nu_E E - \mu_M M \end{pmatrix}.$$

According to the explicit writing of (E^*, F^*, M^*) in (3.4) and since $\mathcal{R}_0 > 1$, we have that

$$\det(D_{E,F,M}\mathbf{f_2}(E^*, F^*, M^*, 0)) = -\mu_M\left[b\rho\nu_E - \mu_F(\mu_E + \nu_E)\right] < 0.$$

Then, the implicit function theorem provides the existence of ε_0. Still thanks to the implicit function theorem, there holds

$$\begin{aligned} \begin{pmatrix} \partial_\varepsilon E^*_\varepsilon \\ \partial_\varepsilon F^*_\varepsilon \\ \partial_\varepsilon M^*_\varepsilon \end{pmatrix} &= -\left(D_{E,F,M}\mathbf{f_2}\right)^{-1} \cdot \nabla_\varepsilon \mathbf{f_2}(E^*_\varepsilon, F^*_\varepsilon, M^*_\varepsilon, \varepsilon) \\ &= \frac{\rho\nu_E E^*_\varepsilon}{(1+\varepsilon)^2(\det\ D_{E,F,M}\mathbf{f_2}(E^*_\varepsilon, F^*_\varepsilon, M^*_\varepsilon, \varepsilon))} \begin{pmatrix} b\Big(1 - \dfrac{E_*}{K}\Big)\mu_M \\ \Big(\dfrac{bF^*_\varepsilon}{K} + \mu_E + \nu_E\Big)\mu_M \\ \Big(\dfrac{bF^*_\varepsilon}{K} + \mu_E + \nu_E\Big)\mu_F \end{pmatrix}. \end{aligned}$$

Recalling, that $\det(D_{E,F,M}\mathbf{f_2}(E^*, F^*, M^*, 0)) < 0$, we deduce by continuity that $\begin{pmatrix} \partial_\varepsilon E^*_\varepsilon \\ \partial_\varepsilon F^*_\varepsilon \\ \partial_\varepsilon M^*_\varepsilon \end{pmatrix} < \begin{pmatrix} 0 \\ 0 \\ 0 \end{pmatrix}$ and the conclusion follows. □

Because of our choice of $\underline{\phi_s}$, we construct a subsolution that converges to $(E_\varepsilon, F_\varepsilon, M_\varepsilon)$ for some positive ε. We construct a sub-solution $(\underline{\phi_E}, \underline{\phi_F}, \underline{\phi_M})$ for system (3.23) by two parts. The first part of $(\underline{\phi_E}, \underline{\phi_F}, \underline{\phi_M})$ is equal to 0 on $[x_\varepsilon, +\infty)$ and the second part on $(-\infty, x_\varepsilon)$ converges to $(E^*_\varepsilon, F^*_\varepsilon, M^*_\varepsilon)$ when $x \to -\infty$. The construction of the sub-solution on $(-\infty, x_\varepsilon)$ is the third difficulty. To cope with this problem, we use the fact that $\underline{\phi_E} \leqslant E_\varepsilon$. We present the result of the existence of a sub-solution as follows

Proposition 3.4.3. *For a speed $c < 0$, there exists $\varepsilon_1 \in (0, \varepsilon_0)$ and $\varepsilon < \varepsilon_1$ a constant small enough such that for the control function $\psi = \underline{\phi_s}$ defined in (3.35), there exists a non-negative sub-solution $(\underline{\phi_E}, \underline{\phi_F}, \underline{\phi_M})$ of system (3.23) such that $\underline{\phi_E} \leqslant E^*_{\varepsilon_1}, \underline{\phi_F} \leqslant F^*_{\varepsilon_1}, \underline{\phi_M} \leqslant M^*_{\varepsilon_1}$. Moreover, when $x \to -\infty$, $(\underline{\phi_E}, \underline{\phi_F}, \underline{\phi_M})(x)$ converges to $(E^*_{\varepsilon_1}, F^*_{\varepsilon_1}, M^*_{\varepsilon_1})$.*

Proof. We fix $c < 0$ and $\varepsilon_1 \in (0, \varepsilon_0)$ (where ε_0 is defined in Proposition 3.4.2). Then, we consider $(\widehat{E}, \widehat{F}, \widehat{M})$ a solution of the following linear system in $\mathbb{R}_-$

$$-c\widehat{E}' = b\widehat{F}\Big(1 - \frac{E^*_{\varepsilon_1}}{K}\Big) - (\nu_E + \mu_E)\widehat{E}, \tag{3.37a}$$

$$-c\widehat{F}' - D\widehat{F}'' = \frac{\rho\nu_E}{1+\varepsilon_1}\widehat{E} - \mu_F\widehat{F}, \tag{3.37b}$$

$$-c\widehat{M}' - D\widehat{M}'' = (1-\rho)\nu_E\widehat{E} - \mu_M\widehat{M}, \tag{3.37c}$$

with $\widehat{E}(-\infty) = E^*_{\varepsilon_1}, \widehat{F}(-\infty) = F^*, \widehat{M}(-\infty) = M^*$.

Now, we will study this linear system by denoting $U = \begin{pmatrix} \widehat{E} \\ \widehat{F} \\ \widehat{M} \\ \widehat{F}' \\ \widehat{M}' \end{pmatrix}$. Then system (3.37) becomes $U' = BU$ where

$B = \begin{pmatrix} \frac{\nu_E+\mu_E}{c} & -\frac{\mu_F(\nu_E+\mu_E)}{b\rho\nu_E/(1+\varepsilon_1)} & 0 & 0 & 0 \\ 0 & 0 & 0 & 1 & 0 \\ 0 & 0 & 0 & 0 & 1 \\ -\frac{\rho\nu_E}{D(1+\varepsilon_1)} & \frac{\mu_F}{D} & 0 & -\frac{c}{D} & 0 \\ -\frac{(1-\rho)\nu_E}{D} & 0 & \frac{\mu_M}{D} & 0 & -\frac{c}{D} \end{pmatrix}$, since $1 - \frac{E^*_{\varepsilon_1}}{K} = \frac{\mu_F(\nu_E+\mu_E)}{b\rho\nu_E/(1+\varepsilon_1)}$. Hence, the characteristic polynomial is

$$\det(B - \lambda I) = \lambda \underbrace{\Big(\lambda^2 + \frac{c}{D}\lambda - \frac{\mu_M}{D}\Big)}_{P_M(\lambda)} \underbrace{\Big[-\lambda^2 + \Big(\frac{\nu_E+\mu_E}{c} - \frac{c}{D}\Big)\lambda + \frac{\nu_E+\mu_E}{c} + \frac{\mu_F}{D}\Big]}_{P_F(\lambda)}.$$

It is clear that $\lambda_0 = 0$ is an eigenvalue associated to the eigenvector $U_0 = \begin{pmatrix} E^*_{\varepsilon_1} \\ F^*_{\varepsilon_1} \\ M^*_{\varepsilon_1} \\ 0 \\ 0 \end{pmatrix}$. Denote eigenvalues $\lambda^+_M > 0, \lambda^-_M < 0$ which are the roots of $P_M(\lambda)$, $\lambda^+_F > 0, \lambda^-_F < 0$ which are the roots of $P_F(\lambda)$. We aim at building a solution $U(x)$ that converges to U_0 when $x \to -\infty$, then we construct U of the following form

$$U(x) = U_0 + e^{\lambda^+_M x}U^+_M + e^{\lambda^+_F x}U^+_F,$$

where U^+_M, U^+_F the corresponding eigenvectors of λ^+_M, λ^+_F. We consider the following cases:

Case 1: $\lambda^+_M \neq \lambda^+_F$: Since λ^+_M is a root of $P_M(\lambda)$, then $U^+_M = \begin{pmatrix} 0 \\ 0 \\ a \\ 0 \\ a\lambda^+_M \end{pmatrix}$ for some $a \in \mathbb{R}$. Denote $U^+_F = \begin{pmatrix} b_1 \\ b_2 \\ b_3 \\ b_4 \\ b_5 \end{pmatrix}$ an eigenvector associated to λ^+_F. We have $BU^+_F = \lambda^+_F U^+_F$, and since $\operatorname{rank}(B - \lambda^+_F I) = 4$ then all entries b_2, b_3, b_4, b_5 depend explicitly on $b_1 \in \mathbb{R}$. More precisely, using the formula of $E^*_{\varepsilon_1}, F^*_{\varepsilon_1}, M^*_{\varepsilon_1}$, we have

$$b_2 = b_1\frac{F^*_{\varepsilon_1}}{E^*_{\varepsilon_1}}\left(1 - \frac{c\lambda^+_F}{\nu_E + \mu_E}\right), \quad b_3 = b_1\frac{M^*_{\varepsilon_1}}{E^*_{\varepsilon_1}}\frac{\mu_M}{-D[(\lambda^+_F)^2 + \frac{c}{D}\lambda^+_F - \frac{\mu_M}{D}]}, \quad b_4 = \lambda^+_F b_2. \tag{3.38}$$

For any $x<0$, we have

$$\widehat{E}(x)=E^*_{\varepsilon_1}+b_1e^{\lambda_F^+x},\quad \widehat{F}(x)=F^*_{\varepsilon_1}+b_2e^{\lambda_F^+x},\quad \widehat{M}(x)=M^*_{\varepsilon_1}+ae^{\lambda_M^+x}+b_3e^{\lambda_F^+x}.$$

We choose $b_1=-E^*_{\varepsilon_1}, a=-M^*_{\varepsilon_1}-b_3$. Thus we obtain that $\widehat{E}(0)=0, \widehat{M}(0)=0, \widehat{F}(0)=\dfrac{cF^*_{\varepsilon_1}\lambda_F^+}{\nu_E+\mu_E}<0$. Then, there exists a unique constant $y_F<0$ such that $\widehat{F}(y_F)=0$.

Claim: For any $x<0$, one has $\widehat{E}(x)<E^*_{\varepsilon_1}, \widehat{F}(x)<F^*_{\varepsilon_1}, \widehat{M}(x)<M^*_{\varepsilon_1}$.

Indeed, since $b_1<0$, we deduce from (3.38) that $b_2<0$, then for any $x<0$, $\widehat{E}(x)<E^*_{\varepsilon_1}, \widehat{F}(x)<F^*_{\varepsilon_1}$. It remains to show that $\widehat{M}(x)<M^*_{\varepsilon_1}$ for any $x<0$. One has

$$\widehat{M}(x)=M^*_{\varepsilon_1}(1-e^{\lambda_M^+x})+b_3(e^{\lambda_F^+x}-e^{\lambda_M^+x}).$$

We only need to show that $b_3(e^{\lambda_F^+x}-e^{\lambda_M^+x})<0$ for any $x<0$. Indeed,

∘ if $\lambda_F^+<\lambda_M^+$, then $e^{\lambda_F^+x}-e^{\lambda_M^+x}>0$ for any $x<0$ and $(\lambda_F^+)^2+\frac{c}{D}\lambda_F^+-\frac{\mu_M}{D}<0$. From (3.38), we deduce that $b_3<0$;

∘ if $\lambda_F^+>\lambda_M^+$, we have $e^{\lambda_F^+x}-e^{\lambda_M^+x}<0$ for any $x<0$ and $b_3>0$.

Case 2: $\lambda_F^+=\lambda_M^+=\lambda^+$: Now λ^+ has one-dimensional eigenspace generated by $U^+=\begin{pmatrix}0\\0\\a\\0\\a\lambda^+\end{pmatrix}$ for some constant a. The solution of $U'=BU$ becomes $U(x)=U_0+xe^{\lambda^+x}U^++e^{\lambda^+x}V^+$, with V^+ some vector to be determined. Plugging this $U(x)$ into the equation yields

$$e^{\lambda^+x}U^++\lambda^+xe^{\lambda^+x}U^++\lambda^+e^{\lambda^+x}V^+=U'(x)=BU=\lambda^+xe^{\lambda^+x}U^++e^{\lambda^+x}BV^+.$$

Hence, $(B-\lambda^+I)V^+=U^+$. Denote $V^+=\begin{pmatrix}b_1\\b_2\\b_3\\b_4\\b_5\end{pmatrix}$, one has $\begin{cases}b_2=b_1\dfrac{F^*_{\varepsilon_1}}{E^*_{\varepsilon_1}}\left(1-\dfrac{c\lambda^+}{\nu_E+\mu_E}\right),\\ b_4=\lambda^+b_2,\\ b_5=\lambda^+b_3+a,\\ a=-\dfrac{M^*_{\varepsilon_1}}{E^*_{\varepsilon_1}}\dfrac{1}{1+\frac{2D\lambda^+}{\mu_M}}b_1.\end{cases}$

Then, we have

$$\widehat{E}(x)=E^*_{\varepsilon_1}+b_1e^{\lambda^+x},\quad \widehat{F}(x)=F^*_{\varepsilon_1}+b_2e^{\lambda^+x},\quad \widehat{M}(x)=M^*_{\varepsilon_1}+axe^{\lambda^+x}+b_3e^{\lambda^+x}.$$

We choose $b_1=-E^*_{\varepsilon_1}, b_3=-M^*_{\varepsilon_1}$, then $\widehat{E}(0)=0, \widehat{M}(0)=0, \widehat{F}(0)=\dfrac{cF^*_{\varepsilon_1}\lambda^+}{\nu_E+\mu_E}<0$. Thus, there exists a unique constant $y_F<0$ such that $\widehat{F}(y_F)=0$.

Since we have $a=\dfrac{M^*_{\varepsilon_1}}{1+\frac{2D\lambda^+}{\mu_M}}>0$, we obtain that for any $x<0$, $\widehat{E}(x)<E^*_{\varepsilon_1}, \widehat{F}(x)<F^*_{\varepsilon_1}, \widehat{M}(x)<M^*_{\varepsilon_1}$.

Hence, in both cases, we constructed solution $(\widehat{E}(x),\widehat{F}(x),\widehat{M}(x))$ of (3.37) such that $\widehat{E}(x)<E^*_{\varepsilon_1}, \widehat{F}(x)<F^*_{\varepsilon_1}, \widehat{M}(x)<M^*_{\varepsilon_1}$. Moreover, $(\widehat{E},\widehat{F},\widehat{M})$ converges to $(E^*_{\varepsilon_1},F^*_{\varepsilon_1},M^*_{\varepsilon_1})$ at $-\infty$. Now, we use these functions to construct a sub-solution for (3.23).

Construction of a sub-solution:

Now, we construct $\underline{\phi_E},\underline{\phi_F},\underline{\phi_M}$ a sub-solution of system (3.16) taking $\phi_s=\underline{\phi_s}$ defined in (3.35) with $\varepsilon\in(0,\varepsilon_1)$ that will be fixed later on. Due to a translation of space, without loss of generality, we can assume here that $x^*_{\varepsilon_1}=0$. Next, we define

$$\underline{\phi_E}(x)=\begin{cases}\widehat{E}(x) & \text{when } x\leqslant 0,\\ 0 & \text{when } x>0,\end{cases}\quad \underline{\phi_F}(x)=\begin{cases}\widehat{F}(x) & \text{when } x\leqslant y_F,\\ 0 & \text{when } x>y_F,\end{cases}\quad \underline{\phi_M}(x)=\begin{cases}\widehat{M}(x) & \text{when } x\leqslant 0,\\ 0 & \text{when } x>0.\end{cases}\tag{3.39}$$

Note that, by the definitions of $\underline{\phi_s}$, the fraction $\dfrac{\underline{\phi_M}}{\underline{\phi_M}+\gamma_s\underline{\phi_s}}$ is well-defined in $\mathbb{R}$. We now check the sub-solution inequalities for $(\underline{\phi_E},\underline{\phi_F},\underline{\phi_M})$. We can see that for any $x>0$, the inequalities are trivial.

◦ **Checking for $\underline{\phi_E}(x)$:** For any $x \leqslant y_F < 0$, since $\underline{\phi_E} \leqslant E^*_{\varepsilon_1}$, thus

$$-c\underline{\phi_E}' - b\underline{\phi_F}\Big(1 - \frac{\underline{\phi_E}}{K}\Big) + (\nu_E + \mu_E)\underline{\phi_E} \leqslant -c\widehat{E}' - b\widehat{F}\Big(1 - \frac{E^*_{\varepsilon_1}}{K}\Big) - (\nu_E + \mu_E)\widehat{E} = 0,$$

For any x such that $y_F < x \leqslant 0$, we have

$$-c\underline{\phi_E}' - b\underline{\phi_F}\Big(1 - \frac{\underline{\phi_E}}{K}\Big) + (\nu_E + \mu_E)\underline{\phi_E} = -c\widehat{E}' + (\nu_E + \mu_E)\widehat{E} = b\widehat{F}\left(1 - \frac{E^*_{\varepsilon_1}}{K}\right) < 0,$$

since $\widehat{F} < 0$ on $(y_F, 0]$. At $x = 0$, we also have $\lim\limits_{x\to 0^-} \underline{\phi_E}'(x) = \widehat{E}'(0) = -\lambda^+ E^*_{\varepsilon_1} < 0 = \lim\limits_{x\to 0^+} \underline{\phi_E}(x)$.

◦ **Checking for $\underline{\phi_F}(x)$:** First, we consider the case where $x \leqslant y_F$. Taking $\varepsilon < \min\big(\frac{\varepsilon_1}{2}, \frac{1}{\gamma_s}\varepsilon_1 \min\limits_{x\leqslant y_F} \phi_M\big)$ it follows, recalling that in this case, $\underline{\phi_s} = \varepsilon$, one has

$$-c\underline{\phi_F}' - D\underline{\phi_F}'' - \rho\nu_E\underline{\phi_E}\frac{\underline{\phi_M}}{\underline{\phi_M} + \gamma_s\underline{\phi_s}} + \mu_F\underline{\phi_F} = \rho\nu_E\underline{\phi_E}\left[\frac{1}{1+\varepsilon_1} - \frac{\widehat{M}}{\widehat{M} + \gamma_s\varepsilon}\right] \leqslant 0,$$

due to the fact that $(\widehat{E}, \widehat{F}, \widehat{M})$ is a solution of (3.37).

For $y_F < x \leqslant 0$, we have $\underline{\phi_F}(x) = 0$, $\underline{\phi_E}(x) = \widehat{E}(x) \geqslant 0$, $\phi(x) = A$, $\underline{\phi_M}(x) = \widehat{M}(x) > 0$, thus

$$-c\underline{\phi_F}' - D\underline{\phi_F}'' - \rho\nu_E\underline{\phi_E}\frac{\underline{\phi_M}}{\underline{\phi_M} + \gamma_s\phi} + \mu_F\underline{\phi_F} = -\rho\nu_E\widehat{E}\frac{\widehat{M}}{\widehat{M} + \gamma_s A} \leqslant 0.$$

At $x = y_F$, we have $\lim\limits_{x\to y_F^-} \underline{\phi_F}'(x) = \widehat{F}'(0) = -\lambda^+ F^*_{\varepsilon_1}\left(1 - \frac{c\lambda^+}{\nu_E + \mu_E}\right) < 0 = \lim\limits_{x\to y_F^+} \underline{\phi_F}'(x)$.

◦ **Checking for $\underline{\phi_M}(x)$:** For any $x \leqslant 0$, one has

$$-c\underline{\phi_M}' - D\underline{\phi_M}'' - (1-\rho)\nu_E\underline{\phi_E} + \mu_M\underline{\phi_M} = -c\widehat{M}' - D\widehat{M}'' - (1-\rho)\nu_E\widehat{E} + \mu_M\widehat{M} = 0.$$

Similarly, at $x = 0$, in both cases $\lim\limits_{x\to 0^-} \underline{\phi_M}'(x) = \widehat{M}'(0) < 0 = \lim\limits_{x\to 0^+} \underline{\phi_M}'(x)$.

It finishes the establishment of the sub-solution. □

3.4.5 Conclusion: Construction of the traveling wave for (3.9) (Proof of Theorem 3.1.2)

As mentioned above, we prove the existence of traveling wave solutions using the sub and the super solutions constructed before. We underline the following

Remark 3.4.1. *For a certain speed $c < 0$ and function $\phi(x - ct) = \Lambda(t, x)$ defined in (3.7), there exists a solution ϕ_s of equation*

$$-c\phi_s' - D\phi_s'' = \phi - \mu_s\phi_s, \quad \phi_s(\pm\infty) = 0,$$

such that for $A > C_s$ large enough and $\eta > 0$ small enough, one has $\overline{\phi_s} \leqslant \phi_s \leqslant \underline{\phi_s}$ in $\mathbb{R}$.

Thanks to Remark 3.4.1, we are able to prove Theorem 3.1.2.

Proof of Theorem 3.1.2. First, notice that since the equation for ϕ_s is independent from the other equations, we deduce that ϕ_s exists and is provided in the proof of Lemma 3.4.1. Next, in section 3.4.3, we obtained that $(\overline{\phi_E}, \overline{\phi_F}, \overline{\phi_M}, \overline{\phi_s})$ is a super-solution of the original system. In section 3.4.4, we obtain that $(\underline{\phi_E}, \underline{\phi_F}, \underline{\phi_M}, \underline{\phi_s})$ is a sub-solution of the original system. Moreover, we have by construction that $(\underline{\phi_E}, \underline{\phi_F}, \underline{\phi_M}) \leqslant (\overline{\phi_E}, \overline{\phi_F}, \overline{\phi_M})$ and according to Remark 3.4.2, we have $\overline{\phi_s} \leqslant \phi_s \leqslant \underline{\phi_s}$.

By applying the comparison principle for the cooperative system (3.9), we deduce that there exists a traveling wave solution $(\phi_E, \phi_F, \phi_M, \phi_s)$ for system (3.9) with

$$(\underline{\phi_E}, \underline{\phi_F}, \underline{\phi_M}) \leqslant (\phi_E, \phi_F, \phi_M) \leqslant (\overline{\phi_E}, \overline{\phi_F}, \overline{\phi_M})$$

Thus (ϕ_E, ϕ_F, ϕ_M) converges to 0 at $+\infty$, and at $-\infty$, one has

$$(E^*_{\varepsilon_1}, F^*_{\varepsilon_1}, M^*_{\varepsilon_1}) \leqslant (\phi_E, \phi_F, \phi_M) < (E^*, F^*, M^*).$$

It only remains to prove by contradiction that $(\phi_E, \phi_F, \phi_M) \underset{x\to-\infty}{\longrightarrow} (E^*, F^*, M^*)$.
Assume it is not the case, we denote

$$(E_*, F_*, M_*) = (\liminf_{x\to-\infty} \phi_E(x),\ \liminf_{x\to-\infty} \phi_F(x),\ \liminf_{x\to-\infty} \phi_M(x)).$$

It follows

$$\max\left(E^* - E_*\ ,\ F^* - F_*\ ,\ M^* - M_*\right) > 0.$$

Next, we introduce

$$\varepsilon_2 = \inf\{\varepsilon > 0\ :\ (E_\varepsilon, F_\varepsilon, M_\varepsilon) \leqslant (E_*, F_*, M_*)\}.$$

Notice that by assumption $\varepsilon_2 > 0$. The end of the proof is split into three claims:

1. Prove by contradiction that $F_* - F^*_{\varepsilon_2} > \delta_F$ (where δ_F is a small positive constant),
2. Prove by contradiction that $E_* - E^*_{\varepsilon_2} > \delta_E$ (where δ_E is a small positive constant),
3. Prove by contradiction that $M_* - M^*_{\varepsilon_2} > \delta_M$ (where δ_M is a small positive constant).

Then the three steps above are in contradiction with the definition of ε_1. Indeed, if the claims are true since the dependence of $(E_\varepsilon, F_\varepsilon, M_\varepsilon)$ with respect to ε is continuous, we deduce the existence of $\varepsilon_3 < \varepsilon_2$ such that

$$(E^*_{\varepsilon_2}, F^*_{\varepsilon_2}, M^*_{\varepsilon_2}) < (E^*_{\varepsilon_3}, F^*_{\varepsilon_3}, M^*_{\varepsilon_3}) \leqslant (E_*, F_*, M_*).$$

Therefore, if the claims are true, the contradiction follows and the proof is achieved.

• **Claim 1.** Assume by contradiction that $F_* = F^*_{\varepsilon_2}$. It follows the existence of a decreasing and unbounded sequence x_n such that $\phi_F(x_n) < F^*_{\varepsilon_2} + 1/n$, $\phi'_F(x_n) = 0$ and $-\phi''_F(x_n) \leqslant 0$. Such sequence exists because if ϕ'_F does not change its sign, it follows that ϕ_F converges and this is absurd since it can only converge to F^*. Notice that we also have by definition of ε_2 that $\phi_E(x_n) > E^*_{\varepsilon_2} + o_1(n)$ and $\phi_M(x_n) > M^*_{\varepsilon_2} + o_n(1)$. Inserting these inequalities in the equation that ϕ_F satisfies, we obtain

$$\rho\nu_E\phi_E(x_n)\frac{1}{1+\gamma_s\phi_s(x_n)/\phi_M(x_n)} - \mu_F\phi_F(x_n) = c\phi'_F(x_n) - \Delta\phi_F(x_n) \leqslant 0.$$

Since $\phi_M(x_n) \geqslant M^*_{\varepsilon_2} + o_n(1)$ and $\phi_s(x_n) = o_n(1)$, we deduce, thanks to (3.36),

$$\begin{aligned}
\rho\nu_E\phi_E(x_n)\frac{1}{1+\gamma_s\phi_s(x_n)/\phi_M(x_n)} - \mu_F\phi_F(x_n) &> \rho\nu_E E^*_{\varepsilon_2}\frac{1}{1+o_n(1)} - \mu_F F^*_{\varepsilon_2} + o_n(1)\\
&> \rho\nu_E E^*_{\varepsilon_2}\frac{1}{1+o_n(1)} - \rho\nu_E E^*_{\varepsilon_2}\frac{1}{1+\varepsilon_2} + o_n(1)\\
&> \rho\nu_E E^*_{\varepsilon_2}\frac{\varepsilon_2 - o_n(1)}{(1+\varepsilon_2)(1+o_n(1))} + o_n(1) > 0.
\end{aligned}$$

Taking n large enough, it follows that $F_* - F^*_{\varepsilon_2} > \delta_F$ for some positive constant δ_F.

• **Claim 2.** Assume by contradiction that $E_* = E^*_{\varepsilon_2}$. It follows the existence of a decreasing and unbounded sequence x_n such that $\phi_E(x_n) < E^*_{\varepsilon_2} + 1/n$, $\phi'_E(x_n) = 0$. Inserting this inequality in the equation satisfied by ϕ_E, we obtain as above

$$\begin{aligned}
0 &= -c\phi'_E(x_n)\\
&= \rho\nu_E\phi_F(x_n)\left(1 - \frac{\phi_E(x_n)}{K}\right) - (\mu_E + \nu_E)\phi_E(x_n)\\
&> \rho\nu_E\phi_F(x_n)\left(1 - \frac{E^*_{\varepsilon_2}}{K}\right) - \rho\nu_E F^*_{\varepsilon_2}\left(1 - \frac{E^*_{\varepsilon_2}}{K}\right) + o_n(1)\\
&> \rho\nu_E\left(1 - \frac{E^*_{\varepsilon_2}}{K}\right)\left[\phi_F(x_n) - F^*_{\varepsilon_2}\right] + o_n(1).
\end{aligned}$$

Recalling that $E^*_{\varepsilon_2} < E^* < K$ (since $\mathcal{R}_0 > 1$ and by the definition of E^*) and using claim 1, it follows the following contradiction by taking n large enough such that $o_n(1)$ is small enough

$$\rho\nu_E\left(1 - \frac{E^*_{\varepsilon_2}}{K}\right)\left[\phi_F(x_n) - F^*_{\varepsilon_2}\right] + o_n(1) > \rho\nu_E\left(1 - \frac{E^*_{\varepsilon_2}}{K}\right)\delta_F + o_n(1) > 0.$$

We conclude to the existence of a positive constant δ_E such that $E_* - E^*_{\varepsilon_2} > \delta_E$.

• **Claim 3.** Assume by contradiction that $M_* = M^*_{\varepsilon_2}$. It follows the existence of a decreasing and unbounded sequence x_n such that $\phi_M(x_n) < M^*_{\varepsilon_2} + 1/n$, $\phi'_M(x_n) = 0$ and $-\phi''_M(x_n) \leqslant 0$. Inserting these inequalities in the equation satisfied by ϕ_M, we obtain as above

$$\begin{aligned} 0 \ &\geqslant \ -c\phi'_M(x_n) - \phi''_M(x_n) \\ &= (1-r)\nu_E\phi_E(x_n) - \mu_M\phi_M(x_n) \\ &> (1-r)\nu_E\phi_E(x_n) - (1-\rho)\nu_E E^*_{\varepsilon_2} + o_n(1) \\ &> (1-\rho)\nu_E\left(\phi_E(x_n) - E^*_{\varepsilon_2}\right) + o_n(1). \end{aligned}$$

Recalling claim 2, it follows the following contradiction by taking n large enough such that $o_n(1)$ is small enough:

$$(1-\rho)\nu_E\left(\phi_E(x_n) - E^*_{\varepsilon_2}\right) + o_n(1) > (1-\rho)\nu_E\delta_E + o_n(1) > 0.$$

We conclude to the existence of a positive constant $\delta_M > 0$ such that $M_* - M^*_{\varepsilon_1} > \delta_M$.

It concludes the proof. □

Chapter 4

Rolling carpet strategy to eliminate mosquitoes: 2D case

This chapter is a joint work with Luis Almeida, Alexis Léculier and Nicolas Vauchelet.

Abstract. "Rolling carpet" is a useful control strategy that consists of actions in a moving set. In this paper, we generalize the analysis of "rolling carpet" in the application of the Sterile Insect Technique for mosquito control to a two-dimensional space. This technique aims to suppress the mosquito population by releasing sterile male mosquitoes to mate with wild females yet produce no fertile offspring. We study a partially degenerate reaction-diffusion system in $\mathbb{R}^2$ with a source term that characterizes the releases moving with a certain speed. The profiles of this release function are generalized from the previous works of the authors in one-dimensional space for both monostable and bistable cases. By the construction of a radially symmetric super-solution, we prove in the present work that the solution of our system spreads with the same speed of the release, in which the zero equilibrium invades the positive one.

4.1 Introduction

The Sterile Insect Technique (SIT) is a classical control technique that has been applied successfully on the field against different kinds of pests or vectors (see [73]). The technique consists of mass releases of males sterilized by ionizing radiation. The released sterile males transfer their sterile sperms to wild females, which results in a decrease or even elimination of the targeted population. For mosquitoes, other sterilization techniques have been developed using either genetics (the RIDL technique) or bacteria (Wolbachia) [108].

Models of mosquito population under the control of the SIT was studied widely in the literature. We refer to [200] which is our starting point. The authors in [200] used a dynamical system approach with an important assumption that the population dynamics exhibit a strong Allee effect. With this assumption, it is sufficient to apply the SIT for a finite time to drive the population below the survival threshold. However, for mosquito population, this assumption could be not realistic in some case. The work [19] dealt with the case where there is no Allee effects in the wild population, and proposed a permanent release strategy which consists of massive release at the beginning to drive the population to a low level, followed by lower release rate, which can be maintained in a long term.

Modeling explicitly the spatial component remains challenging due to the lack of knowledge about vectors in the field, and from the mathematical point of view, the studies of spatial-temporal models are more sophisticated. A reaction-diffusion equation was first used in [144, 128] to model the diffusion in the SIT model. In these classical works, they considered homogeneous releases in the whole space, which is not realistic in practice. How to design the spatial distribution for the control is an interesting question to guarantee and optimize the control results. In the present work, we want to generalize the "rolling carpet" strategy for the SIT studied in [12, 126] by reaction-diffusion models to the two-dimensional space. This strategy consists of local releases on a moving frame with a certain speed in order to block and reverse the propagation of the population. The optimal control problems for this strategy in general frameworks were studied in [45, 46]. In the case of Allee effects, the authors have shown in [15, 12] that sterile males need to be released in a sufficiently large interval to eradicate the mosquitoes. Particularly, in [12] when the "rolling carpet" strategies are applied, it was shown that the critical size of the release area depends on its moving speed. In the case without Allee effects, to avoid the wild population recovers in the controlled zone, the authors considered in [126] the releases that are exponentially decreasing in space. This generalized the idea in [19] in the spatial scale, where the number of sterile males that we keep releasing in the treated zone is low and possible to maintain. All of these results were proved

in one-dimensional space based on the construction of "forced" traveling wave solutions moving with the same speed as the releases. In the present paper, we generalize these release strategies to a two-dimensional space and emphasize that in a long release period, our strategies reduce significantly the number of sterile males required to eradicate the population.

In the higher dimension case, the asymptotic behavior of reaction-diffusion equations with classical nonlinearity such as the monostable, the bistable are well understood. We quote [23] for the study of planar traveling wave solution propagating in a certain direction, and [114] for radially symmetric wave solutions. In the present work, we are interested in the radial framework. The studies of radially symmetric solutions focus on the location of wavefronts (see e.g. [114, 96]). They show that if followed out in a radial direction at the correct speed, the solution starting from compactly supported initial data approaches the one-dimensional traveling wave, shifted by the logarithmic delay plus an additional, of which there is no complete result describing the behavior of this quantity, except the case with radially symmetric initial data [225, 182]. Results about traveling wave solutions and spreading speeds have been provided for both the monostable case [68, 174] and the bistable case [182, 175].

On extending the model and strategies in our previous work to the two-dimensional space, we design a radially symmetric source term Λ that represents the number of released sterile males and moves with a constant speed c. We are interested in the question of whether the solution of our model spreads with the same 'forced' speed c such that the extinction state invades the persistent state. Reaction-diffusion equations of the form $\partial_t u - \Delta u = f(x - ct, u)$ with forced speed c were first studied for the climate change framework in one-dimensional space [33, 3, 34]. The results were extended to the higher dimension in [35, 36, 42] where the authors proved the existence and stability of planar traveling wave solutions $U(x - ct \cdot \nu)$ moving in the same direction ν of the source term f. In the framework of mosquito control, we are interested in a radially symmetric domain since it approximates better the geometry of the controlled areas. In practice, the technique tries to eradicate the population in a specific domain rather than push the propagation in a certain direction. To the best of our knowledge, there is still no result for the spread of a radially symmetric solution of a reaction-diffusion system with forced speed. Moreover, the generalization of the methods studied in the literature to a partially degenerate system as in the present work remains challenging. We answer the question proposed above by the construction of a spreading super-solution. However, constructing traveling wave solutions for our system remains an open question.

4.1.1 Formulation of the model

In $\mathbb{R}^2$, we consider the following system modeling the dynamics of a mosquito population split into several stages : E density of the aquatic phase, F density of fertilized females, M density of males, M_s density of sterile insects.

$$\partial_t E = bF\left(1 - \frac{E}{K}\right) - (\mu_E + \nu_E)E \tag{4.1a}$$

$$\partial_t F - D\Delta F = \rho\nu_E E \frac{M}{M + \gamma_s M_s}\Gamma(M + \gamma_s M_s) - \mu_F F \tag{4.1b}$$

$$\partial_t M - D\Delta M = (1 - \rho)\nu_E E - \mu_M M \tag{4.1c}$$

$$\partial_t M_s - D\Delta M_s = \Lambda - \mu_s M_s \tag{4.1d}$$

In this model, b is the birth rate, μ_E, μ_M, μ_F and μ_s are the death rates for the aquatic phase, the males, the fertilized females, and the sterile males, respectively. Denote K the carrying capacity of the aquatic phase, $D > 0$ the diffusion coefficient, ν_E the emergence rate, and ρ the egg-hatching ratio to female. The release function is $\Lambda(t, x)$. The quantity $\dfrac{M}{M + \gamma_s M_s}\Gamma(M + \gamma_s M_s) \in (0, 1)$ models the probability that a female mates with a fertile male. In the mating process, the parameter γ_s models the competitivity of sterile males, and the function $\Gamma(M)$ represents how the density of males influences the growth of females. In this work, we will consider the two following choices for the function Γ :

$$\Gamma(M) = 1 \ \text{ (monostable case)} , \qquad \Gamma(M) = 1 - e^{-\gamma M} \ \text{ (bistable case).} \tag{4.2}$$

In the bistable case, function $\Gamma(M)$ models the Allee effects, that is, the difficulty of finding a partner when the density is low, such function stabilizes the extinction equilibrium.

System (4.1) is complemented with some given initial data in $L^\infty(\mathbb{R}^2)$

$$E(t = 0, x) = E^0(x), \quad M(t = 0, x) = M^0(x), \quad F(t = 0, x) = F^0(x), \quad M_s(t = 0, x) = M_s^0(x).$$

The existence of a unique solution of system (4.1) may be obtained by using the classical theory of nonlinear

parabolic system (see e.g. [103]) and has already been proved for such a system in [17]. To study this problem, some appropriate initial conditions will be expected later on.

In the following part, we present some preliminary results of the models and the comparison principle that will be used as the main tool in the present work.

4.1.2 Preliminaries

We first provide some information about the steady states of the underlying ODE system

$$\frac{dE}{dt} = bF\left(1-\frac{E}{K}\right) - (\mu_E+\nu_E)E, \tag{4.3a}$$

$$\frac{dF}{dt} = \rho\nu_E E\frac{M}{M+\gamma_s M_s}\Gamma(M+\gamma_s M_s) - \mu_F F, \tag{4.3b}$$

$$\frac{dM}{dt} = (1-\rho)\nu_E E - \mu_M M, \tag{4.3c}$$

$$\frac{dM_s}{dt} = \Lambda - \mu_s M_s, \tag{4.3d}$$

with Λ is a constant number of sterile males released per time unit. We introduce two constants

$$\mathcal{N} := \frac{b\rho\nu_E}{\mu_F(\nu_E+\mu_E)}, \quad \zeta := \frac{\mu_M}{(1-\rho)\nu_E\gamma K}, \tag{4.4}$$

where $\mathcal{N}$ is the classical basic offspring number, ζ is the ratio between the male population density at which the Allee effect applies and the male population size at wild equilibrium, as prescribed by the egg carrying capacity [200]. We assume that

$$\mathcal{N} > 1, \tag{4.5a}$$

$$\mathcal{N} > 4\zeta, \quad \text{and} \quad \max_{\theta\in(\theta_0,1)}\left[-\ln\theta - \frac{1}{2\zeta}\left(1-\sqrt{1+\frac{4\zeta}{\mathcal{N}}\frac{\ln\theta}{1-\theta}}\right)\right] > 0, \tag{4.5b}$$

Then we recall the following results concerning the existence and stability of the positive equilibria.

Proposition 4.1.1. *Let us consider system* (4.3) *with the function* Γ *define in* (4.2). *When* $\Lambda = 0$, *we have the following results*

- *In the monostable case (*$\Gamma \equiv 1$*), system* (4.3a)-(4.3c) *has a unique positive equilibrium* (E^*, F^*, M^*) *if and only if* (4.5a) *holds, where*

$$E^* = K\left(1-\frac{1}{\mathcal{N}}\right), \quad F^* = \frac{\rho\nu_E}{\mu_F}E^*, \quad M^* = \frac{(1-\rho)\nu_E}{\mu_M}E^*. \tag{4.6}$$

  All trajectories of (4.3) *resulting from positive initial data converge to this equilibrium.*

- *In the bistable case (*$\Gamma(M) = 1-e^{-\gamma M}$*), system* (4.3a)-(4.3c) *has two positive equilibria* $(e^*, f^*, m^*) \ll (E^*, F^*, M^*)$ *if and only if* (4.5b) *holds. The trivial equilibrium* $(0,0,0)$ *and* (E^*, F^*, M^*) *are locally asymptotically stable.*

When $\Lambda > 0$, *in both cases, there exists a constant* $\Lambda^* > 0$ *such that if* $\Lambda > \Lambda^*$ *then the extinction equilibrium* $(0,0,0)$ *is globally asymptotically stable.*

Concerning the proof of Proposition 4.1.1, we refer to [200, Lemma 3] for the bistable case and [8, Proposition 2.1] for the monostable case.

Next, we indicate that system (4.1) is monotone on the invariant set $[0,K]\times\mathbb{R}^3_+$:

Lemma 4.1.1. *The set* $[0,K]\times\mathbb{R}^3_+$ *is invariant, i.e. if* $0 \leqslant E^0 \leqslant K$, $0 \leqslant F^0$, $0 \leqslant M^0$, $0 \leqslant M_s^0$ *then for all* $t > 0$, *the solution of* (4.1) *verifies* $0 \leqslant E(t) \leqslant K$, $0 \leqslant F(t)$, $0 \leqslant M(t)$, $0 \leqslant M_s^0$.

Notice that since the equation on E does not have partial derivatives in x variable, the result in Lemma 4.1.1 is also true when K is a function of x and verifies (4.8).

Denoting $\mathbf{U} = (E,F,M,M_s)^T$, $\mathbf{f} = (f_E, f_F, f_M, f_s)^T$ where

$$f_E(E,F,M,M_s) = bF\left(1-\frac{E}{K}\right) - (\mu_E+\nu_E)E, \qquad f_M(E,F,M,M_s) = (1-\rho)\nu_E E - \mu_M M,$$

$$f_F(E,F,M,M_s)=\rho\nu_E E\frac{M}{M+\gamma_s M_s}\Gamma(M+\gamma_s M_s)-\mu_F F,\qquad f_s(E,F,M,M_s)=\Lambda-\mu_s M_s.$$

We may rewrite system (4.1) in the form

$$\partial_t\mathbf{U}-\mathbb{D}\Delta\mathbf{U}=\mathbf{f}(\mathbf{U}),\quad \text{with } \mathbb{D}=\begin{pmatrix}0&0&0&0\\0&D&0&0\\0&0&D&0\\0&0&0&D\end{pmatrix}.$$

By simple computations, we get

$$\frac{\partial f_E}{\partial F}\geqslant 0,\quad \frac{\partial f_M}{\partial E}\geqslant 0,\quad \frac{\partial f_F}{\partial E}\geqslant 0,\quad \frac{\partial f_E}{\partial M}=\frac{\partial f_E}{\partial M_s}=\frac{\partial f_M}{\partial F}=\frac{\partial f_M}{\partial M_s}=0,$$
$$\frac{\partial f_F}{\partial M}=\rho\nu_E E\left(\frac{\gamma_s M_s}{(M+\gamma_s M_s)^2}\Gamma(M+\gamma_s M_s)+\frac{\gamma_s M_s}{M+\gamma_s M_s}\Gamma'(M+\gamma_s M_s)\right)\geqslant 0,$$

and

$$\frac{\partial f_F}{\partial M_s}=-\rho\nu_E E\frac{\gamma_s M}{(M+\gamma_s M_s)^2}\leqslant 0 \text{ in the monostable case,}$$
$$\frac{\partial f_F}{\partial M_s}=-\rho\nu_E E\frac{\gamma_s M}{(M+\gamma_s M_s)^2}\left(1-e^{-\gamma(M+\gamma_s M_s)}(1+\gamma(M+\gamma_s M_s)\right)\leqslant 0,\ \text{in the bistable case,}$$

by applying the inequality $1+x\leqslant e^x$. By applying the Kamke lemma for cooperative systems [59] with the variable $\widetilde{\mathbf{U}}=(E,F,M,-M_s)$, we obtain the monotonicity of system (4.1) on the invariant set $[0,K]\times\mathbb{R}^3_+$.

We define the following order in $\mathbb{R}^4$

Definition 4.1.1. *For any vectors $\mathbf{u},\mathbf{v}\in\mathbb{R}^4$, we define an order $\preceq$ such that $\mathbf{u}\preceq\mathbf{v}$ if and only if*

$$\begin{cases}u_i\leqslant v_i & \text{for } i\in\{1,2,3\},\\ u_4\geqslant v_4.\end{cases}$$

Moreover, we write $\mathbf{u}\prec\mathbf{v}$ if $\mathbf{u}\preceq\mathbf{v}$ and $\mathbf{u}\neq\mathbf{v}$.

We define the super- and sub- solution of system (4.1) as follows

Definition 4.1.2. *We say that $\overline{\mathbf{U}}=(\overline{E},\overline{F},\overline{M},\overline{M_s})$ is a **super-solution** of system (4.1), if it verifies, in the distributional sense, $\partial_t\overline{\mathbf{U}}-\mathbb{D}\Delta\overline{\mathbf{U}}\succeq\mathbf{f}(\overline{\mathbf{U}})$ and $\overline{\mathbf{U}}(t=0)\succeq(E^0,F^0,M^0,M_s^0)$.*

*We say that $\underline{\mathbf{U}}=(\underline{E},\underline{F},\underline{M},\underline{M_s})$ is a **sub-solution** of system (4.1), if it verifies, in the distributional sense, $\partial_t\underline{\mathbf{U}}-\mathbb{D}\Delta\underline{\mathbf{U}}\preceq\mathbf{f}(\underline{\mathbf{U}})$ and $\underline{\mathbf{U}}(t=0)\preceq(E^0,F^0,M^0,M_s^0)$.*

We can deduce the following comparison principle [167, 126] for system (4.1)

Lemma 4.1.2 (Comparison principle)**.** *Let us consider two initial data $(E_1^0,F_1^0,M_1^0,M_{s,1}^0)$ and $(E_2^0,F_2^0,M_2^0,M_{s,2}^0)$ in $[0,K]\times\mathbb{R}^3_+$ satisfying that*

$$(E_1^0,F_1^0,M_1^0,M_{s,1}^0)\preceq(E_2^0,F_2^0,M_2^0,M_{s,2}^0).$$

Suppose that $(E_1,F_1,M_1,M_{s,1})$ is a sub-solution of (4.1) with initial data $(E_1^0,F_1^0,M_1^0,M_{s,1}^0)$, and $(E_2,F_2,M_2,M_{s,2})$ is a super-solution of (4.1) with initial data $(E_2^0,F_2^0,M_2^0,M_{s,2}^0)$. Then, for all $t>0$, we have

$$(E_1,F_1,M_1,M_{s,1})\preceq(E_2,F_2,M_2,M_{s,2}).$$

For the sake of the simplicity of notations, up to a rescaling, we assume that the diffusion coefficient $D=1$ in the rest of this work.

4.1.3 Presentation of the main result

In order to obtain such a spreading solution of (4.1) with a forced speed, we must assume that the initial date is well-prepared, that is, we have already eliminated mosquitoes in a ball. Such an assumption is natural since in practice, to extend a control strategy to a large area, we need to ensure the success in elimination in a smaller area first. More precisely, we consider the following assumption

Assumption 4.1.1. *There exist constants $R > 0, C_0 > 0$, and $u_0 \in (0,1)$ such that for all $x \in \mathbb{R}^2$, we have the initial data (E^0, F^0, M^0, M_s^0) satisfies that*

$$0 \leqslant F^0(x) \leqslant F^*(u_0 \mathbf{1}_{\{|x|\leqslant R\}} + \mathbf{1}_{\{|x|>R\}}), \quad 0 \leqslant E^0(x) \leqslant \min\{K, C_0 F^0(x)\},$$

$$M^0(x) \leqslant C_0 F^0(x), \quad M_s^0 \geqslant \frac{\overline{\Lambda}}{\mu_s} \mathbf{1}_{\{|x|\leqslant R\}},$$

with (E^*, F^*, M^*) is the persistent equilibirum defined in Proposition 4.1.1 and $\overline{\Lambda}$ given in Theorem 4.1.1. Moreover, assume that $(E^0, F^0, M^0)(x) = (E^*, F^*, M^*)$ for $|x|$ large enough,

The main result of this paper is presented as follows.

Theorem 4.1.1. *Assume that* (4.5a) *holds in the monostable case and* (4.5b) *holds in the bistable case on the parameters. Consider constants $c > 0$, $0 < R_1 < R_2$, and the release function given by*

$$\Lambda(t,x) = \overline{\Lambda} \mathbf{1}_{\{R_1+ct\leqslant|x|\leqslant R_2+ct\}}, \qquad \text{in the bistable case,} \tag{4.7a}$$

$$\Lambda(t,x) = \overline{\Lambda} \mathbf{1}_{\{R_1+ct\leqslant|x|\leqslant R_2+ct\}} + \overline{\Lambda} e^{\eta(|x|-(R_1+ct))} \mathbf{1}_{\{|x|<R_1+ct\}}, \qquad \text{in the monostable case.} \tag{4.7b}$$

Then, there exist $\overline{\Lambda} > 0$ large enough, $\overline{\eta}$ small enough and $\overline{L} > 0$ large enough such that for all $\Lambda \geqslant \overline{\Lambda}$, $R_2 - R_1 > \overline{L}$, $0 < \eta \leqslant \overline{\eta}$, the solution of (4.1) *with the release function given in* (4.7) *and initial data satisfying Assumption 4.1.1 for $R > R_2$ and u_0 small enough, verifies*

$$\forall \underline{c} < c, \quad \lim_{t\to+\infty} \sup_{|x|<\underline{c}t} \|(E, M, F)(t,x)\| = 0.$$

Theorem 4.1.1 showed that with the release profiles as in (4.7), if the number of sterile males is large enough, the population spread with the same forced speed c of Λ and the extinction equilibrium invades the persistent equilibrium.

Remark 4.1.1. *Consider the release function Λ as in* (4.7) *in a time period $[0,T]$, then it requires a significantly smaller amount of sterile males compared to the constant release when T gets large. Indeed, if we release a constant number $\overline{\Lambda}$ in a time period $[0,T]$ and in a ball $\mathcal{B}_{R+ct}$, the amount of sterile males required is*

$$\int_0^T \iint_{|x|\leqslant R+ct} \overline{\Lambda} dx dt = \mathcal{O}(T^3).$$

While in the bistable case, our release in (4.7a) *requires an amount of*

$$\int_0^T \iint_{R_1+ct\leqslant|x|\leqslant R_2+ct} \overline{\Lambda} dx dt = \mathcal{O}(T^2).$$

In the monostable case, the release in (4.7b) *requires*

$$\int_0^T \iint_{R_1+ct\leqslant|x|\leqslant R_2+ct} \overline{\Lambda} dx dt + \int_0^T \iint_{|x|\leqslant R_1+ct} \overline{\Lambda} e^{\eta(|x|-(R_1+ct))} dx dt = \mathcal{O}(T^2)$$

We leave the computation for the reader.

For practical application, it seems natural to consider the heterogeneous case where the carrying capacity K depends on the space variable. More precisely, let us assume the following :

$$\exists\, K_2 > K_1 > 0, \text{ such that, for all } x \in \mathbb{R}^2,\ K_1 \leqslant K(x) \leqslant K_2. \tag{4.8}$$

Then, we keep the same assumption on the initial data as in Assumption 4.1.1, except that we modify obviously the assumption on E^0 in the following way :

$$0 \leqslant E^0(x) \leqslant \min\{K(x), C_0 F^0(x)\} \text{ for all } x \in \mathbb{R}^2.$$

The constant ζ defined in (4.4) depends on x. We assume that in the bistable case, the assumption in (4.5b) holds for all $x \in \mathbb{R}^2$. As a consequence of Theorem 4.1.1 we have

Corollary 4.1.1. *Under the same assumption of Theorem 4.1.1. Let $c > 0$ and $0 < R_1 < R_2$, we consider the release function Λ as in* (4.7). *Then, there exist $\overline{\Lambda}$ large enough, $\overline{\eta}$ small enough and $\overline{L} > 0$ large enough such*

that for all $\Lambda \geqslant \overline{\Lambda}$, $R_2 - R_1 > \overline{L}$, $0 < \eta \leqslant \overline{\eta}$, *the solution of* (4.1) *with the release function given in* (4.7) *and initial data satisfying Assumption 4.1.1 for* $R > R_2$ *and* u_0 *small enough, verifies*

$$\forall \underline{c} < c, \quad \lim_{t\to+\infty} \sup_{|x|<\underline{c}t} \|(E, M, F)(t, x)\| = 0.$$

4.1.4 Idea of the proof & Organisation of the paper

The principal idea of the proof is to use the comparison principle and construct a radially symmetric super-that goes to 0 in the set $\{|x| < \underline{c}t\}$ for any $\underline{c} < c$.

To construct the super-solution, we split the spatial domain into four subdomains : Consider some positive constants c', r_1, r_2 such that $\max\left\{\frac{2}{3}c, \frac{\underline{c}+c}{2}\right\} < c' < c$ and $0 < R_1 < r_1 < r_2 < R_2$,

1. $\Omega_t^0 = B_{r_1+c't}$ (where B_r denotes the ball of radius r and center at the origin) with c' that will be fixed later on,
2. $\Omega_t^1 = T(0, r_1 + c't, r_1 + ct)$ (where $T(z, r, R)$ denotes the torus of center z, small radius r and big radius R, i.e. $T(z, r, R) = \{x \in \mathbb{R}^2,\ r \leqslant \|x - z\| \leqslant R\}$),
3. $\Omega_t^2 = T(0, r_1 + ct, r_2 + ct)$ (it is the torus of action),
4. $\Omega_t^3 = B^c_{r_2+ct}$, the rest of the field.

Notice that $\mathbb{R}^2 = \overline{\Omega_t^0 \cup \Omega_t^1 \cup \Omega_t^2 \cup \Omega_t^3}$ and $\Omega_t^0 < \Omega_t^1 < \Omega_t^2 < \Omega_t^3$ (in term of modulus). We underline that the distance $L = r_2 - r_1$ has not been fixed yet.

In the rest of the paper, we present the construction of a super-solution in order to prove the Theorem 4.1.1. Section 4.2 is devoted to the construction of the super-solution, where we construct different parts of the super-solution on each subdomain Ω_t^i with $i = 1, \ldots, 4$. We provide the proof of Theorem 4.1.1 and Corollary 4.1.1 in Section 4.3 and provide numerical illustration in Section 4.4.

4.2 Construction of a radially symmetric super-solution

In this part, we construct in 4.2.1 a profile of the super-solution in each sub-domain Ω_t^i of the space defined in 4.1.4 with $i = 1, \ldots, 4$. We emphasize that μ, ε, c', and L are free parameters and can be fixed later in the construction. Then in 4.2.2, we construct a super-solution by the following steps:

- **Step 1:** We construct $\overline{F}$ by parts according to the profiles set up in 4.2.1.
- **Step 2:** We obtain solution $\overline{E}$ of equation (4.1a) by inserting $F = \overline{F}$, and show that by taking $\mu > 0$, $\varepsilon > 0$ small enough, there exists a constant $C_1 > 0$ such that $\overline{E} \leqslant C_1\overline{F}$.
- **Step 3:** We obtain solution $\overline{M}$ of equation (4.1c) by inserting $E = \overline{E}$, and show that by taking $\mu > 0$, $\varepsilon > 0$ small enough, there exists a constant $C_2 > 0$ such that $\overline{M} \leqslant C_2\overline{F}$.
- **Step 4:** We provide some lower bound for M_s depending on the release function Λ defined in (4.7).
- **Step 5:** We show that by taking appropriate values of c' and L, $(\overline{E}, \overline{F}, \overline{M})$ is a super-solution of system (4.1a)-(4.1c) with initial data satisfying Assumption 4.1.1.

4.2.1 Preparation of the construction

On the torus Ω_t^1

We first construct a function $\phi_1(t, x)$ on the torus Ω_t^1 which will serve as the shape of the super-solution on this torus.

Lemma 4.2.1. *Let* $\mu > 0$, $r_1 > 0$, *and* $u_0 > 0$, *and let* $0 < \underline{c} < c' < c$ *with* $c' > \frac{2}{3}c$. *Let us define*

$$\alpha(t) := \frac{u_0}{\lambda_+ e^{\lambda_-[c-c']t} - \lambda_- e^{\lambda_+[c-c']t}}, \qquad \beta(r) := \lambda_+ e^{\lambda_- r} - \lambda_- e^{\lambda_+ r}. \tag{4.9}$$

where $\lambda_\pm = \dfrac{-(c' + \frac{1}{r_1}) \pm \sqrt{(c' + \frac{1}{r_1})^2 + 2\mu}}{2}$. *Then, the following hold :*

(i) The function $t \mapsto \alpha(t)$ is positive and decreasing for $t \geqslant 0$, $\lim_{t\to+\infty} \alpha(t) = 0$, and for all $t \geqslant 0$, we have $\alpha'(t) > -\frac{\mu}{4}\alpha(t)$.

(ii) The function $r \mapsto \beta(r)$ is positive and increasing for $r \geqslant 0$, moreover for all $r > 0$, we have $\beta'(r) < \sqrt{\frac{\mu}{2}}\beta(r)$.

(iii) The function ϕ_1 defined by

$$\phi_1(t,x) = \alpha(t)\beta(|x| - (r_1 + c't)), \tag{4.10}$$

is a super-solution on Ω_t^1 of the equation $\partial_t u - \Delta u = -\mu u$ which verifies the Dirichlet condition $u = u_0$ on the boundary $\{|x| = r_1 + ct\}$ and Neumann condition $\partial_\nu u = 0$ on the boundary $\{|x| = r_1 + c't\}$.

Remark 4.2.1. *Notice that for $t > 0$ fixed, the function $\psi_1(r) := \alpha(t)\beta(r - (r_1 + c't))$ is a solution of the boundary value problem*

$$\begin{cases} -(c' + \dfrac{1}{r_1})\psi_1' - \psi_1'' = -\dfrac{\mu}{2}\psi_1 \\ \psi_1(r_1 + ct) = u_0, \\ \psi_1'(r_1 + c't) = 0. \end{cases}$$

Proof of Lemma 4.2.1. For the point (i), we notice that by definition of $\lambda_\pm$, we have $0 < \lambda_+ < -\lambda_-$. Then, clearly α is positive and goes to 0 as t grows to $+\infty$. Then, we compute

$$\alpha'(t) = -\frac{u_0\lambda_+\lambda_-[c-c']\left(e^{\lambda_-[c-c']t} - e^{\lambda_+[c-c']t}\right)}{(\lambda_+ e^{\lambda_-[c-c']t} - \lambda_- e^{\lambda_+[c-c']t})^2} = \lambda_+\lambda_-[c-c'] \cdot \frac{e^{\lambda_+[c-c']t} - e^{\lambda_-[c-c']t}}{\lambda_+ e^{\lambda_-[c-c']t} - \lambda_- e^{\lambda_+[c-c']t}}\alpha(t).$$

By definition of $\lambda_\pm$, we have $\lambda_+\lambda_- = -\frac{\mu}{2}$, and since $0 < \lambda_+ < -\lambda_-$. We have

$$\frac{e^{\lambda_+[c-c']t} - e^{\lambda_-[c-c']t}}{\lambda_+ e^{\lambda_-[c-c']t} - \lambda_- e^{\lambda_+[c-c']t}} \leqslant \frac{e^{\lambda_+[c-c']t} - e^{\lambda_-[c-c']t}}{-\lambda_- e^{\lambda_+[c-c']t}} \leqslant -\frac{1}{\lambda_-} < \frac{1}{c'}.$$

Then, for all $c' \in (\frac{2}{3}c, c)$, which is equivalent to $\frac{c-c'}{c'} \in (0, \frac{1}{2})$, we have

$$\alpha'(t) > -\frac{\mu}{2}\frac{[c-c']}{c'}\alpha(t) > -\frac{\mu}{4}\alpha(t).$$

For the point (ii), the positivity of β is clear since $\lambda_- < 0 < \lambda_+$, then we have

$$\beta'(r) = -\lambda_+\lambda_-(e^{\lambda_+ r} - e^{\lambda_- r}) = \frac{\mu}{2}(e^{\lambda_+ r} - e^{\lambda_- r}) > 0.$$

And

$$\beta'(r) = -\lambda_+\lambda_-(e^{\lambda_+ r} - e^{\lambda_- r}) < -\lambda_+\lambda_- e^{\lambda_+ r} < \lambda_+\beta(r) < \sqrt{\frac{\mu}{2}}\beta(r).$$

For the point (iii), we first notice that according to Remark 4.2.1 we have

$$-\left(c' + \frac{1}{r_1}\right)\beta' - \beta'' + \frac{\mu}{2}\beta = 0.$$

Then, we compute, denoting $r = |x|$,

$$\begin{aligned} \partial_t\phi_1 - \Delta\phi_1 + \mu\phi_1 &= \left(\alpha' + \frac{\mu}{2}\alpha\right)(t)\beta(r - [r_1 + c't]) + \alpha(t)\left[-(c' + \frac{1}{r})\beta' - \beta'' + \frac{\mu}{2}\beta\right](r - [r_1 + c't]) \\ &= \left(\alpha' + \frac{\mu}{2}\alpha\right)(t)\beta(r - [r_1 + c't]) + \alpha(t)\left(\frac{1}{r_1} - \frac{1}{r}\right)\beta'(r - [r_1 + c't]). \end{aligned}$$

Recalling that $r_1 + c't < r < r_1 + ct$, $\alpha(t) > 0$ and β is increasing, it implies

$$\alpha(t)\left(\frac{1}{r_1} - \frac{1}{r}\right)\beta'(r - [r_1 + c't]) > 0.$$

Then, we arrive at

$$\partial_t\phi_1 - \Delta\phi_1 + \mu\phi_1 > \left(\alpha' + \frac{\mu}{2}\alpha\right)(t)\beta(r - [r_1 + c't]). \tag{4.11}$$

Then, we use the inequality in point (i) and deduce that, for all $c' \in (\frac{2}{3}c, c)$,

$$(\alpha' + \frac{\mu}{2}\alpha)\beta > \frac{\mu\alpha\beta}{4} > 0. \tag{4.12}$$

We conclude thanks to (4.11). □

On the torus Ω_t^2

Now, we construct a function ϕ_2 on the torus Ω_t^2 using a similar result as in [12, Lemma 2]. First, we provide the following Lemma

Lemma 4.2.2. *Let $\varepsilon > 0$, $u_0 \in (0,1)$, $c > 0$, and $r_1 > 0$. There exists a constant L large enough such that the following system admits a solution ψ_2 :*

$$\begin{cases} -(c + \dfrac{1}{r_1})\psi_2' - \psi_2'' = -\varepsilon\psi_2, \\ \psi_2(0) = u_0, \quad \psi_2'(0) = 0, \\ \psi_2(L) = 1, \quad \psi_2'(L) > 0. \end{cases}$$

Moreover, ψ_2 is positive, increasing on $(0, L)$, and we have $0 < \psi_2'(r) < \sqrt{\varepsilon}\psi_2(r)$.

Proof. Denoting

$$\widetilde{\lambda}_\pm = \frac{1}{2}\left(-\left(c + \frac{1}{r_1}\right) \pm \sqrt{\left(c + \frac{1}{r_1}\right)^2 + 4\varepsilon}\right), \qquad \widetilde{\lambda}_- < 0 < \widetilde{\lambda}_+,$$

we define

$$\psi_2(r) = \frac{u_0}{\sqrt{(c + \frac{1}{r_1})^2 + 4\varepsilon}}\left(\widetilde{\lambda}_+ e^{\widetilde{\lambda}_- r} - \widetilde{\lambda}_- e^{\widetilde{\lambda}_+ r}\right).$$

We verify easily that ψ_2 is a continuous, differentiable, and increasing function on $\mathbb{R}^+$. Moreover, $\psi_2(0) = u_0 < 1$, $\lim_{r\to+\infty} \psi_2(r) = +\infty$. Hence there exists L large enough such that $\psi_2(L) = 1$. Furthermore, by the same token as for β in the point (ii) Lemma 4.2.1, we obtain by simple computations that $\psi_2'(r) < \widetilde{\lambda}_+\psi_2(r) < \sqrt{\varepsilon}\psi_2(r)$. □

We define the function ϕ_2 as follows

Lemma 4.2.3. *Under the same assumption as in Lemma 4.2.2, let us fix $r_2 = L + r_1$ and define*

$$\phi_2(x,t) = \psi_2(|x| - (r_1 + ct)), \tag{4.13}$$

where ψ_2 is defined in Lemma 4.2.2. Then, the function ϕ_2 is a super-solution of the equation $\partial_t u - \Delta u = -\varepsilon u$ on Ω_t^2 with Dirichlet boundary conditions $u = u_0$ on $\{|x| = r_1 + ct\}$ and $u = 1$ on $\{|x| = r_2 + ct\}$.

Moreover, on the set $\{|x| = r_1 + ct\}$, we have $\partial_\nu\phi_2(t,x) = 0$, and on $\{|x| = r_2 + ct\}$, we have $\partial_\nu\phi_2(t,x) > 0$, with ν is the normal outward vector on the boundary.

Proof. We denote $r = |x|$ and verify easily that,

$$\partial_t\phi_2 - \Delta\phi_2 + \varepsilon\phi_2 = -(c + \frac{1}{r})\psi_2' - \psi_2'' + \varepsilon\psi_2 = \left(\frac{1}{r_1} - \frac{1}{r}\right)\psi_2'.$$

This latter quantity is nonnegative since on Ω_t^2 we have $r_1 + ct < r < r_2 + ct$ and ψ_2 is increasing. Finally, the Dirichlet boundary conditions follows straightforwardly from the definition of ψ_2 in Lemma 4.2.2. □

4.2.2 Construction of a super-solution

In this part, we construct a radially symmetric super-solution $(\overline{E}, \overline{F}, \overline{M})$ of system (4.1a)-(4.1c).

Construction of $\overline{F}$

We first recall the notation (E^*, M^*, F^*) for the positive equilibrium of system (4.1a)–(4.1b). With the notations of Lemma 4.2.1 and Lemma 4.2.3, we define $\overline{F}(t,x)$ on $\mathbb{R}^2$ by

$$\overline{F}(t,x) = \begin{cases} F^*\alpha(t)\beta(0) & \text{on } \Omega_t^0, \\ F^*\phi_1(t,x) & \text{on } \Omega_t^1, \\ F^*\phi_2(t,x) & \text{on } \Omega_t^2, \\ F^* & \text{on } \Omega_t^3. \end{cases} \tag{4.14}$$

By this construction, the function $\overline{F}$ is radially symmetric and nondecreasing with respect to $|x|$.

Lemma 4.2.4. *Let $\mu > 0$, $r_1 > 0$, $\varepsilon > 0$, and $u_0 \in (0,1)$, and let $0 < \underline{c} < c' < c$ with $c' > \frac{2}{3}c$. Let $L = r_2 - r_1$ be large enough as in Lemma 4.2.2. We define $g(t,x)$ by*

$$g(t,x) = \frac{\mu}{4}\mathbf{1}_{\Omega_t^0} + \mu\mathbf{1}_{\Omega_t^1} + \varepsilon\mathbf{1}_{\Omega_t^2}.$$

Then, $\overline{F}$ defined in (4.14) is a super-solution in $\mathbb{R}^2$ of the equation

$$\partial_t v - \Delta v + g(t,x)v = 0, \quad v(t=0) \leqslant \overline{F}(0,x).$$

Proof. By construction, $\overline{F}$ is continuous on $\mathbb{R}^2$, and for all fixed $t > 0$, and increasing with respect to $|x|$. on Ω_t^1 and Ω_t^2, from the definition of ϕ_1 and ϕ_2 in Lemma 4.2.1 and Lemma 4.2.3, it is clear that

$$\partial_t\overline{F} - \Delta\overline{F} + g(t,x)\overline{F} \geqslant 0, \quad \text{on } \Omega_t^1 \cup \Omega_t^2.$$

Noticing also that on the boundary $\{|x| = r_1 + ct\}$, we have $\partial_\nu\phi_1(t,x) \geqslant \partial_\nu\phi_2(t,x) = 0$, with ν is the normal outward vector on the boundary.

On Ω_t^3, $\overline{F}$ is a constant therefore it is a super-solution since g is nonnegative and on the boundary $\{|x| = r_2 + ct\}$ we have $\partial_\nu\phi_2(t,x) \geqslant 0 = \partial_\nu\overline{F}(t,x)$.

Finally, on Ω_t^0, we have $\Delta\overline{F} = 0$ and $\partial_t\overline{F} > -\frac{\mu}{4}\overline{F}$ (see Lemma 4.2.1 (i)). We conclude by noticing also that the derivatives coincide at the boundary $\{|x| = r_1 + c't\}$. □

Construction of $\overline{E}$

Lemma 4.2.5. *Under the same assumptions as in Lemma 4.2.4, let us define $\overline{E}$ as the solution of the equation*

$$\partial_t\overline{E} = b\overline{F}\left(1 - \frac{\overline{E}}{K}\right) - (\mu_E + \nu_E)\overline{E}, \qquad \overline{E}(t=0) = E^0 \leqslant \min\{K, C_0\overline{F}(x,0)\}, \tag{4.15}$$

for some positive constant C_0, $\overline{F}$ being defined in (4.14). Then, there exists $C_1 \geqslant C_0$ large enough and $0 < \mu$, $0 < \varepsilon$ small enough such that for all $t > 0$ and $x \in \mathbb{R}^2$, $\overline{E}(t,x) \leqslant C_1\overline{F}(t,x)$.

Proof. We verify that there exist $C > 0$ large enough and $\mu > 0, \varepsilon > 0$ small enough such that $C\overline{F}$ is a super-solution of the equation for $\overline{E}$, i.e.

$$C\partial_t\overline{F} - b\overline{F}\left(1 - \frac{C\overline{F}}{K}\right) + (\mu_E + \nu_E)C\overline{F} \geqslant 0.$$

On Ω_t^0, we compute

$$\begin{aligned} C\partial_t\overline{F} - b\overline{F}\left(1 - \frac{C\overline{F}}{K}\right) + (\mu_E + \nu_E)C\overline{F} &= F^*\beta(0)\left[C\alpha'(t) + \alpha(t)\left(C(\mu_E + \nu_E) - b + \frac{CbF^*\alpha(t)\beta(0)}{K}\right)\right] \\ &\geqslant F^*C\alpha(t)\beta(0)\left(-\frac{\mu}{4} + \mu_E + \nu_E - \frac{b}{C} + \frac{bF^*\alpha(t)\beta(0)}{K}\right). \end{aligned}$$

Then, if C is large enough and μ small enough, this latter term is nonnegative.

On Ω_t^1, we have

$$C\partial_t\overline{F} - b\overline{F}\left(1 - \frac{C\overline{F}}{K}\right) + (\mu_E + \nu_E)C\overline{F} = F^*\left[C\partial_t\phi_1 - b\phi_1\left(1 - \frac{CF^*\phi_1}{K}\right) + (\mu_E + \nu_E)C\phi_1\right]$$

$$= F^* \left[C\alpha'\beta - c'C\alpha\beta' - b\phi_1 \left(1 - \frac{CF^*\phi_1}{K}\right) + (\mu_E + \nu_E)C\phi_1 \right]$$
$$> F^* \left[-C\left(\frac{\mu}{4} + c'\sqrt{\frac{\mu}{2}}\right)\phi_1 - b\phi_1 \left(1 - \frac{CF^*\phi_1}{K}\right) + (\mu_E + \nu_E)C\phi_1 \right],$$

where we use Lemma 4.2.1 (i) and (ii). We arrive at

$$C\partial_t\overline{F} - b\overline{F}\left(1 - \frac{C\overline{F}}{K}\right) + (\mu_E + \nu_E)C\overline{F} > CF^*\phi_1 \left[-\left(\frac{\mu}{4} + c'\sqrt{\frac{\mu}{2}}\right) - \frac{b}{C} + \mu_E + \nu_E \right].$$

This latter term is nonnegative provided C is large enough and μ is small enough.

On Ω_t^2, by the same token as above, by using the construction of ϕ_2 in Lemma 4.2.3, we compute

$$\begin{aligned} C\partial_t\overline{F} - b\overline{F}\left(1 - \frac{C\overline{F}}{K}\right) + (\mu_E + \nu_E)C\overline{F} &= CF^* \left[\partial_t\phi_2 - b\phi_2 \left(\frac{1}{C} - \frac{F^*\phi_2}{K}\right) + (\mu_E + \nu_E)\phi_2 \right] \\ &= CF^* \left[c\psi_2' - b\psi_2 \left(\frac{1}{C} - \frac{F^*\psi_2}{K}\right) + (\mu_E + \nu_E)\psi_2 \right] \\ &> CF^*\psi_2 \left(-c\sqrt{\varepsilon} - \frac{b}{C} + \mu_E + \nu_E \right). \end{aligned}$$

The latter term is nonnegative provided ε is small enough and C is large enough.

Finally, on Ω_t^3, we have $\overline{F} = F^*$ is a constant and $\overline{E}$ is bounded. Therefore, $\overline{E} \leqslant C\overline{F}$ on Ω_t^3 for C large enough. We conclude the proof by taking $C_1 = \max\{C, C_0\}$. □

Construction of $\overline{M}$

Lemma 4.2.6. *Under the same assumptions as in Lemma 4.2.4, let us define $\overline{M}$ as the solution of the equation*

$$\partial_t\overline{M} - \Delta\overline{M} = (1-\rho)\nu_E\overline{E} - \mu_M\overline{M}, \qquad \overline{M}(t=0) = M^0 \leqslant C_0\overline{F}(x,0), \tag{4.16}$$

with $\overline{E}$ defined in Lemma 4.2.5. Then, if $\mu > 0$ and $\varepsilon > 0$ are small enough, there exists $C_2 \geqslant C_0$ large enough such that for all $t > 0$ and $x \in \mathbb{R}^2$, $\overline{M}(t,x) \leqslant C_2\overline{F}(t,x)$.

Proof. We compute for some constant $C > 0$, using Lemma 4.2.4,

$$\begin{aligned} C\partial_t\overline{F} - C\Delta\overline{F} + \mu_M C\overline{F} - (1-\rho)\nu_E\overline{E} &\geqslant -Cg(t,x)\overline{F} + C\mu_M\overline{F} - (1-r)\nu_E\overline{E} \\ &= (-Cg(t,x) + C\mu_M - (1-\rho)\nu_E C_1)\overline{F}, \end{aligned}$$

where we use Lemma 4.2.5 for the last inequality. Hence, if we take μ and ε small enough such that $\mu_M - \underline{g} > 0$, we make take C large enough such that $C(\mu_M - g) \geqslant C_1(1-r)\nu_E$. It implies that for C large enough $C\overline{F}$ is a super-solution of the equation (4.16), we conclude the proof by taking $C_2 = C$. □

Conditions on M_s

In this part, we provide in Lemma 4.2.7 some lower bounds for M_s depending on Λ defined in (4.7). Then, in Proposition 4.2.1, we show that for Λ large enough, $(\overline{E}, \overline{F}, \overline{M})$ defined in (4.15), (4.14), and (4.16) is the super-solution of system (4.1a)-(4.1c). This condition is natural since the number of sterile males needs to be large enough to drive the wild population to elimination.

Lemma 4.2.7. *Let $c > 0$, $0 < R_1 < r_1 < r_2 < R_2$ be fixed. Let M_s be the solution to the equation*

$$\partial_t M_s - \Delta M_s = \Lambda - \mu_s M_s, \qquad M_s(t=0) = M_s^0, \tag{4.17}$$

with M_s^0 satisfies Assumption 4.1.1 with $R > R_2$, and Λ defined in (4.7). Then,there exists a constant $\overline{M_s} > 0$ proportional to $\overline{\Lambda}$ and depending on $c + \frac{1}{r_2}$, $r_1 - R_1$, $R_2 - r_2$, and μ_s such that the solution of the above equation (4.17) verifies that

(i) in the bistable case with Λ as in (4.7a),

$$M_s(t,x) \geqslant \overline{M_s}\mathbf{1}_{\{r_1+ct<|x|<r_2+ct\}}, \tag{4.18}$$

(ii) in the monostable case with Λ *as in* (4.7b),

$$M_s(t,x) \geqslant \overline{M_s}\left(\mathbf{1}_{\{r_1+ct<|x|<r_2+ct\}} + e^{\eta(|x|-r_1-ct)}\mathbf{1}_{\{|x|\leqslant r_1+ct\}}\right), \tag{4.19}$$

Remark 4.2.2. *In the monostable case (ii), by the condition* (4.19) *in Lemma 4.2.7 on* M_s*, we deduce that for* $\eta > 0$ *small enough, we have* $M_s \geqslant \overline{M_s}\frac{\overline{F}}{F^* u_0}\mathbf{1}_{\{|x|<r_1+ct\}}$ *with* $\overline{F}$ *defined in* (4.14).

Proof. The proof relies on the construction of a sub-solution for the equation (4.17). First, it is clear that M_s^0 verifies the inequalities announced.

(i) Let us introduce the function m defined on $\mathbb{R}$ by

$$m(r) = \widehat{\mathrm{M}}\begin{cases} e^{-a(r-r_1)^2}, & \text{on } (-\infty, r_1), \\ 1, & \text{on } [r_1, r_2], \\ e^{-b(r-r_2)^2}, & \text{on } (r_2, +\infty), \end{cases}$$

for some positive constants a, b, $\widehat{\mathrm{M}}$ which will be fixed later. Then, for $t > 0$, $x \in \mathbb{R}^2$, we define the function $m_s(t,x) = m(|x| - ct)$. Clearly, $m_s \geqslant \widehat{\mathrm{M}}\mathbf{1}_{\{r_1+ct<|x|<r_2+ct\}}$. We compute

$$\partial_t m_s - \Delta m_s + \mu_s m_s = -m'' - \left(c + \frac{1}{|x|}\right)m' + \mu_s m$$

$$= \widehat{\mathrm{M}}\begin{cases} e^{-a(|x|-r_1-ct)^2}\left(\mu_s + 2a(|x|-r_1-ct)\Big(c+\frac{1}{|x|}\Big) + 2a - 4a^2(|x|-r_1-ct)^2\right), & \text{if } |x| < r_1+ct, \\ \mu_s, & \text{if } |x| \in [r_1+ct, r_2+ct], \\ e^{-b(|x|-r_2-ct)^2}\left(\mu_s + 2b(|x|-r_2-ct)\Big(c+\frac{1}{|x|}\Big) + 2b - 4b^2(|x|-r_2-ct)^2\right), & \text{if } |x| > r_2+ct. \end{cases}$$

• For all $|x| \leqslant r_1 + ct$, we have

$$\mu_s + 2a(|x|-r_1-ct)\left(c+\frac{1}{|x|}\right) + 2a - 4a^2(|x|-r_1-ct)^2 \leqslant \mu_s + 2a.$$

In particular, for $|x| < R_1 + ct < r_1 + ct$,

$$\mu_s + 2a(|x|-r_1-ct)\left(c+\frac{1}{|x|}\right) + 2a - 4a^2(|x|-r_1-ct)^2 \leqslant \mu_s + 2a - 4a^2(R_1-r_1)^2.$$

This right hand side is non-positive if $a \geqslant \dfrac{1+\sqrt{1+4(r_1-R_1)^2\mu_s}}{4(r_1-R_1)^2}$. Hence, if $\widehat{\mathrm{M}} \leqslant \dfrac{\overline{\Lambda}}{2a+\mu_s}$, we arrive at the estimate, for all $|x| \leqslant r_1 + ct$,

$$\widehat{\mathrm{M}}\left[\mu_s + 2a(|x|-r_1-ct)\Big(c+\frac{1}{|x|}\Big) + 2a - 4a^2(|x|-r_1-ct)^2\right] \leqslant \overline{\Lambda}\mathbf{1}_{\{R_1+ct<|x|<r_1+ct\}}. \tag{4.20}$$

• For all $|x| \geqslant r_2 + ct$, we have, for all $t > 0$,

$$\begin{aligned} &\mu_s + 2b(|x|-r_2-ct)\Big(c+\frac{1}{|x|}\Big) + 2b - 4b^2(|x|-r_2-ct)^2 \\ &\quad\leqslant \mu_s + 2b(|x|-r_2-ct)\Big(c+\frac{1}{r_2}\Big) + 2b - 4b^2(|x|-r_2-ct)^2 = \mathrm{P}(|x|-r_2-ct), \end{aligned}$$

where $\mathrm{P}(X) = \mu_s + 2b + 2b\Big(c+\dfrac{1}{r_2}\Big)X - 4b^2X^2$. This polynomial is maximum at $X = \dfrac{1}{4b}(c+\dfrac{1}{r_2})$ with maximum value given by $2b + \mu_s + \dfrac{1}{4}(c+\dfrac{1}{r_2})^2$. Hence, if

$$\widehat{\mathrm{M}} \leqslant \frac{\overline{\Lambda}}{2b+\mu_s+\frac{1}{4}(c+\frac{1}{r_2})^2}, \tag{4.21}$$

we deduce that $\widehat{\mathrm{M}}\mathrm{P}(|x|-r_2-ct) \leqslant \overline{\Lambda}$.

Then, for all $|x| \geqslant R_2 + ct$, we have $X \geqslant R_2 - r_2$. We obtain that $P(X) \leqslant P(R_2 - r_2)$ for all $X \geqslant R_2 - r_2$ if $R_2 - r_2 \geqslant \dfrac{1}{4b}\left(c + \dfrac{1}{r_2}\right)$ which is equivalent to $b \geqslant \dfrac{1}{4(R_2 - r_2)}\left(c + \dfrac{1}{r_2}\right)$. Moreover, we verify easily that $\mathrm{P}(R_2 - r_2) \leqslant 0$ for any

$$b \geqslant \frac{1}{4(R_2 - r_2)^2}\left[\left(c + \frac{1}{r_2}\right)(R_2 - r_2) + 1 + \sqrt{\left(1 + \left(c + \frac{1}{r_2}\right)(R_2 - r_2)\right)^2 + 4\mu_s(R_2 - r_2)^2}\right]. \quad (4.22)$$

As a consequence, we have proved that when b and $\widehat{\mathrm{M}}$ verify respectively (4.22) and (4.21), then for all $|x| \geqslant r_2 + ct$,

$$\widehat{\mathrm{M}}\left[\mu_s + 2b(|x| - r_2 - ct)\left(c + \frac{1}{|x|}\right) + 2b - 4b^2(|x| - r_2 - ct)^2\right] \leqslant \overline{\Lambda}\mathbf{1}_{\{r_2+ct<|x|<R_2+ct\}}. \quad (4.23)$$

• For all $|x| \in [r_1 + ct, r_2 + ct]$, if $\widehat{\mathrm{M}} \leqslant \dfrac{\overline{\Lambda}}{\mu_s}$, then

$$\partial_t m_s - \Delta m_s + \mu_s m_s \leqslant \overline{\Lambda}\mathbf{1}_{\{r_1+ct<|x|<r_2+ct\}} \quad (4.24)$$

Combining (4.20),(4.23), and (4.24), it shows that for all $t > 0$, $x \in \mathbb{R}^2$,

$$\partial_t m_s - \Delta m_s + \mu_s m_s \leqslant \Lambda.$$

Hence m_s is a sub-solution for equation (4.17) which implies $M_s \geqslant m_s \geqslant \widehat{\mathrm{M}}\mathbf{1}_{\{r_1+ct<|x|<r_2+ct\}}$. We conclude the proof of this first point by taking

$$\widehat{\mathrm{M}} = \overline{\Lambda}\min\left\{\frac{1}{2b + \mu_s + \frac{1}{4}\left(c + \frac{1}{r_2}\right)^2}, \frac{1}{2a + \mu_s}\right\},$$

with a and b chosen as above.

(ii) We proceed in the same way for the proof of the second point. We first fix $\varepsilon > 0$ such that $\eta(r_1 - R_1) = (1 + \varepsilon)\ln(1 + \varepsilon)$ and we define $a_\varepsilon = \dfrac{\eta}{(1 + \varepsilon)(r_1 - R_1)}$. Then, we introduce the function

$$m(r) = \widehat{\mathrm{M}}\begin{cases} e^{\eta(r - R_1)}, & \text{on } (-\infty, R_1), \\ (1 + \varepsilon)e^{-a_\varepsilon(r - r_1)^2} & \text{on } (R_1, r_1), \\ 1 + \varepsilon, & \text{on } (r_1, r_2), \\ (1 + \varepsilon)e^{-b(r - r_2)^2}, & \text{on } (r_2, +\infty), \end{cases}$$

for some constant $\widehat{\mathrm{M}}$ which will be fixed later. With this choice of ε and a_ε, we have $m \in C^1(\mathbb{R})$. As above, we define $m_s(t, x) = m(|x| - ct)$ for $t > 0$ and $x \in \mathbb{R}^2$, we notice that

$$m_s(t, x) \geqslant \widehat{\mathrm{M}}\left(\mathbf{1}_{\{r_1+ct<|x|<r_2+ct\}} + e^{\eta(|x| - r_1 - ct)}\mathbf{1}_{\{|x|\leqslant r_1+ct\}}\right). \quad (4.25)$$

We show that we may find constants b, and $\widehat{\mathrm{M}}$ such that m_s is a sub-solution of (4.17).

For $|x| < R_1 + ct$, we have

$$\begin{aligned} \partial_t m_s - \Delta m_s + \mu_s m_s &= -m'' - \left(c + \frac{1}{|x|}\right)m' + \mu_s m \\ &= \widehat{\mathrm{M}}e^{\eta(|x| - R_1 - ct)}\left[\mu_s - \left(c + \frac{1}{|x|}\right)\eta - \eta^2\right] \\ &\leqslant \widehat{\mathrm{M}}\mu_s e^{\eta(|x| - R_1 - ct)}. \end{aligned}$$

For $R_1 + ct < |x| < r_1 + ct$, we compute

$$\begin{aligned}
&\partial_t m_s - \Delta m_s + \mu_s m_s = -m'' - \left(c + \frac{1}{|x|}\right) m' + \mu_s m \\
&= \widehat{\mathrm{M}}(1+\varepsilon) e^{-a_\varepsilon(|x|-r_1-ct)^2} \left(\mu_s + 2a_\varepsilon(|x|-r_1-ct)\Big(c+\frac{1}{|x|}\Big) + 2a_\varepsilon - 4a_\varepsilon^2(|x|-r_1-ct)^2\right) \\
&\leqslant \widehat{\mathrm{M}}(1+\varepsilon) e^{-a_\varepsilon(|x|-r_1-ct)^2} \left(\mu_s + 2a_\varepsilon\right)
\end{aligned}$$

For $r_1 + ct < |x| < r_2 + ct$, we compute

$$\partial_t m_s - \Delta m_s + \mu_s m_s = \widehat{\mathrm{M}}(1+\varepsilon)\mu_s.$$

We treat the domain $|x| > r_2 + ct$ as in the point (i).

Finally, by taking b verifying (4.22) and

$$\widehat{\mathrm{M}} = \frac{\overline{\Lambda}}{1+\varepsilon} \min\left(\frac{1}{2b + \mu_s + \frac{1}{4}(c+\frac{1}{r_2})^2}, \frac{1}{2a_\varepsilon + \mu_s}\right),$$

we deduce that

$$\partial_t m_s - \Delta m_s + \mu_s m_s \leqslant \Lambda.$$

Hence, m_s is a sub-solution and thanks to estimate (4.25), we conclude the proof by taking $\overline{M_s} = \widehat{\mathrm{M}}$.

□

Proposition 4.2.1. *Let $\mu > 0$, $r_1 > 0$, $\varepsilon > 0$, $u_0 \in (0,1)$, and $0 < \underline{c} < c' < c$ with $c' > \frac{2}{3}c$. Let $L = r_2 - r_1$ be large enough as in Lemma 4.2.2. Consider function Λ defined in* (4.7) *with some constants $\overline{\Lambda} > 0$, $\eta > 0$.*

Then, for μ, $\varepsilon \in (0, \mu_F)$ and $u_0 \in (0,1)$ small enough, $\overline{\Lambda} > 0$ large enough, and $\eta > 0$ small enough (in the monostable case), $(\overline{E}, \overline{M}, \overline{F})$ defined respectively in (4.15), (4.14), (4.16)*, is a super solution of system* (4.1a)–(4.1c) *with initial data satisfying Assumption 4.1.1.*

Proof. We first notice that due to Assumption 4.1.1, the conditions on the initial data are clearly satisfied. Moreover, from the construction in Lemma 4.2.5 and Lemma 4.2.6, we already know that $\overline{E}$ and $\overline{M}$ are super-solutions. Then, we are left to prove that $\overline{F}$ is a super-solution for (4.1b). From Lemma 4.2.4 it is enough to prove that

$$\rho\nu_E \overline{E} \frac{\overline{M}}{\overline{M} + \gamma_s M_s} \Gamma(\overline{M} + \gamma_s M_s) - \mu_F \overline{F} \leqslant -g(t,x)\overline{F}, \tag{4.26}$$

where we recall that g is defined in the statement of Lemma 4.2.4.

We recall constant $\overline{M_s}$ in Lemma 4.2.7, which is proportional to $\overline{\Lambda}$. Thus when we take $\overline{\Lambda}$ large, we obtain large $\overline{M_s}$. We apply the inequalities in Lemma 4.2.7 in this proof.

• On the set Ω_t^2, we have $\overline{M} \leqslant C_2\overline{F} \leqslant C_2 F^*$, and

$$\begin{aligned}
\rho\nu_E \overline{E} \frac{\overline{M}}{\overline{M} + \gamma_s M_s} \Gamma(\overline{M} + \gamma_s M_s) - \mu_F \overline{F} &\leqslant \rho\nu_E \overline{E} \frac{C_2 F^*}{C_2 F^* + \gamma_s \overline{M_s}} - \mu_F \overline{F} \\
&\leqslant \rho\nu_E C_1 \overline{F} \frac{C_2 F^*}{C_2 F^* + \gamma_s \overline{M_s}} - \mu_F \overline{F} < -\varepsilon \overline{F},
\end{aligned}$$

for $\overline{M_s}$ large enough.

• On the set $\{|x| < r_1 + ct\} = \Omega_t^0 \cup \Omega_t^1$, we have $\overline{F} \leqslant F^* u_0$ by definition in (4.14). It implies from Lemma 4.2.5 and Lemma 4.2.6 that $\overline{E} \leqslant C_1 F^* u_0$ and $\overline{M} \leqslant C_2 F^* u_0$. Then, we have, using also the fact that $M_s \mapsto \frac{\overline{M}}{\overline{M} + \gamma_s M_s} \Gamma(\overline{M} + \gamma_s M_s)$ is non-increasing, we have for $M_s \geqslant 0$,

$$\frac{\overline{M}}{\overline{M} + \gamma_s M_s} \Gamma(\overline{M} + \gamma_s M_s) \leqslant \Gamma(\overline{M}) \leqslant \Gamma(C_2 F^* u_0).$$

Therefore, in the bistable case (i), we have

$$\rho\nu_E \overline{E} \frac{\overline{M}}{\overline{M} + \gamma_s M_s} \Gamma(\overline{M} + \gamma_s M_s) \leqslant \rho\nu_E \overline{E} \left(1 - e^{-\gamma C_2 F^* u_0}\right) \leqslant \rho\nu_E C_1 \left(1 - e^{-\gamma C_2 F^* u_0}\right) \overline{F},$$

where we use Lemma 4.2.5 for the last inequality. Hence, for $\mu < \mu_F$, there exists u_0 small enough such that

$$\rho\nu_E C_1 \left(1 - e^{-\gamma C_2 F^* u_0}\right) \overline{F} \leqslant (\mu_F - \mu)\overline{F}.$$

It implies that on the set $\{|x| < r_1 + ct\}$, in the bistable case (i), we have

$$\rho\nu_E \overline{E} \frac{\overline{M}}{\overline{M} + \gamma_s M_s} \Gamma(\overline{M} + \gamma_s M_s) - \mu_F \overline{F} \leqslant -\mu \overline{F}.$$

In the monostable case (ii), by Remark 4.2.2, we have that for $\eta > 0$ small enough, on the set $\{|x| < r_1 + ct\}$, we have $M_s \geqslant \overline{M_s} \frac{\overline{F}}{F^* u_0}$. Hence,

$$\begin{aligned}\rho\nu_E \overline{E} \frac{\overline{M}}{\overline{M} + \gamma_s M_s} \Gamma(\overline{M} + \gamma_s M_s) &\leqslant \rho\nu_E \overline{E} \frac{C_2 \overline{F}}{C_2 \overline{F} + \gamma_s \overline{M_s} \frac{\overline{F}}{F^* u_0}} \\ &\leqslant \rho\nu_E C_1 \frac{C_2 F^* u_0}{C_2 F^* u_0 + \gamma_s \overline{M_s}} \overline{F},\end{aligned}$$

where we use the estimate $\overline{E} \leqslant C_1 \overline{F}$ from Lemma 4.2.5 for the last inequality. Then, for $\overline{M_s}$ large enough or u_0 small enough, we have the desired estimate

$$\rho\nu_E \overline{E} \frac{\overline{M}}{\overline{M} + \gamma_s M_s} \Gamma(\overline{M}) - \mu_F \overline{F} \leqslant -\mu \overline{F}.$$

Hence, (4.26) was proved. □

4.3 Proof of the main result

4.3.1 Proof of Theorem 4.1.1

Proof of Theorem 4.1.1. Recall the super-solution $(\overline{E}, \overline{F}, \overline{M})$ constructed in 4.2.2, then for any $\underline{c} \leqslant c' \leqslant c$, on $\Omega_t^0 = B_{r_1 + ct}$, we have

$$\|(\overline{E}, \overline{F}, \overline{M})\| \leqslant C\alpha,$$

for some constant $C > 0$ and α defined in Lemma 4.2.1, which is decreasing towards 0 when t goes to $+\infty$. Thus, we can conclude the result of Theorem 4.1.1. □

4.3.2 Proof of Corollary 4.1.1

Proof of Corollary 4.1.1. Let us denote (E_1, M_1, F_1) the solution of system (4.1a)–(4.1b) with $K = K_1$, and (E_2, M_2, F_2) the solution of system (4.1a)–(4.1b) with $K = K_2$. By the comparison principle, since $K_1 \leqslant K(x) \leqslant K_2$, we deduce that on $\mathbb{R}_+ \times \mathbb{R}^2$,

$$(E_1, M_1, F_1)(t, x) \leqslant (E, M, F)(t, x) \leqslant (E_2, M_2, F_2)(t, x).$$

Then, by applying Theorem 4.1.1 for (E_1, M_1, F_1) and (E_2, M_2, F_2) we obtained the desired result. □

4.4 Numerical simulations

Following [69, 200], we consider the values of biological parameters are chosen as follows for mosquitoes of species *Aedes albopictus* and presented in Table 4.1.

To make an observation in a ball B_R, we carry out a simulation in a ball $B_{R'}$ with a very large radius R', and use a Neumann boundary condition on the boundary. It is well-known that such a spatial domain approximates correctly $\mathbb{R}$, or at least regarding spreading properties of reaction–diffusion systems. We take $R = 5$(km) and $R' = 10$(km) and observe the dynamics of system (4.1). Consider the following function

$$\phi(x, y) = 0.1 e^{0.8\sqrt{x^2 + y^2}}.$$

We choose the initial data

$$E^0(x, y) = 2.5\phi(x, y), \quad F^0(x, y) = \phi(x, y), \quad M^0(x, y) = 0.8\phi(x, y), \quad M_s^0(x, y) = 0.$$

Table 4.1 – Parameter values of *Aedes albopictus* mosquitoes used for the numerical simulation

Symbol	Description	Value	Unit
b	Birth rate of fertile females	10	day^{-1}
ν_E	Emerging rate of viable eggs	0.08	day^{-1}
μ_E	Death rate of aquatic phase	0.05	day^{-1}
μ_F	Female death rate	0.1	day^{-1}
μ_M	Wild male death rate	0.14	day^{-1}
μ_s	Sterile male death rate	0.14	day^{-1}
K	Carrying capacity of aquatic phase in patch 1	200	_
γ_s	Mating competitiveness of sterile male	1	_
r	Ratio of female hatch	0.5	_

Then, we have (E^0, F^0, M^0) satisfies Assumption 4.1.1. The torus of action is

$$\left\{x \in \mathbb{R}^2 \quad | \quad R_1 \leqslant |x| \leqslant R_2\right\}$$

A finite element method was applied to simulate the dynamics of the system using the FreeFem++ software.

4.4.1 Monostable case

In the monostable case, we plot the density of females in Figure 4.1.

When there is no control with the SIT, the population spreads to the center of the ball, reaches the value of the positive equilibrium at the center, and then spreads in the whole observed area $\mathcal{B}(R)$ (see Figure 4.1a from left to right).

In the control case, the release function Λ in the monostable case is defined below

$$\Lambda(x,t) = \overline{\Lambda}\mathbf{1}_{\{R_1+ct\leqslant|x|\leqslant R_2+ct\}} + \overline{\Lambda}e^{\eta(|x|-(R_1+ct))}\mathbf{1}_{\{|x|<R_1+ct\}}$$

We take $R_1 = 2,\ R_2 = 3, \eta = 0.01,\ \overline{\Lambda} = 1000$ ($\text{day}^{-1}\text{km}^{-1}$), and $c = 0.01$. The distribution of females is now presented in Figure 4.1b. We observe that at first, it spreads to the center more slowly compared to the non-controlled case until the density in the whole domain reaches some value. Then, it starts to decrease and finally vanishes in the whole domain (see Figure 4.1b from left to right).

4.4.2 Bistable case

The release function Λ in the bistable case is defined as below

$$\Lambda(x,t) = \overline{\Lambda}\mathbf{1}_{\{R_1+ct\leqslant|x|\leqslant R_2+ct\}},$$

We choose $c = 0.01,\ \overline{\Lambda} = 1000$. Considering the same initial data as above, the dynamic of the female population under the control in different areas is presented in Figure 4.2. We observe that when the control is carried out in a larger area with $R_1 = 2,\ R_2 = 3.5$, the population spreads more quickly and vanishes at time $t = 35$ (days) (see Figure 4.2b). While in the control area with $R_1 = 2,\ R_2 = 2.5$, the density of the population remains positive (see Figure 4.2a).

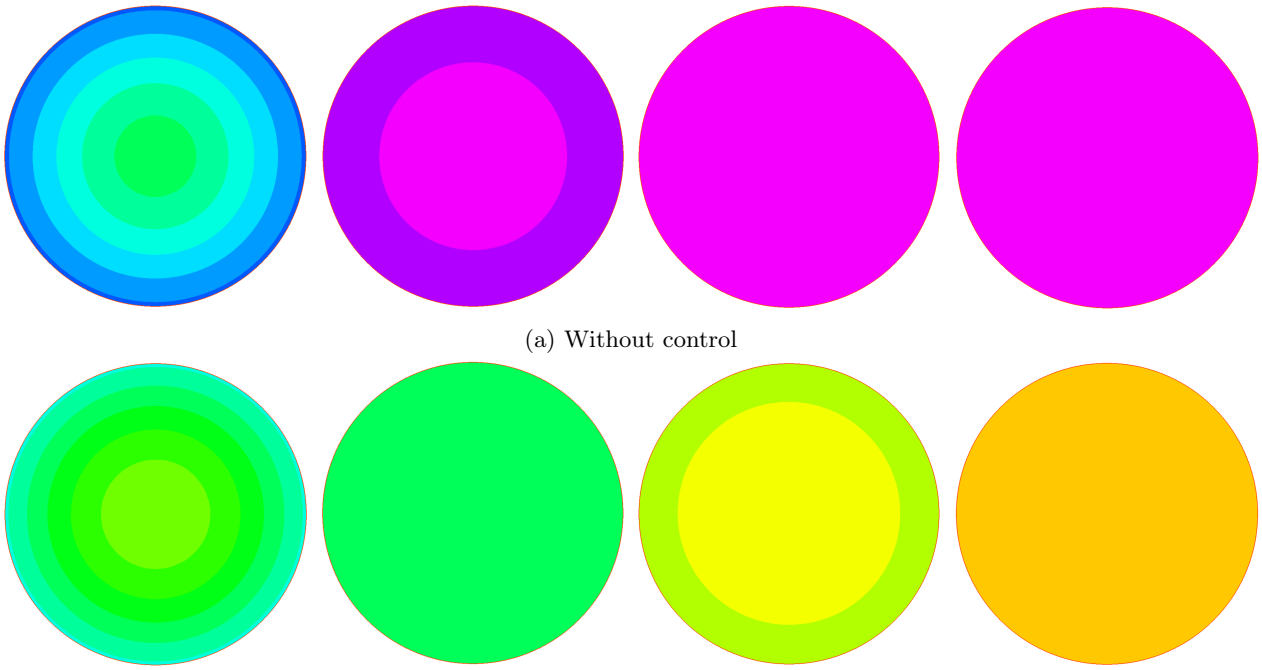

(a) Without control

(b) control with $\overline{\Lambda} = 1000, \eta = 0.01$.

Figure 4.1 – Distribution of females in the monostable case at time $t = 5,\ 15,\ 30$, and 35 (days) from left to right respectively.

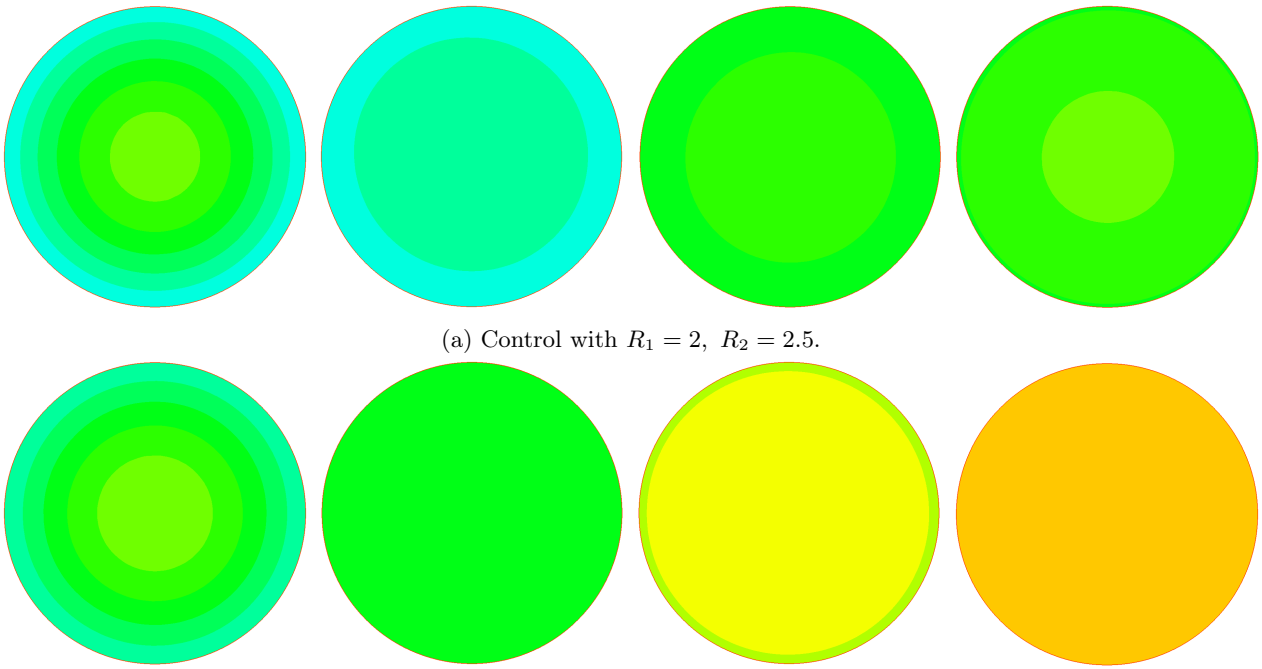

(a) Control with $R_1 = 2,\ R_2 = 2.5$.

(b) Control with $R_1 = 2,\ R_2 = 3.5$.

Figure 4.2 – Distribution of females in the bistable case at time $t = 5,\ 15,\ 30$, and 35 (days) from left to right respectively.

Part II

Metapopulation models with discrete diffusions

Chapter 5

Efficacy of the Sterile Insect Technique in an inaccessible area: A study using two-patch models

This chapter is a joint work with Pierre-Alexandre Bliman and Nicolas Vauchelet.

Abstract. The Sterile Insect Technique (SIT) is one of the sustainable strategies for the control of disease vectors, which consists of releasing sterilized males that will mate with the wild females, resulting in a reduction and, eventually a local elimination, of the wild population. The implementation of the SIT in the field can become problematic when there are inaccessible areas where the release of sterile insects cannot be carried out directly, and the migration of wild insects from these areas to the treated zone may influence the efficacy of this technique. However, we can also take advantage of the movement of sterile individuals to control the wild population in these unreachable places. In this paper, we derive a two-patch model for *Aedes* mosquitoes where we consider the discrete diffusion between the treated area and the inaccessible zone. We investigate two different release strategies (constant and impulsive periodic releases), and by using the monotonicity of the model, we show that if the number of released sterile males exceeds some threshold, the technique succeeds in driving the whole population in both areas to extinction. This threshold depends on not only the biological parameters of the population but also the diffusion between the two patches.

5.1 Introduction

Mosquitoes of genus *Aedes aegypti* and *Aedes albopictus* play a crucial role in transmitting various arboviruses to humans including dengue, chikungunya, and Zika virus. Unfortunately, there are no specific vaccines or drugs available for these diseases. Consequently, the primary prevention lies in controlling the mosquito population [93]. However, traditional insecticide-based methods have limitations, prompting the need for innovative and sustainable strategies [2], [29]. Biological controls involve releasing large numbers of mosquitoes that are either sterile or incapable of transmitting diseases, which recently gained much attention. The Sterile Insect Technique is among these sustainable alternative methods which consist of the release of sterilized male mosquitoes that will mate with wild females [118], [73]. These wild females, unable to lay viable eggs, will gradually drive the wild population to decline. The efficacy of SIT relies on a comprehensive understanding of the vector behavior, as well as accurate modeling of its dispersal, to optimize the release strategies.

Spatial heterogeneity in mosquito populations and mosquito-borne diseases occurs due to differences in the quality and quantity of their habitats, as well as variations in host density, temperature, and rainfall [56], [199], [145]. Especially, the number and accessibility of sites where mosquitoes lay their eggs play a significant role in determining the size of adult mosquito populations by increasing the carrying capacity of the environment [1]. Developing models that capture mosquito behavior in response to environmental heterogeneity is crucial for designing effective control strategies, especially in the face of rapid global land-use changes. Models using monotone dynamical systems were introduced (see e.g. [18], [70], [200]) and applied efficiently (see e.g. [38], [19], [39]) to study the SIT. Not many mosquito modeling studies have incorporated migration or dispersal effects due to insufficient information on individual movement in the field as well as the complex analysis of models. Most of them used the diffusion approach, which considers space as a continuous variable. They were first developed in one-dimensional space using scalar reaction-diffusion equations [144], [128], then extended to sex-structured compartmental systems to consider the different behaviors of aquatic phases, wild females, males, and sterile males (see e.g. [15], [12], [126]) and in higher dimension (see e.g. [69], [10]). However, it remains challenging to

explicitly incorporate the factors that affect the movement of sterile males. For instance, when resources are concentrated in patches or distinct locations, a metapopulation approach in which we treat space as a discrete set of patches and describe how the population on each patch varies with time is more suitable for modeling mosquito dispersal [25], [140], [143].

The application of the SIT in the field encounters a difficulty of the limitation in space when there are some inaccessible areas where people can not release sterile insects directly. For example, mosquitoes of the genus *Aedes polynesiensis* primarily exploit land crab burrows for oviposition in certain French Polynesian atolls [41], [124], [125], [102]. The larvae in the crab burrows emerge into adult mosquitoes that can fly out to search for food and human blood for fertility. However, one standout advantage of the SIT is that it relies on the natural ability of the male mosquitoes to move, locate and mate with females. This behavior will take place in those areas that cannot be reached with conventional control techniques (i.e. insecticides). Therefore, we are interested in the mosquito population dynamics in the presence of such reservoirs and the elimination of the whole populations while considering that the released sterile males can fly into the unreachable sites. The patchy models with discrete diffusion mentioned above are a useful approach to describe the mosquito dynamic taking into account the inaccessibility to the burrows. We develop a two-patch model and in each patch, we consider a monotone dynamical system inspired by the models in [200] where the population is divided into different compartments characterizing the aquatic phase, wild females, wild males, and sterile males. Except for the aquatic phase, individuals in other states move between patches at specific rates. The SIT is only carried out in the first patch and only affects the second one through these movements. In this framework, we are interested in how to guarantee the successful elimination of the SIT in both areas and how the diffusion rates as well as other biological parameters influence the efficacy.

To tackle this problem, we focus on studying the global stability of the extinction equilibrium in our system. Results of global asymptotic behavior for the single-species model depending on the discrete diffusion were provided in the literature[4], [202], [138]. Lyapunov's second method was used in [134] to investigate the multi-species system with discrete diffusion. Many works have been done to design robust strategies for releasing sterile males to drive a population to elimination [38], [39]. We extend these control strategies to our two-patch system and prove the sufficient conditions for both constant continuous and periodic impulsive releases to drive the whole system to extinction. We obtain that when the number of released sterile males exceeds some threshold, the populations in both the treated and the inaccessible zone reach elimination. We also show in the present work how the diffusion rates between two areas and other biological parameters influence these conditions. These results may help estimate the possibility and the surplus of sterile mosquitoes necessary to complete elimination in the presence of hidden, inaccessible, reservoirs.

The organization of this Chapter is as follows. In Section 5.2, we present the formulation of the two-patch model and prove the monotonicity of the systems and some other preliminary results that be applied in our proofs. Section 5.3 is devoted to the study of the system without sterile insects. In Theorem 5.3.1, we provide conditions for the persistence and extinction of the wild population on each patch. In section 5.4, we study the dynamics of mosquito population in the presence of the SIT with two release strategies: constant and impulsive releases. Theorem 5.4.1 presents sufficient conditions on the average number of sterile males released per time unit to drive the population to elimination. We provide the principle of the method used to treat the system in 5.4.1 and then apply this principle to prove Theorem 5.4.1. Section 5.5 is focused on the dependence of the critical number of sterile males on parameters. The results in 5.5.1 show that when the diffusion rates are large, the dynamics of the whole system are the same as in the case when there is no separation between the two sub-populations. Then, Theorem 5.5.2 shows that the critical number of released sterile males depends monotonically on the biological parameters. Finally, some numerical illustrations are provided in Section 5.6.

5.2 Model

In this section, we present the formulation of the model using to study the population dynamics in 5.2.1. Then, in 5.2.2, we provide some preliminary results that will be used later in the present work.

5.2.1 Formulation of the model

Consider two patches and denote E_i, F_i, M_i, and M_i^s respectively the density of aquatic phase (eggs, larvae, pupae), fertile females, males, and sterile males on the patch i depending on time t. We consider a two-patch model coupled by the diffusion terms as follows where the dynamic in each patch is inspired by the model in [200]

$$\dot{E}_1 = bF_1\left(1 - \frac{E_1}{K_1}\right) - (\nu_E + \mu_E)E_1, \tag{5.1a}$$

$$\dot{F}_1 = \rho\nu_E E_1 \frac{M_1}{M_1 + \gamma_s M_1^s} - \mu_F F_1 - d_{12}F_1 + d_{21}F_2, \tag{5.1b}$$

$$\dot{M}_1 = (1-\rho)\nu_E E_1 - \mu_M M_1 - \beta d_{12}M_1 + \beta d_{21}M_2, \tag{5.1c}$$

$$\dot{M}_1^s = \Lambda - \mu_s M_1^s - \alpha d_{12}M_1^s + \alpha d_{21}M_2^s, \tag{5.1d}$$

$$\dot{E}_2 = bF_2\left(1 - \frac{E_2}{K_2}\right) - (\nu_E + \mu_E)E_2, \tag{5.1e}$$

$$\dot{F}_2 = \rho\nu_E E_2 \frac{M_2}{M_2 + \gamma_s M_2^s} - \mu_F F_2 - d_{21}F_2 + d_{12}F_1, \tag{5.1f}$$

$$\dot{M}_2 = (1-\rho)\nu_E E_2 - \mu_M M_2 - \beta d_{21}M_2 + \beta d_{12}M_1, \tag{5.1g}$$

$$\dot{M}_2^s = -\mu_s M_2^s - \alpha d_{21}M_2^s + \alpha d_{12}M_1^s. \tag{5.1h}$$

The interpretation of the parameters used in the model, with $i, j \in \{1, 2\}$, is as below

- $\Lambda(t)$ is the number per time unit of sterile mosquitoes that are released at time t on the first patch;
- the fraction $\frac{M_i}{M_i+\gamma_s M_i^s}$ corresponds to the probability that a female mates with a fertile male;
- $b > 0$ is the birth rate; $\mu_E > 0$, $\mu_M > 0$, and $\mu_F > 0$ denote the death rates for the mosquitoes in the aquatic phase, for adult males, and for adult females, respectively;
- K_i is an environmental capacity for the aquatic phase on patch ith, accounting also for the intraspecific competition;
- $\nu_E > 0$ is the rate of emergence;
- $\rho \in (0, 1)$ is the probability that a female emerges, then $(1 - \rho)$ is the probability that a male emerges.
- $d_{ij} > 0$ is the moving rate of female mosquitoes from patch ith to patch jth; the fertile males and sterile males move slower but with proportional rates respectively βd_{ij}, αd_{ij} where typically $0 < \alpha < \beta < 1$ in practice.

We recall the basic offspring number of the sub-population in one patch as introduced in [200]

$$\mathcal{N} = \frac{b\rho\nu_E}{\mu_F(\mu_E + \nu_E)}. \tag{5.2}$$

The persistence and extinction of the population in the patch depend strongly on the value of this number. In Section, 5.3, we will show that $\mathcal{N}$ is also the basic offspring number of the whole two-patch system.

5.2.2 Preliminary results

First, we provide some definition and denotation of the order used in the present work.

Definition 5.2.1. *A matrix $A \in \mathcal{M}^{m\times n}$ is called non-negative, denote $A \geqslant 0$, if all of its entries are non-negative.*
It is called positive, denote $A > 0$, if if is non-negative and there is at least one positive entry.
It is called strictly positive, denote $A \gg 0$, if all of its entries are strictly positive.

In the present work, we also use the above definition of order for vectors in $\mathbb{R}^n$. Next, we present a property of a Metzler matrix that will be used in this paper.

Lemma 5.2.1. *Assume that a square matrix A is Metzler and irreducible, then e^A is strictly positive.*

Proof. Since A is Metzler, then there exists a constant $\delta > 0$ large enough such that $A + \delta I$ is a non-negative matrix with a positive element on the main diagonal. Moreover, A is irreducible so $A + \delta I$ is also irreducible. Thus, $A + \delta I$ is primitive, that is, there exists an integer $n > 0$ such that $(A + \delta I)^n \gg 0$. Hence, we have $e^{A+\delta I} \gg 0$, and since δI commutes with all matrices, one has $e^A = e^{A+\delta I}e^{-\delta I} \gg 0$. □

We present in this section the so-called Kamke [59] or Chaplygin [55] lemma for a cooperative system (Lemma 5.2.2). Then, we apply this lemma to show the monotonicity of system (5.1) in Lemma 5.2.3.

Lemma 5.2.2. *For any $n \in \mathbb{N}^*$, consider a smooth function $\mathbf{f} : \mathbb{R}^n \to \mathbb{R}^n$, and a vector function $\mathbf{u}(t)$ satisfying a differential equation*

$$\dot{\mathbf{u}} = \mathbf{f}(\mathbf{u}).$$

Moreover, we assume that the above system is cooperative, that is,

$$\frac{\partial f_i}{\partial u_j}(t) \geqslant 0, \qquad \text{for } i \neq j,\ t > 0. \tag{5.3}$$

If a vector function $\mathbf{v}(t)$ satisfies a differential inequality $\dot{\mathbf{v}} \leqslant \mathbf{f}(\mathbf{v})$ then, for initial data $\mathbf{v}(0) \leqslant \mathbf{u}(0)$, we have $\mathbf{v}(t) \leqslant \mathbf{u}(t)$ for all $t > 0$.

To apply this Lemma to system (5.1), we first define the following order in $\mathbb{R}^8$ as follows

Definition 5.2.2. *For any vectors $\mathbf{u}, \mathbf{v} \in \mathbb{R}^8$, we define an order $\preceq$ such that $\mathbf{u} \preceq \mathbf{v}$ if and only if*

$$\begin{cases} u_i \leqslant v_i & \text{for } i \in \{1, 2, 3, 5, 6, 7\}, \\ u_i \geqslant v_i & \text{for } i \in \{4, 8\}. \end{cases}$$

Moreover, we write $\mathbf{u} \prec \mathbf{v}$ if $\mathbf{u} \preceq \mathbf{v}$ and $\mathbf{u} \neq \mathbf{v}$.

The monotonicity of system (5.1) is shown in the following result

Lemma 5.2.3. *By denoting $\mathbf{u} = (E_1, F_1, M_1, M_1^s, E_2, F_2, M_2, M_2^s) \in \mathbb{R}^8$, we can write system (5.1) as the form $\dot{\mathbf{u}} = \mathbf{f}(\mathbf{u})$ with $\mathbf{f}$ is $\mathcal{C}^1$ in $\mathbb{R}^8$. In the invariant subset $\{0 \leqslant E_1 \leqslant K_1\} \cap \{0 \leqslant E_2 \leqslant K_2\}$ of $\mathbb{R}^8_+$, system (5.1) is monotone in the sense that if a vector function $\mathbf{v}(t)$ satisfies a differential inequality $\dot{\mathbf{v}} \preceq \mathbf{f}(\mathbf{v})$ then, for initial data $\mathbf{v}(0) \preceq \mathbf{u}(0)$, we have $\mathbf{v}(t) \preceq \mathbf{u}(t)$ for all $t > 0$.*

Proof. By changing the variable to $\widetilde{\mathbf{u}} = (E_1, F_1, M_1, -M_1^s, E_2, F_2, M_2, -M_2^s)$, we can write system (5.1) as

$$\dot{\widetilde{\mathbf{u}}} = \widetilde{\mathbf{f}}(\widetilde{\mathbf{u}}).$$

This system is cooperative since in $\{0 \leqslant E_1 \leqslant K_1\} \cap \{0 \leqslant E_2 \leqslant K_2\}$ of $\mathbb{R}^8_+$, we have

$$\frac{\partial \widetilde{f}_1}{\partial \widetilde{u}_2} = b\left(1 - \frac{E_1}{K_1}\right) \geqslant 0, \quad \frac{\partial \widetilde{f}_1}{\partial \widetilde{u}_j} = 0 \ \text{ for any } j > 2,$$

$$\frac{\partial \widetilde{f}_2}{\partial \widetilde{u}_1} = \rho\nu_E \frac{M_1}{M_1 + \gamma_s M_1^s} \geqslant 0, \quad \frac{\partial \widetilde{f}_2}{\partial \widetilde{u}_3} = \rho\nu_E \frac{\gamma_s M_1^s}{(M_1 + \gamma_s M_1^s)^2} \geqslant 0,$$

$$\frac{\partial \widetilde{f}_2}{\partial \widetilde{u}_4} = \rho\nu_E E_1 \frac{\gamma_s M_1}{(M_1 + \gamma_s M_1^s)^2} \geqslant 0, \quad \frac{\partial \widetilde{f}_2}{\partial \widetilde{u}_6} = d_{21} > 0, \quad \frac{\partial \widetilde{f}_2}{\partial \widetilde{u}_j} = 0 \ \text{ for } j \in \{5, 7, 8\}.$$

$$\frac{\partial \widetilde{f}_3}{\partial \widetilde{u}_1} = (1-\rho)\nu_E \geqslant 0, \quad \frac{\partial \widetilde{f}_3}{\partial \widetilde{u}_7} = \beta d_{21} > 0, \quad \frac{\partial \widetilde{f}_1}{\partial \widetilde{u}_j} = 0 \ \text{ for } j \in \{2, 4, 5, 6, 8\},$$

$$\frac{\partial \widetilde{f}_4}{\partial \widetilde{u}_8} = \alpha d_{21} > 0, \frac{\partial \widetilde{f}_4}{\partial \widetilde{u}_j} = 0 \ \text{ for } j \in \{1, 2, 3, 5, 6, 7\}.$$

Similarly for $\widetilde{f}_i$ with $i > 4$, so $\widetilde{\mathbf{f}}$ is cooperative.

For any vector function $\mathbf{v}$ such that $\mathbf{v} \preceq \mathbf{f}(\mathbf{v})$, by the same variable change, one has $\widetilde{\mathbf{v}} \leqslant \widetilde{\mathbf{f}}(\widetilde{\mathbf{v}})$. The initial data $\mathbf{v}(0) \preceq \mathbf{u}(0)$ implies that $\widetilde{\mathbf{v}}(0) \leqslant \widetilde{\mathbf{u}}(0)$. Therefore, by applying Lemma 5.2.2, one has $\widetilde{\mathbf{v}}(t) \leqslant \widetilde{\mathbf{u}}(t)$ for any $t > 0$ which is equivalent to $\mathbf{v}(t) \preceq \mathbf{u}(t)$. □

In order to define the solution of (5.1), we make some assumptions for the release function $\Lambda(t)$

Assumption 5.2.1. *Assume that function $\Lambda(t)$ satisfies*

$$\Lambda(t) = \Lambda_1(t) + \Lambda_2(t), \tag{5.4}$$

where $\Lambda_1 \in L^1_{\text{loc}}(0, +\infty)$, $\Lambda_1(t) \geqslant 0$ for almost every t, and Λ_2 is a sum of Dirac masses with positive weights. Assume moreover that there exists a time $T > 0$ such that the average value of Λ over any T-time interval is finite, that is,

$$C_\Lambda := \frac{1}{T} \sup_{t \geqslant 0} \int_t^{t+T} \Lambda(s) ds < +\infty. \tag{5.5}$$

Assumption 5.2.1 is natural since in practice, the total amount of the sterile males released in a finite time interval is finite. The term Λ_2 corresponds to impulsive releases.

The next result shows that any trajectory of system (5.1) resulting from any non-negative initial data is bounded.

Lemma 5.2.4. *Let Λ satisfy Assumption 5.2.1. For any non-negative initial data $(E_1^0, F_1^0, M_1^0, M_1^{s,0}, E_2^0, F_2^0, M_2^0, M_2^{s,0})$, there exists a unique solution $(E_1, F_1, M_1, M_1^s, E_2, F_2, M_2, M_2^s)$ of system (5.1), and it is non-negative. If $E_i^0 < K_i$ with $i = 1, 2$, then $E_i(t) \leqslant K_i$ for any $t > 0$. Moreover, for all $t \geqslant 0$, we have the uniform bounds*

$$F_1 + F_2 \leqslant \max\left\{F_1^0 + F_2^0,\ C_F\right\}, \quad M_1 + M_2 \leqslant \max\left\{M_1^0 + M_2^0,\ C_M\right\},$$

where

$$C_F := \frac{\rho\nu_E(K_1 + K_2)}{\mu_F},\ C_M := \frac{(1-\rho)\nu_E(K_1 + K_2)}{\mu_M},$$

and

$$M_1^s(t) + M_2^s(t) \leqslant \max\left\{M_1^{s,0} + M_2^{s,0}, \frac{TC_\Lambda}{1 - e^{-\mu_s T}}\right\} + TC_\Lambda,$$

with T and C_Λ defined in Assumption 5.2.1. One also has

$$\limsup_{t\to+\infty}(F_1 + F_2)(t) \leqslant C_F, \quad \limsup_{t\to+\infty}(M_1 + M_2)(t) \leqslant C_M, \quad ,$$

and

$$\limsup_{t\to+\infty}(M_1^s + M_2^s)(t) \leqslant \frac{TC_\Lambda}{1 - e^{-\mu_s T}} + TC_\Lambda =: C_{M^s}.$$

Remark 5.2.1. *In the case $\Lambda \in L^\infty(0, +\infty)$, one can let T tend to zero and obtain that $C_\Lambda = \sup_{t>0}\Lambda(t)$ and $\limsup_{t\to+\infty}(M_1^s + M_2^s) \leqslant \frac{C_\Lambda}{\mu_s}$. The condition of Λ that we made in Assumption 5.2.1 is weaker than the L^∞ assumption since we also include impulsive releases, represented by the Dirac masses.*

Proof of Lemma 5.2.4. By applying the Lemma 5.2.3, one deduces that system (5.1) preserves the positivity.

For $i = 1, 2$, we have $E_i(t = 0) = E_i^0 < K_i$ and assume that there exists a value $t_0 < \infty$ such that

$$t_0 = \inf\{t > 0 : E_i(t) = K_i\}$$

then $\dot{E}_i(t_0) > 0$ but from (5.1a) and (5.1e), one has $\dot{E}_i(t_0) = -(\nu_E + \mu_E)K_i < 0$ (contradictory). Then we deduce that $E_i(t) \leqslant K_i$ for any $t > 0$.

From equations (5.1b) and (5.1f), since for $i = 1, 2$, $\dfrac{M_i}{M_i + \gamma_s M_i^s} \leqslant 1$ one has

$$\dot{F}_1 + \dot{F}_2 \leqslant \rho\nu_E(E_1 + E_2) - \mu_F(F_1 + F_2).$$

Since $E_1,\ E_2$ are bounded then we deduce that

$$(F_1 + F_2)(t) \leqslant (F_1^0 + F_2^0)e^{-\mu_F t} + \frac{\rho\nu_E(K_1 + K_2)}{\mu_F}(1 - e^{-\mu_F t}) \leqslant \max\left\{F_1^0 + F_2^0,\ \frac{\rho\nu_E(K_1 + K_2)}{\mu_F}\right\},$$

for any $t \geqslant 0$. For $i = 1, 2$, one has $F_i \geqslant 0$, thus $F_i(t) \leqslant \max\left\{F_1^0 + F_2^0,\ C_F\right\}$ for any $t \geqslant 0$. Let t goes to infinity we get $\limsup_{t\to+\infty}(F_1 + F_2)(t) \leqslant C_F$. One obtains similarly the inequalities for M_1, M_2.

For M_1^s and M_2^s, by denoting $X_s(t) = M_1^s(t) + M_2^s(t)$, then from equations (5.1d) and (5.1h), one has

$$\dot{X}_s(t) = -\mu_s X_s(t) + \Lambda(t).$$

For any integer k, by integrating both sides of this equality in $((k-1)T, kT)$ with T defined in Assumption 5.2.1, one gets

$$X_s(kT) = e^{-\mu_s T}X_s((k-1)T) + \int_{(k-1)T}^{kT} e^{-\mu_s(t-(k-1)T)}\Lambda(t)dt.$$

Since $e^{-\mu_s(t-(k-1)T)} < 1$ for any $t \in ((k-1)T, kT)$ and by Assumption 5.2.1, we deduce that

$$X_s(kT) \leqslant e^{-\mu_s T}X_s((k-1)T) + TC_\Lambda,$$

with C_Λ defined in (5.5). Using the iteration with respect to k, we deduce that

$$X_s(kT) \leqslant e^{-\mu_s kT} X_s^0 + TC_\Lambda \left(1 + e^{-\mu_s T} + \cdots + e^{-\mu_s (k-1)T}\right) = e^{-\mu_s kT} X_s^0 + TC_\Lambda \frac{1 - e^{-\mu_s kT}}{1 - e^{-\mu_s T}}.$$

Now for any time $t > 0$, there exists an integer k such that $t \in [kT, (k+1)T)$. Then, we obtain that

$$\begin{aligned} X_s(t) &= e^{-\mu_s (t-kT)} X_s(kT) + \int_{kT}^{t} e^{-\mu_s (t-s)} \Lambda(s) ds \\ &\leqslant e^{-\mu_s t} X_s^0 + TC_\Lambda \frac{e^{-\mu_s (t-kT)} - e^{-\mu_s t}}{1 - e^{-\mu_s T}} + TC_\Lambda. \\ &\leqslant e^{-\mu_s t} X_s^0 + \frac{TC_\Lambda}{1 - e^{-\mu_s T}} \left(1 - e^{-\mu_s t}\right) + TC_\Lambda \end{aligned}$$

since $e^{-\mu_s (t-kT)} < 1$. The inequality of $M_1^s + M_2^s$ follows. □

5.3 Mosquito dynamics without sterile males

First, we describe the dynamics of wild mosquitoes in the two areas by considering the following system which is re-obtained from system (5.1) in the absence of sterile males

$$\dot{E}_1 = bF_1 \left(1 - \frac{E_1}{K_1}\right) - (\nu_E + \mu_E) E_1, \tag{5.6a}$$

$$\dot{F}_1 = \rho \nu_E E_1 - \mu_F F_1 - d_{12} F_1 + d_{21} F_2, \tag{5.6b}$$

$$\dot{M}_1 = (1-\rho) \nu_E E_1 - \mu_M M_1 - \beta d_{12} M_1 + \beta d_{21} M_2, \tag{5.6c}$$

$$\dot{E}_2 = bF_2 \left(1 - \frac{E_2}{K_2}\right) - (\nu_E + \mu_E) E_2, \tag{5.6d}$$

$$\dot{F}_2 = \rho \nu_E E_2 - \mu_F F_2 - d_{21} F_2 + d_{12} F_1, \tag{5.6e}$$

$$\dot{M}_2 = (1-\rho) \nu_E E_2 - \mu_M M_2 - \beta d_{21} M_2 + \beta d_{12} M_1, \tag{5.6f}$$

It is clear that the subset $\{0 \leqslant E_1 \leqslant K_1\} \cap \{0 \leqslant E_2 \leqslant K_2\}$ of the positive cone of $\mathbb{R}^6$ is positively invariant over time. The following result shows the nature of the equilibrium points of system (5.6).

Theorem 5.3.1. *For $\mathcal{N} < 1$, zero is the unique equilibrium of system* (5.6)*, and all trajectories of* (5.6) *resulting from non-negative initial data converge to zero as time evolves.*

For $\mathcal{N} > 1$, system (5.6) has two equilibrium points: zero and $\mathbf{u}^+ = (E_1^+, F_1^+, M_1^+, E_2^+, F_2^+, M_2^+)$ strictly positive. Moreover, the zero equilibrium is unstable. All trajectories of (5.6) *resulting from any positive initial data $(E_1^0, F_1^0, M_1^0, E_2^0, F_2^0, M_2^0)$ such that $(E_1^0, F_1^0, E_2^0, F_2^0) > 0$ converge to $\mathbf{u}^+$ when $t \to +\infty$.*

Theorem 5.3.1 shows that the constant $\mathcal{N}$ defined in (5.2) is the basic offspring number of the whole two-patch system (5.1). When $\mathcal{N} > 1$, the populations in both areas remain persistent for any diffusion rates as time evolves. In the rest of the paper, we only consider the case $\mathcal{N} > 1$.

To prove this theorem, we first consider the sub-system of $E_1,\ E_2,\ F_1,\ F_2$. From equations (5.6b) and (5.6e), the positive equilibrium satisfies

$$\rho \nu_E \begin{pmatrix} E_1^+ \\ E_2^+ \end{pmatrix} = \begin{pmatrix} \mu_F + d_{12} & -d_{21} \\ -d_{12} & \mu_F + d_{21} \end{pmatrix} \begin{pmatrix} F_1^+ \\ F_2^+ \end{pmatrix},$$

then

$$\begin{pmatrix} F_1^+ \\ F_2^+ \end{pmatrix} = \frac{\rho \nu_E}{\mu_F (\mu_F + d_{12} + d_{21})} \begin{pmatrix} \mu_F + d_{21} & d_{21} \\ d_{12} & \mu_F + d_{12} \end{pmatrix} \begin{pmatrix} E_1^+ \\ E_2^+ \end{pmatrix}. \tag{5.7}$$

On the other hand, from equation (5.6a) and (5.6d), we also have

$$F_1^+ = \frac{\nu_E + \mu_E}{b} \frac{E_1^+}{1 - \frac{E_1^+}{K_1}}, \qquad F_2^+ = \frac{\nu_E + \mu_E}{b} \frac{E_2^+}{1 - \frac{E_2^+}{K_2}}. \tag{5.8}$$

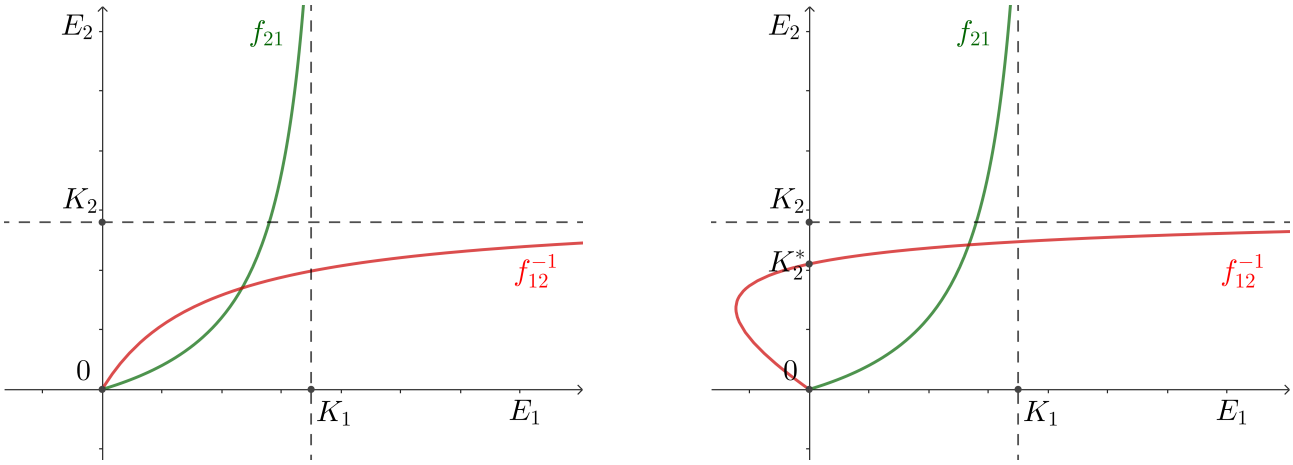

(a) $\mathcal{N} \leqslant \min_{\substack{i,j\in\{1,2\}\\ i\neq j}} \frac{\mu_F + d_{ij} + d_{ji}}{\mu_F + d_{ij}}$ (b) $\mathcal{N} > \min_{\substack{i,j\in\{1,2\}\\ i\neq j}} \frac{\mu_F + d_{ij} + d_{ji}}{\mu_F + d_{ij}}$

Figure 5.1 – Behaviors of f_{21} and f_{12}^{-1}

From (5.7) and (5.8), we deduce that

$$E_2^+ = \frac{\mu_F + d_{12} + d_{21}}{d_{21}} \frac{1}{\mathcal{N}} \frac{E_1^+}{1 - \frac{E_1^+}{K_1}} - \frac{\mu_F + d_{21}}{d_{21}} E_1^+ =: f_{21}(E_1^+), \tag{5.9}$$

$$E_1^+ = \frac{\mu_F + d_{12} + d_{21}}{d_{12}} \frac{1}{\mathcal{N}} \frac{E_2^+}{1 - \frac{E_2^+}{K_2}} - \frac{\mu_F + d_{12}}{d_{12}} E_2^+ =: f_{12}(E_2^+). \tag{5.10}$$

The following lemma provides information for these functions.

Lemma 5.3.1. *For $\{i,j\} = \{1,2\}$, function $f_{ij}(x)$ is defined and convex on $(0, K_j) \subset \mathbb{R}$.*
If $\mathcal{N} \leqslant \frac{\mu_F + d_{ij} + d_{ji}}{\mu_F + d_{ij}}$, then f_{ij} has no positive root and it is increasing on $(0, K_j)$.
Otherwise, it has a unique positive root

$$K_j^+ := K_j \left(1 - \frac{\mu_F + d_{ji} + d_{ij}}{\mu_F + d_{ij}} \frac{1}{\mathcal{N}}\right) < K_j \tag{5.11}$$

Moreover, $f_{ij} < 0$ on $(0, K_j^+)$, $f_{ij} > 0$ and increasing on (K_j^+, K_j).

Proof of Lemma 5.3.1. We recall function $f_{ij}(x) := \frac{\mu_F + d_{ij} + d_{ji}}{d_{ij}} \frac{1}{\mathcal{N}} \frac{x}{1 - \frac{x}{K_j}} - \frac{\mu_F + d_{ij}}{d_{ij}} x$. One has $f_{ij} = 0$ if and only if

$$\frac{\mu_F + d_{ij}}{K_j} x^2 + \left(\frac{\mu_F + d_{ij} + d_{ji}}{d_{ij}} - \mu_F - d_{ij}\right) x = 0.$$

We deduce that $f_{ij} = 0$ at 0 and K_j^+ as in (5.11) , and $K_j^+ > 0$ if and only if $\mathcal{N} \leqslant \frac{\mu_F + d_{ij} + d_{ji}}{\mu_F + d_{ij}}$. Moreover, $f_{ij} < 0$ on $(0, K_j^+)$, $f_{ij} > 0$ and is increasing on (K_j^+, K_j). It is defined and convex on $(0, K_j) \subset \mathbb{R}$ since

$$f_{ij}''(x) = 2 \frac{\mu_F + d_{ij} + d_{ji}}{d_{ij}} \frac{1}{K_j \mathcal{N}} \frac{1}{\left(1 - \frac{x}{K_j}\right)^3} > 0,$$

for any $x \in (0, K_j)$. We also have $f_{ij}(0) = 0$, $\lim_{x \to K_j} f_{ij}(x) = +\infty$. □

Proof of Theorem 5.3.1. **Existence and uniqueness of the positive equilibrium.** System (5.6) has a positive equilibrium iff system (5.9)-(5.10) has a solution (E_1^+, E_2^+) in $(0, K_1) \times (0, K_2)$.

First, we study the case where $0 < \mathcal{N} \leqslant \min_{\substack{i,j\in\{1,2\}\\ i\neq j}} \dfrac{\mu_F + d_{ij} + d_{ji}}{\mu_F + d_{ij}}$, then according to Lemma 5.3.1, we have $f_{12} : [0, K_2) \to [0, +\infty)$ is positive and increasing, so this function is invertible (see Figure 5.1). We denote $f_{12}^{-1} : [0, K_1] \to [0, K_2)$ the restriction of the invert function of f_{12} on $[0, K_1]$, then

$$E_2^+ = f_{21}(E_1^+) = f_{12}^{-1}(E_1^+).$$

Thus, E_1^+ is a positive root of function $f_{21} - f_{12}^{-1}$. For any $x \in (0, K_1)$, one has

$$(f_{21} - f_{12}^{-1})'(x) = f_{21}'(x) - \frac{1}{f_{12}'(f_{12}^{-1}(x))},$$

then

$$(f_{21} - f_{12}^{-1})''(x) = f_{21}''(x) + \frac{f_{12}''(f_{12}^{-1}(x))}{(f_{12}'(f_{12}^{-1}(x)))^3} > 0$$

since f_{ij} is convex on $(0, K_j)$. Hence, $f_{21} - f_{12}^{-1}$ is convex on $(0, K_1)$. Moreover, we have $(f_{21} - f_{12}^{-1})(0) = 0$, and $\lim_{x\to K_1}(f_{21} - f_{12}^{-1})(x) = +\infty$. Therefore, this function has a unique positive root if and only if the derivative at zero is negative. We have

$$(f_{21} - f_{12}^{-1})'(0) = \frac{\frac{1}{\mathcal{N}}(\mu_F + d_{12} + d_{21}) - \mu_F - d_{21}}{d_{21}} - \frac{d_{12}}{\frac{1}{\mathcal{N}}(\mu_F + d_{12} + d_{21}) - \mu_F - d_{12}}.$$

Then, $(f_{21} - f_{12}^{-1})'(0) < 0$ if and only if $1 < \mathcal{N} < \dfrac{\mu_F + d_{12} + d_{21}}{\mu_F}$.

Now, without loss of generality, we assume that $d_{12} > d_{21}$, then $\dfrac{\mu_F + d_{12} + d_{21}}{\mu_F + d_{12}} < \dfrac{\mu_F + d_{12} + d_{21}}{\mu_F + d_{21}}$. If $\mathcal{N} > \dfrac{\mu_F + d_{12} + d_{21}}{\mu_F + d_{12}} > 1$, again according to Lemma 5.3.1, function f_{12} has a unique positive root K_2^+ and is invertible on $[K_2^+, K_2]$ (see Figure 5.1). We denote again $f_{12}^{-1} : [0, K_1] \to [K_2^+, K_2)$ the restriction of the invert function of f_{12} on $[0, K_1]$, then we also have $f_{21} - f_{12}^{-1}$ convex on $(0, K_1)$, and $(f_{21} - f_{12}^{-1})(0) = -f_{12}^{-1}(0) = -K_2^+ < 0$, $\lim_{x\to K_1}(f_{21} - f_{12}^{-1})(x) = +\infty > 0$. We can deduce that $f_{21} - f_{12}^{-1}$ has a unique positive root on $(0, K_1)$.

Instability of the zero equilibrium. At the origin $\mathbf{0} = (0, 0, 0, 0, 0, 0)$ of $\mathbb{R}^6$, the Jacobian matrix of system (5.6) is

$$J(\mathbf{0}) = \begin{pmatrix} -\nu_E - \mu_E & b & 0 & 0 & 0 & 0 \\ \rho\nu_E & -\mu_F - d_{12} & 0 & 0 & d_{21} & 0 \\ (1-\rho)\nu_E & 0 & -\mu_M - \beta d_{12} & 0 & 0 & \beta d_{21} \\ 0 & 0 & 0 & -\nu_E - \mu_E & b & 0 \\ 0 & d_{12} & 0 & \rho\nu_E & -\mu_F - d_{21} & 0 \\ 0 & 0 & \beta d_{12} & (1-\rho)\nu_E & 0 & -\mu_F - \beta d_{21} \end{pmatrix},$$

with the characteristic polynomial

$$\det(J(0) - \lambda I) = [(\lambda + \mu_F)(\lambda + \mu_M) + \beta(d_{12} + d_{21} + d_{12}\mu_F + d_{21}\mu_M)]\,[(\lambda + \nu_E + \mu_E)(\lambda + \mu_F) - b\rho\nu_E]$$

$$\times\,[(\lambda + \nu_E + \mu_E)(\lambda + \mu_F + d_{12} + d_{21}) - b\rho\nu_E].$$

Since $\mathcal{N} > 1$, we have $\mu_F(\nu_E+\mu_E) - b\rho\nu_E < 0$. Thus, we can deduce that the factor $(\lambda+\nu_E+\mu_E)(\lambda+\mu_F) - b\rho\nu_E = \lambda^2 + \lambda(\nu_E + \mu_E + \mu_F) + \mu_F(\nu_E + \mu_E) - b\rho\nu_E$ has one positive root $\lambda > 0$. Hence, the Jacobian at zero has at least one positive eigenvalue so the zero equilibrium is unstable.

Stability of the positive equilibrium. First, we can see that the system (5.6a)-(5.6b), (5.6d)-(5.6e) of (E_1, F_1, E_2, F_2) does not depend on M_1, M_2, and it is cooperative and irreducible. By applying Theorem 1.1 in Chapter 4 of [191], one deduces that this system is strongly monotone. When $\mathcal{N} > 1$, this system admits exactly two equilibria: $(0, 0, 0, 0)$, and $(E_1^+, F_1^+, E_2^+, F_2^+)$. But the zero equilibrium is unstable, so by Theorem 2.2 in Chapter 2 of [191], if the initial data satisfies that $0 < (E_1^0, F_1^0, E_2^0, F_2^0) \leqslant (E_1^+, F_1^+, E_2^+, F_2^+)$, the solution (E_1, F_1, E_2, F_2) converges to $(E_1^+, F_1^+, E_2^+, F_2^+)$ when $t \to +\infty$.

Now if the initial data satisfies that $(E_1^0, F_1^0, E_2^0, F_2^0) > (E_1^+, F_1^+, E_2^+, F_2^+)$, then there exists a constant $\lambda > 1$

large enough such that $\lambda(E_1^+, F_1^+, E_2^+, F_2^+) \geqslant (E_1^0, F_1^0, E_2^0, F_2^0)$. Since $1 - \dfrac{\lambda E_i^+}{K_i} < 1 - \dfrac{E_i^+}{K_i}$, one has

$$b\lambda F_i^+ \left(1 - \frac{\lambda E_i^+}{K_i}\right) - (\nu_E + \mu_E)\lambda E_i^+ < \lambda \left[bF_i^+ \left(1 - \frac{E_i^+}{K_i}\right) - (\nu_E + \mu_E)E_i^+\right] = 0,$$

and the right-hand side of system (5.6a)-(5.6b), (5.6d)-(5.6e) at $\lambda(E_1^+, F_1^+, E_2^+, F_2^+)$ is non positive. Thus, the trajectory resulting from the initial data $\lambda(E_1^+, F_1^+, E_2^+, F_2^+)$ is non-increasing, and therefore converges to $(E_1^+, F_1^+, E_2^+, F_2^+)$. By applying the Lemma 5.2.2 to system (5.6a)-(5.6b), (5.6d)-(5.6e), we deduce that the trajectory resulting from the initial data $(E_1^0, F_1^0, E_2^0, F_2^0)$ lies between $(E_1^+, F_1^+, E_2^+, F_2^+)$ and the trajectories resulting from $\lambda(E_1^+, F_1^+, E_2^+, F_2^+)$. Hence, it also converges to $(E_1^+, F_1^+, E_2^+, F_2^+)$ when time t goes to infinity.

Moreover, since the trajectories issued from the initial data above and below $(E_1^+, F_1^+, E_2^+, F_2^+)$ all converge to the same limit, then by the comparison principle, we deduce that the trajectory resulting from any positive initial data with values between these initial values converges to this equilibrium.

Secondly, if we denote matrix $A = \begin{pmatrix} -\mu_M - \beta d_{12} & \beta d_{21} \\ \beta d_{12} & -\mu_M - \beta d_{21} \end{pmatrix}$, this matrix is Hurwitz. Functions $M_1,\ M_2$ satisfy $\begin{pmatrix} \dot{M}_1 \\ \dot{M}_2 \end{pmatrix} = A \begin{pmatrix} M_1 \\ M_2 \end{pmatrix} + (1-\rho)\nu_E \begin{pmatrix} E_1 \\ E_2 \end{pmatrix}$. Thus, for any $t > 0$,

$$\begin{pmatrix} M_1(t) \\ M_2(t) \end{pmatrix} = e^{tA} \begin{pmatrix} M_1^0 \\ M_2^0 \end{pmatrix} + (1-\rho)\nu_E \int_0^t e^{(t-s)A} \begin{pmatrix} E_1(s) \\ E_2(s) \end{pmatrix} ds. \tag{5.12}$$

Moreover, the equilibrium satisfies

$$\begin{pmatrix} M_1^+ \\ M_2^+ \end{pmatrix} = -(1-\rho)\nu_E A^{-1} \begin{pmatrix} E_1^+ \\ E_2^+ \end{pmatrix}. \tag{5.13}$$

Hence, from (5.13) and (5.12), we deduce that

$$\begin{pmatrix} M_1(t) \\ M_2(t) \end{pmatrix} - \begin{pmatrix} M_1^+ \\ M_2^+ \end{pmatrix} = e^{tA} \begin{pmatrix} M_1^0 \\ M_2^0 \end{pmatrix} + (1-\rho)\nu_E \left[\int_0^t e^{(t-s)A} \begin{pmatrix} E_1(s) \\ E_2(s) \end{pmatrix} ds + A^{-1} \begin{pmatrix} E_1^+ \\ E_2^+ \end{pmatrix}\right]. \tag{5.14}$$

Moreover, when $t \to +\infty$, we have that $\begin{pmatrix} E_1(t) \\ E_2(t) \end{pmatrix}$ converges to $\begin{pmatrix} E_1^+ \\ E_2^+ \end{pmatrix}$ and $e^{tA} \to 0$ since A is Hurwitz. Thus, for any $\varepsilon > 0$, there exists a time $T_\varepsilon > 0$ large enough such that for any $t > T_\varepsilon$,

$$E_i^+ - \varepsilon < E_i(t) < E_i^+ + \varepsilon, \qquad i = 1, 2, \tag{5.15}$$

and $\|e^{tA}\| < \|e^{T_\varepsilon A}\| \leqslant \varepsilon$.

Since matrix A is Metzler and irreducible, then by applying Lemma 5.2.1, one has that e^{At} is strictly positive for any $t > 0$. Moreover, one has $E_i \in (0, K_i)$ in $(0, +\infty)$, then for any $t > 2T_\varepsilon$,

$$0 < \int_0^{T_\varepsilon} e^{(t-s)A} \begin{pmatrix} E_1(s) \\ E_2(s) \end{pmatrix} ds < \int_0^{T_\varepsilon} e^{(t-s)A} ds \begin{pmatrix} K_1 \\ K_2 \end{pmatrix},$$

then

$$\left\| \int_0^{T_\varepsilon} e^{(t-s)A} \begin{pmatrix} E_1(s) \\ E_2(s) \end{pmatrix} ds \right\| < \left\| \int_0^{T_\varepsilon} e^{(t-s)A} ds \right\| \left\| \begin{pmatrix} K_1 \\ K_2 \end{pmatrix} \right\| = \left\| A^{-1} \left(e^{tA} - e^{(t-T_\varepsilon)A}\right) \right\| \left\| \begin{pmatrix} K_1 \\ K_2 \end{pmatrix} \right\| < \varepsilon C_1,$$

with some positive constant C_1 not depending on ε. Using the second inequality in (5.15), one has

$$\int_{T_\varepsilon}^t e^{(t-s)A} \begin{pmatrix} E_1(s) \\ E_2(s) \end{pmatrix} ds \leqslant A^{-1}(e^{(t-T_\varepsilon)A} - I) \begin{pmatrix} E_1^+ + \varepsilon \\ E_2^+ + \varepsilon \end{pmatrix} = A^{-1} e^{(t-T_\varepsilon)A} \begin{pmatrix} E_1^+ + \varepsilon \\ E_2^+ + \varepsilon \end{pmatrix} - \varepsilon A^{-1} - A^{-1} \begin{pmatrix} E_1^+ \\ E_2^+ \end{pmatrix}.$$

Proving similarly for the other inequality, we can deduce that

$$\left\| \int_{T_\varepsilon}^t e^{(t-s)A} \begin{pmatrix} E_1(s) \\ E_2(s) \end{pmatrix} ds + A^{-1} \begin{pmatrix} E_1^+ \\ E_2^+ \end{pmatrix} \right\| \leqslant \varepsilon C_2,$$

with some positive constant C_2 not depending on ε. Hence, from (5.14), we deduce that for any $t > 2T_\varepsilon$,

$$\left\| \begin{pmatrix} M_1(t) \\ M_2(t) \end{pmatrix} - \begin{pmatrix} M_1^+ \\ M_2^+ \end{pmatrix} \right\| < \varepsilon \left[\left\| \begin{pmatrix} M_1^0 \\ M_2^0 \end{pmatrix} \right\| + C_1 + C_2 \right].$$

Therefore, $(M_1(t), M_2(t))$ converges to (M_1^+, M_2^+) when t tends to $+\infty$. □

In the following section, by considering the releases of sterile males, we look for a condition of release functions Λ such that the positive equilibrium disappears.

5.4 Elimination with releases of sterile males

In this section, we consider $\Lambda(t)$ in system (5.1) the number of sterile males released per time unit and our goal is to adjust its values such that the wild population reaches elimination. We consider two release strategies as follows

Constant release: Let the release function $\Lambda(t) \equiv \Lambda > 0$. As time goes to infinity, the density of sterile males (M_1^s, M_2^s) converges to (M_1^{s*}, M_2^{s*}) that is the solution of system

$$\begin{cases} \Lambda - \mu_s M_1^{s*} - \alpha d_{12} M_1^{s*} + \alpha d_{21} M_2^{s*} = 0 \\ -\mu_s M_2^{s*} - \alpha d_{21} M_2^{s*} + \alpha d_{12} M_1^{s*} = 0 \end{cases} \tag{5.16}$$

By denoting

$$\tau_1 := \frac{(\mu_s + \alpha d_{21})}{\mu_s(\mu_s + \alpha d_{12} + \alpha d_{21})}, \quad \tau_2 := \frac{\alpha d_{12}}{\mu_s(\mu_s + \alpha d_{12} + \alpha d_{21})}, \tag{5.17}$$

we have $M_1^{s*} = \tau_1 \Lambda$, and $M_2^{s*} = \tau_2 \Lambda$ and $M_1^{s*} + M_2^{s*} = \dfrac{\Lambda}{\mu_s}$.

Impulsive periodic releases: Consider the release function

$$\Lambda(t) = \sum_{k=0}^{+\infty} \tau \Lambda_k^{\text{per}} \delta_{k\tau}, \tag{5.18}$$

with period $\tau > 0$ and Λ_k^{per} is the average number of sterile males released per time unit during the time interval $(k\tau, (k+1)\tau)$ for $k = 0, 1, \ldots$. We choose in this work Λ_k^{per} constant, and drop consequently the sub-index k. The release function $\Lambda(t)$ in (5.18) means that we release a total amount of $\tau \Lambda^{\text{per}}$ mosquitoes at the beginning of each time period ($t = k\tau$).

Denote vector $X(t) = \begin{pmatrix} M_1^s(t) \\ M_2^s(t) \end{pmatrix}$, then with $k = 0, 1, \ldots$, the density of sterile males satisfies the following system

$$X'(t) = A_s X(t) \qquad \text{for any } t \in \bigcup_{k=0}^{\infty} (k\tau, (k+1)\tau), \tag{5.19a}$$

$$X(k\tau^+) = X(k\tau^-) + \begin{pmatrix} \tau \Lambda^{\text{per}} \\ 0 \end{pmatrix}, \tag{5.19b}$$

with matrix $A_s = \begin{pmatrix} -\alpha d_{12} - \mu_s & \alpha d_{21} \\ \alpha d_{12} & -\alpha d_{21} - \mu_s \end{pmatrix}$, and $X(k\tau^\pm)$ denote the right and left limits of $X(t)$ at time $k\tau$ and by convention, we set $X(0^-) = 0$. The densities of the sterile males evolve according to (5.19a) on the union of open intervals $(k\tau, (k+1)\tau)$ while X is submitted to jump at each point $k\tau$ as in (5.19b). For such a release schedule, the solution of system (5.19) satisfies

$$X(k\tau^+) = \sum_{i=0}^{k} e^{iA_s\tau} \begin{pmatrix} \tau \Lambda^{\text{per}} \\ 0 \end{pmatrix}, \qquad X(t) = e^{A_s t} X(k\tau^+) \quad \text{for any } t \in \bigcup_{k=0}^{\infty} (k\tau, (k+1)\tau).$$

Since matrix A_s is Hurwitz, when $t \to +\infty$, we have that X converges to the periodic solution $X^{\text{per}} = \begin{pmatrix} M_1^{s,\text{per}} \\ M_2^{s,\text{per}} \end{pmatrix}$

that satisfies that, for $k = 0, 1, \ldots$

$$X^{\rm per}(k\tau^+) = (I - e^{A_s\tau})^{-1}\begin{pmatrix}\tau\Lambda^{\rm per}\\ 0\end{pmatrix}, \qquad X^{\rm per}(t) = e^{A_s t}X^{\rm per}(k\tau^+) \quad \text{for any } t \in \bigcup_{k=0}^{\infty}(k\tau,(k+1)\tau). \tag{5.20}$$

The following lemma shows that the periodic solution $X^{\rm per}$ is strictly positive at any time t.

Lemma 5.4.1. *There exists positive constant $\tau_1^{\rm per}$, $\tau_2^{\rm per}$ which depends on A_s and period τ such that for any $t > 0$, one has $X^{\rm per}(t) \geqslant \Lambda^{\rm per}\begin{pmatrix}\tau_1^{\rm per}\\ \tau_2^{\rm per}\end{pmatrix}$.*

Proof. We have matrix A_s is Metzler and irreducible, then by applying Lemma 5.2.1, we deduce that $e^{A_s} \gg 0$.

On the other hand, matrix A_s is Hurwitz so $(I - e^{A_s\tau})^{-1} = \sum_{i=0}^{+\infty} e^{iA_s\tau} \gg 0$ for any $\tau > 0$. Moreover, we have $e^{A_s t}$ is also strictly positive for any $t > 0$, thus there exist positive constants $\tau_1^{\rm per}$, $\tau_2^{\rm per}$ depending on τ and A_s such that

$$\inf_{t>0} X^{\rm per}(t) = \min_{t\in[0,\tau]} X^{\rm per}(t) = \min_{t\in[0,\tau]} e^{A_s t}(I - e^{A_s\tau})^{-1}\begin{pmatrix}\tau\Lambda^{\rm per}\\ 0\end{pmatrix} \geqslant \Lambda^{\rm per}\begin{pmatrix}\tau_1^{\rm per}\\ \tau_2^{\rm per}\end{pmatrix}.$$

The result of Lemma 5.4.1 follows. □

Remark 5.4.1. *The parameters τ_i defined in* (5.17) *and $\tau_i^{\rm per}$ play a similar role to each other: they define a relationship between an average release rate Λ per time unit and a (minimum) level of the sterile mosquito density.*

We provide in the following result a condition on $\Lambda(t)$ for the wild population to reach elimination.

Theorem 5.4.1. *Consider system* (5.1) *with the release function $\Lambda(t)$. Then*

- *In the constant release case, for $\Lambda(t) \equiv \Lambda$, there exists a positive number $\overline{\Lambda}$ satisfying*

$$\overline{\Lambda} \leqslant \max_{i=1,2}\frac{1}{\gamma_s\tau_i}(\mathcal{N}-1)C_M \qquad i = 1, 2,$$

with τ_i defined in (5.17)*, C_M defined in Lemma 5.2.4 such that if $\Lambda > \overline{\Lambda}$, system (5.1) has a unique equilibrium*

$$\mathbf{u}_0^* = (0, 0, 0, M_1^{s*}, 0, 0, 0, M_2^{s*}).$$

Moreover, in this case, for any non-negative initial data, the solution of (5.1) *converges to this equilibrium when $t \to +\infty$.*

- *In the periodic release case, for $\Lambda(t)$ defined in* (5.19)*, There exists a positive constant $\overline{\Lambda}^{\rm per}$ satisfying*

$$\overline{\Lambda}^{\rm per} \leqslant \max_{i=1,2}\frac{1}{\gamma_s\tau_i^{\rm per}}(\mathcal{N}-1)C_M,$$

with $\tau_i^{\rm per}$ defined in Lemma 5.4.1, C_M defined in Lemma 5.2.4 such that if $\Lambda^{\rm per} > \overline{\Lambda}^{\rm per}$, then for any non-negative initial data, the solution of the initial value problem of system (5.1) *converges to the unique steady state*

$$\mathbf{u}_0^{\rm per} = (0, 0, 0, M_1^{s,{\rm per}}, 0, 0, 0, M_2^{s,{\rm per}}),$$

as time $t \to +\infty$.

This result shows that with a sufficiently large number of sterile males released in the first zone, we can succeed in driving the wild population in both areas to elimination. In the following, we describe the principle idea to prove this result.

5.4.1 Principle of the method

To provide conditions for the release Λ to stabilize the zero equilibrium, our strategy is as follows:

Step 1: We consider $\rho_i = \sup_{t>0}\dfrac{M_i(t)}{M_i(t) + \gamma_s M_i^s(t)}$, for $i = 1,\ 2$, in system (5.1) to be smaller than some level, then we study the system with the fractions replaced by some constant.

Step 2: We show how to realize, through an adequate choice of Λ, the above behavior of M_i^s.

Step 1: Setting the sterile population level directly

Theorem 5.3.1 shows us that when the basic offspring number is smaller than 1, the zero equilibrium is globally asymptotically stable. For the controlled system, the basic offspring numbers is smaller than $\rho_i\mathcal{N}$. It suggests that, for stabilizing the origin of system (5.1), it is sufficient to ensure $\rho_i\mathcal{N} \leqslant 1$.

Proposition 5.4.1. *If the trajectory resulting from any positive initial data of system* (5.1) *satisfies that for* $\mathcal{N}$ *defined in* (5.2)*,*

$$\frac{M_i(t)}{M_i(t)+\gamma_s M_i^s(t)} \leqslant \frac{1}{\mathcal{N}}, \qquad t \geqslant 0,\ i=1,2. \tag{5.21}$$

then $\mathbf{u}' = (E_1, F_1, M_1, E_2, F_2, M_2)$ *converges to* $\mathbf{0}_6$ *as time* $t \to +\infty$*.*

Proof. Assume that we can set M_i^s to be large enough such that (5.21) holds, and we consider the following system

$$\dot{E}_1 = bF_1\left(1-\frac{E_1}{K_1}\right) - (\nu_E+\mu_E)E_1, \tag{5.22a}$$

$$\dot{F}_1 = \frac{1}{\mathcal{N}}\rho\nu_E E_1 - \mu_F F_1 - d_{12}F_1 + d_{21}F_2, \tag{5.22b}$$

$$\dot{M}_1 = (1-\rho)\nu_E E_1 - \mu_M M_1 - \beta d_{12}M_1 + \beta d_{21}M_2, \tag{5.22c}$$

$$\dot{E}_2 = bF_2\left(1-\frac{E_2}{K_2}\right) - (\nu_E+\mu_E)E_2, \tag{5.22d}$$

$$\dot{F}_2 = \frac{1}{\mathcal{N}}\rho\nu_E E_2 - \mu_F F_2 - d_{21}F_2 + d_{12}F_1, \tag{5.22e}$$

$$\dot{M}_2 = (1-\rho)\nu_E E_2 - \mu_M M_2 - \beta d_{21}M_2 + \beta d_{12}M_1, \tag{5.22f}$$

Denote $\widetilde{\mathbf{u}} = (\widetilde{E_1}, \widetilde{F_1}, \widetilde{M_1}, \widetilde{E_2}, \widetilde{F_2}, \widetilde{M_2})$ solution of system (5.22). Since system (5.22) is cooperative and the inequality (5.21) holds, one obtains that $\widetilde{\mathbf{u}}$ is a super-solution of the system (5.1a)-(5.1c), (5.1e)-(5.1g), and by applying Lemma 5.2.2, we have $\widetilde{\mathbf{u}} \geqslant \mathbf{u}'$.

Denote $\mathbf{u}^* = (E_1^*, F_1^*, M_1^*, E_2^*, F_2^*, M_2^*)$ a positive equilibrium of system (5.22) if exists. Similar to the previous section, we have

$$E_2^* = \frac{\mu_F+d_{12}+d_{21}}{d_{21}}\frac{E_1^*}{1-\frac{E_1^*}{K_1}} - \frac{\mu_F+d_{21}}{d_{21}}E_1^* =: g_{21}(E_1^*), \tag{5.23}$$

$$E_1^* = \frac{\mu_F+d_{12}+d_{21}}{d_{12}}\frac{E_2^*}{1-\frac{E_2^*}{K_2}} - \frac{\mu_F+d_{12}}{d_{12}}E_2^* =: g_{12}(E_2^*). \tag{5.24}$$

The analysis of g_{ij} is analogous to f_{ij} in Lemma 5.3.1. It is easy to check that g_{12} is increasing on $(0, K_2)$, so it is invertible. Then, E_1^* satisfies $(g_{21} - g_{12}^{-1})(E_1^*) = 0$. Function g_{21} is convex and g_{12}^{-1} is concave in $(0, K_1)$, and

$$g_{21}'(0) = \frac{\mu_F+d_{12}+d_{21}}{d_{21}} - \frac{(\mu_F+d_{21})}{d_{21}} = \frac{d_{12}}{d_{21}},$$

$$(g_{12}^{-1})'(0) = \frac{1}{g_{12}'(0)} = \frac{1}{\frac{\mu_F+d_{12}+d_{21}}{d_{12}} - \frac{\mu_F+d_{12}}{d_{12}}} = \frac{d_{12}}{d_{21}}.$$

We obtain that $g_{21}'(0) = (g_{12}^{-1})'(0)$ (see Figure 5.2), so zero is the unique equilibrium of system (5.22). By applying Theorem 3.1 in Chapter 2 of [191], we deduce that when $t \to +\infty$, the solution $\widetilde{\mathbf{u}}(t)$ converges to the equilibrium zero. Since $\mathbf{u}'(t) \leqslant \widetilde{\mathbf{u}}(t)$ for all $t > 0$, we deduce that the $\mathbf{u}'$ also converges to zero when t large. □

Step 2: Shaping the release function

We now want to choose Λ such that the condition (5.21) holds, which means

$$\gamma_s M_i^s(t) \geqslant (\mathcal{N}-1)\, M_i(t), \qquad t \geqslant 0,\ i=1,\ 2$$

The upper bound of M_i can be obtained from Lemma 5.2.4. For time $t > 0$ large enough, it is sufficient to choose Λ such that $\gamma_s M_i^s(t) \geqslant (\mathcal{N}-1)\, C_M$.

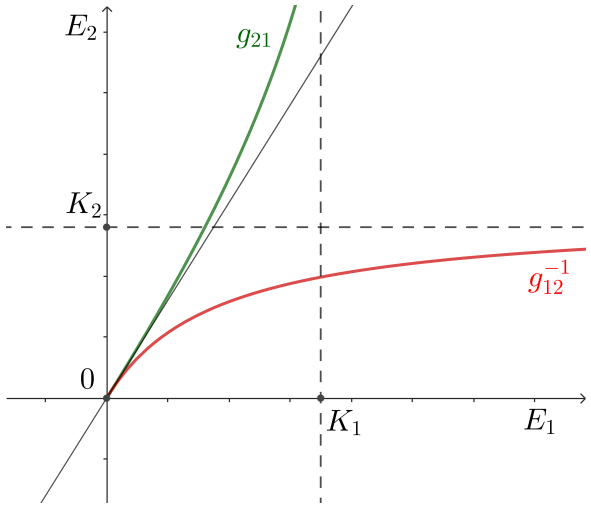

Figure 5.2 – The relation between E_1 and E_2 in the case when the positive root disappears

5.4.2 Proof of Theorem 5.4.1

Proof of Theorem 5.4.1. **Constant release:** For $\Lambda(t) \equiv \Lambda$, let us recall $A_s = \begin{pmatrix} -\mu_s - \alpha d_{12} & \alpha d_{21} \\ \alpha d_{12} & -\mu_s - \alpha d_{21} \end{pmatrix}$, and it is a Hurwitz matrix. And we have

$$\begin{pmatrix} M_1^s(t) \\ M_2^s(t) \end{pmatrix} = e^{tA_s} \begin{pmatrix} M_1^{s0} \\ M_2^{s0} \end{pmatrix} + (1-\rho)\nu_E \int_0^t e^{(t-s)A_s} ds \begin{pmatrix} \Lambda \\ 0 \end{pmatrix}.$$

Thus, when $t \to +\infty$, we can deduce that $\begin{pmatrix} M_1^s(t) \\ M_2^s(t) \end{pmatrix}$ converges to $\begin{pmatrix} M_1^{s*} \\ M_2^{s*} \end{pmatrix}$ for any initial data since $e^{tA_s} \to 0$ when $t \to +\infty$. Hence, for any $\varepsilon > 0$, there exists a value $T_\varepsilon > 0$ such that for any $t > T_\varepsilon$, $i = 1, 2$,

$$M_i^s(t) \geqslant M_i^{s*} - \varepsilon.$$

If we take Λ such that $\gamma_s(M_i^{s*} - \varepsilon) \geqslant (\mathcal{N} - 1)\, C_M$ with C_M defined in Lemma 5.2.4, then condition (5.21) holds. By applying Proposition 5.4.1, we deduce that for $i = 1, 2$, if $\Lambda > \max_{i=1,2} \dfrac{1}{\gamma_s \tau_i} (\mathcal{N} - 1) C_M$, system (5.1) has $\mathbf{u}_0^*$ as a unique equilibrium point, and every trajectory converges to this equilibrium when $t \to +\infty$. The dynamics of system (5.1) depend continuously and monotonically on Λ, then we deduce that there exists a positive critical value $\overline{\Lambda} \leqslant \max_{i=1,2} \dfrac{1}{\gamma_s \tau_i} (\mathcal{N} - 1) C_M$ such that for any $\Lambda > \overline{\Lambda}$, and for any non-negative initial data, solution $\mathbf{u}' = (E_1, F_1, M_1, E_2, F_2, M_2)(t)$ converges to $\mathbf{0}_6$ when $t \to +\infty$.

Impulsive periodic releases: Consider $\Lambda(t)$ defined in (5.19), denote $(E_1^{\text{per}}, F_1^{\text{per}}, M_1^{\text{per}}, E_2^{\text{per}}, F_2^{\text{per}}, M_2^{\text{per}})$ a solution of (5.1a)-(5.1c), (5.1e)-(5.1g) with $M_i^s \equiv M_i^{s,\text{per}}$ defined in (5.20). From Lemma 5.4.1, one has $M_i^{s,\text{per}}(t) \geqslant \Lambda^{\text{per}} \tau_i^{\text{per}}$ for all $t > 0$. Therefore, if we take Λ^{per} such that $\gamma_s \Lambda^{\text{per}} \tau_i^{\text{per}} \geqslant (\mathcal{N} - 1)\, C_M$, then condition (5.21) holds. By applying Proposition 5.4.1, we deduce that $\mathbf{u}^{\text{per}} = (E_1^{\text{per}}, F_1^{\text{per}}, M_1^{\text{per}}, E_2^{\text{per}}, F_2^{\text{per}}, M_2^{\text{per}})$ converges to zero as t grows. Since (M_1^s, M_2^s) converges to $(M_1^{s,\text{per}}, M_2^{s,\text{per}})$ as $t \to +\infty$, we have $\mathbf{u}' = (E_1, F_1, M_1, E_2, F_2, M_2)$ appoaches $\mathbf{u}^{\text{per}}$ and thus converges to $\mathbf{0}_6$ as time t goes to infinity.

Since the dynamics of system (5.1) depends continuously and monotonically on Λ, there exists a positive critical value $\overline{\Lambda}^{\text{per}} \leqslant \max_{i=1,2} \dfrac{1}{\gamma_s \tau_i^{\text{per}}} (\mathcal{N} - 1) C_M$ such that if $\Lambda^{\text{per}} > \overline{\Lambda}^{\text{per}}$ the equilibrium $\mathbf{u}_0^{\text{per}}$ of (5.1) with $\Lambda(t)$ defined in (5.18) is globally asymptotically stable. □

5.5 Parameter dependence of the critical values of the release rate

In this section, we consider the constant release case and examine how the critical value $\overline{\Lambda}$ depends on the parameters of system (5.1). In this model, the elimination of the population depends not only on the diffusion rate between the inaccessible area and the treated area, but also on the biological intrinsic values like the birth/death rates, and the carrying capacity.

5.5.1 Diffusion rates

In this part, we want to compare the critical values of Λ corresponding to different values of $d_{12},\ d_{21}$. We show that when the diffusion rates are large enough, the critical number of sterile males released is the same as in the case when there is no separation between the two sub-populations.

The case $d_{12},\ d_{21}$ large

First, we present a result of uniform convergence of system (5.1) when $d_{12},\ d_{21}$ go to $+\infty$ and d_{12} is proportional to d_{21}.

Proposition 5.5.1. *For $\varepsilon > 0$, consider the diffusion rates $d_{12} = \dfrac{1}{\varepsilon},\ d_{21} = \dfrac{\eta}{\varepsilon}$ with $\eta = \dfrac{d_{21}}{d_{12}} > 0$. Denote $\mathbf{u}^\varepsilon = (E_1^\varepsilon, F_1^\varepsilon, M_1^\varepsilon, M_1^{s,\varepsilon}, E_2^\varepsilon, F_2^\varepsilon, M_2^\varepsilon, M_2^{s,\varepsilon})$ the solution of system (5.1) with the initial date $\mathbf{u}^{\varepsilon,0}$ satisfying that*

$$\{E_i^{\varepsilon,0}\}_\varepsilon,\ \{F_i^{\varepsilon,0}\}_\varepsilon,\ \{M_i^{\varepsilon,0}\}_\varepsilon \text{ converge to } E_i^{0,0}, F_i^{0,0}, M_i^{0,0} \text{ respectively as } \varepsilon \to 0,\ \text{with } i = 1,\ 2,$$

and

$$E_1^{\varepsilon,0} - \eta E_2^{\varepsilon,0} = \mathcal{O}(\varepsilon), \quad F_1^{\varepsilon,0} - \eta F_2^{\varepsilon,0} = \mathcal{O}(\varepsilon), \quad M_1^{\varepsilon,0} - \eta M_2^{\varepsilon,0} = \mathcal{O}(\varepsilon), \quad M_1^{s,\varepsilon,0} = M_2^{s,\varepsilon,0} = 0. \tag{5.25}$$

Then, when $\varepsilon \to 0$, the sequence $\{\mathbf{u}^\varepsilon\}_\varepsilon$ converges uniformly to a limit $(E_1, F_1, M_1, M_1^s, E_2, F_2, M_2, M_2^s)$ on $[0, +\infty)$. Moreover, we have

$$F_1 = \eta F_2, \quad M_1 = \eta M_2, \quad M_1^s = \eta M_2^s. \tag{5.26}$$

If we denote $F = F_1 + F_2,\ M = M_1 + M_2,\ M^s = M_1^s + M_2^s$, then (E_1, E_2, F, M, M^s) solves the following system

$$\dot{E}_1 = \frac{\eta}{\eta+1} bF\left(1 - \frac{E_1}{K_1}\right) - (\nu_E + \mu_E)E_1, \tag{5.27a}$$

$$\dot{E}_2 = \frac{1}{\eta+1} bF\left(1 - \frac{E_2}{K_2}\right) - (\nu_E + \mu_E)E_2, \tag{5.27b}$$

$$\dot{F} = \rho\nu_E(E_1 + E_2)\frac{M}{M + \gamma_s M^s} - \mu_F F, \tag{5.27c}$$

$$\dot{M} = (1-\rho)\nu_E(E_1 + E_2) - \mu_M M, \tag{5.27d}$$

$$\dot{M^s} = \Lambda_\infty - \mu_s M^s, \tag{5.27e}$$

with the corresponding initial data $E_1^{0,0},\ E_2^{0,0},\ F^{0,0} = F_1^{0,0} + F_2^{0,0},\ M^{0,0} = M_1^{0,0} + M_2^{0,0},\ M^{s,0,0} = 0$.

It is straightforward to see that the previous result implies that the functions F_1, F_2, M_1, M_2 fulfil the following identities:

$$F_1 = \frac{\eta}{1+\eta}F, \quad F_2 = \frac{1}{1+\eta}F, \quad M_1 = \frac{\eta}{1+\eta}M, \quad M_2 = \frac{1}{1+\eta}M.$$

Proof of Proposition 5.5.1. To prove this result, we first apply the Arzela-Ascoli theorem for the sequence of smooth solution $\{\mathbf{u}^\varepsilon\}_\varepsilon$ on a close interval $[0, T]$ with any $T > 0$. Then, we extend the convergence at infinity.

• **Uniform convergence on $[0, T]$:** First, we check the uniform boundedness of this sequence. For $i = 1, 2$, from Lemma 5.2.4, one has $E_i^\varepsilon(t) \leqslant K_i$ for all $t > 0$ and $\varepsilon > 0$. Again by this Lemma, for any $t > 0$, one has

$$F_i^\varepsilon(t) \leqslant \max\left\{F_1^{\varepsilon,0} + F_2^{\varepsilon,0},\ \frac{\rho\nu_E(K_1+K_2)}{\mu_F}\right\} \leqslant C_F^0$$

here C_F^0 does not depend on ε since the initial data converge as ε goes to zero. Similarly, we can show that there are positive constants $C_M^0,\ C_{M^s}^0$ not depending on ε such that for any $t > 0$, one has $M_i^\varepsilon(t) < C_M^0,\ M_i^{s,\varepsilon}(t) < C_{M^s}^0$.

Next, we prove that the sequence of derivative $\{\dot{\mathbf{u}^\varepsilon}\}_\varepsilon$ is also uniformly bounded. For any $t > 0$,

$$\dot{F_1^\varepsilon} < \rho\nu_E K_1 - \frac{1}{\varepsilon}\left(F_1^\varepsilon - \eta F_2^\varepsilon\right).$$

We show that $\dfrac{F_1^\varepsilon - \eta F_2^\varepsilon}{\varepsilon}$ is uniformly bounded on $[0,T]$. Indeed, we have for all $t>0$ and $\varepsilon>0$,

$$\dot{F}_1^\varepsilon - \eta \dot{F}_2^\varepsilon = \rho\nu_E \left(E_1^\varepsilon \frac{M_1^\varepsilon}{M_1^\varepsilon + \gamma_s M_1^{s,\varepsilon}} - \eta E_2^\varepsilon \frac{M_2^\varepsilon}{M_2^\varepsilon + \gamma_s M_2^{s,\varepsilon}} \right) - \left(\mu_F + \frac{\eta+1}{\varepsilon} \right) (F_1^\varepsilon - \eta F_2^\varepsilon)$$

$$= A^\varepsilon - \left(\frac{\eta+1}{\varepsilon} \right) (F_1^\varepsilon - \eta F_2^\varepsilon),$$

where $A^\varepsilon := \rho\nu_E \left(E_1^\varepsilon \dfrac{M_1^\varepsilon}{M_1^\varepsilon + \gamma_s M_1^{s,\varepsilon}} - \eta E_2^\varepsilon \dfrac{M_2^\varepsilon}{M_2^\varepsilon + \gamma_s M_2^{s,\varepsilon}} \right) - \mu_F (F_1^\varepsilon - \eta F_2^\varepsilon)$ is uniformly bounded since we already proved that $\mathbf{u}^\varepsilon$ is uniformly bounded. Then, for any $\varepsilon>0$, we have $|A^\varepsilon(t)| < C$ for any $t>0$ and some constant $C>0$. By the Duhamel formula, we obtain

$$(F_1^\varepsilon - \eta F_2^\varepsilon)(t) = (F_1^{\varepsilon,0} - \eta F_2^{\varepsilon,0}) e^{-\frac{\eta+1}{\varepsilon}t} + \int_0^t A^\varepsilon(s) e^{-\frac{\eta+1}{\varepsilon}(t-s)} ds.$$

So for all $t \geqslant 0$, one has

$$\frac{|F_1^\varepsilon - \eta F_2^\varepsilon|(t)}{\varepsilon} \leqslant \frac{\left| F_1^{\varepsilon,0} - \eta F_2^{\varepsilon,0} \right|}{\varepsilon} e^{-\frac{\eta+1}{\varepsilon}t} + \frac{C}{\eta+1} \left(1 - e^{-\frac{\eta+1}{\varepsilon}t} \right).$$

For any $t \in [0,+\infty)$ and $\varepsilon>0$, one has $0 < e^{-\frac{\eta+1}{\varepsilon}t} < 1$. And due to the Assumption (5.25) for the initial data, the right-hand side is uniformly bounded with respect to ε. Hence, we deduce that $\dot{F}_1^\varepsilon$ is uniformly bounded on $[0,T]$. We obtain analogously the uniform boundedness of $\dot{F}_i^\varepsilon$, $\dot{M}_i^\varepsilon$, and $\dot{M}_i^{s,\varepsilon}$. Due to the positivity of system (5.1), one has $\dot{E}_i^\varepsilon(t) < bC_{F_i}^0$ for all $t>0$ and $\varepsilon>0$.

Since the sequence of derivatives $\{\dot{\mathbf{u}}^\varepsilon\}_\varepsilon$ is uniformly bounded on $[0,T]$, we deduce the equicontinuity of the sequence $\{\mathbf{u}^\varepsilon\}_\varepsilon$. Hence, by the Arzela-Ascoli theorem, this sequence has a uniformly convergent subsequence. We denote its limit $\mathbf{u} = (E_1, F_1, M_1, M_1^s, E_2, F_2, M_2, M_2^s)$. If we multiply system (5.1) with ε and let it go to zero, we obtain the equalities (5.26) and system (5.27).

With the initial data satisfying the assumptions in Proposition 5.5.1, the solution of system (5.27) on $(0,+\infty)$ is unique. Since all the subsequence of $\{\mathbf{u}^\varepsilon\}_\varepsilon$ converge to the same limit, we deduce that the whole sequence converges uniformly to this limit on $[0,T]$.

• **Extension to $+\infty$:** For all $t \geqslant 0$, we prove that for all $\delta>0$, there exists $\varepsilon_0>0$ such that for all $\varepsilon \in (0,\varepsilon_0)$, we have $\|\mathbf{u}^\varepsilon(t) - \mathbf{u}(t)\| < \delta$.

Indeed, the solution of both (5.1) and (5.27) converges to a constant as time t goes to infinity, then there exists a time $T>0$ large enough and $\varepsilon_1>0$ such that for any $\varepsilon \in (0,\varepsilon_1)$ and all $t>T$, one has

$$\|\mathbf{u}^\varepsilon(t) - \mathbf{u}^\varepsilon(T)\| < \frac{\delta}{3}, \quad \|\mathbf{u}(t) - \mathbf{u}(T)\| < \frac{\delta}{3}.$$

Moreover, we have that the sequence $\{\mathbf{u}^\varepsilon\}_\varepsilon$ converges uniformly to $\mathbf{u}$ in the closed interval $[0,T]$. Thus, there exists a positive value $\varepsilon_0 < \varepsilon_1$ such that for all $\varepsilon \in (0,\varepsilon_0)$,

$$\sup_{[0,T]} \|\mathbf{u}^\varepsilon - \mathbf{u}\| < \frac{\delta}{3}.$$

Hence, we have $\|\mathbf{u}^\varepsilon(T) - \mathbf{u}(T)\| < \dfrac{\delta}{3}$ and we deduce that

$$\|\mathbf{u}^\varepsilon(t) - \mathbf{u}(t)\| \leqslant \|\mathbf{u}^\varepsilon(t) - \mathbf{u}^\varepsilon(T)\| + \|\mathbf{u}^\varepsilon(T) - \mathbf{u}(T)\| + \|\mathbf{u}(t) - \mathbf{u}(T)\| < \delta.$$

It is clear that for $t \leqslant T$, one has $\|\mathbf{u}^\varepsilon(t) - \mathbf{u}(t)\| < \dfrac{\delta}{3} < \delta$. So we obtain the convergence on $[0,+\infty)$. □

In the next result, we study the limit system (5.27).

Theorem 5.5.1. *Consider system* (5.27) *with the release function given by*

(i) constant release $\Lambda_\infty(t) \equiv \Lambda_\infty$.

Then there exists $\overline{\Lambda}_\infty > 0$ *such that for any* $\Lambda_\infty > \overline{\Lambda}_\infty$, *system* (5.27) *has a unique equilibrium* $u_\infty^0 = \left(0,0,0,0,\frac{\Lambda_\infty}{\mu_s}\right)$ *and it is globally asymptotically stable.*

(ii) impulsive periodic release $\Lambda_\infty(t) = \sum_{k=0}^{+\infty} \tau \Lambda_\infty^{\text{per}} \delta_{k\tau}$ *with period* τ.

Then there exists $\overline{\Lambda}_\infty^{\text{per}} > 0$ *such that for any* $\Lambda_\infty^{\text{per}} > \overline{\Lambda}_\infty^{\text{per}}$, *all trajectories of* (5.27) *resulting from any non-negative initial data satisfy that* (E_1, E_2, F, M) *converges to the equilibrium* $\mathbf{0}_4 \in \mathbb{R}^4$.

Proof. Firstly, we show that for $\Lambda_\infty(t)$ large enough such that $\dfrac{M}{M+\gamma_s M^s} \leqslant \dfrac{1}{\mathcal{N}}$, then all trajectories of (5.27) resulting from any non-negative initial data satisfy that (E_1, E_2, F, M) converges to the equilibrium $\mathbf{0}_4 \in \mathbb{R}^4$. Indeed, consider the first four equations of system (5.27) with $\dfrac{M}{M+\gamma_s M^s}$ replaced by $\dfrac{1}{\mathcal{N}}$, and we denote the equilibrium (E_1^*, E_2^*, F^*, M^*) of this system satisfy

$$F^* = \frac{\rho\nu_E(E_1^* + E_2^*)}{\mathcal{N}\mu_F}, \qquad M^* = \frac{(1-\rho)\nu_E(E_1^* + E_2^*)}{\mu_M},$$

and

$$(E_1^* + E_2^*) = \frac{E_1^* + E_2^*}{\frac{\eta}{\eta+1}\left(1 - \frac{E_1^*}{K_1}\right) + \frac{1}{\eta+1}\left(1 - \frac{E_2^*}{K_2}\right)}.$$

This is equivalent to either $E_1^* + E_2^* = 0$ or

$$\frac{\eta}{\eta+1}\left(1 - \frac{E_1^*}{K_1}\right) + \frac{1}{\eta+1}\left(1 - \frac{E_2^*}{K_2}\right) = 1.$$

The left-hand side of this equality is smaller than 1 since $E_i^* < K_i$ with $i = 1, 2$, thus we deduce that $E_1^* = E_2^* = F^* = M^* = 0$. Hence, this system has exactly one equilibrium $\mathbf{0}_4$ and all trajectories converge to this steady state by using Theorem 3.1 in Chapter 2 of [191]. Then, by applying the comparison Lemma 5.2.2, we deduce the convergence of system (5.27).

Analogously to system (5.1), we have the boundedness for the solution of (5.27) and the monotonicity of the system with respect to Λ_∞. Therefore, we can deduce the existence of the critical values for both the constant and periodic cases. □

Next, we make a comparison between the previous case and the case where there is no separation between the two sub-populations.

The non-separation case

When there is no separation between the two sub-populations of mosquitoes, we consider one population (E, F, M, M^s) in a habitat with aquatic carrying capacity $K = K_1 + K_2$. Then (E, F, M, M^s) satisfies the following system

$$\dot{E} = bF\left(1 - \frac{E}{K}\right) - (\nu_E + \mu_E)E, \tag{5.28a}$$

$$\dot{F} = \rho\nu_E E \frac{M}{M + \gamma_s M^s} - \mu_F F, \tag{5.28b}$$

$$\dot{M} = (1-\rho)\nu_E E - \mu_M M, \tag{5.28c}$$

$$\dot{M}^s = \Lambda - \mu_s M^s. \tag{5.28d}$$

For the constant release, the positive equilibrium (E^*, F^*, M^*, M^{s*}) satisfies

$$M^* = \frac{(1-\rho)\nu_E}{\mu_M}E^*, \quad M^{s*} = \frac{\Lambda}{\mu_s}, \quad F^* = \frac{\rho\nu_E}{\mu_F}\frac{E^*}{1 + \frac{\mu_M\gamma_s\Lambda}{(1-\rho)\nu_E\mu_s E^*}};$$

and from (5.28a), we deduce that

$$\frac{b\rho\nu_E}{\mu_F}\frac{E^*}{1 + \frac{\mu_M\gamma_s\Lambda}{(1-\rho)\nu_E\mu_s E^*}}\left(1 - \frac{E^*}{K}\right) - (\nu_E + \mu_E)E^* = 0.$$

This equation has no positive solution if and only if $\Lambda > \overline{\Lambda}_0 = \dfrac{(1-\rho)\nu_E K\mu_s(1-\mathcal{N})^2}{4\mathcal{N}\mu_M\gamma_s}$.

Remark 5.5.1. *We can see that in the special case where $K_1 = \eta K_2$, by taking $E = E_1 + E_2$, we can write system (5.27) as system (5.28) for (E, F, M, M^s) with carrying capacity $K = K_1 + K_2$. Hence, we deduce that $\overline{\Lambda}_\infty = \overline{\Lambda}_0$. This suggests that the critical number of sterile males released in the case with very large diffusion rate is the same as in the non-separation case in 5.5.1.*

5.5.2 Biological intrinsic values

In this section, we compare the critical value of Λ corresponding to different values of the parameters namely the birth rate b, the death rate $\mu_E,\ \mu_F,\ \mu_M,\ \mu_s$, and the carrying capacities $K_1,\ K_2$. In this section, we show that the critical value $\overline{\Lambda}$ is monotone with respect to these parameters. To prove this claim, we first define in $\mathbb{R}^7_+$ an order such that $(\mu_E, \mu_F, \mu_M, \mu_s, b, K_1, K_2) \trianglelefteq (\mu'_E, \mu'_F, \mu'_M, \mu'_s, b', K'_1, K'_2)$ if and only if

$$\mu_E \leqslant \mu'_E,\ \mu_F \leqslant \mu'_F,\ \mu_M \leqslant \mu'_M,\ \mu_s \geqslant \mu'_s,\ b \geqslant b',\ K_1 \geqslant K'_1,\ K_2 \geqslant K'_2.$$

Moreover, we write $(\mu_E, \mu_F, \mu_M, \mu_s, b, K_1, K_2) \triangleleft (\mu'_E, \mu'_F, \mu'_M, \mu'_s, b', K'_1, K'_2)$ if the two vectors are not identical. With this order relation, we have the following result

Theorem 5.5.2. *Consider system (5.1) and the basic offspring number $\mathcal{N} > 1$, consider the critical values $\overline{\Lambda}$ and $\overline{\Lambda}^{\mathrm{per}}$ as defined in Theorem 5.4.1, then we have the mappings from $\mathbb{R}^7_+$ to $\mathbb{R}_+$*

$$(\mu_E, \mu_F, \mu_M, \mu_s, b, K_1, K_2) \mapsto \overline{\Lambda}, \quad (\mu_E, \mu_F, \mu_M, \mu_s, b, K_1, K_2) \mapsto \overline{\Lambda}^{\mathrm{per}},$$

are non-increasing with respect to the order $\trianglelefteq$.

Proof. First, we consider system (5.1) with two sets of parameters

$$\Theta = (\mu_E, \mu_F, \mu_M, \mu_s, b, K_1, K_2), \quad \Theta' = (\mu'_E, \mu'_F, \mu'_M, \mu'_s, b', K'_1, K'_2),$$

where $\Theta \trianglelefteq \Theta'$. We fix the same value of Λ in both cases and consider

$$\mathbf{u} = (E_1, F_1, M_1, M_1^s, E_2, F_2, M_2, M_2^s), \quad \mathbf{v} = (\widetilde{E_1}, \widetilde{F_1}, \widetilde{M_1}, \widetilde{M_1^s}, \widetilde{E_2}, \widetilde{F_2}, \widetilde{M_2}, \widetilde{M_2^s})$$

where $\mathbf{u},\ \mathbf{v}$ are the solutions of (5.1) with the parameters $\Theta,\ \Theta'$, respectively. We have $\dot{\mathbf{u}} = \mathbf{f}_\Theta(\mathbf{u})$, and $\dot{\mathbf{v}} = \mathbf{f}_{\Theta'}(\mathbf{v}) \preceq \mathbf{f}_\Theta(\mathbf{v})$ in the subset $\{0 \leqslant E_1 \leqslant K_1\} \cap \{0 \leqslant E_2 \leqslant K_2\}$ of $\mathbb{R}^8_+$. Moreover, functions $\mathbf{f}_\Theta$ and $\mathbf{f}_{\Theta'}$ satisfy the assumptions in Lemma 5.2.3, then by applying this lemma, we obtain that $\mathbf{v} \preceq \mathbf{u}$ for the same initial data, so

$$E_i(t) \geqslant \widetilde{E_i}(t),\ F_i(t) \geqslant \widetilde{F}_i(t),\ M_i(t) \geqslant \widetilde{M_i}(t) \qquad \text{for all } t > 0,\ i = 1, 2.$$

On the other hand, for any $\Lambda > \overline{\Lambda}_\Theta$, by Theorem 5.4.1 we have that $E_i(t),\ F_i(t),\ M_i(t)$ converge to zero as t goes to infinity. As a consequence of the above inequalities, we deduce that $\widetilde{E_i}(t),\ \widetilde{F}_i(t),\ \widetilde{M_i}(t)$ also converge to zero for all initial data. So $\Lambda > \overline{\Lambda}_{\Theta'}$, and we can deduce that $\overline{\Lambda}_\Theta \geqslant \overline{\Lambda}_{\Theta'}$. □

5.6 Numerical simulations

Following [69, 200], we consider the parameters as in Table 5.1.

5.6.1 Trajectories and Equilibria

We fix the moving rate $d_{12} = 0.06,\ d_{21} = 0.04$ (day^{-1}), and plot the numerical solutions of system (5.1) with different releases functions $\Lambda(t)$. In each case, we numerically solve the system with different initial data $(E_1^0, F_1^0, M_1^0, E_2^0, F_2^0, M_2^0) : \{(2, 5, 6, 3, 5, 6),\ (10, 20, 60, 25, 40, 60),\ (100, 50, 60, 120, 80, 60)\}$. In the following section, we present several numerical simulations showing the trajectories and approximated equilibria according to different release strategies.

Constant continuous releases

We take three different constant values of $\Lambda \in \{0, 200, 500\}$ (day^{-1}). The initial density of sterile males is equal to zero. We approximate the positive equilibria in each case and plot the trajectories of E_1 and E_2 in Figures 5.3 according to different values of Λ. We observe the following:

- When $\Lambda = 0$, there is one positive equilibrium

$$(E_1^*, E_2^*) = (192.62, 174.82).$$

Table 5.1 – Parameter values of *Aedes albopictus* mosquitoes used for the numerical simulation

Symbol	Description	Value	Unit
b	Birth rate of fertile females	10	day^{-1}
ν_E	Emerging rate of viable eggs	0.08	day^{-1}
μ_E	Death rate of aquatic phase	0.05	day^{-1}
μ_F	Female death rate	0.1	day^{-1}
μ_M	Wild male death rate	0.14	day^{-1}
μ_s	Sterile male death rate	0.14	day^{-1}
K_1	Carrying capacity of aquatic phase in patch 1	200	_
K_2	Carrying capacity of aquatic phase in patch 2	180	_
γ_s	Mating competitiveness of sterile male	1	_
r	Ratio of female hatch	0.5	_
α	Ratio between diffusion rates of sterile males and female	0.5	_
β	Ratio between diffusion rates of sterile males and female	0.8	_

All positive trajectories converge to the positive steady state (E_1^*, E_2^*).

- When $\Lambda = 200$ (day^{-1}), there are two positive equilibria

$$(E_1^+, E_2^+) = (17.29, 49.98), \qquad (E_1^*, E_2^*) = (85.79, 130.02).$$

All positive trajectories also converge to the larger positive steady state (E_1^*, E_2^*).

- When $\Lambda = 500$ (day^{-1}), there is no positive equilibrium. All the trajectories converge to the zero equilibrium.

This validates the result in Theorem 5.4.1 that when Λ exceeds some critical value, zero is the unique equilibrium of system (5.1). The observation for $\Lambda = 0$ illustrates the result in Theorem 5.3.1 that there is one positive equilibrium and it is globally asymptotically stable. The introduction of sterile males ($\Lambda = 200 > 0$) reduces the value of the positive steady state (see Figure 5.3b), and when $\Lambda = 500$ (day^{-1}) exceeds some critical value (at most equal to 500), all trajectories converge to the zero equilibrium (see Figure 5.3c). This illustrates the first point of Theorem 5.4.1. To approximate the critical value of Λ, we provide some numerical bifurcation diagrams in Section 5.6.2.

Periodic impulsive releases

In this part, we consider the periodic impulsive releases with $\Lambda(t)$ defined in (5.18), with Λ^{per} equal to 200 and 300 (day^{-1}), the period $\tau = 10$ (days). The trajectories of $E_1,\ E_2$ shown in Figure 5.4 converge to the periodic solution when $\Lambda^{\text{per}} = 200$ (day^{-1}) and go to zero when $\Lambda^{\text{per}} = 300$ (day^{-1}). This illustrates the second point of Theorem 5.4.1 that when the number of sterile males released exceeds a critical value $\overline{\Lambda}^{\text{per}}$, the wild populations of mosquitoes in both areas reach elimination.

5.6.2 Critical values and bifurcation

Our aim in this section is to approximate the critical value of Λ where the bifurcation occurs.

Bifurcation diagram in the constant release case

We solve a system of nonlinear stationary problem $\mathcal{F}(u;\Lambda) = 0$ for all values of the parameter Λ, knowing that the solutions are continuous with respect to Λ. Solving by numerical approximations can be done using numerical continuation methods (see [170]).

Here we present the simplest method called *Natural Parameter Continuation* (incremental methods, see [170]): Iteratively find approximate roots of $\mathcal{F}(u,\Lambda) = 0$ for several values of Λ_i with index $i \in \mathbb{N}^*$. The root of step i is used as an initial guess for the numerical solver at step $i+1$. The first initial guess is the root for the smallest Λ. To approximate the critical value $\overline{\Lambda}$ in the constant case and examine what happens when $0 < \Lambda \leqslant \overline{\Lambda}$, we draw the bifurcation diagram for $\Lambda \in [0.1, 500]$. The initial positions of the numerical continuation are taken at the approximated equilibria when $\Lambda = 0.1$.

We obtain the bifurcation diagrams in Figure 5.5 for two scenarios. We observed that the critical value of Λ decreases when the diffusion rates increase.

- For $d_{12} = 1,\ d_{21} = 2$, the critical value $\overline{\Lambda} = 106.45$ (day^{-1}).

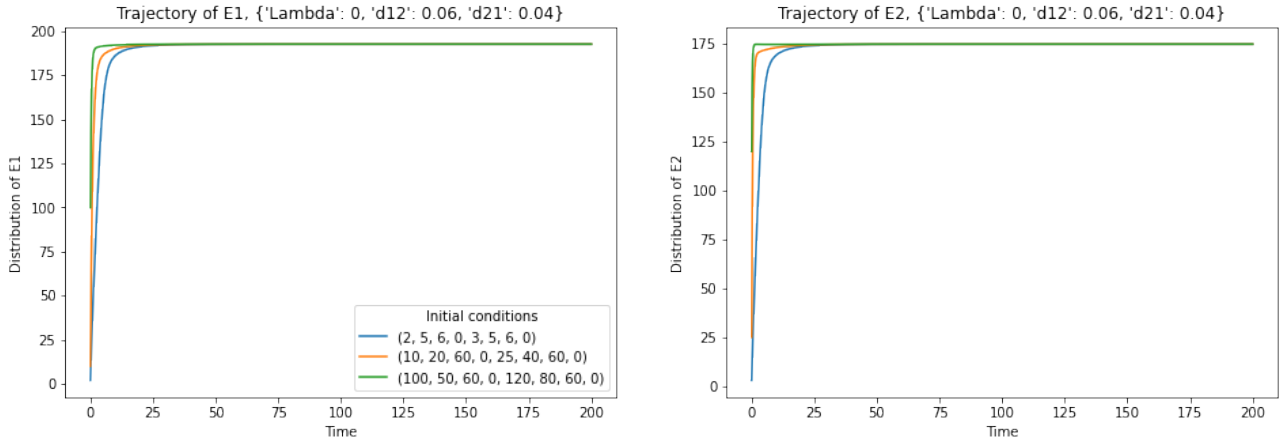

(a) $\Lambda = 0$

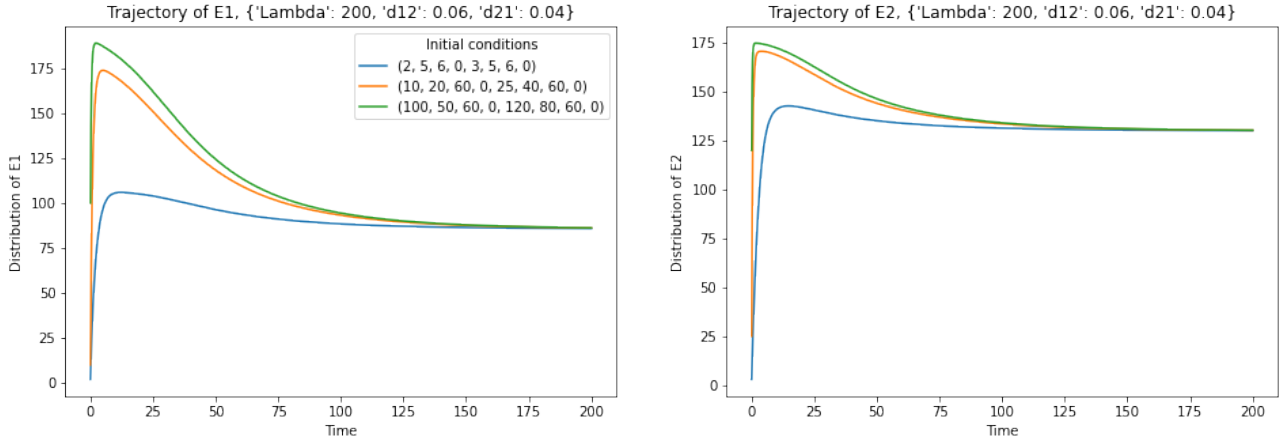

(b) $\Lambda = 200$ (day^{-1}).

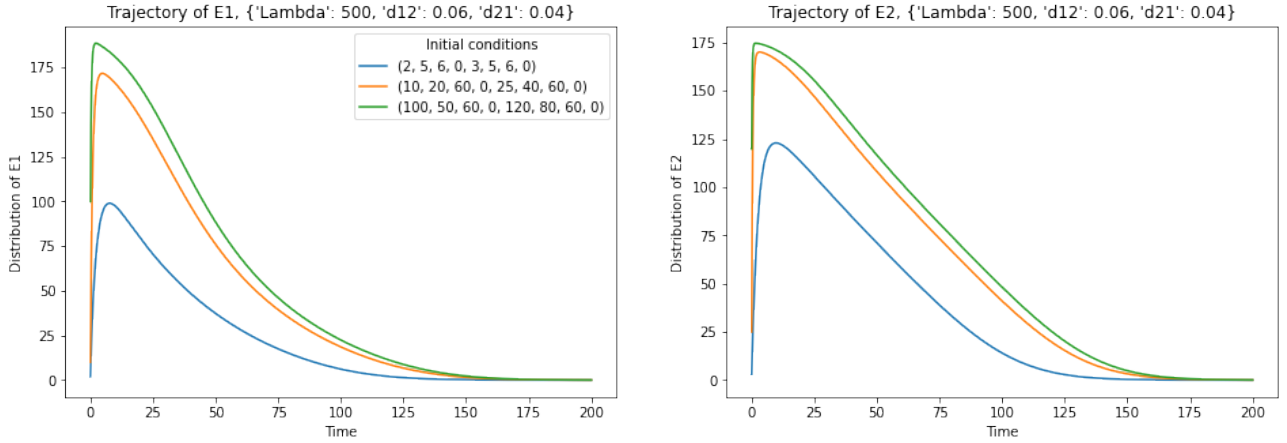

(c) $\Lambda = 500$ (day^{-1}).

Figure 5.3 – Trajectories of E_1 and E_2 in the constant release case with diffusion rates $d_{12} = 0.06$, $d_{21} = 0.04$ (day^{-1}).

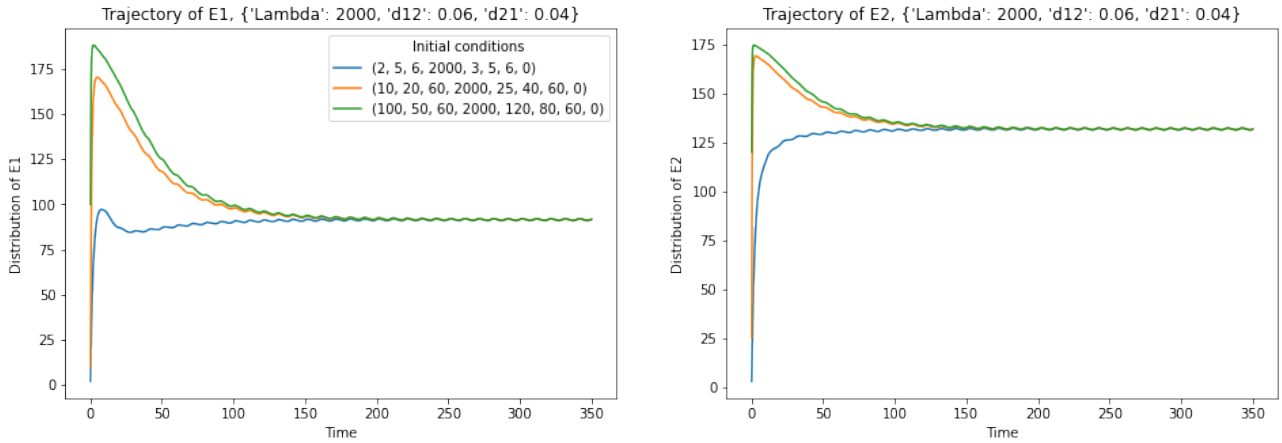

(a) $\Lambda^{\text{per}} = 200$

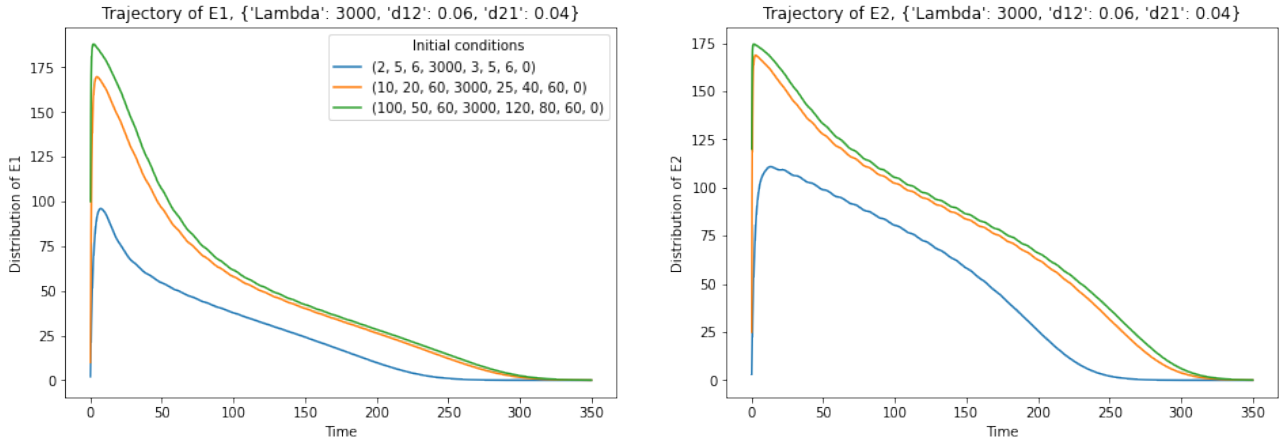

(b) $\Lambda^{\text{per}} = 300$

Figure 5.4 – Trajectories of E_1 and E_2 in the periodic release case with period $\tau = 10$ (days), diffusion rates $d_{12} = 0.06,\ d_{21} = 0.04$ (day^{-1}).

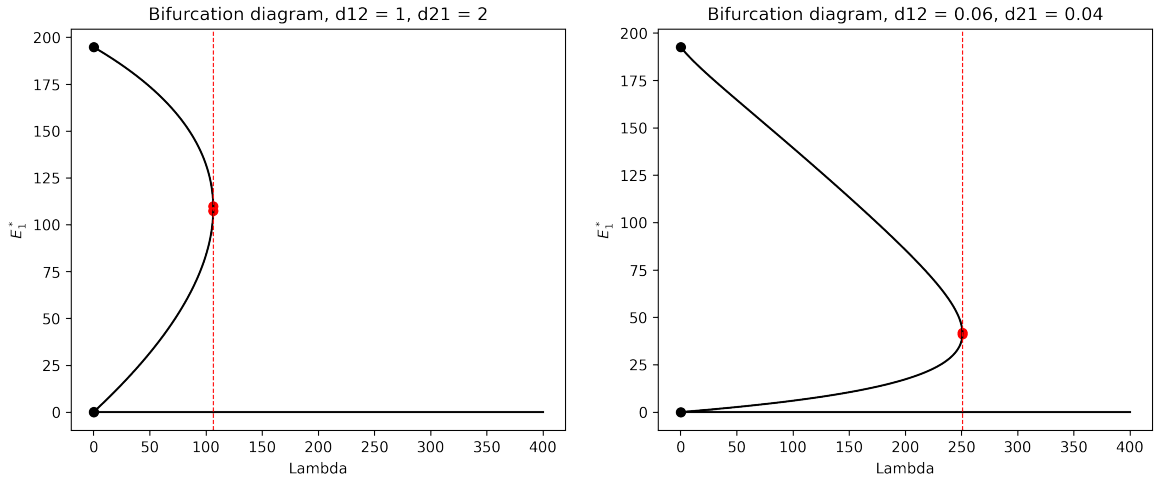

Figure 5.5 – Bifucation diagrams of E_1^* with parameter Λ in the constant continuous release case.

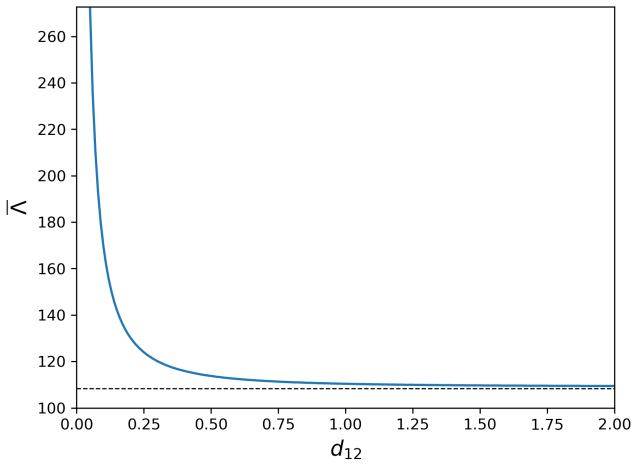

Figure 5.6 – Dependence of $\overline{\Lambda}$ on the diffusion rate d_{12}.

- For $d_{12} = 0.06,\ d_{21} = 0.04$, the critical value $\overline{\Lambda} = 250.88$ (day^{-1}).

Taking $d_{12} = d_{21}$, we plot the critical value $\overline{\Lambda}$ corresponding to the moving rates d_{12} (see Figure 5.6). This shows that the value of $\overline{\Lambda}$ decreases when the diffusion rate gets larger, and converges to a value $\overline{\Lambda}_\infty \approx 109.45$ (day^{-1}) as d_{12} goes to infinity. This validates the result provided by Proposition 5.5.1 where $\overline{\Lambda}_\infty$ is the critical value of Λ corresponding to system (5.27). We also found that $\overline{\Lambda}_\infty = \overline{\Lambda}_0$ where $\overline{\Lambda}_0$ is the critical value of the system when there is no separation between the two sub-populations defined in 5.5.1.

Comparison of release strategies

In practice, the strategy using impulsive releases is more realistic than the constant strategy. In this section, we make a comparison between these two strategies.

For the fixed diffusion rates $d_{12} = 0.06,\ d_{21} = 0.04$, we approximated the critical number of sterile males released in both cases using the method in 5.6.2

- When $\Lambda(t) \equiv \Lambda$ constant, the critical value $\overline{\Lambda} \approx 250.88$ (day^{-1});
- When $\Lambda(t) = \sum_{k=0}^{+\infty} \tau \Lambda^{\text{per}} \delta_{k\tau}$ with period $\tau = 10$, the critical value of Λ^{per} is $\overline{\Lambda}^{\text{per}} \approx 255.15$ (day^{-1}).

We can see that $\overline{\Lambda}$ and $\overline{\Lambda}^{\text{per}}$ are consistent. We also present numerical simulations in both cases with the same total amount of sterile males released where $\Lambda^{\text{per}} = \Lambda = 300$. The densities of sterile males in both cases are shown in Figure 5.7. We obtained in Figure 5.8 that in both cases, the wild mosquito population reaches elimination at time $t \approx 300$. Again we can see that the two strategies provide the same performance.

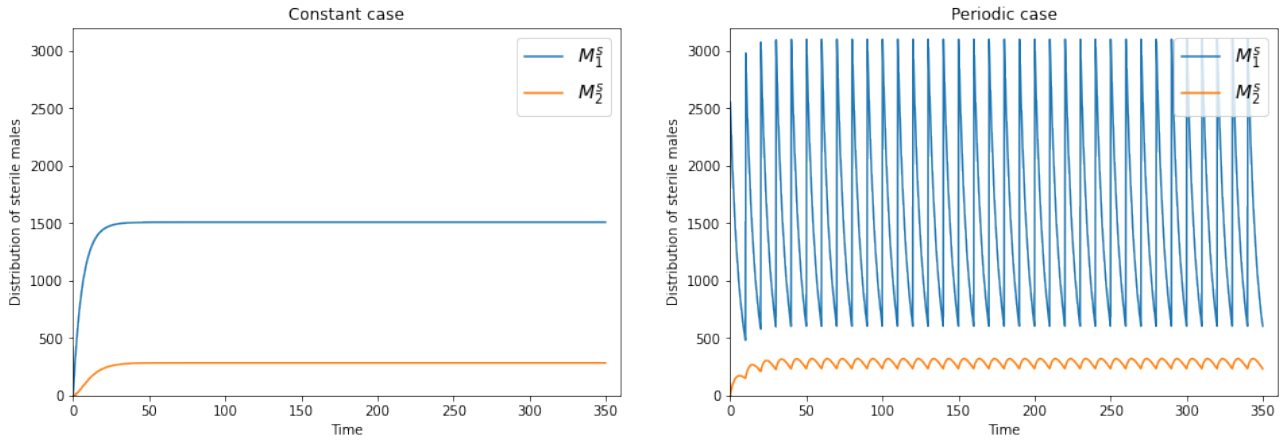

Figure 5.7 – Densities of M_1^s and M_2^s in both cases. *Left:* constant continuous releases with $\Lambda = \overline{\Lambda} = 250.88$ (day^{-1}), *Right:* periodic impulsive releases with $\Lambda^{\text{per}} = \overline{\Lambda}^{\text{per}} = 255.15$ (day^{-1}).

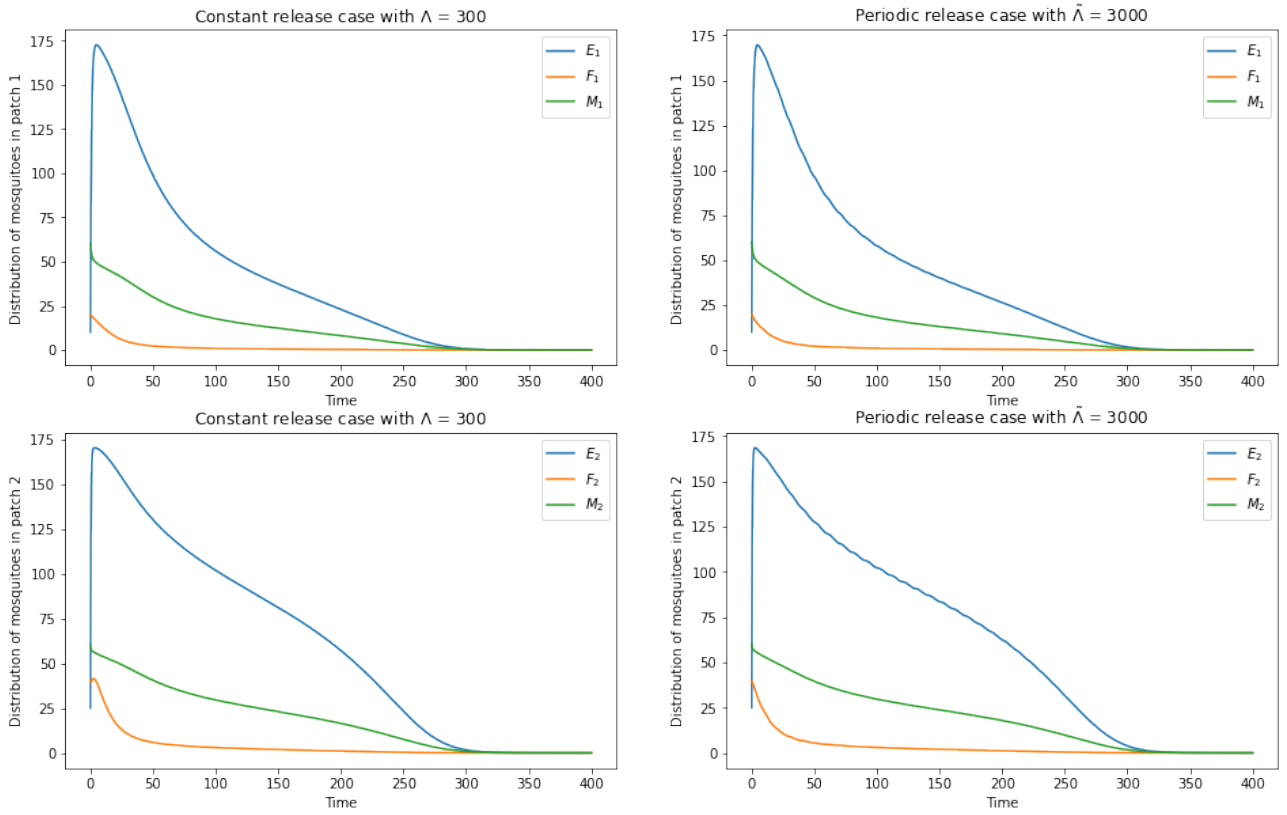

Figure 5.8 – Densities of wild mosquitoes in two patches in both cases. *Left:* constant continuous release with $\Lambda = 300$ mosquitoes released per day, *Right:* periodic impulsive releases with $\tau\Lambda^{\text{per}} = 3000$ mosquitoes released at the beginning of each time period.

5.7 Discussion and conclusion

The existence of some hidden areas (e.g. crab burrows) that can not be accessed by the SIT hinders the population from reaching elimination. Without the implementation of this technique, Theorem 5.3.1 showed that the wild populations in both areas are persistent and converge towards the unique positive equilibrium (see Figure 5.3a) and are independent of the diffusion rates between them. The main results obtained in the present work indicated that with a sufficient number of sterile males released, the SIT succeeds in driving both sub-populations to extinction. We investigated both continuous constant releases and impulsive periodic releases in Theorem 5.4.1. The two strategies provided almost similar performance but the periodic release is more realistic in practice. The idea in our proof can also be used to design a feedback release strategy and this could be studied in future works.

The results also pointed out that the critical numbers of released sterile males are monotone with respect to the biological parameters of the population (see Section 5.5.2). A population with a larger birth rate of wild mosquitoes and a bigger carrying capacity of the environment requires more sterile males to reach elimination. A larger death rate in any compartment of the wild mosquitoes reduces this critical value, and on the contrary larger death rate for the sterile males increases this value.

Moreover, the critical number of sterile males also depends on the diffusion rates between the treated area and the inaccessible zone. More precisely, if the diffusion rates are large, this system approaches the case when there is no separation between two sub-populations (see Theorem 5.5.1). Numerically, we showed that the larger the values of diffusion rates, the smaller the threshold we need to exceed to obtain elimination (see Figure 5.6). This also showed that when the movement is at a low level, the leak of wild mosquitoes from the inaccessible area impedes the eradication in the treated zone and it requires a large number of sterile males to break through this obstacle. In practice, this could be an unrealistic amount of sterile mosquitoes. It is not surprising that the scenario with larger diffusion between two areas is better since more sterile males can arrive at the unreachable zone.

Part III

Model calibration: A multi-scale approach

Chapter 6

Unveiling Mosquito Dynamics through a Mechanistic-Statistical Framework: Mark-Release-Recapture Analysis

This chapter is a joint work with Lionel Roques, Olivier Bonnefon, Luis Almeida and Réné Gato in the framework of an interdisciplinary secondment of the MathInParis2020 doctoral programs.

Abstract. Control of mosquito populations recently become a significant task worldwide to protect humans from many mosquito-borne diseases. Biological controls relying on releases of modified mosquitoes to reduce the reproduction and vectorial capacity of the wild population are studied widely due to their sustainability. The mark-release-recapture (MRR) experiment is an essential technique to examine the results of the controls which involves marking the released individuals, releasing them into the population, and then determining the ratio (proportion of marked to unmarked animals) of the population when individuals are captured at a later date. The dispersal can also be examined by setting up traps at different positions in the study zone. We develop in the present work a method to estimate the biological parameters of mosquitoes from MRR data of population density. An individual-based model is built considering some specific characteristics of mosquitoes in MRR experiments to study the dynamics of each individual. We derive a reaction-diffusion model to describe the dynamics in the population scale where we impose the same parameters as in the individual scale. We propose a mechanistic-statistical approach to estimate parameters and validate our method with simulated data. We provide interesting insights on dispersal as well as survival and capture effects for the real data.

6.1 Introduction

Mosquitoes are the primary arthropod vectors of human disease globally, transmitting malaria, lymphatic filariasis, and arboviruses such as dengue and the Zika virus. Existing treatments are only symptomatic, and there are no specific vaccines or drugs available for most of these diseases. In such conditions, the main form of prevention is to focus on the control of the mosquito population. Due to the limitations of classical insecticide-based controls, there has been an increasing necessity to develop innovative strategies that are more sustainable and eco-friendly [2], [29]. Among these alternative methods, biological controls such as the sterile insect technique (SIT), the release of mosquitoes carrying a dominant lethal (RIDL), or Wolbachia-based strategies require the release of large numbers of mosquitoes that are either sterile or unable to transmit disease. Knowledge about ecological parameters of released insects, such as the dispersal and survival dynamics in the field, may provide significant aid in designing more effective vector control strategies.

Mark-release-recapture (MRR) experiments applied to animal populations allow researchers to estimate population densities and key demographic parameters including survival rates, longevity, and emigration rates [60], [187]. In the case of the control method using releases of mosquitoes, the MRR technique plays an important role in examining the efficiency and designing release protocols. Marking released mosquitoes allows researchers to keep track of and study the fitness of individuals under field conditions. The survival and dispersal information that MRR experiments provide can indicate better timelines and positions for releases. However, mosquito MRR experiments have some specific limitations (see [187], [213]) such as marking difficulty due to small individual sizes, short lifespan under natural conditions, low recapture rate often ranging from 5 to 10% [85], and removal of individuals due to capturing. These restrictions hinder many models that consider multiple captures and reduce the accuracy of the well-known Lincoln-Petersen index [187] for abundance estimation. To overcome these obstacles, various works in the literature have developed estimation methods for ecological parameters of

mosquitoes from MRR experiments using both deterministic models and Bayesian models (see [48], [57], [213] and references therein).

On the other hand, the data collected from MRR experiments are commonly at the level of population density, so they cannot be applied directly at the individual level. Our idea of breaking through the limitations of mosquito MRR analysis is to study the dynamics of released mosquitoes by tying together two modeling frameworks for population dynamics: an individual-based model (IBM) and a reaction-diffusion model describing population densities. The question of the relationship between deterministic population models and individual-based approaches has been studied in the literature [76], [223]. The difficulty of combining these two frameworks lies in the difference between the timescales of population and individual behaviors. In the present work, we derived a reaction-diffusion model mathematically from the stochastic rules defining the individual-based model.

IBMs describe all individuals in a population as individual entities and consider the stochastic nature of processes. These models also allow accounting for differences among individuals [65]. In the mosquito context, we derive an individual-based model based on a stochastic process that expresses the movement of a mosquito. The survival rate, in terms of life duration, and the capturing rate are described explicitly as random variables, knowing the fact that once collected at traps, the individuals do not survive for new releases. Different approaches have been used to analyze and calibrate IBMs [203], especially the Bayesian inference using a Particle Markov Chain Monte Carlo method was carried out in [115]. However, parameter inference of IBMs, in general cases, is not an easy task and often relies on manual tuning due to their complexity and stochastic nature. Since the outcome of simulations can vary significantly even with fixed parameters, due to the inherent randomness in individual actions and interactions, determining the optimal set of parameters that best explains observed data becomes a non-trivial task.

An effective way to describe the density of a population with dispersal properties is to use reaction-diffusion models. They can be derived mechanistically via individual movements which are based on random walks [208], [160]. So, by using this idea, we develop such a reaction-diffusion model from the individual-based model with the same ecological parameters imposed in the equation. Then, a mechanistic-statistical approach can be applied to estimate reaction-diffusion parameters even with extremely sparse and noisy data [197]. This method has been used in several studies (see e.g., [221], [195], [196]) to estimate parameters and states of models built on deterministic and stochastic differential equations based on coupling (a) the mechanistic vision of the equations and (b) the statistical vision of observation data. In the present work, we apply this method to both the simulated data and real data from biologists. The estimation obtained from the simulated data generated by the individual-based model validates the accuracy of the mechanistic-statistical method. Then, by applying this approach to the real data, we provide some insights about survival and dispersal of released mosquitoes. Our models and techniques can be used to investigate the mark-release-recapture data in other contexts.

The remainder of this paper is organized as follows: Section 6.2 provides details of the mosquito MRR experiments as well as describes the models we have developed to exploit the data. The mechanistic-statistical approach for our models is described precisely in 6.2.4. Section 6.3 provides the main results obtained in the present work. The validation of our method with simulated data is presented in 6.3.1, and the application to the real data is shown in 6.3.2.

6.2 Material and Methods

6.2.1 Mark-release-recapture data

Aedes aegypti is the main dengue vector in the world. This mosquito lives close to people and has a notable preference for feeding on human blood. Their larvae can grow in a variety of water reservoirs connected to household activities [98]. These characteristics make it a perfect vector for the spread of the dengue virus, particularly in big cities with dense populations and a lot of artificial water containers. A progressive evaluation of the SIT from laboratory to big cages was conducted. This evaluation was important to systematically examine potential impacts on mosquito performance and survival under increasing natural conditions [87], [88]. A mark-release-recapture trial was carried out to evaluate the efficiency of the SIT to suppress a field population of *Aedes aegypti*, as a first step towards the development of a program with an SIT component against this major vector species.

The field trial was carried out in El Cano ($23°01'59.8''$ N, $82°27'32.''$W), an urban area of the southwestern suburb of Havana City, Cuba. The study sites were selected based on a predefined set of entomological, ecological, sociological, and logistical criteria [47], [161].

The Mark-Release-Recapture process is as follows:

- **Mark - Release:** There are four releases of sterile males carried out each week. In each release, 10,000 mosquitoes were marked with different colors respectively yellow, red, blue, and pink, and released at a fixed position.

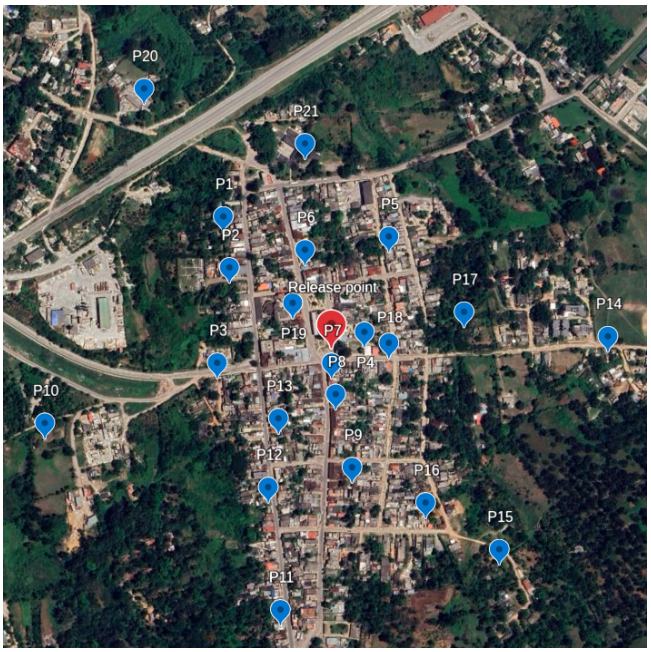

Figure 6.1 – Satellite images showing the study sites. The red mark shows the release position. The blue marks present the position of 21 traps set up for recapture. Photo via Google Earth.

- **Recapture:** There were 21 traps set up in different places within 400m around the release point to capture and count the number of marked mosquitoes each day. The traps were distributed in different rings with a radius of 50, 100, 150, 200, 250, 300, and 400m. The locations of traps P_i with $i = 1, 2, \ldots, 21$ according to the data (see Figure 6.2).

The numbers of mosquitoes captured each day in each trap were stored as tables in the datasets. There are four datasets corresponding to four different releases that were carried out. Our aim in the present work is to estimate some essential parameters from these datasets such as the **dispersal**, the **survival rate** as well as the **effects of recapture** on the released mosquitoes.

The landscape in which the experiments were carried on is made of various habitats that can deduce different dispersal rates of mosquitoes. To investigate the heterogeneity, we consider two cases. In the first case, we assume that the diffusion of mosquitoes is homogenous in the whole area, while in the second case, it performs differently in the urban area and the non-residential areas including forests, rivers, agricultural land, ... (see Figure 6.2).

6.2.2 Models

Microscopic Model

We describe the mosquito dynamics in the mark-release-recapture analysis by an individual-based model as below:

Movement. We assume that each mosquito follows an Itô diffusion process without drift. At the beginning of the release experiment, there are $N_0 = 10^4$ mosquitoes, and their positions $X_t^k \in \mathbb{R}^2$ at time t are governed by the following stochastic differential equation:

$$dX_t^k = \sigma(X_t^k)dB_t, \quad X_0^k = x_0, \tag{6.1}$$

where B is a 2-dimensional Brownian motion, and σ is a Lipschitz-continuous function on $\mathbb{R}^2$ that describes the local mosquito mobility, which may vary depending on local conditions.

Life expectancy and death times. In the absence of trapping, the mosquito's life expectancy is given by $1/\nu > 0$. Their death times follow an exponential distribution with parameter ν.

Trapping. The traps, indexed by $i = 1, \ldots, 21$, are located at positions $x_i \in \mathbb{R}^2$. For a mosquito with position X_t, the probability of being trapped follows an exponential distribution with parameter $f_i(X_t) = \gamma \exp(-\|X_t - x_i\|^2/R^2)$. This implies that the average duration before capturing at position x is $1/f_i(x)$. The constant $R > 0$ measures the rate at which the trap loses its effectiveness as one moves farther away from x_i.

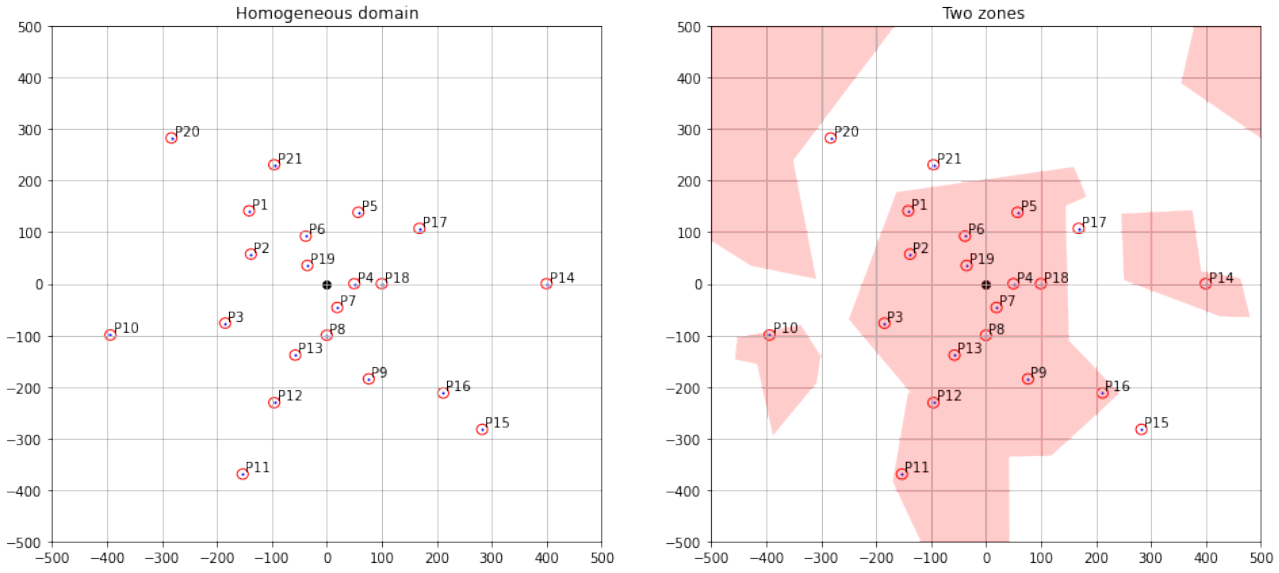

Figure 6.2 – Two types of domains are considered for study. *Left:* a homogeneous domain. *Right:* a domain consisting of two zones, urban (red) and non-residential (white) zones.

Macroscopic Model

Let's first consider a 1D model, discretized in time and space. We assume that the mosquito stays in place with a probability $N(x)$, moves to the left by a distance $\lambda > 0$ with a probability $M(x)$, or moves to the right by a distance $\lambda > 0$ with a probability $M(x)$, where $N + 2M = 1$. At each time step τ, it dies with a probability of $1 - e^{-\nu\tau}$ and gets captured with a probability of $1 - e^{-F(x)\tau}$. Let $p(t, x)$ be the probability that the mosquito is alive and not captured at position x at time t. We start by calculating $p(t + \tau, x)$:

$$p(t+\tau,x) = e^{-\nu\,\tau}\left[N\,p(t,x)\,e^{-F(x)\,\tau} + M(x-\lambda)\,p(t,x-\lambda)\,e^{-F(x-\lambda)\,\tau} + M(x+\lambda)\,p(t,x+\lambda)\,e^{-F(x+\lambda)\,\tau}\right].$$

Next, by Taylor's expansion we write:

$$M(x\pm\lambda)p(t,x\pm\lambda)e^{-F(x\pm\lambda)\tau} = M(x)p(t,x)e^{-F(x)\tau} \pm \lambda\frac{\partial(Mpe^{-F\tau})}{\partial x}(t,x) + \frac{\lambda^2}{2}\frac{\partial^2(Mpe^{-F\tau})}{\partial x^2}(t,x) + \mathcal{O}(\lambda^3),$$

which leads to:

$$p(t+\tau,x) = e^{-\nu\tau}\left[p(t,x)e^{-F(x)\tau} + \lambda^2\frac{\partial^2(Mpe^{-F\tau})}{\partial x^2}(t,x) + \mathcal{O}(\lambda^3)\right].$$

Again by Taylor's expansion, we have

$$\begin{aligned} p + \tau\frac{\partial p}{\partial t} &= (1-\nu\tau)\left[p(t,x)(1-F(x)\tau) + \lambda^2\frac{\partial^2(Mp(1-F\tau))}{\partial x^2}(t,x) + \mathcal{O}(\lambda^3) + \mathcal{O}(\tau^2)\right], \\ &= p - \nu\tau p - F(x)\tau p + \lambda^2\frac{\partial^2 Mp}{\partial x^2}(t,x) \quad - \lambda^2\tau\frac{\partial^2(MpF)}{\partial x^2}(t,x) + \mathcal{O}(\lambda^3) + \mathcal{O}(\tau^2). \end{aligned}$$

By dividing by τ and taking the limit as $\lambda \to 0$ and $\tau \to 0$, such that $\sigma^2(x) = \lim_{\tau\to 0,\lambda\to 0} 2M(x)\lambda^2/\tau$, we obtain:

$$\frac{\partial p}{\partial t} \approx \frac{\partial^2}{\partial x^2}\left(\frac{\sigma(x)^2}{2}p\right) - \nu p - F(x)p.$$

To extend this result to the two-dimensional space, let's now consider a 2D model, discretized in time and space. We assume that the mosquito moves to the left, right, up, or down by a distance $\lambda > 0$ with a probability $M(x_1, x_2)$ for each direction, or stays in place with a probability $N(x_1, x_2)$, where $N + 4M = 1$. At each time

step τ, it dies with a probability of $1 - e^{-\nu\tau}$ and gets captured with a probability of $1 - e^{-F(x_1,x_2)\tau}$. Let $p(t, x_1, x_2)$ be the probability that the mosquito is alive and not captured at position (x_1, x_2) at time t. We start by calculating $p(t + \tau, x_1, x_2)$:

$$\begin{aligned} p(t+\tau, x_1, x_2) = e^{-\nu\tau}\Big[& N(x_1, x_2)p(t, x_1, x_2)e^{-F(x_1,x_2)\tau} + \\ & M(x_1 - \lambda, x_2)p(t, x_1 - \lambda, x_2)e^{-F(x_1-\lambda,x_2)\tau} + \\ & M(x_1 + \lambda, x_2)p(t, x_1 + \lambda, x_2)e^{-F(x_1+\lambda,x_2)\tau} + \\ & M(x_1, x_2 - \lambda)p(t, x_1, x_2 - \lambda)e^{-F(x_1,x_2-\lambda)\tau} + \\ & M(x_1, x_2 + \lambda)p(t, x_1, x_2 + \lambda)e^{-F(x_1,x_2+\lambda)\tau}\Big]. \end{aligned}$$

Similarly, to the previous case, we obtain the formulation in 2D of the corresponding Fokker-Plank equation of $p(t, x)$ the product of the probability distribution function associated with the mosquito's position (conditioned on being alive and not captured) and the probability of being alive and not captured. According to the assumption we made in the microscopic model, we take $F(x) := \sum_{i=1}^{21} f_i(x)$.

$$\begin{cases} \dfrac{\partial p}{\partial t} &= \Delta\left(\dfrac{\sigma(x)^2}{2}p\right) - \nu\, p - p\displaystyle\sum_{i=1}^{21} f_i(x), \quad t > 0, \quad x \in \mathbb{R}^2, \\ p(0, x) &= \delta_{x=x_0}. \end{cases} \tag{6.2}$$

Next, we define the probability $\pi_i(t)$ as the probability that the mosquito has been trapped in the trap i before time t. It follows the following equation:

$$\pi_i'(t) = \int_{\mathbb{R}^2} f_i(x)\, p(t, x)\, dx. \tag{6.3}$$

Note that the expected mosquito population density $h(t, x)$ is the solution to the following equation:

$$\begin{cases} \dfrac{\partial h}{\partial t} &= \Delta\left(\dfrac{\sigma(x)^2}{2}h\right) - \nu\, h - h\displaystyle\sum_{i=1}^{21} f_i(x), \quad t > 0, \quad x \in \mathbb{R}^2, \\ h(0, x) &= N_0\, \delta_{x=x_0}. \end{cases} \tag{6.4}$$

6.2.3 Simulated data

From the microscopic model developed in 6.2.2, we generate datasets that mimic the real data and check if Θ is correctly identified by our inference procedure. We first fixed a parameter $\overline{\Theta} = (\overline{\sigma}, \overline{\nu}, \overline{\gamma})$ and used the individual-based model built in subsection 6.2.2 to generate simulated data $\{\tilde{y}_i^j,\ i = 1, \ldots, 21,\ j = 0, \ldots, 19\}$ by the following steps

- We create the maps of landscapes and positions of $n_P = 21$ traps $\omega_i = B_R(x_i)$, with $i = 1, \ldots, 21$ (see Figure 6.2). We fix $R = 10$m.
- We generate $N_0 = 10^4$ stochastic processes X_t^k with $k = 1, \ldots, N_0$, following (6.1) with n time steps, and the release point $x_0 = (0, 0)$.
- For each individual, we generate its lifetime as a random variable $T_k \sim Exp(\nu)$ with the life expectancy $\frac{1}{\nu}$.
- We calculate the distances between N_0 individuals and the centers of n_P traps at each time step, then store them in a matrix $dist$ of dimension $n_P \times n \times N_0$ where

$$dist(i, s, k) = \text{distance between } X_{s\Delta t}^k \text{ and } x_i.$$

- For the individual k, we take the **first** step s such that it belongs to some trap ω_i (that is, $dist(i, s, k) \leqslant R$). When a trajectory X_t belongs to some ω_i, the probability that the mosquito is captured between two

timesteps t and $t + dt$, conditionally on the fact that it has not been captured before is

$$\gamma \int_t^{t+dt} e^{-f_i(X_t)\,\tau}\, d\tau / e^{-f_i(X_t)\,t} = 1 - e^{-f_i(X_t)\,\Delta t} \approx f_i(X_t)\,\Delta t. \tag{6.5}$$

Take a number c uniformly distributed in $[0, 1]$, if c is smaller than the above probability and the time $s\Delta t$ is smaller than the individual's lifetime T_k, it is captured. If it is not captured in this step, we find the next step that satisfies this condition.

- We count the number of mosquitoes captured in trap ω_i on day j and obtain the simulated observation $\{\tilde{y}_i^j\}$.

6.2.4 Parameter estimation with the mechanistic-statistical approach

Observation process and likelihood

The dataset Obs $:= \{\hat{y}_i^j,\ i = 1, \ldots, 21,\ j = 0, \ldots, 19\}$ corresponds to the number of mosquitoes trapped in trap i during day j (i.e., for $t \in [j, j+1)$). Based on the microscopic model described above, each day, any mosquito is trapped in ω_i with a probability $\pi_i(j+1) - \pi_i(j)$. Thus, $\hat{y}_i^j$ can be viewed as the sum of N_0 independent Bernoulli trials. Since $\pi_i(j+1) - \pi_i(j) \mathcal{L} 1$ and $N_0 \gg 1$, the Poisson limit theorem leads to the following observation model for the number of mosquitoes captured in the trap i during day j:

$$Y_i^j | \Theta \sim \text{Poisson}\left[N_0(\pi_i(j+1) - \pi_i(j))\right], \tag{6.6}$$

with $\Theta := (\sigma(x), \nu, \gamma, R)$. Assuming that the observations are independent, conditionally on the diffusion-mortality-capture process, the likelihood associated with Θ is:

$$\begin{aligned} \mathcal{L}(\Theta) := P(\text{Obs}|\Theta) &= \prod_{j=0}^{30} \prod_{i=1}^{21} P(Y_i^j = \hat{y}_i^j) \\ &= \prod_{j=0}^{30} \prod_{i=1}^{21} \exp[-N_0(\pi_i(j+1) - \pi_i(j))] \frac{[N_0(\pi_i(j+1) - \pi_i(j))]^{\hat{y}_i^j}}{\hat{y}_i^j!}. \end{aligned} \tag{6.7}$$

Unknown parameters and prior distribution

Our goal is to estimate the vector of parameters Θ. Firstly, we assume that the function σ has the following specific form:

$$\sigma(x) = \int_{\mathbb{R}^2} J(x - y) \sum_{k=1}^{n_\sigma} \sigma_k \mathbf{1}_{y \in \Omega_k}\, dy, \tag{6.8}$$

where the sets Ω_k tile the entire plane $\mathbb{R}^2$ without any gaps or overlaps, $\sigma_k > 0$ $(k = 1, \ldots, n_\sigma)$ and J is a Gaussian kernel with fixed variance (standard deviation in meters, to be specified). In other words, σ is the regularization of a piecewise constant function.

Second, we note that, if $p(t, x)$ is approached by a spatially constant function $P(t)$ in a given trap ω_i, then $\pi_i'(t) = |\omega_i|/\gamma$ only depends on the product R^2/γ. Thus, the two parameters γ, R describing the capture are probably not identifiable, and one must be fixed. We fix here $R = 10$m.

Then, we define some a priori bounds for the parameters (prior distribution).

- Each σ_k follows a uniform prior distribution in (σ_m, σ_M). We know that $\sigma(x)^2/2 = D(x) \approx \lambda^2/(4\,\tau)$, with λ the distance in straight line crossed by the mosquito during a small time step τ. We take $\tau = 1/1440$ day, and for σ_m we assume that $\lambda = 0.1$m and for σ_M we assume that $\lambda = 10$m. This gives $\sigma_m = 2.7$ and $\sigma_M = 268.3$.

- The parameter ν follows a uniform prior distribution in (ν_m, ν_M). Using a minimal life expectancy of 1 day and a maximum life expectancy of 50 days, we get $\nu_m = 0.02$ and $\nu_M = 1$.

- The parameter γ follows a uniform prior distribution in (γ_m, γ_M). We assume that the mean duration in ω_i before capture is between 1 hour and 10 days. This gives $\gamma_m = 0.1$ and $\gamma_M = 24$.

Table 6.1 – Real values and parameter estimation in simulated datasets

Homogeneous case				
Parameters	σ		ν	γ
Real values	19.0000		0.1000	0.6667
Posterior median	17.5246		0.1378	0.8039
Heterogeneous case				
Parameters	σ_1	σ_2	ν	γ
Real values	50.0000	15.0000	0.1000	0.6667
Posterior median	48.8783	18.6424	0.1057	0.5953

Method of parameter estimation

We apply the mechanistic-statistical approach to estimate the parameter Θ.

Step 1: (mechanistic part) Considering the prior distribution defined above, for each Θ belonging to the prior distribution, we simulated the reaction-diffusion equation (6.2) to approximate the value of $p(t, x)$ using the finite element method carried out by a simulator in FreeFem++.

Step 2: (statistical part) Compute $\pi_i(j)$ by using (6.3). Base on the observation process described in 6.2.4, we approximate the likelihood function using the formula in (6.7).

The posterior distribution for Θ is provided by using Bayes' theorem, the posterior distribution satisfies

$$P(\Theta|\text{Obs}) = \frac{P(\text{Obs}|\Theta)\, P(\Theta)}{P(\text{Obs})} = \frac{\mathcal{L}(\Theta)\,\text{Prior}(\Theta)}{P(\text{Obs})}.$$

We draw a sample from the posterior distribution by an Monte-Carlo Markov Chain (MCMC) method with a Metropolis-Hasting algorithm.

6.3 Results and discussion

6.3.1 Parameters estimation for simulated datasets

As mentioned in the previous section, we consider two scenarios. In the homogeneous case, we assume that all individuals move with the same rule in the whole domain. In the heterogeneous case, there are two types of habitat: urban area and forest area which are denoted respectively Ω_1 (red) and Ω_2 (white) (see Figure 6.2). The diffusion rate in the latter case is heterogeneous where

$$\sigma(x) = \begin{cases} \sigma_1 & \text{if } x \in \Omega_1, \\ \sigma_2 & \text{if } x \in \Omega_2. \end{cases}$$

We generated for each case above one dataset and then applied our mechanistic-statistical method as in 6.2.4 to these datasets. We compare the estimators to the real values of parameters that we used to generate simulated data to assess the performance of our parameter estimation.

Estimations of Θ for both homogeneous and heterogeneous data are presented in Table 6.1. Here, we present an estimator using the posterior median $\overline{\Theta}$. Then we make a comparison to the real values of parameters that we used to generate the simulated datasets. We can observe that the estimators are relatively close to the real parameter Θ given the fact that the observations were only carried out in a subset $\bigcup_{1 \leqslant i \leqslant 21} \omega_i$. It is noteworthy that this subset only represents less than 1 % of the whole area.

Posterior distributions of parameters Θ in the homogeneous and heterogeneous are provided respectively in Figure 6.3 and 6.4.

With this fitness, we succeed in using a mechanistic-statistical approach to offer a possibility of Bayes inference for the individual-based model proposed in 6.2.2 using the population-scale data. This shows that characteristics namely life duration and diffusion rate of mosquito individuals and the effect of capturing can be estimated even with extremely sparse data on the population density. In the next section, we may apply this approach to explore the characteristics of mosquitoes in the mark-release-recapture data provided in 6.2.1.

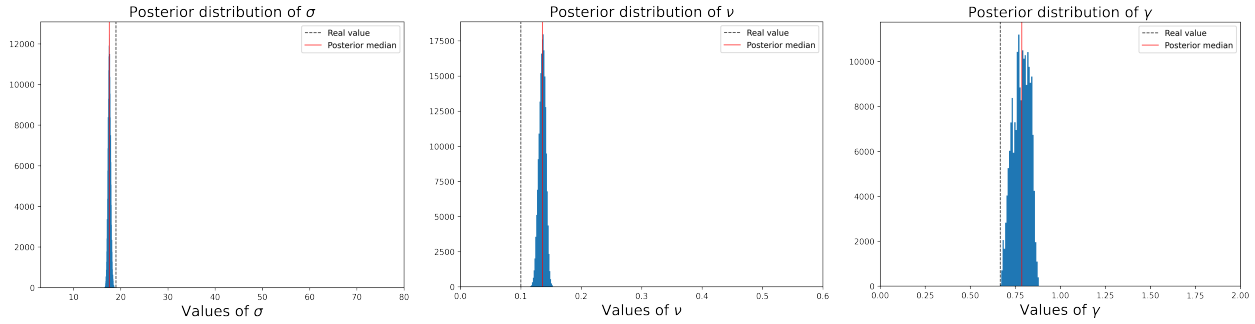

Figure 6.3 – Posterior distribution of Θ of the simulated data in the homogeneous case. Parameters σ [prior $\mathcal{U}(2.7, 268.3)$], ν [prior $\mathcal{U}(0.02, 1)$], γ [prior $\mathcal{U}(0.1, 24)$]. The real values of the parameters are given by the vertical dashed line.

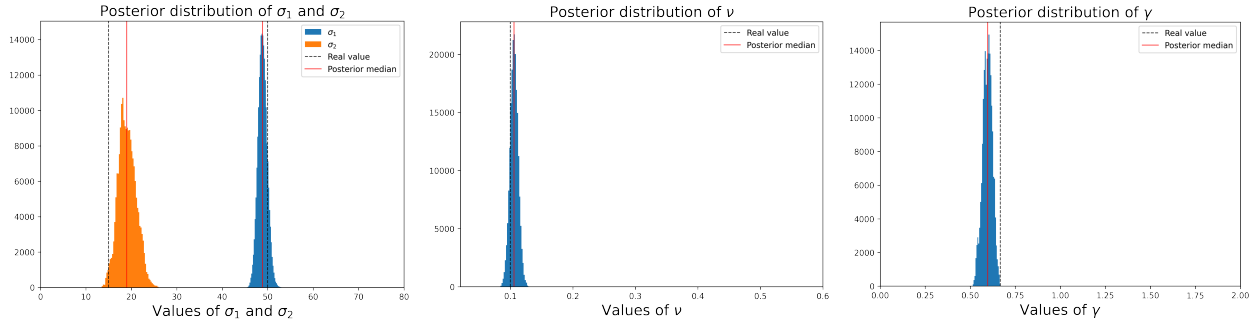

Figure 6.4 – Posterior distribution of Θ of the simulated data in the heterogeneous case. Parameters σ_1, σ_2 [prior $\mathcal{U}(2.7, 268.3)$], ν [prior $\mathcal{U}(0.02, 1)$], γ [prior $\mathcal{U}(0.1, 24)$].

Table 6.2 – Parameter estimation using posterior median of the combined dataset

Homogeneous case					
Parameters	σ		ν	γ	$-\ln \mathcal{L}(\Theta^*)$
Posterior median	63.2209		0.2163	0.1438	980.67
Heterogeneous case					
Parameters	σ_1	σ_2	ν	γ	$-\ln \mathcal{L}(\Theta^*)$
Posterior median	63.1686	67.4266	0.2138	0.1421	980.47

6.3.2 Parameter estimation for real datasets

Now, we apply our technique to the real datasets described in Section 6.2.1. For each dataset, we consider both the homogeneous model with 3 parameters $(\sigma,\ \nu,\ \gamma)$ and the heterogeneous model with 4 parameters $(\sigma_1,\ \sigma_2,\ \nu,\ \gamma)$ where we consider two different diffusion rates in the landscape.

Performance of parameter estimations

The parameter estimations are carried out for each dataset described in 6.2.1 and one dataset combined by these four datasets. We presented in Table 6.2 the estimation Θ for the combined dataset. The posterior distributions are shown in Figure 6.5. We can observe in the heterogeneous case that the distributions of parameters σ_1 and σ_2 almost overlap. The estimation by the posterior median of σ_1 and σ_2 are also very close (62.8119 and 62.3148) and the same as in the homogeneous case. It suggests that the diffusion rates in the two zones Ω_1 and Ω_2 are similar. The estimations for ν and γ in both cases also match each other.

Using the setting of parameters in the previous section, we obtain a mechanistic interpretation of some parameter values. From the homogeneous model, the parameter values corresponding to the posterior median of the combined dataset can be interpreted as follows:

- $\sigma = 63.2209$: the length of a the one-minute straight-line move is about $\lambda = 2.355$ (m);
- $\nu = 0.2163$: the life expectancy of a mosquito is about 5 days;
- $\gamma = 0.1438$: during each hour a mosquito rests inside the trap, there are $\gamma/24 \approx 0.6\%$ that it is captured.

Our estimations are relevant to what has been done by biologists in [88] using classical methods where the average life expectancy of sterile males was calculated from the probability of sterile male daily survival [152] and the flight behavior of released males was assessed as mean distance traveled and flight range [151]. They showed that the mean distance dispersed was 98.7m, the average life expectancy was around 4.4 days and the recapture rate was 0.54%.

Model comparison

We can compare the performance of the homogeneous and heterogeneous models by comparing the maximum values of the likelihood function defined in (6.7) in both models. From Table 6.1, we can see that the value of $-\ln \mathcal{L}(\Theta^*)$ in the heterogeneous case is slightly smaller than in the homogeneous case (980.47 vs 980.67) which implies that the maximum likelihood in the heterogeneous case is larger. Since, the heterogeneous model contains more parameters, to better compare these two models, we can use the Bayesian information criterion (BIC) in which a penalty term for the number of parameters in the model is introduced.

$$BIC = -2 \ln \mathcal{L} + n \ln N,$$

where $\mathcal{L}$ is the maximum likelihood, n is the number of parameters ($n = 3$ for the homogeneous model and $n = 4$ for the heterogeneous model), and $N = 420$ is the number of observations used in the computation of the likelihood (21 traps $\times$ 20 days).

For the combined dataset, the homogeneous model obtains a lower BIC (1979.5 vs 1985.1), indicating that the heterogeneous case does not provide a better fit than the homogeneous model. Moreover, the estimated values of σ_1 and σ_2 in the heterogeneous case are very close indicating that the diffusion in the study area is likely homogeneous.

Simulation results

With the parameters estimated in the previous section, we can provide a simulation of mosquito dynamics that can not be observed by the data by solving numerically the reaction-diffusion model derived in 6.2.2. The simulations are carried out in the domain $\Omega = (-500, 500) \times (-500, 500)$. The initial number of sterile males released at the point $(0, 0)$ is $N_0 = 10^4$.

We present in Figure 6.6 the dynamics in the heterogeneous case with parameters $\sigma_1 = 63.1686$, $\sigma_2 = 67.4266$, $\nu = 0.2138$, $\gamma = 0.1421$ estimated in the previous section. We observe that after one day, the mosquitoes almost die out since the density is smaller than 1 almost everywhere (see Figure 6.6b). We can see the heterogeneity of the population density in Figures 6.6d-6.6f, but the population almost died before reaching the second zone Ω_2.

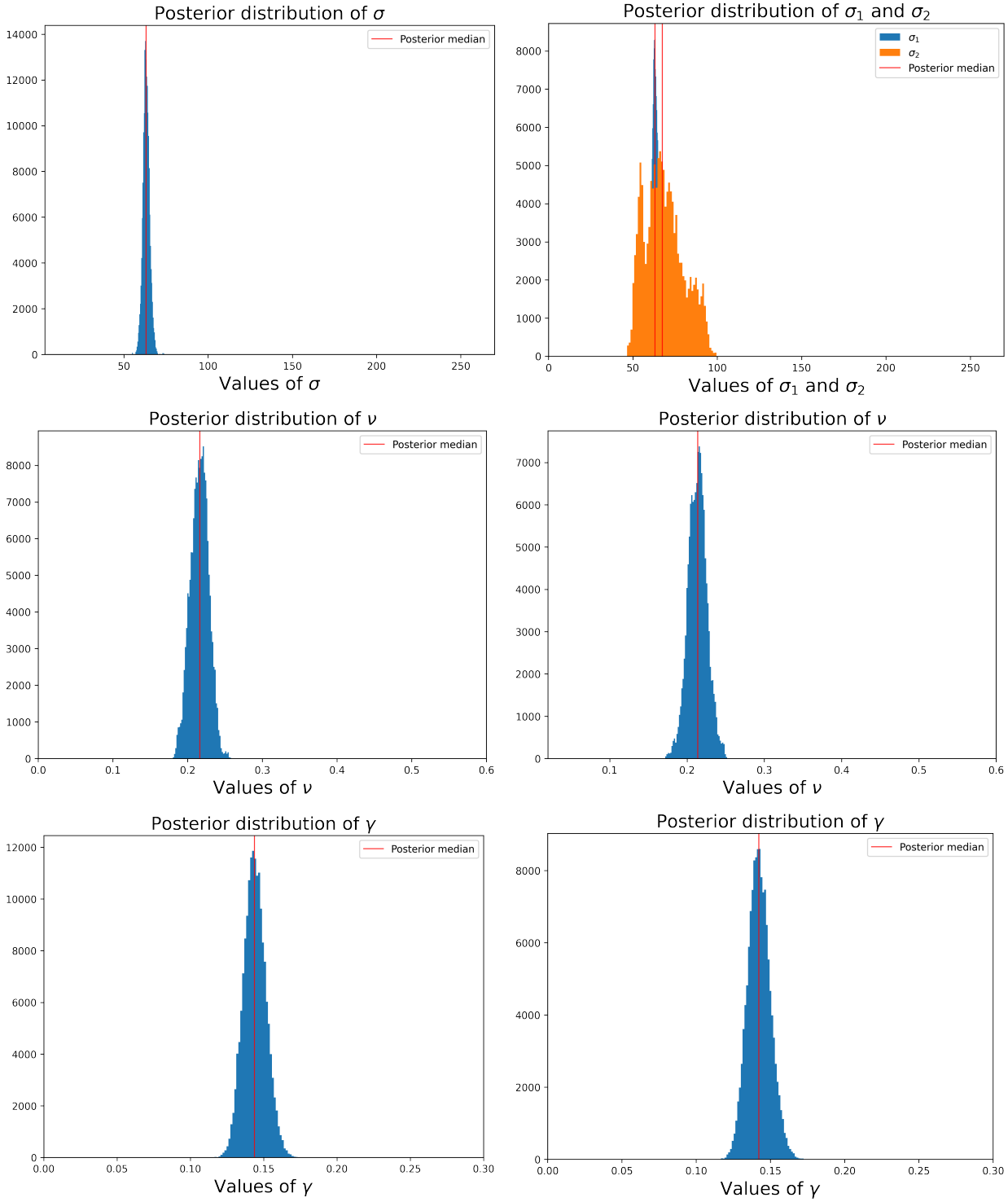

Figure 6.5 – Posterior distribution of Θ of the combined dataset in the homogeneous case (left) and heterogeneous case (right). Parameters σ [prior $\mathcal{U}(2.7, 268.3)$], ν [prior $\mathcal{U}(0.02, 1)$], γ [prior $\mathcal{U}(0.1, 24)$].

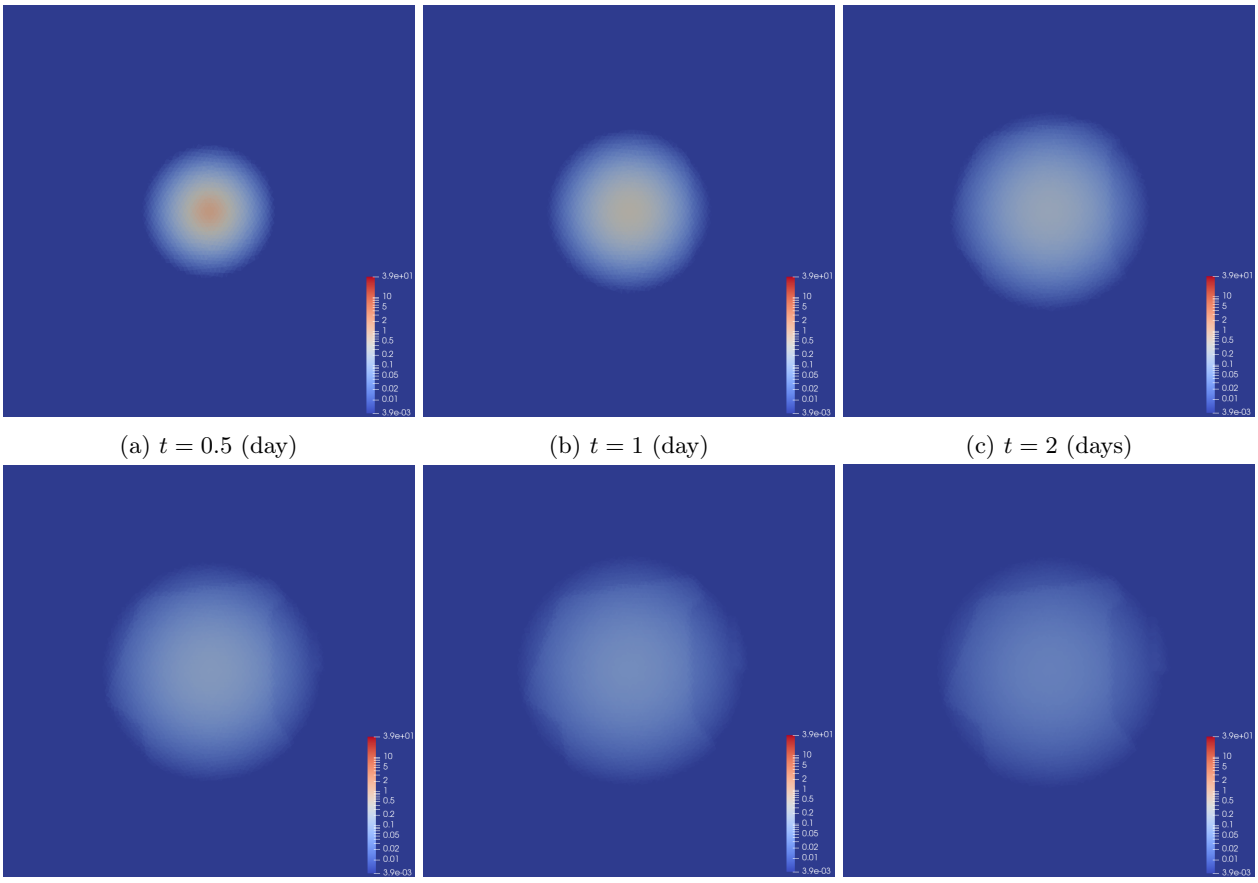

(a) $t = 0.5$ (day) (b) $t = 1$ (day) (c) $t = 2$ (days)

(d) $t = 3$ (days) (e) $t = 4$ (days) (f) $t = 5$ (days)

Figure 6.6 – Numerical simulation in the heterogeneous case with estimated parameter $\sigma_1 = 63.1686$, $\sigma_2 = 67.4266$, $\nu = 0.2138$, $\gamma = 0.1421$.

6.4 Conclusion

In the present work, we unveil the dynamics of mosquito populations in the mark-release-recapture experiments using individual and population modeling frameworks. An individual-based model was developed to describe the behavior of the population by the movement, the lifespan, and the effect of recapture of each individual (see Section 6.2.2). Then, we derived a differential equation population model from the previous model to better express the population densities provided by the mark-release-recapture (MRR) data (see Section 6.2.2). Then, we used a mechanistic-statistical approach for parameter estimations to deal with the heavy loss of information due to the observation process in the MRR experiments (see Section 6.2.4). A simulation study was carried out in Section 6.3.1 to assess the capability to estimate all parameters of the model. The performance of this study showed that our method gave a sufficiently accurate value for the parameters of the dispersal rate, lifespan, and recapture rate. Two kinds of landscape were studied in this paper to investigate the heterogeneity. In the homogeneous case, we assume all individuals move with the same rule in the whole space, while in the heterogeneous case, we assume that the dispersal rates are different in the urban and non-residential areas. The application of our method to real data described in Section 6.2.1 showed that the estimations of the life expectancy and the recapture rate are consistent in both cases, but the homogenous gave a better model for the dispersal estimation. It indicated that the movement of mosquitoes is likely the same in the whole region. Our estimations provided characteristics of *Aedes aegypti* mosquitoes which are relevant to the previous works using traditional approaches.

Conclusion

Summary and Discussion

The works gathered in this thesis studied various questions on two biological control methods of *Aedes* mosquito: the Sterile Insect Technique (SIT) and the population replacement technique using *Wolbachia*. All of these questions emerge from communication with entomologists and are motivated by the real challenges that arise in the application of these techniques in the field concerning the spatial distribution of the population. Various spatial models have been used to study these issues, giving rise to many interesting mathematical problems. Starting with reaction-diffusion models in Part I, we have studied the problem in both bounded domains and the whole space. Reaction-diffusion models provide a way to convert local assumptions on the movement, birth, and death of individuals into global conclusions about the persistence or extinction of populations and the coexistence of interacting species. In the context of mosquito control, we have investigated various conditions to guarantee the extinction of the population. Two important phenomena supported by reaction-diffusion models have been investigated in this thesis: the critical domain size problem and the propagation of wavefront.

In Chapter 2, an inhomogeneous Robin boundary condition was introduced to describe the inflow and outflow of individuals on the border of a bounded domain. We used phase portrait analysis to study the existence of equilibria and provided critical domain sizes that support the population replacement method. We conclude that large and well-isolated domains are better to guarantee the efficacy of the technique in the presence of migration on the boundary. The results obtained in this chapter is in one dimension and a natural continuation is the higher dimension problems. We will provide some perspectives on this direction in the latter of this chapter (see 6.4).

The next interesting phenomenon investigated in this thesis is the propagation of wavefront. The study of propagating solutions, or traveling waves gained much interest since the early 30's and is still an active field of research. In Chapter 3 and 4 of this thesis, we are interested in the existence of propagating solutions with forced speeds. This problem arose naturally in the application of releasing techniques for pest eradication where the releases are shifted in space with a certain speed. Existing results on reaction-diffusion models with forced speed are mostly based on the study of the generalized principal eigenvalue of an associated operator of the scalar model. The generalization of this approach to a partially degenerate system like our model remains challenging. In this thesis, we take advantages of the monotonicity of the system and provide sophisticated constructions of super- and sub-solutions. We emphasize that the constructions depend on the profiles of the release function that we designed as well as the geometries of the release areas. The releases we designed in 3 and 4 provided useful strategies but were still far from realistic protocols since the number of sterile males is finite and the release can only be carried out at some specific time during the release period. A more realistic strategy that could be investigated as a potential future direction is the impulsive releases over time (see 6.4).

Although reaction-diffusion models are a good way of modeling dispersal, their analysis becomes extremely complicated when modeling environmental heterogeneity. Discrete approaches offer a better and simpler way of modeling heterogeneity, especially when resources such as hosts and breeding sites are variable across regions. Part II of this thesis used such a discrete diffusion model to investigate the problem of inaccessibility of the SIT caused by spatial heterogeneity. A two-patch model with discrete diffusions was studied in which the release of sterile males was carried out in only one patch. The theory of a monotone dynamical system was applied to provide conditions on the number of sterile males to guarantee the global extinction of the whole system and examine how this number depends on the diffusion rate between two patches and other biological parameters. In Chapter 5, we explore both constant and impulsive release strategies. Numerical simulations show that the performance of these two strategies is likely the same, while the impulsive release is more realistic. As a potential continuation of this work, the control could be improved by using a feedback strategy and/or combining both constant and impulsive releases.

Potential Future Directions

Critical domain size problems in higher dimensions

The critical domain size for extinction versus persistence of population is a significant problem supported by reaction-diffusion models that have been studied widely in the literature (see [129, 153, 198] and references therein). In higher dimensions, the geometry of the domain has fundamental impacts on the qualitative behavior of solutions. When boundary conditions are hostile, the critical domain results have been provide for the following reaction-diffusion equation with a drift

$$\begin{cases} \partial_t p = \operatorname{div}(D\nabla p - ap) + f(p) & \text{in } (0,T)\times\Omega, \\ p = 0 & \text{on } (0,T)\times\partial\Omega, \end{cases}$$

with different geometries of Ω in $\mathbb{R}^n$ such as an n-hyperrectangle $\Omega = [0, L_1] \times \cdots \times [0, L_n]$, a ball $\Omega = B_R$, or even a more general domain $\Omega \subset \mathbb{R}^n$ with a smooth boundary (see [81]). However, treating other kinds of boundary conditions remains very challenging. The study of phase portrait analysis used in Chapter 2 of this thesis can be combined with the ideas in [81] to generalize the results to other kinds of boundary value problems.

On the other hand, more realistic boundary conditions can be derived to study the persistence and extinction of the population in presence of migration on the boundary. The impacts of domain geometry on the population dynamics in the "core area" of the domain should be examined carefully to derive an appropriate boundary condition. We refer to [75, 49, 50] for the studies of *how habitat edges change species interactions*. A possible and natural generalization of the Robin boundary condition introduced in Chapter 2 is to consider the heterogeneity in the density around the boundary. More precisely, we can consider on $\partial\Omega$,

$$\partial_\nu p = -D_b(p - p^{\text{ext}}),$$

with $\partial\Omega = \bigcup_{i=1,\dots,n} \partial\Omega_i$, and $p^{\text{ext}} = p_i^{\text{ext}}$ on $\partial\Omega_i$.

Impulsive reaction-diffusion models: a more realistic scenario

In practice, biological control agents (e.g. sterile males, *Wolbachia*-carrying mosquitoes) are released impulsively. A possible way to model the population dynamics with impulsive release is to use the impulsive reaction-diffusion model. This equation was proposed in [130] for species with distinct reproductive and dispersal stages. They can be presented in the form of a discrete-time recursion

$$\begin{cases} \partial_t u^{(k)} = \operatorname{div}\left(D\nabla u^{(k)} - a u^{(k)}\right) + f(u^{(k)}) & \text{for } (t,x)\in(0,1]\times\Omega, \\ u^{(k)}(0,x) = g(N_k(x)) & \text{for } x\in\Omega, \\ N_{k+1}(x) := u^{(k)}(1,x) & \text{for } x\in\Omega, \end{cases}$$

with Ω bounded or $\Omega = \mathbb{R}^n$. The population density at the beginning of the period k is denoted by $N_k(x)$. Various works in the literature have studied this kind of model regarding the critical size problems (see e.g. [81]), and the propagation phenomena (see e.g. [131, 219, 130, 80]). We remark that many results of these impulsive models are verified for a class of reaction-diffusion models.

In the context of this thesis, we can consider the impulsive release by taking

$$u^{(k)}(0,x) = u^{(k-1)}(1,x) + \Lambda_k \quad \text{for } x\in\Omega,$$

with Λ_k is the number of mosquitoes released in the period k. The population dynamics in each period can be studied by generalizing the method implemented in this thesis. The recurrence relation needs to be investigated to study the dynamics of the system over time.

Appendices

Appendix A

Monotonicity

We provide in this part some results on monotonicity of the dynamical systems that are used to describe the dynamic of mosquito population (see (1.1), (1.6)).

First, we present the definition of a cooperative and competitive system [191]

Definition A.0.1. *Consider the autonomous system of ordinary differential equation*

$$\dot{\mathbf{u}} = \mathbf{f}(\mathbf{u}), \tag{A.1}$$

with $\mathbf{u} = (u_1, \ldots, u_n) \in \mathbb{R}^n$ *and* $\mathbf{f} = (f_1, \ldots, f_n) : \mathbb{R}^n \to \mathbb{R}^n$ *is a* $\mathcal{C}^1$ *vector function. System* (A.1) *is called cooperative if*

$$\frac{\partial f_i}{\partial x_j}(x) \geqslant 0 \quad i \neq j, \quad x \in D,$$

and it is a competitive system if

$$\frac{\partial f_i}{\partial x_j}(x) \leqslant 0 \quad i \neq j, \quad x \in D,$$

with D *is a convex subset in* $\mathbb{R}^n$.

A.1 The stage-structured system

To be more reader-friendly, we recall the system (1.1) below

$$\begin{aligned} \dot{E}(t) &= bF\left(1 - \frac{E}{K}\right) - (\nu_E + \mu_E)E, \\ \dot{F}(t) &= \rho\nu_E\Gamma(M)E - \mu_F F, \\ \dot{M}(t) &= (1-\rho)\nu_E E - \mu_M M, \end{aligned} \tag{A.2}$$

with

$$\Gamma(M) \equiv 1 \text{ (monostable case)}, \qquad \Gamma(M) = 1 - e^{-\gamma M} \text{ (bistable case)}.$$

We can easily check that system (A.1) is cooperative in $[0, K] \times \mathbb{R}^2$. Indeed, denote $\mathbf{u} = (E, F, M)$ and

$$\mathbf{f} = \begin{pmatrix} f_1(E,F,M) \\ f_2(E,F,M) \\ f_3(E,F,M) \end{pmatrix} = \begin{pmatrix} bF\left(1 - \frac{E}{K}\right) - (\nu_E + \mu_E)E, \\ \rho\nu_E\Gamma(M)E - \mu_F F, \\ (1-\rho)\nu_E E - \mu_M M, \end{pmatrix}.$$

Then, we have

$$\frac{\partial f_1}{\partial F} = b\left(1 - \frac{E}{K}\right) > 0, \quad \frac{\partial f_1}{\partial M} = 0,$$

$$\frac{\partial f_2}{\partial E} = \rho\nu_E\Gamma(M) > 0, \quad \frac{\partial f_2}{\partial M} = \begin{cases} 0 & \text{in the monostable case,} \\ \rho\nu_E\gamma E e^{-\gamma M} > 0 & \text{in the bistable case,} \end{cases}$$

$$\frac{\partial f_3}{\partial E} = (1-\rho)\nu_E > 0, \quad \frac{\partial f_3}{\partial F} = 0.$$

By applying [191, Proposition 1.1, Chapter 3] on cooperative system, we can show that system (A.1) is order-preserving. Consider the orders defined by the following positivity

Definition A.1.1. *A matrix $A \in \mathcal{M}^{m\times n}$ is called non-negative, denote $A \geqslant 0$, if all of its entries are non-negative.*
It is called positive, denote $A > 0$, if if is non-negative and there is at least one positive entry.
It is called strictly positive, denote $A \gg 0$, if all of its entries are strictly positive.

Then, the following result presents the monotonicity of system (A.1).

Proposition A.1.1. *Consider two trajectories $\mathbf{u}_1 = (E_1, F_1, M_1)$ and $\mathbf{u}_2 = (E_2, F_2, M_2)$ of system (A.2) resulting from initial data $\mathbf{u}_1(0)$ and $\mathbf{u}_2(0)$ respectively. Let $<_r$ denote any one of the relations $\leqslant$, $<$, $\ll$ defined in Definition A.1.1. If $\mathbf{u}_1(0) <_r \mathbf{u}_2(0)$, then $\mathbf{u}_1 <_r \mathbf{u}_2$.*

Next, we show that $[0, K] \times \mathbb{R}^2_+$ is the positively invariant set of system (A.2).

Proposition A.1.2. *The set $[0, K] \times \mathbb{R}^2_+$ is invariant, i.e. if $0 \leqslant E^0 \leqslant K$, $0 \leqslant F^0$, $0 \leqslant M^0$ then for all $t > 0$, the solution of (A.2) verifies $0 \leqslant E(t) \leqslant K$, $0 \leqslant F(t)$, $0 \leqslant M(t)$.*

Proof. Due to Proposition A.1.1, we deduce that if $(E(0), F(0), M(0)) \geqslant 0$ then for all $t > 0$, one has $(E(t), F(t), M(t)) \geqslant 0$.

It remains to show that $E(t) \leqslant K$ for all $t \geqslant 0$. Indeed, assume that there exists a time $t_0 > 0$ such that $E(t_0) > K$. Since $0 \leqslant E(0) \leqslant K$, and E is continuous over time, we can deduce that there exists a time $t_1 \in (0, t_0)$ such that $E(t_1) > 0$ and $\dot{E}(t_1) > 0$. However, we also have $\dot{E}(t_1) = bF(t_1)\left(1 - \dfrac{E(t_1)}{K}\right) - (\nu_E + \mu_E)E(t_1) < 0$. This contradiction proves the result. □

By applying the comparison lemma for cooperative system which is known as Kamke's lemma [59] or Chaplygin's lemma [55], we obtain the following result

Proposition A.1.3. *Consider a trajectory $\mathbf{u} = (E_1, F_1, M_1)$ of system (A.2) resulting from an intial datum $\mathbf{u}^0$. Then, in the invariant set $[0, K] \times \mathbb{R}^2_+$, system (A.2) is monotone in the sense that if a vector function $\mathbf{v}(t)$ satisfies a differential inequality $\dot{\mathbf{v}} \leqslant \mathbf{f}(\mathbf{v})$, and $\mathbf{v}(0) \leqslant \mathbf{u}(0)$, then we have $\mathbf{v}(t) \leqslant \mathbf{u}(t)$ for all $t > 0$.*

We also recall system (1.4) modeling the population dynamics with the SIT

$$\begin{aligned}
\dot{E}(t) &= \beta F\left(1 - \frac{E}{K}\right) - (\nu_E + \mu_E)E,\\
\dot{F}(t) &= \rho\nu_E E\frac{M}{M + \gamma_s M_s}\Gamma(M + \gamma_s M_s) - \mu_F F,\\
\dot{M}(t) &= (1-\rho)\nu_E E - \mu_M M,\\
\dot{M}_s(t) &= \Lambda(t) - \mu_s M_s,
\end{aligned} \tag{A.3}$$

with $\Lambda(t)$ is the number of sterile males release at time t. We also have that $[0, K] \times \mathbb{R}^3_+$ is the an invariant set of (A.3). We emphasize that this system is not cooperative. Indeed, if we denote $\mathbf{U} = (E, F, M, M_s)$ and

$$\mathbf{g}(\mathbf{U}) = \begin{pmatrix} g_1(\mathbf{U})\\ g_2(\mathbf{U})\\ g_3(\mathbf{U})\\ g_4(\mathbf{U})\end{pmatrix} = \begin{pmatrix} \beta F\left(1 - \frac{E}{K}\right) - (\nu_E + \mu_E)E,\\ \rho\nu_E E\dfrac{M}{M + \gamma M_s}\Gamma(M + \gamma M_s) - \mu_F F,\\ (1-\rho)\nu_E E - \mu_M M,\\ \Lambda(t) - \mu_s M_s\end{pmatrix}.$$

- In the monostable case, $\dfrac{\partial g_2}{\partial M_s} = -\dfrac{\gamma\rho\nu_E EM}{(M + \gamma M_s)^2} \leqslant 0$
- In the bistable case

$$\frac{\partial g_2}{\partial M_s} = \frac{\gamma\rho\nu_E EM}{M + \gamma M_s}\left[e^{-(M+\gamma M_s)} - \frac{1 - e^{-(M+\gamma M_s)}}{M + \gamma M_s}\right].$$

Consider function $\psi(x) = xe^{-x} + e^{-x} - 1$, then we have $\psi(0) = 0$, and $\psi'(x) = -xe^{-x} \leqslant 0$ for any $x \geqslant 0$. Hence, $\psi(M + \gamma M_s) \leqslant 0$ for any $M \geqslant 0,\ M_s \geqslant 0$. We deduce that $\dfrac{\partial g_2}{\partial M_s} \leqslant 0$ in $[0, K] \times \mathbb{R}^3_+$.

However, by changing the variable to $\widetilde{\mathbf{u}} = (E, F, M, -M_s)$, we can write system (A.3) as follows

$$\widetilde{\mathbf{u}} = \widetilde{\mathbf{f}}(\widetilde{\mathbf{u}}),$$

and this system is cooperative. Thus, the similar comparison result as Proposition A.1.1 is applied to system (A.3) with the order defined as below

Definition A.1.2. *For any vectors* $\mathbf{u}, \mathbf{v} \in \mathbb{R}^4$*, we define an order* $\preceq$ *such that* $\mathbf{u} \preceq \mathbf{v}$ *if and only if*

$$\begin{cases} u_i \leqslant v_i & \text{for } i \in \{1,2,3\}, \\ u_i \geqslant v_i & \text{for } i = 4. \end{cases}$$

Moreover, we write $\mathbf{u} \prec \mathbf{v}$ *if* $\mathbf{u} \preceq \mathbf{v}$ *and* $\mathbf{u} \neq \mathbf{v}$.

A.2 The replacement system

We recall system (1.6) modeling the dynamics of *Wolbachia*-infected and uninfected mosquitoes.

$$\begin{aligned} \dot{n}_i(t) &= b_i n_i \left(1 - \frac{n_i + n_u}{K}\right) - d_i n_i + \Lambda(t), \\ \dot{n}_u(t) &= b_u n_u \left(1 - \frac{n_i + n_u}{K}\right)\left(1 - s_h \frac{n_i}{n_i + n_u}\right) - d_u n_u, \end{aligned} \tag{A.4}$$

This system is positively invariant in the set $D = \{(n_i, n_u) \in \mathbb{R}^2_+ \mid (n_i + n_u) \leqslant K\}$. We can check that system (A.4) is competitive. Indeed, if we denote

$$\begin{aligned} f_i(n_i, n_u) &= b_i n_i \left(1 - \frac{n_i + n_u}{K}\right) - d_i n_i + \Lambda(t), \\ f_u(n_i, n_u) &= b_u n_u \left(1 - \frac{n_i + n_u}{K}\right)\left(1 - s_h \frac{n_i}{n_i + n_u}\right) - d_u n_u, \end{aligned}$$

then in D we have

$$\frac{\partial f_i}{\partial n_u} = -\frac{b_i n_i}{K} \leqslant 0,$$

and

$$\frac{\partial f_u}{\partial n_i} = -\frac{b_u n_u}{K}\left(1 - s_h \frac{n_i}{n_i + n_u}\right) - \frac{b_u n_u^2}{(n_i + n_u)^2}\left(1 - \frac{n_i + n_u}{K}\right) \leqslant 0.$$

The competitive dynamical system preserves the unrelated properties: if two initial data $(n_i^1, n_u^1)(0)$ and $(n_i^2, n_u^2)(0)$ are unrelated, that is, neither $(n_i^1, n_u^1)(0) \geqslant (n_i^2, n_u^2)(0)$ nor $(n_i^1, n_u^1)(0) \leqslant (n_i^2, n_u^2)(0)$, then $(n_i^1, n_u^1)(t)$ and $(n_i^2, n_u^2)(t)$ are also not related.

Appendix B

Asymptotic limit of a Robin boundary problem

B.1 Formulation of the problem

In [201], the authors reduced a 2-by-2 reaction-diffusion system of Lotka-Volterra type modeling two biological populations to a scalar equation as in (2.1) when the fecundity rate is very large. This limit problem was first proved in the whole domain. In the present study, we prove the limit for a system in a bounded domain with inhomogeneous Robin boundary conditions. In the following part, we recall the necessary assumptions and present results about this problem.

Although the main result of the paper is in one-dimensional space, the following result holds in any dimension d. Let $\Omega \subset \mathbb{R}^d$ be a bounded domain and consider the initial-boundary-value problem (B.1) depending on parameter $\epsilon > 0$,

$$\partial_t n_1^\epsilon - \Delta n_1^\epsilon = n_1^\epsilon f_1^\epsilon(n_1^\epsilon, n_2^\epsilon), \qquad (t,x) \in (0,T)\times\Omega, \tag{B.1a}$$

$$\partial_t n_2^\epsilon - \Delta n_2^\epsilon = n_2^\epsilon f_2^\epsilon(n_1^\epsilon, n_2^\epsilon), \qquad (t,x) \in (0,T)\times\Omega, \tag{B.1b}$$

$$n_1^\epsilon(0,x) = n_1^{\text{init},\epsilon}(x), \quad n_2^\epsilon(0,x) = n_2^{\text{init},\epsilon}(x), \qquad x \in \Omega, \tag{B.1c}$$

$$\frac{\partial n_1^\epsilon}{\partial \nu} = -D(n_1^\epsilon - n_1^{\text{ext},\epsilon}), \quad \frac{\partial n_2^\epsilon}{\partial \nu} = -D(n_2^\epsilon - n_2^{\text{ext},\epsilon}), \qquad (t,x) \in (0,T)\times\partial\Omega, \tag{B.1d}$$

where we assume that $f_1^\epsilon, f_2^\epsilon$ are smooth enough to guarantee existence and uniqueness of a classical solution for fixed ϵ. More precisely, the following assumptions are made:

Assumption B.1.1. (Initial and boundary conditions). *Assume that* $n_1^{\text{init},\epsilon}, n_2^{\text{init},\epsilon} \in L^\infty(\Omega)$ *with* $n_1^{\text{init},\epsilon}, n_2^{\text{init},\epsilon} \geqslant 0$ *and* $n_2^{\text{init},\epsilon}$ *is not identical to* 0.

$D > 0$ *is constant,* $n_1^{\text{ext},\epsilon} \geqslant 0, n_2^{\text{ext},\epsilon} > 0$ *do not depend on time* t *and position* x.

To study the limit problem, we define the "rescaled total population" n^ϵ and proportion p^ϵ, by

$$n^\epsilon := \frac{1}{\epsilon} - n_1^\epsilon - n_2^\epsilon, \quad p^\epsilon := \frac{n_1^\epsilon}{n_1^\epsilon + n_2^\epsilon}.$$

Next, we recall some assumptions that were proposed in [201] on the families of functions $(f_1^\epsilon, f_2^\epsilon)_{\epsilon>0}$ to study the convergence of p^ϵ when $\epsilon \to 0$

Assumption B.1.2. *Function* $f_1^\epsilon, f_2^\epsilon$ *are of class* $\mathcal{C}^2(\mathbb{R}^2_+\{0\})$*, and for* $i \in \{1,2\}$ *there exists* $F_i \in \mathcal{C}^2(\mathbb{R}^2)$ *(independent of* ϵ*) such that*

$$f_i^\epsilon(n_1^\epsilon, n_2^\epsilon) = F_i(n^\epsilon, p^\epsilon). \tag{B.2}$$

That is, we may write $f_i^\epsilon(n_1^\epsilon, n_2^\epsilon) = F_i\left(\frac{1}{\epsilon} - n_1^\epsilon - n_2^\epsilon, \frac{n_1^\epsilon}{n_1^\epsilon + n_2^\epsilon}\right)$ for $i \in \{1,2\}$.

Then, we can deduce that p^ϵ and n^ϵ satisfy system (B.3) as follows:
In $(0,T)\times\Omega$, we have

$$\partial_t n^\epsilon - \Delta n^\epsilon = -(\frac{1}{\epsilon} - n^\epsilon)\left[p^\epsilon F_1(n^\epsilon, p^\epsilon) + (1-p^\epsilon)F_2(n^\epsilon, p^\epsilon)\right], \tag{B.3a}$$

$$\partial_t p^\epsilon - \Delta p^\epsilon + \frac{2\epsilon A}{1-\epsilon n^\epsilon}\nabla p^\epsilon \cdot \nabla n^\epsilon = p^\epsilon(1-p^\epsilon)(F_1 - F_2)(n^\epsilon, p^\epsilon), \tag{B.3b}$$

on the boundary $(0,T)\times\partial\Omega$, we have

$$\frac{\partial n^\epsilon}{\partial \nu} = -D(n^\epsilon - n^{\text{ext},\epsilon}), \quad \frac{\partial p^\epsilon}{\partial \nu} = -D(p^\epsilon - p^{\text{ext},\epsilon})\frac{1-\epsilon n^{\text{ext},\epsilon}}{1-\epsilon n^\epsilon}, \tag{B.3c}$$

at time $t=0$, for any $x\in\Omega$, the initial data read

$$n^\epsilon(0,x) = n^{\text{init},\epsilon}(x), \quad p^\epsilon(0,x) = p^{\text{init},\epsilon}(x), \tag{B.3d}$$

where $(F_1-F_2)(n^\epsilon,p^\epsilon) = F_1(n^\epsilon,p^\epsilon) - F_2(n^\epsilon,p^\epsilon)$, and

$$n^{\text{init},\epsilon} := \frac{1}{\epsilon} - n_1^{\text{init},\epsilon} - n_2^{\text{init},\epsilon}, \quad p^{\text{init},\epsilon} := \frac{n_1^{\text{init},\epsilon}}{n_1^{\text{init},\epsilon}+n_2^{\text{init},\epsilon}},$$

$$n^{\text{ext},\epsilon} := \frac{1}{\epsilon} - n_1^{\text{ext},\epsilon} - n_2^{\text{ext},\epsilon}, \quad p^{\text{ext},\epsilon} := \frac{n_1^{\text{ext},\epsilon}}{n_1^{\text{ext},\epsilon}+n_2^{\text{ext},\epsilon}}.$$

Let us denote $H(n,p) = -pF_1(n,p) - (1-p)F_2(n,p)$. The following assumption guarantees existence of zeros of H given by $(n,p) = (h(p),p)$ for each $p\in[0,1]$.

Assumption B.1.3. *In addition to Assumption B.1.2,*
(i) There exists $B>0$ such that for all $n\geqslant 0$, $p\in[0,1]$, $\partial_n H(n,p)\leqslant -B$,
(ii) For all $p>0$, $H(0,p)>0$.

Conditions (i) and (ii) imply that for all $p\in[0,1]$, there exists a unique $n =: h(p)\in\mathbb{R}_+^*$ such that $H(n,p)=0$. We have $H\in\mathcal{C}^2(\mathbb{R}_+^2)$ (from Assumption B.1.2) thus $h\in\mathcal{C}^2(0,1)$, with $H(h(p),p)=0$ for all $p\in[0,1]$.

The following assumptions are made for the initial data and boundary conditions

Assumption B.1.4. *There exists a function $p^{\text{init}}\in L^2(\Omega)$ such that $p^{\text{init},\epsilon}\underset{\epsilon\to 0}{\rightharpoonup} p^{\text{init}}$ weakly in $L^2(\Omega)$. Function $n^{\text{init},\epsilon} - h(0)\in L^2\cap L^\infty(\Omega)$ is uniformly bounded in $\epsilon>0$.*

Assumption B.1.5. *There exists positive constants $\tilde\epsilon>0, \tilde K>0$ such that for any $\epsilon\in(0,\tilde\epsilon)$, we have $|n^{\text{ext},\epsilon}|<\widetilde{K}$.*

There exists a constant $p^{\text{ext}}\in(0,1)$ not depending on ϵ such that $p^{\text{ext},\epsilon}\underset{\epsilon\to 0}{\to} p^{\text{ext}}$

Convergence result. For fixed $\epsilon>0$, existence of solutions of (B.3) is classical (see, e.g. [167]). Following the idea in [201], we present the asymptotic limit of the proportion p^ϵ and n^ϵ in the following theorem.

Theorem B.1.1. *Assume that Assumptions B.1.1-B.1.5 are satisfied and consider the solution (n^ϵ,p^ϵ) of (B.3). Then, for all $T>0$, we have the convergence*

$$\begin{cases} p^\epsilon \xrightarrow[\epsilon\to 0]{} p^0 \text{ strongly in } L^2(0,T;L^2(\Omega)), \text{ weakly in } L^2(0,T;H^1(\Omega)),\\ n^\epsilon - h(p^\epsilon) \xrightarrow[\epsilon\to 0]{} 0 \text{ strongly in } L^2(0,T;L^2(\Omega)), \text{ weakly in } L^2(0,T;H^1(\Omega)),\end{cases}$$

where p^0 is the unique solution of

$$\begin{cases} \partial_t p^0 - \Delta p^0 = p^0(1-p^0)(F_1-F_2)(h(p^0),p^0), & \text{in } (0,T)\times\Omega,\\ p^0(0,\cdot) = p^{\text{init}} & \text{in } \Omega\\ \frac{\partial p^0}{\partial\nu} = -D(p^0 - p^{\text{ext}}) & \text{on } (0,T)\times\partial\Omega.\end{cases}$$

We recall the apriori estimates of [201] without proof and present some bounds on the boundary in Appendix B.2. Then we use the Aubin-Lions lemma and trace theorem to prove the limit in Appendix B.3.

B.2 Uniform a priori estimates

First, we establish the uniform bound with respect to ϵ in L^∞ in the following lemma

Lemma B.2.1. *Under Assumptions B.1.1-B.1.5, for a given value $\epsilon>0$, let (n^ϵ,p^ϵ) be the unique solution of (B.3). Then, for any $T>0$, $0\leqslant p^\epsilon\leqslant 1$ in $[0,T]\times\overline{\Omega}$ for all $\epsilon>0$. Also, there exists $\epsilon_0>0, K_0>0$ such that for any $\epsilon\in(0,\epsilon_0)$, $||n^\epsilon||_{L^\infty([0,T]\times\Omega)}\leqslant K_0$.*

Moreover, n^ϵ is uniformly bounded on $[0,T]\times\partial\Omega$.

Proof. Using the same method as in Lemma 5 of [201], we obtain the uniform bounds for p^ϵ in $[0,T]\times\overline{\Omega}$, and for n^ϵ in $L^\infty([0,T]\times\Omega)$.

Moreover, for any $x\in\partial\Omega$, let ν be the normal outward vector through x. Then, for $\delta>0$ small enough, $x-\delta\nu\in\Omega$. From the boundary condition for n^ϵ in (B.3), one has for $t\in[0,T]$, $\lim\limits_{\delta\to0^+}\dfrac{n^\epsilon(t,x)-n^\epsilon(t,x-\delta\nu)}{\delta}=-D(n^\epsilon(t,x)-n^{\text{ext},\epsilon})$.

So for any $\eta>0$, there exists $\delta>0$ small such that

$$\left|\tfrac{n^\epsilon(t,x)-n^\epsilon(t,x-\delta\nu)}{\delta}+D(n^\epsilon(t,x)-n^{\text{ext},\epsilon})\right|\leqslant\eta.$$

Thus, $n^\epsilon(t,x)(1+\delta D)\leqslant n^\epsilon(t,x-\delta\nu)+\delta Dn^{\text{ext},\epsilon}+\delta\eta$, then for η and δ small enough, for any $\epsilon<\epsilon_0$, $t\in[0,T], x\in\partial\Omega$, since $x-\delta\nu\in\Omega$, one has $|n^\epsilon(t,x)|\leqslant K_0+\delta D\widetilde{K}+\delta\eta<K_1$. Then n^ϵ is uniformly bounded on $[0,T]\times\partial\Omega$ and $||n^\epsilon||_{L^\infty([0,T]\times\partial\Omega)}\leqslant K_1$. □

The following lemmas can be proved analogously to the proof in [201].

Lemma B.2.2. *Under Assumptions B.1.1-B.1.5, for $\epsilon>0$ small enough, let (n^ϵ,p^ϵ) be the unique solution of (B.3). We have the following uniform estimates*

$$\epsilon\int_0^T\int_\Omega|\nabla n^\epsilon|^2dxdt\leqslant C_0,\ \int_0^T\int_\Omega|\nabla p^\epsilon|^2dxdt\leqslant\overline{C},\tag{B.4}$$

for some positive constants C_0 and $\overline{C}$.

Denote $M^\epsilon:=n^\epsilon-h(p^\epsilon)$ where h is defined in Assumption B.1.3. The following provide the convergence of M^ϵ.

Lemma B.2.3. *Let $T>0$, under Assumptions B.1.1-B.1.5, one has $M^\epsilon\to0$ in $L^2(0,T;L^2(\Omega))$ when $\epsilon\to0$.*

Now, we provide a uniform estimate for $\partial_t p^\epsilon$ with respect to ϵ in the following lemma.

Lemma B.2.4. *Under Assumptions B.1.1-B.1.5, for $\epsilon>0$ small enough, $\partial_t p^\epsilon$ is uniformly bounded in $L^2(0,T;X')$ with respect to ϵ, where $X=H^1(\Omega)\cap L^\infty(\Omega)$.*

B.3 Proof of convergence

The idea to prove Theorem B.1.1 is relied on the relative compactness obtained from the Aubin-Lions lemma below (see [188])

Lemma B.3.1 (Aubin-Lions)**.** *Let $T>0$, $q\in(1,\infty)$, and $(\psi_n)_n$ a bounded sequence in $L^q(0,T;B)$, where B is a Banach space. If (ψ_n) is bounded in $L^q(0,T;X)$ and X embeds compactly in B, and if $(\partial_t\psi_n)_n$ is bounded in $L^q(0,T;X')$ uniformly with respect to n, then $(\psi_n)_n$ is relatively compact in $L^q(0,T;B)$.*

Proof of Theorem B.1.1. We use 3 steps to proof Theorem B.1.1. First, we obtain the relative compactness of (p^ϵ) by applying Aubin-Lions lemma, and prove that there exists (up to extracting subsequences) a limit function. Then, we study its behavior on the boundary using the trace theorem. Finally, thanks to our uniform bounds, we show that the limit function satisfies a problem whose solution is unique.

Step 1: In our problem, we need to apply the Lions-Aubin lemma with $q=2, B=L^2(\Omega)$ and $X=H^1(\Omega)\cap L^\infty(\Omega)$ to $(\psi_\epsilon)=(p^\epsilon)_\epsilon$. The compact embedding from X to B is valid by the Rellich-Kondrachov theorem. In the previous section, we have already obtained uniform estimates that are sufficient to apply the Aubin-Lions lemma. The sequence $(p^\epsilon)_\epsilon$ is bounded in $L^2(0,T;L^2(\Omega))$ due to Lemma B.2.1

$$||p^\epsilon||^2_{L^2(0,T;L^2(\Omega))}=\int_0^T\int_\Omega|p^\epsilon|^2dxdt\leqslant||p^\epsilon||^2_{L^\infty(0,T;L^2(\Omega))}\text{meas}(\Omega)T<\infty,$$

for $\epsilon<\epsilon_0$ small enough. Then, due to Lemma B.2.2, this sequence is bounded in $L^2(0,T;X)$. The sequence $(\partial_t p^\epsilon)_\epsilon$ is bounded in $L^2(0,T;X')$ by Lemma B.2.4. Thus, we can apply Aubin-Lions lemma and deduce that $(p^\epsilon)_\epsilon$ is strongly relatively compact in $L^2(0,T;L^2(\Omega))$. Therefore, there exists $p^0\in L^2(0,T;H^1(\Omega))$ such that, up to extraction of subsequences, we have $p^\epsilon\to p^0$ strongly in $L^2((0,T)\times\Omega)$ and a.e., $\nabla p^\epsilon\rightharpoonup\nabla p^0$ weakly in $L^2((0,T)\times\Omega)$.

Moreover, by the triangle inequality we have $|n^\epsilon-h(p^0)|\leqslant|n^\epsilon-h(p^\epsilon)|+|h(p^\epsilon)-h(p^0)|\leqslant|n^\epsilon-h(p^\epsilon)|+||h'||_{L^\infty([0,1])}|p^\epsilon-p^0|$. From the strong convergence of p^ϵ and M^ϵ in Lemma B.2.3 when $\epsilon\to0$, we can deduce the following strong convergence in $L^2(0,T;L^2(\Omega))$

$$n^\epsilon\to n^0:=h(p^0)\tag{B.5}$$

Step 2: Now, let us focus on the behavior on the boundary of the domain. Let the linear operator γ be the trace operator on the boundary $(0,T)\times\partial\Omega$. For any $\epsilon\in(0,\epsilon_0)$ small enough, we have $\gamma(p^\epsilon)=p^\epsilon\mid_{(0,T)\times\partial\Omega}$, then by the trace theorem, one has

$$||\gamma(p^\epsilon)||_{L^2(0,T;L^2(\partial\Omega))}\leqslant C||p^\epsilon||_{L^2(0,T;H^1(\Omega))}$$

where the constant C only depends on Ω. Then

$$||\gamma(p^\epsilon)||^2_{L^2(0,T;L^2(\partial\Omega))}\leqslant C^2\int_0^T\int_\Omega|p^\epsilon|^2dxdt+C^2\int_0^T\int_\Omega|\nabla p^\epsilon(t,\cdot)|^2dxdt<\infty,$$

due to Lemma B.2.1 and B.2.2. Hence, we can deduce that $\gamma(p^\epsilon)$ is weakly convergent in $L^2((0,T)\times\partial\Omega)$. Let $\gamma^0:=\lim\limits_{\epsilon\to0}\gamma(p^\epsilon)$. For any function $\psi\in C^1(\overline{\Omega})$, and for $i=1,\dots,d$, by Green's formula one has

$$\int_\Omega\partial_i p^\epsilon\psi dx=-\int_\Omega p^\epsilon\partial_i\psi+\int_{\partial\Omega}\psi\gamma(p^\epsilon)\nu_i dS.$$

Since p^ϵ converges weakly to p^0 in $H^1(\Omega)$, when $\epsilon\to0$, one has

$$\int_\Omega\partial_i p^0\psi dx=-\int_\Omega p^0\partial_i\psi+\int_{\partial\Omega}\psi\gamma^0\nu_i dS.$$

We can deduce that $\gamma^0=\gamma(p^0)$.

Step 3: We pass to the limit in the weak formulation of (B.3), for any test function ψ such that $\psi\in C^2([0,T]\times\overline{\Omega}),\psi(T,\cdot)=0$ in Ω, one has

$$\underbrace{-\int_0^T\int_\Omega p^\epsilon\partial_t\psi dxdt}_{\text{strong convergence}}+A\underbrace{\int_0^T\int_\Omega\nabla p^\epsilon\cdot\nabla\psi dxdt}_{\text{weak convergence}}=\underbrace{\int_\Omega p^{\text{init},\epsilon}\psi(0,\cdot)dx}_{\text{weak convergence}}$$

$$-2\epsilon A\underbrace{\int_0^T\int_\Omega\frac{\psi}{1-\epsilon n^\epsilon}\nabla p^\epsilon\nabla n^\epsilon dxdt}_{\text{bounded as }\epsilon\to0}+\underbrace{\int_0^T\int_\Omega\psi p^\epsilon(1-p^\epsilon)(F_1-F_2)(n^\epsilon,p^\epsilon)dxdt}_{\text{strong convergence}}$$

$$-DA\underbrace{\int_0^T\int_{\partial\Omega}(p^\epsilon-p^{\text{ext},\epsilon})\frac{1-\epsilon n^{\text{ext},\epsilon}}{1-\epsilon n^\epsilon}dS}_{\text{weak convergence}}.$$

The weak convergence of the last term on the boundary is obtained from Lemma B.2.1 and Assumption B.1.5. When $\epsilon<\epsilon_0$, we have $n^{\text{ext},\epsilon},n^\epsilon$ are uniformly bounded on $(0,T)\times\Omega$ with respect to ϵ, then $\frac{1-\epsilon n^{\text{ext},\epsilon}}{1-\epsilon n^\epsilon}$ converges strongly to 1 when $\epsilon\to0$. From the previous step, one has $p^\epsilon|_{\partial\Omega}=\gamma(p^\epsilon)\rightharpoonup\gamma(p^0)$ weakly in $L^2((0,T)\times\partial\Omega)$. Passing to the limit, we obtain that $p^0\in L^2(0,T;H^1(\Omega))$ is a weak solution of the following problem

$$\begin{cases}\partial_t p^0-A\Delta p^0=p^0(1-p^0)(F_1-F_2)(n^0,p^0) & \text{in }(0,T)\times\Omega,\\ p^0(0,\cdot)=p^{\text{init}} & \text{in }\Omega\\ \frac{\partial p^0}{\partial\nu}=-D(p^0-p^{\text{ext}}) & \text{on }(0,T)\times\partial\Omega.\end{cases}$$

Using (B.5), we can deduce that this problem is a self-contained initial-boundary-value problem. Moreover, since 0 and 1 are respectively sub- and super-solutions of this problem, it admits a unique classical solution with values in $[0,1]$. Hence, all the extracted sub-sequences converge to the same limit p^0 and $p^0|_{\partial\Omega}=\gamma(p^0)$. □

Appendix C

Spread of Invasive Fronts

Propositions 3.1.1 and 3.1.2 in Chapter 3 described the dynamics of the wild mosquito population in the absence of sterile males in the monostable case. We present the proof of these results in the following.

C.1 Priliminary results

We recall [219, Theorem 4.2] which shows the estimate of the spreading speed c^* for the monostable system in discrete setting

$$\mathbf{u}_{n+1} = \mathcal{Q}[\mathbf{u}_n]$$

where the vector-valued function $\mathbf{u_n}(x) = (u_n^1(x), u_n^2(x), ..., u_n^k(x))$ represents the population densities of the populations of k species at the point x and the time $n\tau$, with τ a fixed generation time. Then in section 4 of this work, the authors showed how to apply the results to a reaction-diffusion system by letting $\mathcal{Q}$ be its time τ map. That is, replacing $\mathcal{Q}$ by $\mathcal{Q}_\tau$ where $\mathcal{Q}_\tau[\mathbf{u}_0] := \mathbf{u}(x, \tau)$. Next, we recall the result of this work and apply it to the system (3.3).

Consider the system of reaction-diffusion equations $\partial_t u_i - d_i \partial_{xx} u_i = f_i(\mathbf{u})$, with $1 \leqslant i \leqslant k$ and denote $\mathbf{f} = (f_1, f_2, \dots f_k)$. The reaction function $\mathbf{f}$ needs to satisfy the following assumptions.

Assumption C.1.1.

i. $\mathbf{f}(\mathbf{0}) = \mathbf{0}$ and there is a vector $\overline{\mathbf{u}} \gg \mathbf{0}$ such that $\mathbf{f}(\overline{\mathbf{u}}) = 0$ which is minimal in the sense there are no $\overline{\mathbf{v}}$ other than $\mathbf{0}$ and $\overline{\mathbf{u}}$ such that $\mathbf{f}(\overline{\mathbf{v}}) = 0$ and $\mathbf{0} \ll \overline{\mathbf{v}} \leqslant \overline{\mathbf{u}}$.

ii. The system is cooperative, that is, $f_i(\mathbf{u})$ is nondecreasing in all components of $\mathbf{u}$ with the possible exception of the i^{th} one.

iii. $\mathbf{f}(\mathbf{u})$ is continuous and piecewise continuously differentiable at $\mathbf{u}$ for $\mathbf{0} \leqslant \mathbf{u} \leqslant \overline{\mathbf{u}}$ and differentiable at $\mathbf{0}$.

iv. The Jacobian matrix $\mathbf{f}'(\mathbf{0})$ is in Frobenius form. The principal eigenvalue $\eta_1(\mathbf{0})$ of its upper left diagonal block is positive and strictly larger than the principal eigenvalues $\eta_\sigma(\mathbf{0})$ of its other diagonal blocks, and there is at least one nonzero entry to the left of each diagonal block other than the first one.

For any positive parameter μ, if the initial data are of the form $e^{-\mu x}\mathbf{u}_0$ then the solution of this system has the form $e^{-\mu x}\mathbf{v}$, where the vector-valued function $\mathbf{v}$ is the solution of the system of ordinary differential equations with constant coefficients $\partial_t \mathbf{v} = C_\mu \mathbf{v}$, with $\mathbf{v}(\mathbf{0}) = \mathbf{u}_0$. The coefficient matrix is given by

$$C_\mu = \operatorname{diag}\Big(d_i \mu^2\Big) + \mathbf{f}'(\mathbf{0}), \tag{C.1}$$

and denote $\gamma_\sigma(\mathbf{0})$ the principal eigenvalue of the σth diagonal block of the matrix C_μ. We introduce the constant

$$\overline{c} := \inf_{\mu > 0} \frac{\gamma_1(\mu)}{\mu}. \tag{C.2}$$

Let $\overline{\mu} \in (0, \infty]$ again denote the value of μ at which this minimum is attained, and let $\zeta(\mu)$ be the eigenvector of C_μ which correspond to the eigenvalue $\gamma_1(\mu)$. Then, the following theorem presents the main result

Theorem C.1.1 (Theorem 4.2 in [219])**.** *Suppose that* $\mathbf{f}$ *satisfies the Assumptions C.1.1. Assume that either (a)* $\overline{\mu}$ *is finite,*

$$\gamma_1(\overline{\mu}) > \gamma_\sigma(\overline{\mu}) \text{ for all } \sigma > 1, \tag{C.3}$$

and

$$\mathbf{f}(\rho\zeta(\overline{\mu})) \leqslant \rho\mathbf{f}'(\mathbf{0})\zeta(\overline{\mu}), \tag{C.4}$$

for all positive ρ;

or

(b) There is a sequence $\mu_\nu \nearrow \overline{\mu}$ such that for each ν the inequalities (C.3) and (C.4) with $\overline{\mu}$ replaced by μ_ν are valid.

Then the system has a unique speed $c^* = \overline{c}$ with c^* defined in Proposition 3.1.1.

C.2 Proof of Propositions 3.1.1 and 3.1.2

Now we apply this theorem to system (3.3) with $\mathbf{f}(E,F,M) = \begin{pmatrix} \beta F\left(1-\frac{E}{K}\right) - (\nu_E+\mu_E)E \\ \rho\nu_E E - \mu_F F \\ (1-\rho)\nu_E E - \mu_M M \end{pmatrix}$, and we provide the proof as follows

Proof of Propositions 3.1.1 and 3.1.2. First, we need to show that $\mathbf{f}$ satisfies Assumptions C.1.1. With $\beta r\nu_E > \mu_F(\nu_E+\mu_E)$, we can deduce that $\mathbf{f}$ has two zeros $(0,0,0)$, (E^*,F^*,M^*), and satisfies (i). When $E \leqslant K$, one has $\mathbf{f}$ is cooperative, thus $\mathbf{f}$ satisfies (ii). It is easy to see that $\mathbf{f}$ satisfies (iii). Now we only need to check the assumption (iv). The Jacobian of $\mathbf{f}$ at $(0,0,0)$

$$\mathbf{f}'(\mathbf{0}) = \begin{pmatrix} -\nu_E-\mu_E & \beta & 0 \\ \rho\nu_E & -\mu_F & 0 \\ (1-\rho)\nu_E & 0 & -\mu_M \end{pmatrix} \tag{C.5}$$

is in Frobenius form with two diagonal blocks $B_1 = \begin{pmatrix} -\nu_E-\mu_E & \beta \\ \rho\nu_E & -\mu_F \end{pmatrix}$ and $B_2 = -\mu_M$. There is a positive entry $(1-\rho)\nu_E$ to the left of B_2.

The block B_1 has two eigenvalues $\eta_\pm = \dfrac{-(\nu_E+\mu_E+\mu_F) \pm \sqrt{(\nu_E+\mu_E-\mu_F)^2+4\beta\rho\nu_E}}{2}$. Denote $\begin{pmatrix} e_\pm \\ f_\pm \end{pmatrix}$ the eigenvectors corresponding to eigenvalues $\eta_\pm$ of B_1. Then, one has

$$-(\nu_E+\mu_E)e_\pm + \beta f_\pm = \frac{-(\nu_E+\mu_E+\mu_F) \pm \sqrt{(\nu_E+\mu_E-\mu_F)^2+4\beta\rho\nu_E}}{2} e_\pm.$$

So

$$\beta f_\pm = \frac{\nu_E+\mu_E-\mu_F \pm \sqrt{(\nu_E+\mu_E-\mu_F)^2+4\beta\rho\nu_E}}{2} e_\pm.$$

Since $\dfrac{\nu_E+\mu_E-\mu_F - \sqrt{(\nu_E+\mu_E-\mu_F)^2+4\beta\rho\nu_E}}{2} < 0$, then e_- and f_- always have different signs. Hence, η_+ is the only eigenvalue that has the corresponding positive eigenvector, and it is the principal eigenvalue of B_1. Moreover, due to the assumption $\beta\rho\nu_E > \mu_F(\nu_E+\mu_E)$, one has $\eta_1(\mathbf{0}) = \eta_+ > 0 > -\mu_M = \eta_2(\mathbf{0})$. This concludes that $\mathbf{f}$ satisfies (iv).

Now, one has the matrix

$$C_\mu = \begin{pmatrix} -\nu_E-\mu_E & \beta & 0 \\ \rho\nu_E & D\mu^2-\mu_F & 0 \\ (1-\rho)\nu_E & 0 & D\mu^2-\mu_M \end{pmatrix}.$$

Similarly to the matrix $\mathbf{f}'(\mathbf{0})$, the principal eigenvalue of the first block of C_μ is

$$\gamma_1(\mu) = \frac{D\mu^2-\nu_E-\mu_E-\mu_F+\sqrt{(D\mu^2+\nu_E+\mu_E-\mu_F)^2+4\beta\rho\nu_E}}{2}$$

By the assumption $\beta\rho\nu_E > \mu_F(\nu_E+\mu_E)$ and $D>0$, we have $\gamma_1(\mu) > 0$. It is easy to see that $\dfrac{\gamma_1(\mu)}{\mu} \sim \dfrac{1}{\mu}$ when $\mu \to 0^+$, and $\dfrac{\gamma_1(\mu)}{\mu} \sim \mu$ when $\mu \to +\infty$. Hence, one can deduce that there exists a finite constant $\overline{\mu} \in (0,+\infty)$ such that $\dfrac{\gamma_1(\overline{\mu})}{\overline{\mu}} = \inf\limits_{\mu>0} \dfrac{\gamma_1(\mu)}{\mu}$.

Consider $\zeta(\overline{\mu}) = \begin{pmatrix} e \\ f \\ m \end{pmatrix}$ the eigenvector corresponding to the eigenvalue $\gamma_1(\overline{\mu})$ of $C_{\overline{\mu}}$, where $\begin{pmatrix} e \\ f \end{pmatrix}$ is the positive eigenvector associated to the principal eigenvalue $\gamma_1(\overline{\mu})$ of the first diagonal block. So $m > 0$ if and only if $\gamma_1(\overline{\mu}) > \gamma_2(\overline{\mu}) = D\overline{\mu}^2 - \mu_M$, that is

$$2\mu_M - D\overline{\mu}^2 - \nu_E - \mu_E - \mu_F + \sqrt{(D\overline{\mu}^2 + \nu_E + \mu_E - \mu_F)^2 + 4\beta\rho\nu_E} > 0. \tag{C.6}$$

Hence, whenever the parameters satisfy condition (C.6), the inequality (C.3) holds, the eigenvector $\zeta(\overline{\mu}) = \begin{pmatrix} e \\ f \\ m \end{pmatrix}$ is positive, and for any positive ρ, $\mathbf{f}(\rho\zeta(\overline{\mu})) - \rho\mathbf{f}'(\mathbf{0})\zeta(\overline{\mu}) = \rho \begin{pmatrix} -\frac{\beta}{K}ef\rho \\ 0 \\ 0 \end{pmatrix} < 0$, then (C.4) holds. Now, applying the result of Theorem C.1.1, we obtain the spreading speed $c^* = \overline{c}$. By applying Theorem 4.1 in [219], the solution of (3.3) satisfies

$$\lim_{t\to+\infty} \left[\max_{|x|\geqslant t(c^*+\varepsilon)} \max(E, F, M)(t, x) \right] = 0,$$

if the initial data (E^0, F^0, M^0) is compactly supported and $0 \leqslant (E^0, F^0, M^0) \ll (E^*, F^*, M^*)$. Furthermore, for any strictly positive constant ω, there is a positive R_ω with the property that if $\min(E^0, F^0, M^0) \geqslant \omega$ on an interval of length $2R_\omega$, then

$$\lim_{t\to+\infty} \left[\max_{|x|\leqslant t(c^*-\varepsilon)} \max(E^* - E, F^* - F, M^* - M)(t, x) \right] = 0.$$

Moreover, Proposition 3.3 in the work of Lui [139] provides, in a discrete setting, some conditions in which the constant R_ω can be chosen to be arbitrarily small and independent of ω. This result can be transposed to the continuous case like what has been done in section 4 of [219] and it is simple to verify that, when $\min E_0 > 0$ or $\min F_0 > 0$, our system satisfies those conditions so we leave it to the readers. Hence, by applying this result, we deduce that if the initial data E^0 or F^0 are strictly positive on a set with a positive measure, then the result in Proposition 3.1.1 holds.

Now, to prove Proposition 3.1.2, the paper [77] provides some conditions in which the spreading speed estimated in [219] of the monostable system is the minimum speed of the traveling wave. The authors in [17] have checked all the conditions for the same system as (3.3), hence we obtain the same result for our system. □

Bibliography

[1] F. V. S. d. Abreu, M. M. Morais, S. P. Ribeiro, and A. E. Eiras. "Influence of breeding site availability on the oviposition behaviour of *Aedes aegypti*". en. In: *Memorias do Instituto Oswaldo Cruz* 110 (July 2015). Publisher: Instituto Oswaldo Cruz, Ministério da Saúde, pp. 669–676.

[2] N. L. Achee et al. "Alternative strategies for mosquito-borne arbovirus control". en. In: *PLOS Neglected Tropical Diseases* 13.1 (Jan. 2019). Publisher: Public Library of Science, e0006822.

[3] M. Alfaro, H. Berestycki, and G. Raoul. "The Effect of Climate Shift on a Species Submitted to Dispersion, Evolution, Growth, and Nonlocal Competition". In: *SIAM Journal on Mathematical Analysis* 49.1 (Jan. 2017). Publisher: Society for Industrial and Applied Mathematics, pp. 562–596.

[4] L. J. S. Allen. "Persistence, extinction, and critical patch number for island populations". en. In: *Journal of Mathematical Biology* 24.6 (Feb. 1987), pp. 617–625.

[5] L. Almeida, J. B. Arnau, M. Duprez, and Y. Privat. "Minimal cost-time strategies for mosquito population replacement". In: ed. by R. Herzog, M. Heinkenschloss, D. Kalise, G. Stadler, and E. Trélat. Berlin, Boston: De Gruyter, 2022, pp. 73–90.

[6] L. Almeida, J. Bellver Arnau, and Y. Privat. "Optimal Control Strategies for Bistable ODE Equations: Application to Mosquito Population Replacement". en. In: *Applied Mathematics & Optimization* 87.1 (Nov. 2022), p. 10.

[7] L. Almeida, P.-A. Bliman, N. Nguyen, and N. Vauchelet. "Steady-state solutions for a reaction–diffusion equation with Robin boundary conditions: Application to the control of dengue vectors". en. In: *European Journal of Applied Mathematics* (Sept. 2023), pp. 1–27.

[8] L. Almeida, M. Duprez, Y. Privat, and N. Vauchelet. "Optimal control strategies for the sterile mosquitoes technique". In: *Journal of Differential Equations* 311 (2022), pp. 229–266.

[9] L. Almeida, J. Estrada, and N. Vauchelet. "The sterile insect technique used as a barrier control against reinfestation". In: *Optimization and Control for Partial Differential Equations*. Ed. by R. Herzog, M. Heinkenschloss, D. Kalise, G. Stadler, and E. Trélat. Berlin, Boston: De Gruyter, 2022, pp. 91–112.

[10] L. Almeida, A. Leculier, N. Nguyen, and N. Vauchelet. "Rolling carpet strategies to eliminate mosquitoes: two-dimensional case". (paper in preparation). 2023.

[11] L. Almeida, A. Léculier, G. Nadin, and Y. Privat. *Optimal control of bistable travelling waves: looking for the spatial distribution of a killing action to block a pest invasion*. Oct. 2022.

[12] L. Almeida, A. Léculier, and N. Vauchelet. "Analysis of the Rolling Carpet Strategy to Eradicate an Invasive Species". In: *SIAM Journal on Mathematical Analysis* 55.1 (Feb. 2023). Publisher: Society for Industrial and Applied Mathematics, pp. 275–309.

[13] L. Almeida, Y. Privat, M. Strugarek, and N. Vauchelet. "Optimal Releases for Population Replacement Strategies: Application to Wolbachia". In: *SIAM Journal on Mathematical Analysis* 51.4 (Jan. 2019). Publisher: Society for Industrial and Applied Mathematics, pp. 3170–3194.

[14] L. Almeida et al. "Optimal release of mosquitoes to control dengue transmission". en. In: *ESAIM: ProcS* 67 (2020). Publisher: EDP Sciences, pp. 16–29.

[15] L. Almeida, J. Estrada, and N. Vauchelet. "Wave blocking in a bistable system by local introduction of a population: application to sterile insect techniques on mosquito populations". en. In: *Mathematical Modelling of Natural Phenomena* 17 (2022). Publisher: EDP Sciences, p. 22.

[16] M. Andraud, N. Hens, C. Marais, and P. Beutels. "Dynamic Epidemiological Models for Dengue Transmission: A Systematic Review of Structural Approaches". en. In: *PLOS ONE* 7.11 (Nov. 2012). Publisher: Public Library of Science, e49085.

[17] R. Anguelov, Y. Dumont, and I. V. Y. Djeumen. *On the use of Traveling Waves for Pest/Vector elimination using the Sterile Insect Technique*. arXiv:2010.00861 [math]. Oct. 2020.

[18] R. Anguelov, Y. Dumont, and J. Lubuma. "Mathematical modeling of sterile insect technology for control of anopheles mosquito". In: *Computers & Mathematics with Applications*. Mathematical Methods and Models in Biosciences 64.3 (Aug. 2012), pp. 374–389.

[19] R. Anguelov, Y. Dumont, and I. V. Yatat Djeumen. "Sustainable vector/pest control using the permanent sterile insect technique". en. In: *Mathematical Methods in the Applied Sciences* 43.18 (2020), pp. 10391–10412.

[20] J. Arino, J. R. Davis, D. Hartley, R. Jordan, J. M. Miller, and P. van den Driessche. "A multi-species epidemic model with spatial dynamics". In: *Mathematical Medicine and Biology: A Journal of the IMA* 22.2 (June 2005), pp. 129–142.

[21] J. Arino, R. Jordan, and P. van den Driessche. "Quarantine in a multi-species epidemic model with spatial dynamics". In: *Mathematical Biosciences*. Alcala Special Issue 206.1 (Mar. 2007), pp. 46–60.

[22] J. B. Arnau. "Optimal mosquito release strategies for vector-borne disease control". en. PhD thesis. Sorbonne Université, Dec. 2022.

[23] D. G Aronson and H. F Weinberger. "Multidimensional nonlinear diffusion arising in population genetics". en. In: *Advances in Mathematics* 30.1 (Oct. 1978), pp. 33–76.

[24] D. G. Aronson and H. F. Weinberger. "Nonlinear diffusion in population genetics, combustion, and nerve pulse propagation". en. In: *Partial Differential Equations and Related Topics*. Ed. by J. A. Goldstein. Lecture Notes in Mathematics. Berlin, Heidelberg: Springer, 1975, pp. 5–49.

[25] P. Auger, E. Kouokam, G. Sallet, M. Tchuente, and B. Tsanou. "The Ross–Macdonald model in a patchy environment". In: *Mathematical Biosciences* 216.2 (Dec. 2008), pp. 123–131.

[26] N. H. Barton and M. Turelli. "Spatial waves of advance with bistable dynamics: cytoplasmic and genetic analogues of Allee effects". In: *The American Naturalist* 178.3 (Sept. 2011), pp. 48–75.

[27] B. J. Beaty and T. H. G. Aitken. "In vitro transmission of yellow fever virus by geographic strains of Aedes aegypti." In: *Mosquito News* 39.2 (1979), pp. 232–238.

[28] N. Becker, B. Pluskota, A. Kaiser, and F. Schaffner. "Exotic Mosquitoes Conquer the World". en. In: *Arthropods as Vectors of Emerging Diseases*. Ed. by H. Mehlhorn. Parasitology Research Monographs. Berlin, Heidelberg: Springer, 2012, pp. 31–60.

[29] N. Becker et al. *Mosquitoes: Identification, Ecology and Control*. en. Fascinating Life Sciences. Cham: Springer International Publishing, 2020.

[30] R. Bellini, A. Medici, A. Puggioli, F. Balestrino, and M. Carrieri. "Pilot Field Trials With Aedes albopictus Irradiated Sterile Males in Italian Urban Areas". In: *Journal of Medical Entomology* 50.2 (Mar. 2013), pp. 317–325.

[31] M. Q. Benedict, R. S. Levine, W. A. Hawley, and L. P. Lounibos. "Spread of The Tiger: Global Risk of Invasion by The Mosquito Aedes albopictus". In: *Vector-Borne and Zoonotic Diseases* 7.1 (Mar. 2007). Publisher: Mary Ann Liebert, Inc., publishers, pp. 76–85.

[32] G. Benelli, C. L. Jeffries, and T. Walker. "Biological Control of Mosquito Vectors: Past, Present, and Future". en. In: *Insects* 7.4 (Dec. 2016). Number: 4 Publisher: Multidisciplinary Digital Publishing Institute, p. 52.

[33] H. Berestycki, O. Diekmann, C. J. Nagelkerke, and P. A. Zegeling. "Can a Species Keep Pace with a Shifting Climate?" en. In: *Bull. Math. Biol.* 71.2 (Feb. 2009), pp. 399–429.

[34] H. Berestycki and J. Fang. "Forced waves of the Fisher–KPP equation in a shifting environment". en. In: *Journal of Differential Equations* 264.3 (Feb. 2018), pp. 2157–2183.

[35] H. Berestycki and L. Rossi. "Reaction-diffusion equations for population dynamics with forced speed I - The case of the whole space". en. In: *Discrete and Continuous Dynamical Systems* 21.1 (Jan. 2008). Publisher: Discrete and Continuous Dynamical Systems, pp. 41–67.

[36] H. Berestycki and L. Rossi. "Reaction-diffusionequations for population dynamics with forced speed II -cylindrical-type domains". en. In: *Discrete and Continuous Dynamical Systems* 25.1 (May 2009). Publisher: Discrete and Continuous Dynamical Systems, pp. 19–61.

[37] P.-A. Bliman. "A feedback control perspective on biological control of dengue vectors by Wolbachia infection". In: *European Journal of Control* 59 (May 2021), pp. 188–206.

[38] P.-A. Bliman, D. Cardona-Salgado, Y. Dumont, and O. Vasilieva. "Implementation of control strategies for sterile insect techniques". In: *Mathematical Biosciences* 314 (Aug. 2019), pp. 43–60.

[39] P.-A. Bliman and Y. Dumont. “Robust control strategy by the Sterile Insect Technique for reducing epidemiological risk in presence of vector migration”. In: *Mathematical Biosciences* 350 (Aug. 2022), p. 108856.

[40] P.-A. Bliman, Y. Dumont, O. E. Escobar-Lasso, H. J. Martinez-Romero, and O. Vasilieva. “Sex-structured model of Wolbachia invasion and design of sex-biased release strategies in Aedes spp mosquitoes populations”. In: *Applied Mathematical Modelling* 119 (July 2023), pp. 391–412.

[41] D. D. Bonnet and H. Chapman. “The larval habitats of Aedes polynesiensis Marks in Tahiti and methods of control.” English. In: *American Journal of Tropical Medicine and Hygiene* 7.5 (1958). Publisher: Baltimore, Md.

[42] J. Bouhours and T. Giletti. “Spreading and Vanishing for a Monostable Reaction–Diffusion Equation with Forced Speed”. en. In: *Journal of Dynamics and Differential Equations* 31.1 (Mar. 2019), pp. 247–286.

[43] K. Bourtzis et al. “Harnessing mosquito–Wolbachia symbiosis for vector and disease control”. In: *Acta Tropica*. Biology and behaviour of male mosquitoes in relation to new approaches to control disease transmitting mosquitoes 132 (Apr. 2014), S150–S163.

[44] M. A. Braks, N. A. Honório, R. Lourenço-De-Oliveira, S. A. Juliano, and L. P. Lounibos. “Convergent Habitat Segregation of Aedes aegypti and Aedes albopictus (Diptera: Culicidae) in Southeastern Brazil and Florida”. In: *Journal of Medical Entomology* 40.6 (Nov. 2003), pp. 785–794.

[45] A. Bressan, M. T. Chiri, and N. Salehi. “On the optimal control of propagation fronts”. In: *Mathematical Models and Methods in Applied Sciences* 32.06 (June 2022). Publisher: World Scientific Publishing Co., pp. 1109–1140.

[46] A. Bressan, M. T. Chiri, and N. Salehi. “Optimal control of moving sets”. In: *Journal of Differential Equations* 361 (July 2023), pp. 97–137.

[47] D. M. Brown, L. S. Alphey, A. McKemey, C. Beech, and A. A. James. “Criteria for Identifying and Evaluating Candidate Sites for Open-Field Trials of Genetically Engineered Mosquitoes”. In: *Vector-Borne and Zoonotic Diseases* 14.4 (Apr. 2014). Publisher: Mary Ann Liebert, Inc., publishers, pp. 291–299.

[48] J. P. Buonaccorsi, L. C. Harrington, and J. D. Edman. “Estimation and Comparison of Mosquito Survival Rates with Release-Recapture-Removal Data”. In: *Journal of Medical Entomology* 40.1 (Jan. 2003), pp. 6–17.

[49] R. S. Cantrell and C. Cosner. “Spatial Heterogeneity and Critical Patch Size: Area Effects via Diffusion in Closed Environments”. In: *Journal of Theoretical Biology* 209.2 (Mar. 2001), pp. 161–171.

[50] R. S. Cantrell and C. Cosner. *Spatial ecology via reaction-diffusion equations*. John Wiley & Sons, 2004.

[51] B. Caputo et al. “A bacterium against the tiger: preliminary evidence of fertility reduction after release of Aedes albopictus males with manipulated Wolbachia infection in an Italian urban area”. In: *Pest Management Science* 76 (Oct. 2019).

[52] E. Caspari and G. S. Watson. “ON THE EVOLUTIONARY IMPORTANCE OF CYTOPLASMIC STERILITY IN MOSQUITOES”. In: *Evolution* 13.4 (Dec. 1959), pp. 568–570.

[53] M. H. T. Chan and P. S. Kim. “Modelling a Wolbachia Invasion Using a Slow–Fast Dispersal Reaction–Diffusion Approach”. In: *Bull Math Biol* 75.9 (June 2013).

[54] M. H. T. Chan and P. S. Kim. “Modelling a Wolbachia Invasion Using a Slow–Fast Dispersal Reaction–Diffusion Approach”. en. In: *Bull Math Biol* 75.9 (Sept. 2013), pp. 1501–1523.

[55] S. Chaplygin. “Selected Works on Mechanics and Mathematics”. In: *State Publ. House, Technical-Theoretical Literature, Moscow* (1954).

[56] L. F. Chaves, G. L. Hamer, E. D. Walker, W. M. Brown, M. O. Ruiz, and U. D. Kitron. “Climatic variability and landscape heterogeneity impact urban mosquito diversity and vector abundance and infection”. en. In: *Ecosphere* 2.6 (2011). _eprint: https://onlinelibrary.wiley.com/doi/pdf/10.1890/ES11-00088.1, art70.

[57] D. Cianci et al. “Estimating Mosquito Population Size From Mark–Release–Recapture Data”. In: *Journal of Medical Entomology* 50.3 (May 2013), pp. 533–542.

[58] H. Comins, M. Hassell, and R. May. “The Spatial Dynamics of Host–Parasitoid Systems”. In: *Journal of Animal Ecology* (1992), pp. 735–748.

[59] W. A. Coppel. *Stability and Asymptotic Behavior of Differential Equations*. en. Heath, 1965.

[60] A. Cordero-Rivera and R. Stoks. "Mark–recapture studies and demography". en. In: *Dragonflies and Damselflies*. Ed. by A. Córdoba-Aguilar. 1st ed. Oxford University PressOxford, Aug. 2008, pp. 7–20.

[61] F. Courchamp, L. Berec, and J. Gascoigne. *Allee Effects in Ecology and Conservation*. en. Google-Books-ID: fQpREAAAQBAJ. OUP Oxford, Feb. 2008.

[62] U. A. Danbaba and S. M. Garba. "Modeling the transmission dynamics of Zika with sterile insect technique". en. In: *Mathematical Methods in the Applied Sciences* 41.18 (2018), pp. 8871–8896.

[63] D. Daners. "Robin boundary value problems on arbitrary domains". In: *Trans. Amer. Math. Soc.* 352.9 (Mar. 2000), pp. 4207–4236.

[64] P. David, ed. *Biological Invasions: Economic and Environmental Costs of Alien Plant, Animal, and Microbe Species*. Boca Raton: CRC Press, June 2002.

[65] D. L. DeAngelis and W. M. Mooij. "Individual-Based Modeling of Ecological and Evolutionary Processes". In: *Annual Review of Ecology, Evolution, and Systematics* 36.1 (2005), pp. 147–168.

[66] *Dengue and severe dengue*. en. `https://www.who.int/news-room/fact-sheets/detail/dengue-and-severe-dengue`. World Health Organization. 2023.

[67] DGS_Céline.M and DGS_Céline.M. *Cartes de présence du moustique tigre (Aedes albopictus) en France métropolitaine*. fr. Mar. 2024.

[68] A. Ducrot. "On the large time behaviour of the multi-dimensional Fisher–KPP equation with compactly supported initial data". en. In: *Nonlinearity* 28.4 (Mar. 2015). Publisher: IOP Publishing, p. 1043.

[69] C. Dufourd and Y. Dumont. "Impact of environmental factors on mosquito dispersal in the prospect of sterile insect technique control". en. In: *Computers & Mathematics with Applications*. BioMath 2012 66.9 (Nov. 2013), pp. 1695–1715.

[70] Y. Dumont and J. M. Tchuenche. "Mathematical studies on the sterile insect technique for the Chikungunya disease and Aedes albopictus". en. In: *Journal of Mathematical Biology* 65.5 (Nov. 2012), pp. 809–854.

[71] M. Duprez, R. Hélie, Y. Privat, and N. Vauchelet. "Optimization of spatial control strategies for population replacement, application to Wolbachia". en. In: *ESAIM: Control, Optimisation and Calculus of Variations* 27 (2021). Publisher: EDP Sciences, p. 74.

[72] H. L. C. Dutra, M. N. Rocha, F. B. S. Dias, S. B. Mansur, E. P. Caragata, and L. A. Moreira. "Wolbachia Blocks Currently Circulating Zika Virus Isolates in Brazilian Aedes aegypti Mosquitoes". In: *Cell Host & Microbe* 19.6 (June 2016), pp. 771–774.

[73] V. A. Dyck, J. Hendrichs, and A. S. Robinson, eds. *Sterile Insect Technique: Principles and Practice in Area-Wide Integrated Pest Management*. 2nd ed. Boca Raton: CRC Press, Jan. 2021.

[74] M. Equihua, S. Ibáñez-Bernal, G. Benítez, I. Estrada-Contreras, C. A. Sandoval-Ruiz, and F. S. Mendoza-Palmero. "Establishment of Aedes aegypti (L.) in mountainous regions in Mexico: Increasing number of population at risk of mosquito-borne disease and future climate conditions". In: *Acta Tropica* 166 (Feb. 2017), pp. 316–327.

[75] W. F. Fagan, R. S. Cantrell, and C. Cosner. "How Habitat Edges Change Species Interactions." In: *The American Naturalist* 153.2 (Feb. 1999), pp. 165–182.

[76] L. Fahse, C. Wissel, and V. Grimm. "Reconciling Classical and Individual-Based Approaches in Theoretical Population Ecology: A Protocol for Extracting Population Parameters from Individual-Based Models". In: *The American Naturalist* 152.6 (Dec. 1998). Publisher: The University of Chicago Press, pp. 838–852.

[77] J. Fang and X.-Q. Zhao. "Monotone Wavefronts for Partially Degenerate Reaction-Diffusion Systems". en. In: *J Dyn Diff Equat* 21.4 (Dec. 2009), pp. 663–680.

[78] J. Z. Farkas, S. A. Gourley, R. Liu, and A.-A. Yakubu. "Modelling Wolbachia infection in a sex-structured mosquito population carrying West Nile virus". en. In: *Journal of Mathematical Biology* 75.3 (Sept. 2017), pp. 621–647.

[79] J. Z. Farkas and P. Hinow. "Structured and Unstructured Continuous Models for Wolbachia Infections". en. In: *Bull. Math. Biol.* 72.8 (Nov. 2010), pp. 2067–2088.

[80] M. Fazly, M. Lewis, and H. Wang. "Analysis of Propagation for Impulsive Reaction-Diffusion Models". In: *SIAM Journal on Applied Mathematics* 80.1 (Jan. 2020). Publisher: Society for Industrial and Applied Mathematics, pp. 521–542.

[81] M. Fazly, M. Lewis, and H. Wang. "On Impulsive Reaction-Diffusion Models in Higher Dimensions". In: *SIAM Journal on Applied Mathematics* 77.1 (Jan. 2017). Publisher: Society for Industrial and Applied Mathematics, pp. 224–246.

[82] P. C. Fife. *Mathematical Aspects of Reacting and Diffusing Systems*. 1st. Berlin, Heidelberg: Springer, 1979.

[83] D. A. Focks, D. G. Haile, E. Daniels, and G. A. Mount. "Dynamic life table model for Aedes aegypti (Diptera: Culicidae): analysis of the literature and model development". In: *Journal of medical entomology* 30.6 (1993), pp. 1003–1017.

[84] S. D. Fretwell. *Populations in a Seasonal Environment.(MPB-5)*. Vol. 106. Princeton University Press, 1972.

[85] G. d. A. Garcia, L. M. B. d. Santos, D. A. M. Villela, and R. Maciel-de Freitas. "Using Wolbachia Releases to Estimate Aedes aegypti (Diptera: Culicidae) Population Size and Survival". en. In: *PLOS ONE* 11.8 (2016). Publisher: Public Library of Science, e0160196.

[86] C. W. Gardiner et al. *Handbook of stochastic methods*. Vol. 3. springer Berlin, 1985.

[87] R. Gato, A. Companioni, R. Y. Bruzón, Z. Menéndez, A. González, and M. Rodríguez. "Release of thiotepa sterilized males into caged populations of Aedes aegypti: Life table analysis". In: *Acta Tropica*. Biology and behaviour of male mosquitoes in relation to new approaches to control disease transmitting mosquitoes 132 (Apr. 2014), S164–S169.

[88] R. Gato et al. "Sterile Insect Technique: Successful Suppression of an Aedes aegypti Field Population in Cuba". en. In: *Insects* 12.5 (May 2021). Number: 5 Publisher: Multidisciplinary Digital Publishing Institute, p. 469.

[89] J. S. M. Gesto et al. "Large-Scale Deployment and Establishment of Wolbachia Into the Aedes aegypti Population in Rio de Janeiro, Brazil". In: *Frontiers in Microbiology* 12 (2021).

[90] L. Girardin and Q. Griette. "A Liouville-type result for non-cooperative Fisher–KPP systems and non-local equations in cylinders". In: *Acta Applicandae Mathematicae* 170 (2020), pp. 123–139.

[91] L. Girardin. "Non-cooperative Fisher–KPP systems: Asymptotic behavior of traveling waves". In: *Math. Models Methods Appl. Sci.* 28.06 (June 2018). Publisher: World Scientific Publishing Co., pp. 1067–1104.

[92] L. Girardin. "Non-cooperative Fisher–KPP systems: traveling waves and long-time behavior". en. In: *Nonlinearity* 31.1 (Dec. 2017). Publisher: IOP Publishing, p. 108.

[93] *Global vector control response 2017-2030*. English. World Health Organization. 2017.

[94] J. Goddard and R. Shivaji. "Stability analysis for positive solutions for classes of semilinear elliptic boundary-value problems with nonlinear boundary conditions". In: *Proceedings of the Royal Society of Edinburgh: Section A Mathematics* 147.5 (2017), 1019–1040.

[95] P. V. Gordon, E. Ko, and R. Shivaji. "Multiplicity and uniqueness of positive solutions for elliptic equations with nonlinear boundary conditions arising in a theory of thermal explosion". In: *Nonlinear Analysis: Real World Applications*. Special Section: Multiscale Problems in Science and Technology. Challenges to Mathematical Analysis and Perspectives III 15 (Jan. 2014), pp. 51–57.

[96] J. Gärtner. "Location of Wave Fronts for the Multi-Dimensional K-P-P Equation and Brownian First Exit Densities". en. In: *Mathematische Nachrichten* 105.1 (1982), pp. 317–351.

[97] F. Hamel and L. Roques. "Fast propagation for KPP equations with slowly decaying initial conditions". In: *Journal of Differential Equations* (2010), p. 1726.

[98] S. N. Hammond et al. "Characterization of Aedes aegypti (Diptera: Culcidae) Production Sites in Urban Nicaragua". In: *Journal of Medical Entomology* 44.5 (Sept. 2007), pp. 851–860.

[99] I. Hanski. "Metapopulation dynamics". en. In: *Nature* 396.6706 (Nov. 1998). Number: 6706 Publisher: Nature Publishing Group, pp. 41–49.

[100] W. A. Hawley. "The biology of Aedes albopictus". eng. In: *Journal of the American Mosquito Control Association. Supplement* 1 (Dec. 1988), pp. 1–39.

[101] W. A. Hawley, P. Reiter, R. S. Copeland, C. B. Pumpuni, and G. B. Craig. "Aedes albopictus in North America: Probable Introduction in Used Tires from Northern Asia". In: *Science* 236.4805 (May 1987). Publisher: American Association for the Advancement of Science, pp. 1114–1116.

[102] K. Heath, M. B. Bonsall, J. Marie, and H. C. Bossin. "Mathematical modelling of the mosquito Aedes polynesiensis in a heterogeneous environment". In: *Mathematical Biosciences* 348 (June 2022), p. 108811.

[103] D. Henry. *Geometric Theory of Semilinear Parabolic Equations*. en. Springer, Nov. 2006.

[104] M. Hertig and S. B. Wolbach. "Studies on Rickettsia-like micro-organisms in insects". In: *The Journal of medical research* 44.3 (1924), p. 329.

[105] K. Hilgenboecker, P. Hammerstein, P. Schlattmann, A. Telschow, and J. H. Werren. "How many species are infected with Wolbachia? – a statistical analysis of current data". In: *FEMS Microbiology Letters* 281.2 (Apr. 2008), pp. 215–220.

[106] D. Hilhorst, M. Iida, M. Mimura, and H. Ninomiya. "Relative compactness in Lp of solutions of some 2m components competition-diffusion systems". In: *Discrete and Continuous Dynamical Systems* 21.1 (May 2008), pp. 233–244.

[107] D. Hilhorst, S. Martin, and M. Mimura. "Singular limit of a competition-diffusion system with large interspecific interaction". In: *Journal of Mathematical Analysis and Applications* 390 (June 2012).

[108] A. A. Hoffmann et al. "Successful establishment of Wolbachia in Aedes populations to suppress dengue transmission". en. In: *Nature* 476.7361 (Aug. 2011). Number: 7361 Publisher: Nature Publishing Group, pp. 454–457.

[109] V. Houé, M. Bonizzoni, and A.-B. Failloux. "Endogenous non-retroviral elements in genomes of Aedes mosquitoes and vector competence". In: *Emerging Microbes & Infections* 8.1 (Jan. 2019), pp. 542–555.

[110] H. Hughes and N. F. Britton. "Modelling the Use of Wolbachia to Control Dengue Fever Transmission". en. In: *Bulletin of Mathematical Biology* 75.5 (May 2013), pp. 796–818.

[111] *Increasing risk of mosquito-borne diseases in EU/EEA following spread of Aedes species*. en. `https://www.ecdc.europa.eu/en/news-events/increasing-risk-mosquito-borne-diseases-eueea-following-spread-aedes-species`. European Centre for Disease Prevention and Control. June 2023.

[112] Y. Jin and W. Wang. "The effect of population dispersal on the spread of a disease". In: *Journal of Mathematical Analysis and Applications* 308.1 (Aug. 2005), pp. 343–364.

[113] M. A. Johansson, J. Hombach, and D. A. T. Cummings. "Models of the impact of dengue vaccines: A review of current research and potential approaches". In: *Vaccine* 29.35 (Aug. 2011), pp. 5860–5868.

[114] C. K. R. T. Jones. "Asymptotic behavior of a reaction-diffusion equation in higher space dimensions". In: *Rocky Mountain Journal of Mathematics* 13.2 (June 1983), pp. 355–364.

[115] M. Kattwinkel and P. Reichert. "Bayesian parameter inference for individual-based models using a Particle Markov Chain Monte Carlo method". In: *Environmental Modelling & Software* 87 (Jan. 2017), pp. 110–119.

[116] M. J. Keeling, F. M. Jiggins, and J. M. Read. "The invasion and coexistence of competing Wolbachia strains". en. In: *Heredity* 91.4 (Oct. 2003). Publisher: Nature Publishing Group, pp. 382–388.

[117] H. Kierstead and L. Slobodkin. "The size of water masses containing plankton blooms". In: *Journal of Marine Research* 12.1 (Jan. 1953).

[118] E. F. Knipling. "Sterile-Male Method of Population Control". In: *Science* 130.3380 (Oct. 1959). Publisher: American Association for the Advancement of Science, pp. 902–904.

[119] A. Kolmogorov, I. Petrovskii, and N. Piscunov. "A study of the equation of diffusion with increase in the quantity of matter, and its application to a biological problem". In: *Byul. Moskovskogo Gos. Univ.* 1.6 (1938), pp. 1–25.

[120] P. Korman. *Chapter 6 Global Solution Branches and Exact Multiplicity of Solutions for Two Point Boundary Value Problems*. Vol. 3. North-Holland, Jan. 2006, pp. 547–606.

[121] P. Korman. "Exact multiplicity of solutions for a class of semilinear Neumann problems". In: *Communications on Applied Nonlinear Analysis* 9 (Jan. 2002).

[122] P. Korman, Y. Li, and T. Ouyang. "An Exact Multiplicity Result for a class of Semilinear Equations". en. In: *Communications in Partial Differential Equations* 22.3-4 (Jan. 1997), pp. 661–684.

[123] P. Korman, Y. Li, and T. Ouyang. "Exact multiplicity results for boundary value problems with nonlinearities generalising cubic". In: *Proceedings of the Royal Society of Edinburgh Section A: Mathematics* 126.3 (1996). Publisher: Royal Society of Edinburgh Scotland Foundation, pp. 599–616.

[124] F. Lardeux, F. Riviere, Y. Sechan, and B. H. Kay. "Release of Mesocyclops aspericornis (Copepoda) for Control of Larval Aedes polynesiensis (Diptera: Culicidae) in Land Crab Burrows on an Atoll of French Polynesia". In: *Journal of Medical Entomology* 29.4 (July 1992), pp. 571–576.

[125] F. Lardeux, Y. Sechan, and M. Faaruia. "Evaluation of Insecticide Impregnated Baits for Control of Mosquito Larvae in Land Crab Burrows on French Polynesian Atolls". In: *Journal of Medical Entomology* 39.4 (July 2002), pp. 658–661.

[126] A. Leculier and N. Nguyen. "A control strategy for the sterile insect technique using exponentially decreasing releases to avoid the hair-trigger effect". en. In: *Mathematical Modelling of Natural Phenomena* 18 (2023). Publisher: EDP Sciences, p. 25.

[127] R. Levins. "Some Demographic and Genetic Consequences of Environmental Heterogeneity for Biological Control1". In: *Bulletin of the Entomological Society of America* 15.3 (Sept. 1969), pp. 237–240.

[128] M. A. Lewis and P. Van Den Driessche. "Waves of extinction from sterile insect release". en. In: *Mathematical Biosciences* 116.2 (Aug. 1993), pp. 221–247.

[129] M. Lewis, T. Hillen, and F. Lutscher. "Spatial Dynamics in ecology". In: June 2009.

[130] M. A. Lewis and B. Li. "Spreading Speed, Traveling Waves, and Minimal Domain Size in Impulsive Reaction–Diffusion Models". en. In: *Bulletin of Mathematical Biology* 74.10 (Oct. 2012), pp. 2383–2402.

[131] M. A. Lewis, B. Li, and H. F. Weinberger. "Spreading speed and linear determinacy for two-species competition models". en. In: *Journal of Mathematical Biology* 45.3 (Sept. 2002), pp. 219–233.

[132] M. A. Lewis, S. V. Petrovskii, and J. R. Potts. *The Mathematics Behind Biological Invasions*. en. Vol. 44. Interdisciplinary Applied Mathematics. Cham: Springer International Publishing, 2016.

[133] B. Li, H. F. Weinberger, and M. A. Lewis. "Spreading speeds as slowest wave speeds for cooperative systems". In: *Mathematical Biosciences* 196.1 (July 2005), pp. 82–98.

[134] M. Y. Li and Z. Shuai. "Global-stability problem for coupled systems of differential equations on networks". In: *Journal of Differential Equations* 248.1 (Jan. 2010), pp. 1–20.

[135] P. Lions. "On the Existence of Positive Solutions of Semilinear Elliptic Equations". In: *SIAM Review* 24 (1982), pp. 441–467.

[136] L. P. Lounibos. "Invasions by Insect Vectors of Human Disease". In: *Annual Review of Entomology* 47.1 (2002), pp. 233–266.

[137] P. Lu, G. Bian, X. Pan, and Z. Xi. "Wolbachia Induces Density-Dependent Inhibition to Dengue Virus in Mosquito Cells". en. In: *PLOS Neglected Tropical Diseases* 6.7 (2012). Publisher: Public Library of Science, e1754.

[138] Z. Lu and Y. Takeuchi. "Global asymptotic behavior in single-species discrete diffusion systems". en. In: *Journal of Mathematical Biology* 32.1 (Nov. 1993), pp. 67–77.

[139] R. Lui. "Biological growth and spread modeled by systems of recursions. I. mathematical theory". en. In: *Mathematical Biosciences* 93.2 (Apr. 1989), pp. 269–295.

[140] A. M. Lutambi, M. A. Penny, T. Smith, and N. Chitnis. "Mathematical modelling of mosquito dispersal in a heterogeneous environment". In: *Mathematical Biosciences* 241.2 (Feb. 2013), pp. 198–216.

[141] R. H. MacArthur and E. O. Wilson. *The theory of island biogeography*. Vol. 1. Princeton university press, 1967.

[142] M. B. Madon, M. S. Mulla, M. W. Shaw, S. Kluh, and J. E. Hazelrigg. "Introduction of Aedes albopictus (Skuse) in southern California and potential for its establishment". eng. In: *Journal of Vector Ecology: Journal of the Society for Vector Ecology* 27.1 (June 2002), pp. 149–154.

[143] M. L. Mann Manyombe, B. Tsanou, J. Mbang, and S. Bowong. "A metapopulation model for the population dynamics of anopheles mosquito". In: *Applied Mathematics and Computation* 307 (Aug. 2017), pp. 71–91.

[144] V. S. Manoranjan and P. Van Den Driessche. "On a diffusion model for sterile insect release". en. In: *Mathematical Biosciences* 79.2 (June 1986), pp. 199–208.

[145] P Martens and L Hall. "Malaria on the move: human population movement and malaria transmission." In: *Emerging Infectious Diseases* 6.2 (2000), pp. 103–109.

[146] J. Martinez, S. Ok, S. Smith, K. Snoeck, J. P. Day, and F. M. Jiggins. "Should Symbionts Be Nice or Selfish? Antiviral Effects of Wolbachia Are Costly but Reproductive Parasitism Is Not". en. In: *PLOS Pathogens* 11.7 (2015). Publisher: Public Library of Science, e1005021.

[147] A. Martín-Park et al. "Pilot trial using mass field-releases of sterile males produced with the incompatible and sterile insect techniques as part of integrated Aedes aegypti control in Mexico". en. In: *PLOS Neglected Tropical Diseases* 16.4 (2022). Publisher: Public Library of Science, e0010324.

[148] A. J. Maynard, L. Ambrose, M. J. Bangs, R. Ahmad, C. Butafa, and N. W. Beebe. "Population structure and invasion history of Aedes aegypti (Diptera: Culicidae) in Southeast Asia and Australasia". en. In: *Evolutionary Applications* 16.4 (2023), pp. 849–862.

[149] C. S. McBride. “Genes and Odors Underlying the Recent Evolution of Mosquito Preference for Humans”. In: *Current Biology* 26.1 (Jan. 2016), R41–R46.

[150] J. M. Medlock et al. “A Review of the Invasive Mosquitoes in Europe: Ecology, Public Health Risks, and Control Options”. In: *Vector-Borne and Zoonotic Diseases* 12.6 (June 2012). Publisher: Mary Ann Liebert, Inc., publishers, pp. 435–447.

[151] C. D. Morris, V. L. Larson, and L. P. Lounibos. “Measuring mosquito dispersal for control programs”. eng. In: *Journal of the American Mosquito Control Association* 7.4 (Dec. 1991), pp. 608–615.

[152] L. E. Muir and B. H. Kay. “Aedes aegypti survival and dispersal estimated by mark-release-recapture in northern Australia.” EN. In: *The American Journal of Tropical Medicine and Hygiene* 58.3 (Mar. 1998). Section: The American Journal of Tropical Medicine and Hygiene, pp. 277–282.

[153] J. D. Murray and R. P. Sperb. “Minimum domains for spatial patterns in a class of reaction diffusion equations”. en. In: *Journal of Mathematical Biology* 18.2 (Nov. 1983), pp. 169–184.

[154] J. D. Murray. *Mathematical Biology*. Berlin, Heidelberg: Springer, 1993.

[155] J. D. Murray. *Mathematical Biology II: Spatial Models and Biomedical Applications*. Springer Science & Business Media, Feb. 2001.

[156] M. Z. Ndii, R. I. Hickson, D. Allingham, and G. N. Mercer. “Modelling the transmission dynamics of dengue in the presence of Wolbachia”. In: *Mathematical Biosciences* 262 (Apr. 2015), pp. 157–166.

[157] R Novak. “The Asian tiger mosquito, Aedes albopictus”. In: *Wing Beats* 3.5 (1992), p. 1.

[158] P. N. Okorie, J. M. Marshall, O. M. Akpa, and O. G. Ademowo. “Perceptions and recommendations by scientists for a potential release of genetically modified mosquitoes in Nigeria”. In: *Malaria Journal* 13.1 (Apr. 2014), p. 154.

[159] A. Okubo. *Diffusion and Ecological Problems: Mathematical Models*. en. Google-Books-ID: YAkJ6aQeCzkC. Springer Berlin Heidelberg, Feb. 1980.

[160] A. Okubo and S. A. Levin. *Diffusion and Ecological Problems: Modern Perspectives*. en. Ed. by S. S. Antman, J. E. Marsden, L. Sirovich, and S. Wiggins. Vol. 14. Interdisciplinary Applied Mathematics. New York, NY: Springer, 2001.

[161] C. F. Oliva et al. “Sterile Insect Technique (SIT) against Aedes Species Mosquitoes: A Roadmap and Good Practice Framework for Designing, Implementing and Evaluating Pilot Field Trials”. en. In: *Insects* 12.3 (Mar. 2021). Number: 3 Publisher: Multidisciplinary Digital Publishing Institute, p. 191.

[162] M. Otero, N. Schweigmann, and H. G. Solari. “A Stochastic Spatial Dynamical Model for Aedes Aegypti”. In: *Bulletin of mathematical biology* 70.5 (2008), pp. 1297–1325.

[163] T. Ouyang and J. Shi. “Exact Multiplicity of Positive Solutions for a Class of Semilinear Problems”. en. In: *Journal of Differential Equations* 146.1 (June 1998), pp. 121–156.

[164] C. V. Pao. *Nonlinear Parabolic and Elliptic Equations*. 1st. Boston, MA: Springer, 1992.

[165] P. Paradisi, R. Cesari, F. Mainardi, and F. Tampieri. “The fractional Fick’s law for non-local transport processes”. In: *Physica A: Statistical Mechanics and its Applications* 293.1 (Apr. 2001), pp. 130–142.

[166] S. Pasquali et al. “Development and calibration of a model for the potential establishment and impact of Aedes albopictus in Europe”. In: *Acta Tropica* 202 (Feb. 2020), p. 105228.

[167] B. Perthame. *Parabolic equations in biology*. Lecture Notes on Mathematical Modelling in the Life Sciences. Springer, 2015.

[168] S. Petrovskii, N. Petrovskaya, and D. Bearup. “Multiscale approach to pest insect monitoring: Random walks, pattern formation, synchronization, and networks”. In: *Physics of Life Reviews* 11.3 (Sept. 2014), pp. 467–525.

[169] R. C. Reiner et al. “A systematic review of mathematical models of mosquito-borne pathogen transmission: 1970–2010”. In: *Journal of The Royal Society Interface* 10.81 (Apr. 2013). Publisher: Royal Society, p. 20120921.

[170] W. C. Rheinboldt. “Numerical continuation methods: a perspective”. en. In: *Journal of Computational and Applied Mathematics*. Numerical Analysis 2000. Vol. IV: Optimization and Nonlinear Equations 124.1 (Dec. 2000), pp. 229–244.

[171] J. G. Rigau-Pérez, G. G. Clark, D. J. Gubler, P. Reiter, E. J. Sanders, and A. V. Vorndam. “Dengue and dengue hemorrhagic fever”. English. In: *The Lancet* 352.9132 (Sept. 1998). Publisher: Elsevier, pp. 971–977.

[172] H. Risken. *The Fokker-Planck Equation*. Ed. by H. Haken. Vol. 18. Springer Series in Synergetics. Berlin, Heidelberg: Springer, 1984.

[173] S. A. Ritchie and K. M. Staunton. "Reflections from an old Queenslander: can rear and release strategies be the next great era of vector control?" In: *Proceedings of the Royal Society B: Biological Sciences* 286.1905 (June 2019). Publisher: Royal Society, p. 20190973.

[174] J.-M. Roquejoffre, L. Rossi, and V. Roussier-Michon. "Sharp large time behaviour in N-dimensional Fisher-KPP equations". en. In: *Discrete and Continuous Dynamical Systems* 39.12 (Nov. 2019), pp. 7265–7290.

[175] J.-M. Roquejoffre and V. Roussier-Michon. "Sharp large time behaviour in N-dimensional reaction-diffusion equations of bistable type". In: *Journal of Differential Equations* 339 (Dec. 2022), pp. 134–151.

[176] L. Roques. *Modèles de réaction-diffusion pour l'écologie spatiale: Avec exercices dirigés*. fr. Editions Quae, Sept. 2013.

[177] L. Roques and O. Bonnefon. "Modelling Population Dynamics in Realistic Landscapes with Linear Elements: A Mechanistic-Statistical Reaction-Diffusion Approach". en. In: *PLOS ONE* 11.3 (Mar. 2016). Publisher: Public Library of Science, e0151217.

[178] L. Roques, E. K. Klein, J. Papaïx, A. Sar, and S. Soubeyrand. "Using Early Data to Estimate the Actual Infection Fatality Ratio from COVID-19 in France". en. In: *Biology* 9.5 (May 2020). Number: 5 Publisher: Multidisciplinary Digital Publishing Institute, p. 97.

[179] N. H. Rose et al. "Climate and Urbanization Drive Mosquito Preference for Humans". In: *Current Biology* 30.18 (Sept. 2020), 3570–3579.e6.

[180] P. A. Ross et al. "A decade of stability for wMel Wolbachia in natural Aedes aegypti populations". en. In: *PLOS Pathogens* 18.2 (2022). Publisher: Public Library of Science, e1010256.

[181] R. Ross. "Malaria and Mosquitoes". en. In: *Nature* 63.1636 (Mar. 1901). Number: 1636 Publisher: Nature Publishing Group, pp. 440–440.

[182] V. Roussier. "Stability of radially symmetric travelling waves in reaction–diffusion equations". In: *Annales de l'Institut Henri Poincaré C, Analyse non linéaire* 21.3 (May 2004), pp. 341–379.

[183] A. K. Sakai et al. "The Population Biology of Invasive Species". In: *Annual Review of Ecology and Systematics* 32.1 (2001), pp. 305–332.

[184] R. Schaaf. "Global behaviour of solution branches for some Neumann problems depending on one or several parameters." In: *Journal für die reine und angewandte Mathematik* 1984.346 (Jan. 1984), pp. 1–31.

[185] S. Seirin Lee, R. E. Baker, E. A. Gaffney, and S. M. White. "Modelling Aedes aegypti mosquito control via transgenic and sterile insect techniques: Endemics and emerging outbreaks". en. In: *Journal of Theoretical Biology* 331 (Aug. 2013), pp. 78–90.

[186] S. Shi and S. Li. "Existence of solutions for a class of semilinear elliptic equations with the Robin boundary value condition". In: *Nonlinear Analysis: Theory, Methods & Applications* 71.7 (Oct. 2009), pp. 3292–3298.

[187] J. B. Silver. *Mosquito Ecology: Field Sampling Methods*. en. Google-Books-ID: VM8MA4E_VT8C. Springer Science & Business Media, Dec. 2007.

[188] J. Simon. "Compact sets in the space $L^p(O,T;B)$". In: *Annali di Matematica pura ed applicata* (Sept. 1986), pp. 65–96.

[189] J. G. Skellam. "Random dispersal in theoretical populations". In: *Biometrika* 38.1/2 (1951), pp. 196–218.

[190] C. E. G. Smith. "The History of Dengue in Tropical Asia and its Probable Relationship to the Mosquito Aedes aegypti." English. In: *Journal of Tropical Medicine and Hygiene* 59.10 (1956), pp. 243–51.

[191] H. L. Smith. *Monotone Dynamical Systems: An Introduction to the Theory of Competitive and Cooperative Systems: An Introduction to the Theory of Competitive and Cooperative Systems*. en. Google-Books-ID: vOfNAwAAQBAJ. American Mathematical Soc., 1995.

[192] J Smoller and A Wasserman. "Global bifurcation of steady-state solutions". In: *Journal of Differential Equations* 39.2 (1981), pp. 269–290.

[193] J. Smoller. *Shock waves and reaction—diffusion equations*. Vol. 258. Springer Science & Business Media, 1983.

[194] J. Smoller. *Shock Waves and Reaction—Diffusion Equations*. en. Springer Science & Business Media, Dec. 2012.

[195] S. Soubeyrand, A. Laine, I. Hanski, and A. Penttinen. "Spatiotemporal Structure of Host-Pathogen Interactions in a Metapopulation." In: *The American Naturalist* 174.3 (Sept. 2009). Publisher: The University of Chicago Press, pp. 308–320.

[196] S. Soubeyrand, S. Neuvonen, and A. Penttinen. "Mechanical-Statistical Modeling in Ecology: From Outbreak Detections to Pest Dynamics". en. In: *Bulletin of Mathematical Biology* 71.2 (Feb. 2009), pp. 318–338.

[197] S. Soubeyrand and L. Roques. "Parameter estimation for reaction-diffusion models of biological invasions". en. In: *Population Ecology* 56.2 (Apr. 2014), pp. 427–434.

[198] D. C. Speirs and W. S. C. Gurney. "Population Persistence in Rivers and Estuaries". en. In: *Ecology* 82.5 (2001), pp. 1219–1237.

[199] S. T. Stoddard et al. "House-to-house human movement drives dengue virus transmission". In: *Proceedings of the National Academy of Sciences* 110.3 (Jan. 2013). Publisher: Proceedings of the National Academy of Sciences, pp. 994–999.

[200] M. Strugarek, H. Bossin, and Y. Dumont. "On the use of the sterile insect release technique to reduce or eliminate mosquito populations". In: *Applied Mathematical Modelling* 68 (Apr. 2019), pp. 443–470.

[201] M. Strugarek and N. Vauchelet. "Reduction to a Single Closed Equation for 2-by-2 Reaction-Diffusion Systems of Lotka–Volterra Type". In: *SIAM Journal on Applied Mathematics* 76.5 (Jan. 2016). Publisher: Society for Industrial and Applied Mathematics, pp. 2060–2080.

[202] Y. Takeuchi. "Cooperative Systems Theory and Global Stability of Diffusion Models". en. In: *Evolution and Control in Biological Systems*. Ed. by A. B. Kurzhanski and K. Sigmund. Dordrecht: Springer Netherlands, 1989, pp. 49–57.

[203] J. C. Thiele, W. Kurth, and V. Grimm. "Facilitating Parameter Estimation and Sensitivity Analysis of Agent-Based Models: A Cookbook Using NetLogo and R". In: *Journal of Artificial Societies and Social Simulation* 17.3 (2014), p. 11.

[204] A. Tran et al. "A Rainfall- and Temperature-Driven Abundance Model for Aedes albopictus Populations". en. In: *International Journal of Environmental Research and Public Health* 10.5 (May 2013). Number: 5 Publisher: Multidisciplinary Digital Publishing Institute, pp. 1698–1719.

[205] E. Trélat, J. Zhu, and E. Zuazua. "Allee optimal control of a system in ecology". In: *Mathematical Models and Methods in Applied Sciences* 28.09 (2018), pp. 1665–1697.

[206] E. Trélat, J. Zhu, and E. Zuazua. "Optimal Population Control Through Sterile Males". working paper or preprint. Oct. 2017.

[207] C.-C. Tsai, S.-H. Wang, and S.-Y. Huang. "Classification and evolution of bifurcation curves for a one-dimensional Neumann–Robin problem and its applications". en. In: *Electron. J. Qual. Theory Differ. Equ.* 85 (2018), pp. 1–30.

[208] P. Turchin. *Quantitative Analysis of Movement: Measuring and Modeling Population Redistribution in Animals and Plants*. en. Google-Books-ID: ZbdmQgAACAAJ. Sinauer, 1998.

[209] M. Turelli. "Cytoplasmic Incompatibility in Populations with Overlapping Generations". en. In: *Evolution* 64.1 (2010). _eprint: https://onlinelibrary.wiley.com/doi/pdf/10.1111/j.1558-5646.2009.00822.x, pp. 232–241.

[210] M. Turelli and A. A. Hoffmann. "Rapid spread of an inherited incompatibility factor in California Drosophila". en. In: *Nature* 353.6343 (Oct. 1991). Publisher: Nature Publishing Group, pp. 440–442.

[211] H. C. Turner, D. L. Quyen, R. Dias, P. T. Huong, C. P. Simmons, and K. L. Anders. "An economic evaluation of Wolbachia deployments for dengue control in Vietnam". en. In: *PLOS Neglected Tropical Diseases* 17.5 (2023). Publisher: Public Library of Science, e0011356.

[212] I. D. Velez et al. "Large-scale releases and establishment of wMel Wolbachia in Aedes aegypti mosquitoes throughout the Cities of Bello, Medellín and Itagüí, Colombia". en. In: *PLOS Neglected Tropical Diseases* 17.11 (Nov. 2023). Publisher: Public Library of Science, e0011642.

[213] D. A. M. Villela, G. d. A. Garcia, and R. Maciel-de Freitas. "Novel inference models for estimation of abundance, survivorship and recruitment in mosquito populations using mark-release-recapture data". en. In: *PLOS Neglected Tropical Diseases* 11.6 (2017). Publisher: Public Library of Science, e0005682.

[214] A. Volpert, V. Volpert, and V. Volpert. *Traveling Wave Solutions of Parabolic Systems*. en. Vol. 140. Translations of Mathematical Monographs. ISSN: 0065-9282, 2472-5137. American Mathematical Society, Oct. 1994.

[215] S.-H. Wang. "A correction for a paper by J. Smoller and A. Wasserman". In: *Journal of Differential Equations* 77.1 (1989), pp. 199–202.

[216] S.-H. Wang and N. D. Kazarinoff. "Bifurcation of steady-state solutions of a scalar reaction-diffusion equation in one space variable". In: *Journal of the Australian Mathematical Society* 52.3 (June 1992), pp. 343–355.

[217] Y. Wang and J. Shi. "Persistence and Extinction of Population in Reaction-Diffusion-Advection Model with Weak Allee Effect Growth". In: *SIAM J. Appl. Math.* 79.4 (Jan. 2019). Publisher: Society for Industrial and Applied Mathematics, pp. 1293–1313.

[218] Y. Wang, J. Shi, and J. Wang. "Persistence and extinction of population in reaction–diffusion–advection model with strong Allee effect growth". en. In: *J. Math. Biol.* 78.7 (June 2019), pp. 2093–2140.

[219] H. F. Weinberger, M. A. Lewis, and B. Li. "Analysis of linear determinacy for spread in cooperative models". en. In: *J Math Biol* 45.3 (Sept. 2002), pp. 183–218.

[220] J. Werren, L. Baldo, and M. Clark. "*Wolbachia*: master manipulators of invertebrate biology". In: *Nat Rev Microbiol* 6 (Oct. 2008), pp. 741–751.

[221] C. K. Wikle. "Hierarchical Models in Environmental Science". en. In: *International Statistical Review* 71.2 (2003). _eprint: https://onlinelibrary.wiley.com/doi/pdf/10.1111/j.1751-5823.2003.tb00192.x, pp. 181–199.

[222] M. Williamson. *Biological Invasions*. en. Google-Books-ID: eWUdzI6j3V8C. Springer Science & Business Media, 1996.

[223] W. Wilson. "Resolving Discrepancies between Deterministic Population Models and Individual-Based Simulations". In: *The American Naturalist* 151.2 (Feb. 1998). Publisher: The University of Chicago Press, pp. 116–134.

[224] *World Mosquito Program: Our Wolbachia method*. en. `https://www.worldmosquitoprogram.org/en/work/wolbachia-method/`.

[225] H. Yagisita. "Nearly Spherically Symmetric Expanding Fronts in a Bistable Reaction-Diffusion Equation". en. In: *Journal of Dynamics and Differential Equations* 13.2 (Apr. 2001), pp. 323–353.

[226] P.-S. Yen and A.-B. Failloux. "A Review: Wolbachia-Based Population Replacement for Mosquito Control Shares Common Points with Genetically Modified Control Approaches". en. In: *Pathogens* 9.5 (May 2020). Number: 5 Publisher: Multidisciplinary Digital Publishing Institute, p. 404.

[227] J. Zhang, S. Li, and X. Xue. "Multiple solutions for a class of semilinear elliptic problems with Robin boundary condition". In: *Journal of Mathematical Analysis and Applications* 388.1 (Apr. 2012), pp. 435–442.

[228] X. Zheng et al. "Incompatible and sterile insect techniques combined eliminate mosquitoes". en. In: *Nature* 572.7767 (Aug. 2019). Number: 7767 Publisher: Nature Publishing Group, pp. 56–61.

[229] Z. Zhu, B. Zheng, Y. Shi, R. Yan, and J. Yu. "Stability and periodicity in a mosquito population suppression model composed of two sub-models". In: *Nonlinear Dynamics* 107 (Jan. 2022), pp. 1–13.